

Near-Zero Emissions Oxy-Combustion Flue Gas Purification

Final Report

January 1, 2009 to June 30, 2012

Authors

Minish Shah (Task 1)
Nick Degenstein (Task 2)
Monica Zafir and Rahul Solunke (Task 3)
Ravi Kumar and Jennifer Bugayong (Task 4)
Ken Burgers (Task 5)

September, 2012

DOE Award No. DE-NT0005341

Recipient

Praxair, Inc.
175 East Park Drive
Tonawanda, NY 14150

Project Director

Minish Shah
Tel: (716) 879-2623
Email: minish_shah@praxair.com

Business Officer

Ray Drnevich
Tel: (716) 879-2595
Email: ray_drnevich@praxair.com

Subcontractors

Foster Wheeler North America Corp.
WorleyParsons Canada
AES Westover LLC

Disclaimer

“This report was prepared as an account of work sponsored by an agency of the United States Government. Neither the United States Government nor any agency thereof, nor any of their employees, makes any warranty, express or implied, or assumes any legal liability or responsibility for the accuracy, completeness, or usefulness of any information, apparatus, product, or process disclosed, or represents that its use would not infringe privately owned rights. Reference herein to any specific commercial product, process, or service by trade name, trademark, manufacturer, or otherwise does not necessarily constitute or imply its endorsement, recommendation, or favoring by the United States Government or any agency thereof. The views and opinions of authors expressed herein do not necessarily state or reflect those of the United States Government or any agency thereof.”

Abstract

The objectives of this project were to carry out an experimental program to enable development and design of near zero emissions (NZE) CO₂ processing unit (CPU) for oxy-combustion plants burning high and low sulfur coals and to perform commercial viability assessment. The NZE CPU was proposed to produce high purity CO₂ from the oxycombustion flue gas, to achieve > 95% CO₂ capture rate and to achieve near zero atmospheric emissions of criteria pollutants. Two SO_x/NO_x removal technologies were proposed depending on the SO_x levels in the flue gas. The activated carbon process was proposed for power plants burning low sulfur coal and the sulfuric acid process was proposed for power plants burning high sulfur coal. For plants burning high sulfur coal, the sulfuric acid process would convert SO_x and NO_x in to commercial grade sulfuric and nitric acid by-products, thus reducing operating costs associated with SO_x/NO_x removal. For plants burning low sulfur coal, investment in separate FGD and SCR equipment for producing high purity CO₂ would not be needed. To achieve high CO₂ capture rates, a hybrid process that combines cold box and VPSA (vacuum pressure swing adsorption) was proposed. In the proposed hybrid process, up to 90% of CO₂ in the cold box vent stream would be recovered by CO₂ VPSA and then it would be recycled and mixed with the flue gas stream upstream of the compressor. The overall recovery from the process will be > 95%.

The activated carbon process was able to achieve simultaneous SO_x and NO_x removal in a single step. The removal efficiencies were >99.9% for SO_x and >98% for NO_x, thus exceeding the performance targets of >99% and >95%, respectively. The process was also found to be suitable for power plants burning both low and high sulfur coals. Sulfuric acid process did not meet the performance expectations. Although it could achieve high SO_x (>99%) and NO_x (>90%) removal efficiencies, it could not produce by-product sulfuric and nitric acids that meet the commercial product specifications. The sulfuric acid will have to be disposed of by neutralization, thus lowering the value of the technology to same level as that of the activated carbon process. Therefore, it was decided to discontinue any further efforts on sulfuric acid process. Because of encouraging results on the activated carbon process, it was decided to add a new subtask on testing this process in a dual bed continuous unit. A 40 days long continuous operation test confirmed the excellent SO_x/NO_x removal efficiencies achieved in the batch operation. This test also indicated the need for further efforts on optimization of adsorption-regeneration cycle to maintain long term activity of activated carbon material at a higher level.

The VPSA process was tested in a pilot unit. It achieved CO₂ recovery of > 95% and CO₂ purity of >80% (by vol.) from simulated cold box feed streams. The overall CO₂ recovery from the cold box VPSA hybrid process was projected to be >99% for plants with low air ingress (2%) and >97% for plants with high air ingress (10%).

Economic analysis was performed to assess value of the NZE CPU. The advantage of NZE CPU over conventional CPU is only apparent when CO₂ capture and avoided costs are compared. For greenfield plants, cost of avoided CO₂ and cost of captured CO₂ are generally about 11-14% lower using the NZE CPU compared to using a conventional CPU. For older plants with high air intrusion, the cost of avoided CO₂ and capture CO₂ are about 18-24% lower using the NZE CPU. Lower capture costs for NZE CPU are due to lower capital investment in FGD/SCR and higher CO₂ capture efficiency.

In summary, as a result of this project, we now have developed one technology option for NZE CPU based on the activated carbon process and coldbox-VPSA hybrid process. This technology is projected to work for both low and high sulfur coal plants. The NZE CPU technology is projected to achieve near zero stack emissions, produce high purity CO₂ relatively free of trace impurities and achieve ~99% CO₂ capture rate while lowering the CO₂ capture costs.

Table of Contents

Disclaimer	2
Abstract	3
Executive Summary	9
Task 1 – Program Management	11
Technology Overview	11
Project Plan	14
Project Execution – Milestones	19
Cost Status	25
Key Accomplishments	26
Path to Commercialization	27
Task 2 – SO _x /NO _x /Hg Removal for High Sulfur Coal	29
Approach	29
Results and Discussion	35
Conclusions	76
Task 3 – SO _x /NO _x /Hg Removal for Low Sulfur Coal	78
Approach	78
Results and Discussion	89
Conclusions	103
Task 4 – High CO ₂ Recovery	104
Approach	104
Results and Discussion	105
Conclusions	128
Task 5 – Commercial Viability Assessment	129
Approach	129
Results and Discussion	135
Conclusions	192
Project Conclusions	194
References	196
Appendix A – Literature Review for Task 4 VPSA Process	198

List of Figures

Figure 1.1 Schematics of Coal Power Plant Without CCS	11
Figure 1.2 Schematics of Oxy-Coal Power Plant With CCS	11
Figure 1.3 Schematics of Conventional CO ₂ Processing Unit	12
Figure 1.4 Schematics of NZE CPU Based on Activated Carbon Process	13
Figure 1.5 Schematics of NZE CPU Based on Sulfuric Acid Process	13
Figure 2.1 Schematic of the Oxy-coal Boiler Island	29
Figure 2.2 A CPU Process Using the Task 2 Process for SO _x /NO _x Removal	30
Figure 2.3 Schematic of the Task 2 Process for SO _x and NO _x Removal	31
Figure 2.4 Schematic of the Task 2 Bench-Scale Unit	33
Figure 2.5 Photograph of the Task 2 Bench-Scale Unit	33
Figure 2.6 Plume Analysis for a 10 Minute Release of NO ₂ through the Fume Hood Exhauster	36
Figure 2.7 Bench Scale Unit Constructed as Part of Subtask 2.1	37
Figure 2.8 Computer Interface Control and Monitoring Panel for the Task 2 Equipment	38

Figure 2.9	Experimental Column Flooding Threshold	39
Figure 2.10	Experimental Column Stage Efficiency	40
Figure 2.11	Percent Conversion of NO to NO ₂ at Various Pressures and Flowrates	41
Figure 2.12	NO _x Absorption by H ₂ SO ₄ ; 100 psia and 130 °F	42
Figure 2.13	NO _x Absorption by H ₂ SO ₄ ; 200 psia and 130 °F	42
Figure 2.14	NO _x Absorption by H ₂ SO ₄ ; 100 psia and 175 °F	43
Figure 2.15	NO _x Absorption by H ₂ SO ₄ ; 100 psia and 195 °F	44
Figure 2.16	NO _x Absorption by H ₂ SO ₄ ; 100 psia and 235 °F	44
Figure 2.17	Accumulation of NO _x in H ₂ SO ₄ during the Test Campaign	45
Figure 2.18	Equilibrium Solubility of SO ₂ in 95wt% Sulfuric Acid vs. Partial Pressure of SO ₂	47
Figure 2.19	Percent SO ₂ Absorption vs. Inlet Gas Concentration of SO ₂	48
Figure 2.20	Impact of Residence Time on SO ₂ Absorption in H ₂ SO ₄ in Absence of NO _x	49
Figure 2.21	Impact of Residence Time on SO ₂ Absorption in H ₂ SO ₄ in Presence of NO _x	49
Figure 2.22	Increase in SO ₂ Absorption in H ₂ SO ₄ by Reaction with NO ₂	50
Figure 2.23	Effect of acid flowrate on SO ₂ absorption	51
Figure 2.24	SO ₂ Absorption in H ₂ SO ₄ vs. NO _x Concentration in Feed at 200 psia	52
Figure 2.25	Absorption in H ₂ SO ₄ vs. NO _x Concentration in Feed at 150 psia	52
Figure 2.26	Impact of Temperature on SO ₂ Absorption in H ₂ SO ₄	53
Figure 2.27	Striping Performance of N ₂ and Air for NO _x Removal from Sulfuric Acid	54
Figure 2.28	Relative rate of NO _x removal for various carbons using N ₂ and air	54
Figure 2.29	Advantages and Disadvantages of the Activated Carbon Filter	58
Figure 2.30	Activated Carbon Mercury Removal System	59
Figure 2.31	Vapor Pressure for Hg, HgS and HgSe	60
Figure 2.32	Typical Operational Parameters for a Selenium Filter	61
Figure 2.33	Advantages and Disadvantages of the Selenium Filter	61
Figure 2.34	Typical Selenium Filter Arrangements	62
Figure 2.35	Pressurized Flue Gas Composition for Feed to the Task 2 Process	63
Figure 2.36	Process Schematic of the Final Task 2 Process	64
Figure 2.37	Stream Summary for Gas Streams of Final Process Simulation	65
Figure 2.38	Stream Summary for Liquid Streams of Final Process Simulation	66
Figure 2.39	US Bureau of Labor statistics – Producer Price Index for Sulfuric Acid	69
Figure 2.40	Sulfuric Acid Pricing 1989-2009	70
Figure 2.41	North American Sulfuric Acid Producers	72
Figure 2.42	Norfolco Supply and Distribution Network for Sulfuric Acid	74
Figure 3.1	Schematic of the Oxy-coal boiler island	78
Figure 3.2	A CPU with Activated Carbon Process for SO _x /NO _x Removal	79
Figure 3.3	Task 3 Activated Carbon Process for SO _x /NO _x Removal	80
Figure 3.4	PI&D of the Experimental Set-up for Material Testing	82
Figure 3.5	P&ID of the Bench Unit for Simultaneous SO _x /NO _x Removal	84
Figure 3.6	Dual Bed Reactor System for Simultaneous SO _x /NO _x Removal	87
Figure 3.7	Workflow to Assess the Activated Carbon Material Longevity	88
Figure 3.8	Relative Retention of SO ₂ for Different Activated Carbon Samples	89
Figure 3.9	Bench Unit for Batch Mode Operation	90
Figure 3.10	Gas Cabinet for Toxic Gas Cylinders Storage and PLC Box	90
Figure 3.11	Schematic of CO ₂ humidifier	91
Figure 3.12	Reactor Outlet SO ₂ and NO _x Concentrations as a Function of Time	91
Figure 3.13	Influence of Temperature on Relative Retention of SO _x and NO _x	93
Figure 3.14	Influence of Operating Pressure on Relative Retention of SO _x and NO _x	94
Figure 3.15	Influence of Operating Pressure on SO _x and NO _x Removal Efficiencies	94
Figure 3.16	Influence of NO/SO ₂ Molar Ratio in Feed on Relative Retention	95

Figure 3.17 Influence of NO/SO ₂ Molar Ratio in Feed on Removal Efficiency	95
Figure 3.18 Influence of Total Feed Flowrate on Relative Retention.....	96
Figure 3.19 Continuous Unit experimental set-up	97
Figure 3.20 Temperature Profiles During the Regeneration Stage	98
Figure 3.21 Depletion of Sulfate Ions in Waste Water with the Number of Washes	99
Figure 3.22 Reactor Effluent Concentrations as a Function of Time.....	100
Figure 3.23 Breakthrough Time for Bed 801	101
Figure 3.24 Reactor effluent concentration profiles for 30th adsorption cycle	102
Figure 4.1 VPSA Process Cycle Steps.....	104
Figure 4.2 Pure Component CO ₂ Equilibrium Data.....	106
Figure 4.3 Pure Component N ₂ Equilibrium Data	107
Figure 4.4 VPSA Bench Unit.....	108
Figure 4.5 Photograph of the VPSA Continuous Operation Unit.....	112
Figure 4.6 VPSA Adsorbents P and Q – CO ₂ Recovery vs. Purity.....	117
Figure 4.7 P and Q - Relative BSF vs. CO ₂ Recovery * Purity	118
Figure 4.8 Process Option A: Vacuum Pump Comparison P vs. Q.....	118
Figure 4.9 Process Option B: Vacuum Pump Comparison P vs. Q.....	119
Figure 4.10 SO _x and NO _x Retention on Adsorbent Q.....	125
Figure 5.1 Near Zero Emissions CPU Process Schematic.....	136
Figure 5.2 Effect of VPSA Product Purity on ASU + CPU Specific Power.....	145
Figure 5.3 Effect of VPSA CO ₂ Recovery on CPU CO ₂ Recovery	145
Figure 5.4 COE of New Plants using Low Sulfur Coal	161
Figure 5.5 Cost of CO ₂ Capture for New Plants using Low Sulfur Coal.....	162
Figure 5.6 COE of New Plants using High Sulfur Coal	163
Figure 5.7 Cost of CO ₂ Capture for New Plants using High Sulfur Coal	164
Figure 5.8 Relative Impact of NZE CPU Components on COE.....	165
Figure 5.9 Relative Impact of NZE CPU Components on CO ₂ Capture Costs	166
Figure 5.10 COE of Old Plants using Low Sulfur Coal.....	166
Figure 5.11 Cost of CO ₂ Capture for Old Plants using Low Sulfur Coal	167
Figure 5.12 COE of Old Plants using High Sulfur Coal	168
Figure 5.13 Cost of CO ₂ Capture for Old Plants using High Sulfur Coal.....	168
Figure 5.14 COE for Greenfield Supercritical Plants with and without CCS.....	170
Figure 5.15 Cost of CO ₂ Capture for Greenfield Supercritical Plants	170
Figure 5.16 COE for Greenfield Ultrasupercritical Plants.....	171
Figure 5.17 Cost of CO ₂ Capture of Greenfield Ultrasupercritical Plants	172
Figure 5.18 COE for Partial Condensation CPU vs. Distillation CPU	174
Figure 5.19 CO ₂ Capture Costs for Partial Condensation CPU vs. Distillation CPU	174
Figure 5.20 Impact on COE when FGD is Partially or Completely Eliminated.....	177
Figure 5.21 CO ₂ Capture Costs when FGD is Partially or Completely Eliminated.....	177
Figure 5.22 COE for New Plant without CCS vs. Old Plants with CCS	179
Figure 5.23 Preliminary Schematic of Oxy-Coal Furnace.....	186
Figure 5.24 Process Schematic of 20 tpd Demonstration CPU	187
Figure 5.25 Dual Purity Cold Box for Pilot Demonstration CPU.....	189

List of Tables

Table 1.1	Milestones Log	14
Table 1.2	Environmental Performance	18
Table 1.3	Final Milestones Status	19
Table 1.4	Final Cost Status	25
Table 1.5	Environmental Performance	27
Table 3.1	Ranges for the Two Level Factorial Design for Selected Parameters	85
Table 3.2	Dual Bed Activated Carbon Unit Cycle Steps	88
Table 3.3	Activated Carbon Process – Bench Unit Results	92
Table 3.4	Removal efficiency for bed 801 over 40 days of continuous operation	101
Table 4.1	Task 4 Schedule	105
Table 4.2	Physical Properties of the VPSA Adsorbents	107
Table 4.3	Breakthrough Data from the VPSA Bench Unit	108
Table 4.4	Results from Cyclic Experiments on the VPSA Bench Unit	109
Table 4.5	Equilibrium Parameters for Adsorbent P and Q	110
Table 4.6	Mass transfer coefficients for adsorbent P and Q	111
Table 4.7	VPSA Process Cycle for Four Beds – One Pressure Equalization	113
Table 4.8	VPSA Process Cycle for Five Beds – Two Pressure Equalizations	113
Table 4.9	VPSA Process Cycle for Six Beds – Three Pressure Equalizations	114
Table 4.10	VPSA Process Cycle for Eight Beds - Four Pressure Equalizations	114
Table 4.11	VPSA Pilot Unit Results – Adsorbent P	115
Table 4.12	VPSA Pilot Unit Results – Adsorbent Q	116
Table 4.13	VPSA Pilot Test Plan	120
Table 4.14	The VPSA Pilot Data – Process A, Adsorbent Q, Shallower Vacuum	121
Table 4.15	Bench-Scale NO ₂ Exposure Experiments for Adsorbent Q	122
Table 4.16	TGA Analysis after Exposure of Adsorbent Q to NO ₂	123
Table 4.17	Bench-Scale SO ₂ Exposure Experiments for Adsorbent Q	124
Table 4.18	TGA Analysis after Exposure of Adsorbent Q to SO ₂	124
Table 4.19	Comparison of VPSA Pilot Data vs. Simulation	126
Table 4.20	Comparison of Pilot Data vs. Simulation for Process B and Adsorbent P	126
Table 4.21	Comparison of Pilot Data vs. Simulation for Process A and Adsorbent Q	127
Table 4.22	Comparison of Pilot Data vs. Simulation for Process A and Adsorbent P	127
Table 5.1	Ambient Conditions	130
Table 5.2	Cooling Water	130
Table 5.3	Oxygen Specification	130
Table 5.4	Coal Specification	130
Table 5.5	Steam Cycle Definition	131
Table 5.6	Boiler Island Environmental Controls	131
Table 5.7	CO ₂ to Pipeline Specification	131
Table 5.8	Economic Feasibility Scenarios	132
Table 5.9	Low Sulfur Coal Case Definitions	133
Table 5.10	High Sulfur Coal Case Definitions	134
Table 5.11	Assumptions Used in Economic Feasibility Study	134
Table 5.12	Stream Summary for NZE CPU -- Low Sulfur Coal	137
Table 5.13	Stream Summary for NZE CPU – High Sulfur Coal	138
Table 5.14	Emissions for Plant using Low Sulfur Coal	138
Table 5.15	Emissions for Plant using High Sulfur Coal	139
Table 5.16	Reductions in Stack Emissions Compared to Air-Fired Power Plant	139

Table 5.17 ASU and CPU Utilities	139
Table 5.18 Power Plant Performance Summary	140
Table 5.19 Power Plant Emissions – Low Sulfur PRB	140
Table 5.20 Power Plant Emissions – High Sulfur Bit	141
Table 5.21 O ₂ -Fired Retrofit Cost Estimate – Low Sulfur Coal	141
Table 5.22 O ₂ -Fired Retrofit Cost Estimate – High Sulfur Coal	142
Table 5.23 CO ₂ Rich Oxy-Fuel Flue Gas	142
Table 5.24 VPSA Feed Using Low Purity CPU	143
Table 5.25 VPSA Feed Using High Purity CPU	144
Table 5.26 Overall Performance – Air Firing of Low Sulfur Coal	146
Table 5.27 Overall Performance – Oxy Firing of Low Sulfur Coal with Conventional CPU	147
Table 5.28 Overall Performance – Oxy Firing of Low Sulfur Coal with NZE CPU	148
Table 5.29 CPU Feed – Low Sulfur Coal with Conventional CPU	148
Table 5.30 CPU Feed – Low Sulfur Coal with NZE CPU	149
Table 5.31 Purified CO ₂ from Conventional CPU (Low Sulfur)	150
Table 5.32 Purified CO ₂ from NZE CPU (Low Sulfur)	150
Table 5.33 Atmospheric Emissions – Air Firing of Low Sulfur Coal	151
Table 5.34 Atmospheric Emissions – Conventional CPU (Low Sulfur Coal)	152
Table 5.35 Atmospheric Emissions – NZE CPU (Low Sulfur Coal)	153
Table 5.36 Overall Performance – Air Firing of High Sulfur Coal	154
Table 5.37 Overall Performance – Oxy Firing of High Sulfur Coal with Conventional CPU	154
Table 5.38 Overall Performance – Oxy Firing of High Sulfur Coal with NZE CPU	155
Table 5.39 CPU Feed – High Sulfur Coal with Conventional CPU	155
Table 5.40 CPU Feed – High Sulfur Coal with NZE CPU	156
Table 5.41 Purified CO ₂ from Conventional CPU (High Sulfur)	157
Table 5.42 Purified CO ₂ from NZE CPU (High Sulfur)	157
Table 5.43 Atmospheric Emissions – Air Firing of High Sulfur Coal	158
Table 5.44 Atmospheric Emissions – Conventional CPU (High Sulfur Coal)	158
Table 5.45 Atmospheric Emissions – NZE CPU (High Sulfur Coal)	159
Table 5.46 Economic Estimates for Greenfield Plants with Low Air Ingress – Low Sulfur Coal	161
Table 5.47 Economic Estimates for Greenfield Plants with Low Air Ingress – High Sulfur Coal	162
Table 5.48 Economic Estimates for Relative Impact of NZE CPU Components	165
Table 5.49 Economic Estimates for Old Plants with High Air Ingress – Low Sulfur Coal	167
Table 5.50 Economic Estimates for Old Plants with High Air Ingress – High Sulfur Coal	169
Table 5.51 Economic Estimates for Greenfield Plants Using the Supercritical Steam Cycle	170
Table 5.52 Economic Estimates for Greenfield Plants Using the Ultrasupercritical Steam Cycle	172
Table 5.53 Impact of Steam Cycle Efficiency on COE and CO ₂ Capture Costs	173
Table 5.54 Economic Estimates for Comparison of Partial Condensation CPU to Distillation CPU	175
Table 5.55 Impact of Partial or Complete FGD Elimination	176
Table 5.56 Economic Estimates for Evaluation of Savings if FGD is Eliminated	178
Table 5.57 Economic Estimates for Comparing New Plant without CCS to Old Plants with CCS	179
Table 5.58 Coal Composition for Pilot Demonstration CPU	189
Table 5.59 Stream Summary – Partial Condensation CPU	190
Table 5.60 Stream Summary – Distillation CPU	191
Table 5.61 Capex of Pilot CPU Demonstration Facility	191
Table 5.62 Operating Scenario for Pilot CPU Demonstration Facility	192
Table 5.63 Opex of Pilot CPU Demonstration Facility	192
Table 5.64 Cost Summary by Year for Pilot CPU Demonstration Facility	192

Executive Summary

The objectives of this project were to carry out an experimental program to enable development and design of near zero emissions (NZE) CO₂ processing unit (CPU) for oxy-combustion plants burning high and low sulfur coals and to perform commercial viability assessment. The NZE CPU was proposed to produce high purity CO₂ from the oxycombustion flue gas, to achieve > 95% CO₂ capture rate and to achieve near zero atmospheric emissions of criteria pollutants. Conventional CPU includes the steps of cooling, compression, pretreatment and final purification in coldbox. In the conventional process, almost all the SO_x and a large portion of NO_x contained in the flue gas end up in the purified CO₂ stream. High air ingress in the existing plants limits the amount of CO₂ that can be recovered using a conventional process (cold box alone) to < 80%. To overcome these limitations, a NZE CPU with additional processing steps for SO_x/NO_x removal and recovery of CO₂ from coldbox vent stream was proposed.

Two SO_x/NO_x removal technologies were proposed depending on the SO_x levels in the flue gas. The activated carbon process was proposed for power plants burning low sulfur coal and the sulfuric acid process was proposed for power plants burning high sulfur coal. By carrying out these unit operations at high pressure within CPU, it was envisioned that capital costs would be reduced while achieving very low levels of SO_x and NO_x in the CO₂ stream. For plants burning high sulfur coal, the sulfuric acid process would convert SO_x and NO_x in to commercial grade sulfuric and nitric acid by-products, thus reducing operating costs associated with SO_x/NO_x removal. For plants with existing FGD and SCR, the operating cost savings could be realized by shutting down those units. For plants burning low sulfur coal, investment in separate FGD and SCR equipment for producing high purity CO₂ would not be needed.

To overcome the CO₂ recovery limitation, a hybrid process that combines cold box and VPSA (vacuum pressure swing adsorption) was proposed. In the proposed hybrid process, up to 90% of CO₂ in the cold box vent stream would be recovered by CO₂ VPSA and then it would be recycled and mixed with the flue gas stream upstream of the compressor. The overall recovery from the process will be > 95%.

Activated carbon process tests were carried out first in a single bed bench-scale unit operating in a batch mode and subsequently in a dual bed continuous unit. This process was able to achieve simultaneous SO_x and NO_x removal in a single step. The removal efficiencies were >99.9% for SO_x and >98% for NO_x. With 450 ppm SO_x and 200 ppm NO_x in the feed, the process was able to achieve < 5ppm for both SO_x and NO_x in the purified flue gas. This process was able to effectively remove up to 4000 ppm SO_x from the simulated feeds corresponding to oxyfuel flue gas from high sulfur coal plants. In summary, the activated carbon process exceeded performance targets for SO_x and NO_x removal efficiencies and it was found to be suitable for power plants burning both low and high sulfur coals. In the longevity tests performed on a batch unit, the retention capacity could be maintained at high level over 20 cycles, however, in similar test on a continuous unit, the retention capacity of carbon for SO_x and NO_x reduced significantly over a 40 day period of operation. These contradictory results indicate the need for optimization of adsorption-regeneration cycle to maintain long term activity of activated carbon material at a higher level and thus minimize the capital cost of the system.

The VPSA process was tested in a pilot unit. It could recover > 95% of CO₂ at >80% purity (by vol.) from simulated cold box feed streams. The VPSA process and system were optimized by performing techno-economic analysis. The six-bed VPSA process with adsorbent Q and one stage of vacuum pump were found to be optimum. The optimum CO₂ purity from VPSA was found to be ≥80% (by vol.) in order to minimize processing costs in CPU. Based on these results, process simulations were performed for the NZE CPU. The overall CO₂ recovery was projected to be >99% for plants with low air ingress (2%) and >97% for plants with high air ingress (10%). Based upon limited data on the bench-scale unit, it was concluded that any residual SO_x and NO_x in the cold box vent stream did not affect the performance of

the VPSA adsorbent. In parallel to the test program, an attempt was made to develop a simulation tool that can be used to design and predict the performance of the VPSA process. However, the simulation tool could not achieve good match with the pilot test data.

Sulfuric acid process did not meet the performance expectations. Although it could achieve high SO_x (>99%) and NO_x (>90%) removal efficiencies, it could not produce by-product sulfuric and nitric acids that meet the commercial product specifications. A key stumbling block for the process was its inability to remove NO_x from the produced sulfuric acid. The acid produced from the process was predicted to contain roughly 2.5wt% NO_x, which is a very high level of NO_x impurity compared to the NO_x impurity spec in commercial grade acid of <5ppmw. The sulfuric acid will have to be disposed of by neutralization, thus lowering the value of the technology to same level as that of the activated carbon process. Although irrelevant now, other factor that would have reduced the value of sulfuric acid technology is a 4000 ppm threshold for SO_x levels allowed in the current generation of boilers. To keep SO_x below 4000 ppm in the recirculated flue gas, >60% SO_x would have to be removed by FGD for plants burning high sulfur coal. As a result, potential for saving operating costs for the sulfuric acid would have been reduced significantly anyway. Since activated carbon process was shown to remove SO_x from flue gas obtained from high sulfur coal plants and since it is a less complex process than the sulfuric acid process, it was decided to discontinue any further efforts on sulfuric acid process after the work proposed in the project was completed.

The commercial viability assessment for retrofitting existing and new power plants with oxyfuel technology was carried out. Foster Wheeler performed power plant performance assessment and concluded that the retrofit is technically feasible. Their study pointed out that the recirculated flue gas stream used as 'primary air' must be treated in FGD for SO_x removal and the SO_x level in the boiler must be below 4000 ppm. The cost of retrofitting boiler island of a 460 MW power plant with oxyfuel technology was estimated to be \$95 MM to \$99 MM. Praxair performed economic feasibility study using the DOE's guidelines for 550 MW net power plants. The efficiency penalty for 99.3% CO₂ capture was estimated to be ~8.0 percentage points assuming advanced air separation unit (ASU) and CPU designs for parasitic load estimates. The cost of electricity (COE) for existing plant without CCS (CO₂ capture and storage) increased from \$35/MWh to \$96/MWh for CCS with conventional CPU and to \$98/MWh for CCS with NZE CPU. The CO₂ avoided costs for NZE CPU and conventional CPU were \$65/ton and \$85/ton, respectively. Large reduction in CO₂ mitigation cost for NZE CPU compared to conventional CPU were due to higher capture rate and savings in capital investment for FGD and SCR. For greenfield plant, the COE increased from \$82/MWh to \$148/MWh for conventional CPU and \$146/MWh for NZE CPU. The CO₂ avoided costs were ~12% lower for NZE CPU at \$63/ton compared to \$72/ton for conventional CPU.

For scale-up towards commercialization, about one year of further development is recommended for the activated carbon process with the emphasis on adsorption-regeneration cycle optimization. Next step for scaling up this technology is a demonstration of entire NZE CPU at a 20 tpd (tons per day) scale. Cost estimation for this demonstration was estimated with U. of Utah as a potential host site. The total capital cost for a demonstration unit was estimated to be ~\$15 MM and the operating costs for a three year operation were estimated to be ~\$16 MM.

In summary, as a result of this project, we now have developed one technology option for NZE CPU based on the activated carbon process and coldbox-VPSA hybrid process. Although proposed for only low sulfur coal plants, activated carbon process is projected to work for high sulfur coal plants as well. The NZE CPU technology is projected to achieve near zero stack emissions, produce high purity CO₂ relatively free of trace impurities and achieve ~99% CO₂ capture rate while lowering the CO₂ capture costs.

Task 1 – Program Management

Technology Overview

Oxyfuel combustion is one of the leading options being considered for capturing and sequestering CO₂ from coal-fired power plants. A schematic diagram of a coal power plant is shown in Figure 1.1. In the oxyfuel technology, coal plant is fitted with air separation unit (ASU) and CO₂ processing unit (CPU) as shown in Figure 1.2 such that boiler and steam cycle process conditions remain similar to those in the air-fired operation. Coal is combusted using a mixture of oxygen and recirculated flue gas as an oxidant to produce flue gas consisting mainly of CO₂ and water vapor. The CO₂ concentration in the flue gas increases from ~14% (by vol. on a dry basis) in air-fired operation to ~80% in the oxy-fired operation. The CO₂-rich flue gas from oxy-coal boiler can be easily compressed and purified using a conventional CPU technology (Figure 1.3) to produce >95% CO₂ at > 2000 psia pressure needed for sequestration.

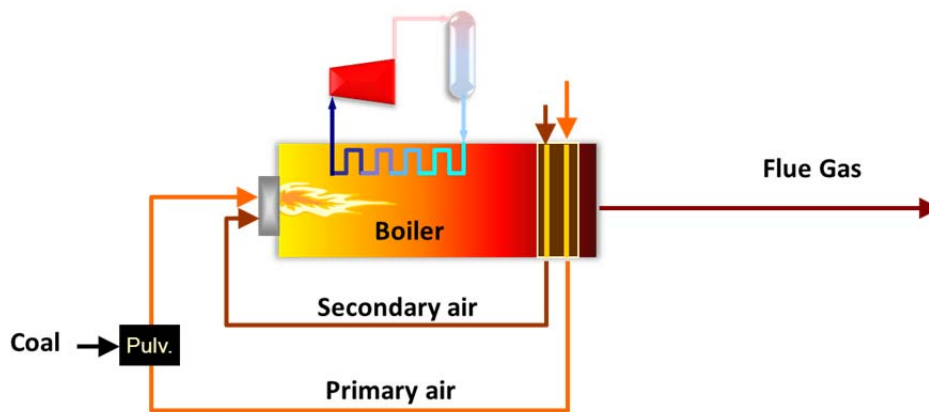


Figure 1.1 Schematics of Coal Power Plant Without CCS

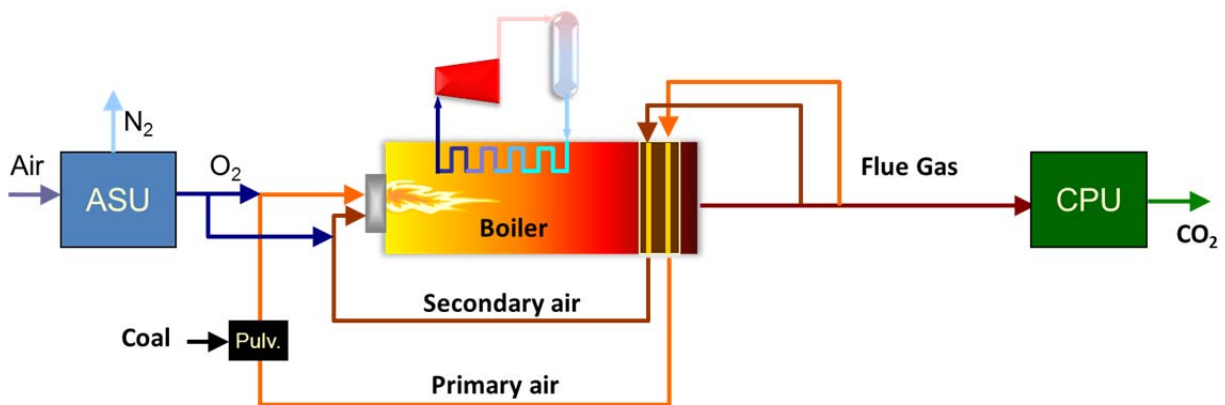


Figure 1.2 Schematics of Oxy-Coal Power Plant With CCS

The conventional CPU process suffers from several limitations when it comes to retrofitting oxyfuel technology to old existing plants. The CO₂ capture rates are limited to < 80% for old plants with high air ingress (~10% of total flue gas volume). A conventional CPU has no unit operations for the purpose of removing SO_x, NO_x and CO from the flue gas. These compounds are typically distributed between the process condensate, the CPU vent and the purified CO₂. To produce CO₂ stream relatively free of SO_x

and NO_x from a conventional CPU, they must be removed in the boiler island using the FGD and SCR units.

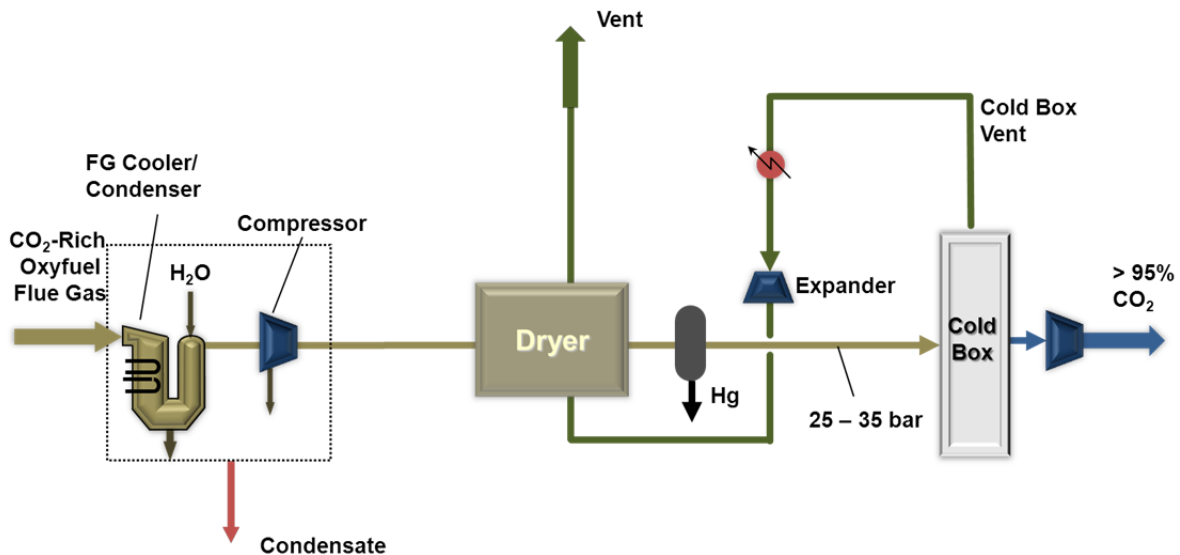


Figure 1.3 Schematics of Conventional CO₂ Processing Unit

The oxyfuel technology presents an excellent opportunity for achieving near zero emissions from the existing PC (pulverized coal) power plants. The volume of net flue gas from boiler that needs to be processed is reduced by a factor of four to five (on a dry basis) due to elimination/reduction of nitrogen from combustion. This reduced volume of CO₂-rich flue gas has to be compressed to 25 to 35 bar (a) for purification, thus further reducing the actual volume of flue gas by a factor of 25 to 35. If the equipment for removing trace impurities (SO_x, NO_x and Hg) are installed downstream of the flue gas compressor, the capital investment could be significantly reduced compared to that for the air-fired operation. Furthermore, by processing the entire volume of flue gas in the CO₂ purification unit, it is possible to remove and concentrate the trace impurities in the solid and liquid waste streams and to produce a vent stream with near zero emissions and a high purity CO₂ relatively free of trace impurities.

Praxair proposed two near zero emissions (NZE) CPU technology concepts that overcome the limitations of conventional CPU while leveraging the synergies offered by the high pressure operation of CPU and reduced flue gas volume. Schematic diagrams of these two concepts are shown in Figures 1.4 and 1.5. Details for these processes are also published in the patents [1, 2] and a patent application [3]. Difference in two concepts is the process used for SO_x and NO_x removal. Two SO_x/NO_x removal technologies were proposed for different SO_x levels in the flue gas. The activated carbon process was proposed for power plants burning low sulfur coal and the sulfuric acid process was proposed for power plants burning high sulfur coal. The sulfuric acid process would convert SO_x and NO_x in to commercial grade sulfuric and nitric acid by-products, while the activated carbon process would produce dilute acid stream that must be disposed of. Common elements in the two concepts are coldbox-VPSA (vacuum pressure swing adsorption) hybrid purification process for achieving high CO₂ capture rate and a catox (catalytic oxidation) unit for minimizing CO emissions to atmosphere. The VPSA captures and recycles CO₂ from the coldbox vent that would otherwise be vented to atmosphere and increases CO₂ capture rates to ~99%. The catox unit eliminates CO emissions to air by converting CO to CO₂. The catox unit was not shown in the original proposal. Since then, Praxair has promoted near zero emissions technology to include the catox unit. As a result, catox unit has been considered as an integral part of the NZE CPU in the present report.

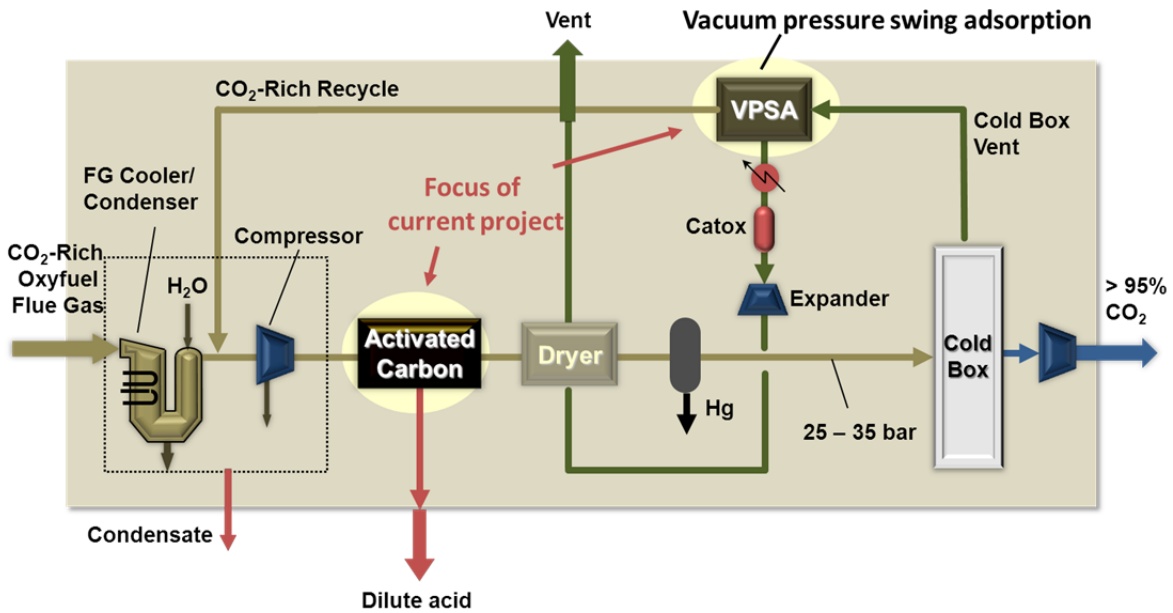


Figure 1.4 Schematics of NZE CPU Based on Activated Carbon Process

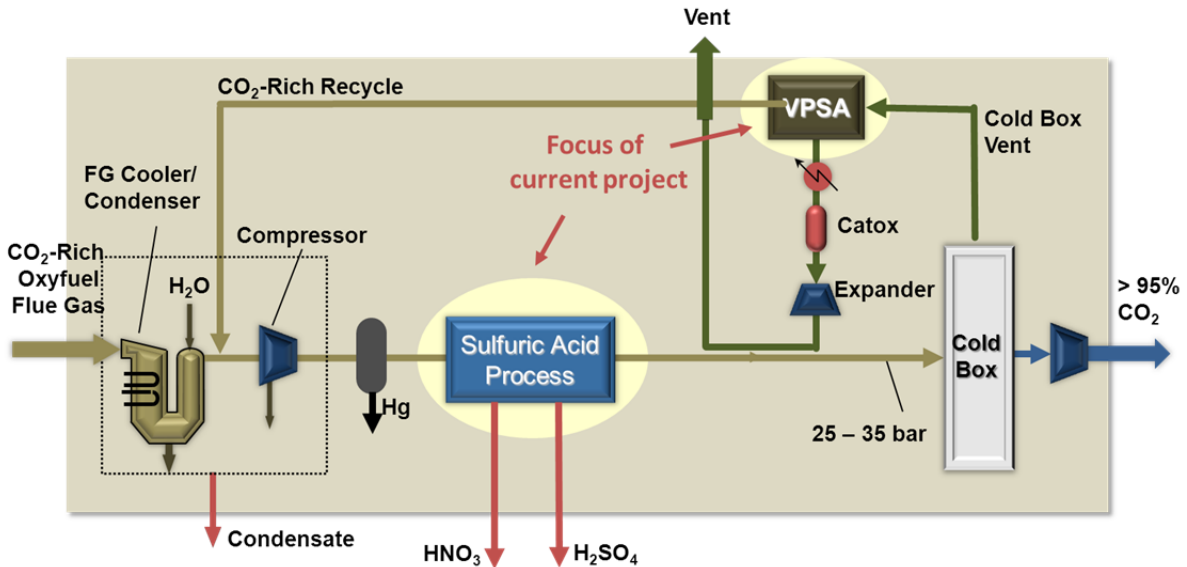


Figure 1.5 Schematics of NZE CPU Based on Sulfuric Acid Process

The NZE CPU technology was projected to reduce emissions of SO_x and Hg by >99% and NO_x emissions by >95% compared to an air-fired power plant. The benefits of the technology include mitigation of air ingress problem, capital and operating cost savings for SO_x and NO_x removal, reduction in CO₂ capture cost and production of high purity CO₂ stream for sequestration. These benefits will translate to lower cost of electricity for power plants with CO₂ capture.

Project Plan

Objectives

The overall objective of the project was to reduce the cost of CO₂ capture and achieve >95% CO₂ recovery with oxy-combustion in existing PC (pulverized coal) power plants while significantly reducing the atmospheric emissions of criteria pollutants and producing purified CO₂ stream containing very low concentrations of trace impurities for sequestration or EOR (enhanced oil recovery). These objectives would be accomplished by integrating a unique combination of existing chemical processing technologies for contaminant removal (NO_x, SO_x, Hg) with Praxair’s advanced CO₂ compression and purification concept. Specific tasks were to carry out an experimental program to enable development and design of separate contaminant removal processes for plants burning high and low sulfur coals and high CO₂ recovery process and to perform commercial viability assessment. Key benefits include high CO₂ recovery even from plants with high air ingress and production of saleable sulfuric acid for plants burning high sulfur coal. The % increase in cost of electricity (COE) for retrofit plants was projected to be in 10 - 35% range when compared to a new coal fired power plant without CO₂ capture.

Scope of Work

The project was divided into five major tasks: a project management Task (1), three Tasks (2, 3 and 4) on experimental programs and a Task (5) on assessing commercial viability. Two of the experimental programs were focused on SO_x/NO_x removal from high sulfur (Task 2) and low sulfur (Task 3) coal oxy-combustion flue gases. Third experimental program was directed towards developing VPSA technology (Task 4), which will enable high CO₂ recovery from a coldbox-VPSA hybrid process. The commercial viability assessment (Task 5) comprised of techno-economic feasibility, operability and market analyses and it involved three other participants – Foster Wheeler, AES and WorleyParsons.

Statement of Work in Brief

Table 1.1 shows a revised list of milestones that was used for measuring the progress of the project.

Table 1.1 Milestones Log

#	MILESTONES	Project Year 1				Project Year 2				Project Year 3			
		Q1	Q2	Q3	Q4	Q1	Q2	Q3	Q4	Q1	Q2	Q3	Q4
M1	2.1 Test Unit for Task 2 Operational		X										
M2	3.2 Test Unit for Task 3 Operational			X									
M3	4.3 Lab Unit for Task 4 Operational			X									
M4	2.3 NO _x Oxidation Catalyst Selection				X								
M5A	5.2 Power Plant Performance Report – Low S coal				X								
M5B	5.2 Power Plant Performance Report – High S Coal					X							
M6	2.2 SO _x /NO _x Removal Target Reached							X					
M7	2.3 By-Product Purity Achieved							X					
M8	3.3 SO _x /NO _x Removal Target Reached						X						
M9	4.3 Separation Agent Selection for Pilot Unit						X						
M10	4.4 Pilot Test Unit Operational						X						
M11	2.5 Process for High Sulfur Coal Defined									X			
M12	5.3 By-Product Commercial Viability									X			
M13	4.4 High CO ₂ Recovery Process Definition										X		
M14	5.4 Cost of Electricity Targets Achieved											X	
M15	5.6 Pilot Demonstration Plan												X
M16	3.5 Continuous Unit Longevity Tests Completed										X		

The following is a brief statement of work extracted from a detailed year by year statement of work submitted in the proposal.

Task 1.0 – Project Management

Provide a single point of contact with DOE for contractual matters and ensure compliance with contract terms and conditions. Assign necessary skills and resources and coordinate activities with participants to ensure that progress remains on schedule and that the milestones (Table 1.1) are delivered on time. Keep DOE informed of the progress on an ongoing basis and prepare reports described under ‘Deliverables’. Adjust the plan as necessary based on the results.

Task 2.0 – SO_x/NO_x/Hg Removal for High Sulfur Coal

Conduct bench-scale experiments for key unit operations of the process that removes SO_x/NO_x/Hg from flue gas obtained by oxy-combustion of high sulfur coal and produces saleable H₂SO₄ and HNO₃. Prove the concept for meeting performance targets and collect data needed for system design.

Subtask 2.1 Bench-Scale Test Unit.

Fabricate and install a bench-scale experimental unit (Milestone **M1**) based on a single vessel capable of testing multiple unit operations in subtasks 2.2 and 2.3.

Subtask 2.2 SO_x/NO_x Removal Tests

Perform experiments at elevated pressures (100 – 300 psia) to collect the required equilibrium vapor pressure data and performance parameters for two NO_x removal unit operations to achieve <50 ppm NO_x in flue gas. Determine optimal conditions for conversion of SO_x into by-product and conclude SO_x/NO_x removal tests upon achieving the performance targets (Milestone **M6**).

Subtask 2.3 NO Oxidation Tests

Screen catalysts using a small batch reactor for selection of the most efficient NO oxidation catalysts (Milestone **M4**).

Subtask 2.4 By-Product Purification

Define an additional unit operation necessary for removing residual NO_x from by-product (Milestone **M7**).

Subtask 2.5 Mercury Removal Research

Collect information on a low pressure version of the mercury removal process from literature. Determine the necessary operating conditions and mercury removal efficiencies from high pressure oxy-coal combustion flue gas, for use in process simulation. Upon completion of this subtask, deliver a report on the SO_x/NO_x/Hg removal process for high sulfur coal (Milestone **M11**).

Task 3.0 – SO_x/NO_x/Hg Removal for Low Sulfur Coal

Conduct bench-scale experiments for key unit operations of the process that removes SO_x/NO_x from flue gas obtained by oxy-combustion of low sulfur coal with the goal of achieving performance targets (Table 1.2). Define unit operations based on conventional technologies for neutralizing dilute acids produced in the process and removing mercury and any residual NO_x from flue gas.

Subtask 3.1 SO_x/NO_x Removal Material Selection

Review literature and contact vendors to identify suitable materials for SO_x/NO_x removal. Obtain samples of potential materials and test them in a laboratory-scale apparatus to screen them based on their

capacity and selectivity of SO_x/NO_x capture from the flue gas stream. Select up to three top performing materials for further testing in a bench-scale unit.

Subtask 3.2 Bench-Scale Test Unit

Fabricate and install a bench-scale test unit based on a single vessel for testing multiple unit operations of the process at pressures expected in the flue gas purification process (Milestone **M2**).

Subtask 3.3 SO_x/NO_x Removal Tests

Test top performing materials selected in subtask 3.1 in a bench-scale unit. Estimate SO_x/NO_x removal effectiveness and utility consumption. Perform tests to select the catalyst based on the durability of catalyst to maintain capacity and activity. Select the best performing materials for process design with the goal of achieving desired SO_x removal and maximum possible NO_x removal (Milestone **M8**).

Subtask 3.4 Hg and Residual NO_x Removal

Define unit operations based on conventional technologies for removal of mercury and residual NO_x for process design activity.

Subtask 3.5 Continuous Operation Unit

Design a dual bed activated carbon continuous operation unit. Complete longevity tests (24 hours/5 days continuous operation repeated over a two months period) in Q3 of Year 3 (Milestone **M16**). Upon completion of this subtask, deliver a topical report on the SO_x/NO_x/Hg removal process for low sulfur coal in Q4 of Year 4.

Task 4.0 – High CO₂ recovery

Subtask 4.1 Separation Agent Identification

Identify top performing separation agents for further testing in Subtask 4.3.

Subtask 4.2 Simulation Tool

Develop a process simulator to simulate the VPSA processes that can produce CO₂ at different purities. Upgrade the simulator when data from laboratory testing and large unit testing become available.

Subtask 4.3 Bench-Scale Tests

Design, construct and commission a bench-scale test unit to process ~ 50 SCFH of feed gas (Milestone **M3**). Test promising separation agents identified from Subtask 4.1. Select two separation agents and several process configurations based on experimental data and results from simulator obtained in Subtask 4.2 (Milestone **M9**).

Subtask 4.4 Continuous Operation Tests

Design, construct and commission the unit with the capability to operate 24/7 to study the complete process (Milestone **M10**). Continue experiments on the pilot test unit for various process configurations. Achieve steady state operation and collect a single data point for each experiment. Analyze data and optimize the process with respect to CO₂ product purity, CO₂ recovery and CO₂ productivity. Deliver a final report on optimized high CO₂ recovery process (Milestone **M14**).

Task 5.0 – Commercial Viability Assessment

Perform techno-economic evaluation to determine the cost of electricity with CO₂ capture and storage for proposed processes relative to existing concepts. Assess operability and ease of integration with the power plants.

Subtask 5.1 Process and Systems Engineering

Define existing power plant cases based on high and low sulfur coal with input from Foster Wheeler and AES. Perform process simulations for the NZE CPUs. Develop heat and mass balances and estimate utilities. Size equipment used in both flue gas purification processes and estimate costs. Estimate equipment cost deltas for different process configurations.

Subtask 5.2 Power Plant Performance

Foster Wheeler to estimate performance of the air and oxyfuel PC power plants burning low and sulfur coals. Define flue gas conditions to enable design of flue gas purification process in Subtask 5.1. Prepare topical report (Milestone **M5**).

Subtask 5.3 By-Product Commercial Viability

With input from WorleyParsons, evaluate technical feasibility of the sulfuric acid process for high sulfur coal. Complete a revised commercial viability assessment and deliver a final report prepared by WorleyParsons in Q1 of Year 3 (Milestone **M12**).

Subtask 5.4 Economic Feasibility

Perform an economic feasibility evaluation of power plants with and without CO₂ capture. Estimate costs based on published reports and Praxair's internal studies. Determine CO₂ recovery, the cost of electricity increase for CCS and the cost of CO₂ capture. Carry out a detailed economic feasibility study based on DOE's guidelines. Determine the impact of the proposed technologies on the overall plant efficiency and on the COE. Determine the CO₂ recovery, the cost of electricity increase for CCS and the cost of CO₂ capture. Estimate COE for various process configurations tested in Task 4 and determine optimum CO₂ purity for the process developed in Task 4 (Milestone **M14**).

Subtask 5.5 Integration and Operability

Obtain consultation from AES on practical aspects of integrating flue gas purification process into a power plant.

Subtask 5.6 Plan for Pilot Scale Demonstration

Assuming successful outcome in achieving DOE's goals, prepare a plan for pilot scale demonstration (Milestone **M15**) including the scope of demonstration, location, scale of operation, timeline for operation and a preliminary budget but excluding a detailed engineering study.

Performance Targets

The performance targets for CO₂ quality and emissions reduction are shown in Table 1.2.

Table 1.2 Environmental Performance

Integrated Acid Process for High Sulfur Coal					
		% Distribution of components Among CO₂ and vent			
Component	CO ₂ Quality	Purified CO ₂ Stream	Vent to Atmosphere	% Removal/ Reduction	Disposition of impurities
Integrated Acid Process for High Sulfur Coal					
CO ₂	> 96%	96%	4%	96%	
SO _x	<100 ppm	<5%	Negligible	>99%	Product H ₂ SO ₄
NO _x	<20 ppm	<5%	<5%	>90%	Product HNO ₃
Hg	Negligible	Negligible	Negligible	>99%	Disposable HgSO ₄
Activated Carbon Based Process for Low Sulfur Coal					
CO ₂	> 96%	96%	4%	96%	
SO _x	<100 ppm	<5%	Negligible	>95%	Gypsum waste
NO _x	<20 ppm	<5%	<5%	>90%	Dilute HNO ₃ waste
Hg	Negligible	Negligible	Negligible	>99%	On disposable carbon

Project Execution – Milestones

Table 1.3 shows final milestones status of the project.

Table 1.3 Final Milestones Status

#	MILESTONES	Planned Start Date	Planned End Date	Actual Start Date	Actual End Date
M1	2.1 Test Unit for Task 2 Operational	1/1/09	6/30/09	1/1/09	7/27/09
M2	3.2 Test Unit for Task 3 Operational	4/1/09	9/30/09	1/1/09	9/30/09
M3	4.3 Lab Unit for Task 4 Operational	4/1/09	9/30/09	1/1/09	9/1/09
M4	2.3 NOx Oxidation Catalyst Selection	7/1/09	12/31/09	8/1/09	12/31/09
M5A	5.2 Power Plant Performance Report Low Sulfur Coal	7/1/09	12/31/09	7/1/09	12/14/09
M5B	5.2 Power Plant Performance Report High Sulfur Coal	1/1/10	6/30/10	1/1/10	7/20/10
M6	2.2 SOx/NOx Removal Target Reached	7/1/09	12/31/10	10/1/09	12/30/10
M7	2.3 By-Product Purity Achieved	4/1/10	12/31/10	4/1/10	12/30/10
M8	3.3 SOx/NOx Removal Target Reached	10/1/09	9/30/10	10/1/09	8/31/10
M9	4.3 Separation Agent Selection for Pilot Unit	10/1/09	9/30/10	10/1/09	7/15/10
M10	4.4 Pilot Test Unit Operational	7/1/09	9/30/10	7/1/09	7/29/10
M11	2.5 Process for High Sulfur Coal Defined	7/1/10	3/31/11	7/1/10	4/29/11
M12	5.3 By-Product Commercial Viability	10/1/09	3/31/11	10/6/09	4/29/11
M13	4.4 High CO ₂ Recovery Process Definition	1/1/11	9/30/11	1/3/11	10/13/11
M14	5.4 Cost of Electricity Targets Achieved	1/1/11	12/31/11	11/9/10	12/21/11
M15	5.6 Pilot Demonstration Plan	7/1/11	12/31/11	9/1/10	12/20/11
M16	3.5 Continuous Unit Longevity Tests Completed	5/1/11	9/30/11	12/28/11	3/16/12

All the tasks associated with the proposed milestones were completed. Detailed discussion on the outcome by Task is described below.

Task 2 SOx/NOx/Hg Removal for High Sulfur Coal

The objective of Task 2 of this project was to evaluate the sulfuric acid process for SOx, NOx and Hg removal from flue gas produced by burning high sulfur coal in oxy-combustion power plants. The goal of the program was not only to investigate a new method of flue gas purification but also to produce useful acid byproduct streams as an alternative to using a traditional FGD and SCR for flue gas processing.

In Q1 2010, it was recognized that the Task 2 progress had fallen behind the original proposal schedule. A number of reasons such as complexity of handling concentrated acid, operational issues identified after commissioning and changes in lab technicians contributed to this delay. With the approval of the DOE manager, the affected Task 2 milestones were reset for measuring progress going forward. Although some of the individual milestones were set back by three quarters, the overall Task 2 completion date was delayed by only four months. Instead of completion in December 2010, Task 2 (Milestone M11) was completed in April 2011.

Milestone M1 – Test Unit for Task 2 Operational

A bench-scale unit for testing the sulfuric acid process was successfully designed and constructed. The unit was designed around a single gas/liquid contacting column with provisions for supplying sulfuric

acid and SO_x/NO_x containing flue gases at different temperatures, pressures and compositions. The process conditions in the column could be varied to simulate various unit operations of the sulfuric acid process. The test unit allowed us to collect data necessary to evaluate technical feasibility of the process as discussed below.

Milestone M1 was completed one month behind schedule (in July 2009) due to resource constraints, higher than anticipated complexity of the test unit and extra effort needed to ensure safe handling of hazardous chemicals. The delay in this milestone did not impact the overall project schedule.

Milestone M4 – NO_x Oxidation Catalyst Selection

Milestone M4 dealt with the catalyst selection for NO_x oxidation step in the sulfuric acid process of Task 2. After sulfuric acid removes NO_x from flue gas, a catalytic reactor in the process was proposed to simultaneously oxidize NO to NO₂ and strip NO₂ from the acid. The test results showed low activity for NO_x removal from NO_x contaminated sulfuric acid. Consequently, this unit operation was dropped from the sulfuric acid process.

Milestone M4 was completed on schedule in December 2009.

Milestone M6 – SO_x/NO_x Removal Target Reached

Various unit operations of the sulfuric acid process were tested under this milestone. They included NO_x stripper (removal of NO_x from NO_x-rich acid), SO₂ oxidation reactor (removal of SO_x from flue gas) and NO_x absorber (removal of NO_x from flue gas). Catalytic NO_x oxidation reactor was not tested due to unsuccessful results in Milestone M4. The results showed that both SO_x and NO_x could be effectively removed from the flue gas by sulfuric acid; however, it was not feasible to strip NO_x from the acid. Inability to remove NO_x from the sulfuric acid was a key stumbling block for the process. Process simulations showed that accumulation of NO_x in the sulfuric acid would reduce the NO_x removal efficiency to only 73%. It also showed that the residual NO_x in the flue gas would be in the form of NO₂. It is possible to add a water scrubber to remove NO₂ from flue gas and produce dilute nitric acid. This additional processing step will increase NO_x removal efficiency to >95%. There was no negative impact of NO_x accumulation on SO_x removal from flue gas and SO_x removal efficiency of >99% could be achieved. Thus, from flue gas purification perspective, this technology could meet SO_x and NO_x removal targets. However, the potential value of technology could not be realized as NO_x-contaminated acid could not be sold for revenue.

Milestone M6 was completed in Q4 2010 as proposed in the revised schedule.

Milestone M7 – By-Product Purity Achieved

Based on the result in Milestone M4, the NO_x stripping reactor was removed from the process, making old Milestone M7 (NO Oxidation Test Complete) unnecessary. This possibility was considered when the proposal was written and Task 2.4 was included to address this concern. The new milestone M7 was proposed to find alternate acid purification method. Task 2.4 was now needed to determine how the process needs to change for removal of NO_x from acid and/or from the process in general. After investigating several options, it was concluded that none of the alternative methods would be economically attractive.

Milestone M11 – Process for High Sulfur Coal Defined

During the project two main constraints were identified that limit the ability of the process to achieve the project goals. 1) Due to boiler island corrosion issues >2/3^{rds} of the fired sulfur must be removed in the boiler island with the use of an FGD. 2). A suitable method could not be found to remove NO_x from the

concentrated sulfuric acid product, which limits marketability of the acid, as well as the cycle's NO_x capture rate. The acid stream would have to be disposed of by neutralization. The value of this technology would be similar to that of the activated carbon process being developed in Task 3. And by the time of this milestone, the results in Task 3 were exceeding our expectations. As a result, it was decided to discontinue further development in the acid process in Q1 2011. A topical report was prepared and submitted to the OSTI site.

Milestone M12 – By-Product Commercial Viability

WorleyParsons Canada performed the commercial viability assessment of the acid process. The capital investment estimated for the acid process was well within the estimates presented by Praxair in the original proposal to the DOE. The amount of acid that can be produced from 10 such plants could be easily absorbed by the existing market. If the sulfuric acid product could be sold at the market prices, the technology would be economically viable. After reviewing the test results and projected sulfuric acid purity, WorleyParsons indicated that the very high levels of NO_x in the product acid would make the acid unmarketable to conventional acid customers, which was the target for the produced acid due to the size of the market. The high levels of NO_x in sulfuric acid presents additional safety and corrosion issues because dilution or neutralization of acid would liberate gas phase NO_x, which would have to then be contained via an elaborate vent and scrubbing system.

Task 3 SO_x/NO_x/Hg Removal for Low Sulfur Coal

The objective of Task 3 of this project was to evaluate the activated carbon process for SO_x, NO_x and Hg removal from flue gas produced by burning low sulfur coal in oxy-combustion power plants. This technology was envisioned to replace traditional FGD and SCR for flue gas processing and save capital costs when CO₂ capture was required.

Original project plan called for testing this technology in a single column bench-scale unit operated in a batch mode. The bench-scale testing was completed in Q3 2010 as planned. Based on the encouraging results, additional scope of testing the process in a dual-bed continuous unit was added to this Task.

Milestone M2 – Test Unit (Single-Bed Unit) for Task 3 Operational

A bench-scale unit for testing the activated carbon process was successfully designed and constructed. The unit was designed around a single column containing carbon bed with provisions for supplying SO_x/NO_x containing flue gases at different temperatures, pressures and compositions and water and nitrogen for regeneration of carbon bed. It was designed to operate during the day shift

Milestone M2 was completed in Q3 2009 as planned.

Milestone M8 – SO_x/NO_x Removal Target Reached

Removal of SO_x and NO_x on activated carbon was investigated by varying key operating conditions such as temperature, pressure, inlet NO/SO₂ molar ratio, residence time and water vapor presence in the feed. Excellent simultaneous removal of SO_x and NO_x was achieved at high pressures (> 200 psia) and ambient temperatures, with efficiency higher than 99.9% for SO_x and up to 98% for NO_x. This performance was maintained when flue gas containing 4000 ppm SO_x corresponding to high sulfur coal plant was fed to the unit. In the longevity tests performed on a batch unit, the retention capacity could be maintained at high level over 20 cycles. In summary, the activated carbon process exceeded performance targets for SO_x and NO_x removal efficiencies and it was found to be suitable for power plants burning both low and high sulfur coals.

The SO_x/NO_x removal targets for the activated carbon process were achieved one month ahead of schedule in August 2010. Based on the encouraging results, additional subtask of testing the process in a continuous unit was proposed (Milestone M16).

Milestone M16 – Continuous Unit Longevity Tests Completed

A new Milestone M16 was added for Task 3 with a target of completing longevity tests on a continuous activated carbon test unit by the end of Q3 2011.

The design and development of a continuous process capable to process adequate flue gas flowrates requires additional study in order to address the challenges related to the process scale-up, optimization, material longevity and waste minimization. In order to achieve some of these objectives a dual bed continuous unit with a capacity of 0.125 TPD CO₂ was designed, built and operated. The unit was designed for an automated operation with minimum supervision. The plan was to start the unit on Monday morning and shut it down on Friday afternoon repeating adsorption and regeneration steps alternatively on both the beds and run the unit in this manner for 8 weeks (32 days of operation). After commissioning the unit, it was decided to run the unit 24/7. First such run was carried out for about 25 days. After this run, the unit was modified to improve switching of beds from adsorption to regeneration. A second run was carried out for 40 days resulting in higher than planned operating time without any interruptions. In both of these runs, activated carbon achieved excellent SO_x/NO_x removal. However, retention capacity of activated carbon for SO_x/NO_x was significantly declined. The tests conducted on a single-bed bench unit showed that retention capacity was maintained over 20 cycles. Because of these contradictory results, future work should focus on optimization of adsorption-regeneration cycle to maintain long term activity of activated carbon material at a higher level and thus minimize the capital cost of the system.

The longevity tests were begun in December 2012, which was seven months later than originally planned. Complexity of the unit and unavailability of some key resources for wiring and control system design caused delays. A no-cost time extension was obtained from the DOE to allow us to complete these tests. Milestone M16 was completed in March 2012.

Task 4 – High CO₂ Recovery

The objective in this Task was to perform experiments at bench-scale and pilot-scale to enable development and design of a “vacuum pressure swing adsorption” (VPSA) unit that will enable a coldbox-VPSA hybrid process to attain > 95% CO₂ recovery even from plants with high air ingress. Additional objective was to determine optimum CO₂ purity from VPSA that will result in maximum overall system efficiency.

All the milestones and associated tasks were met either earlier or on-time. We will now discuss some details:

Milestone M3 - Lab Unit for Task 4 Operational

The lab unit was designed to measure the equilibrium capacity of various adsorbents and to carry out cyclic tests that mimic process cycle steps of a multi-bed VPSA unit. The bench unit was designed with a small diameter (17.5 mm) short length (1524 mm) single column. This helps to speed up the experiments and test several adsorbents in a timely manner.

Work for building experimental test system began in Q1 and finished somewhat ahead of schedule in Q3 2009. After safety inspection and approval, the bench-unit for Task 4 was tested and actual tests started in early October 2009.

Milestone M9 - Separation Agent Selection for Pilot Unit

Literature search, an essential part of any R&D project was finished in Q2 2009. As a result, we identified six potential adsorbents for further testing. One process concept was also identified. The bench tests identified three adsorbents with a potential for achieving the target CO₂ recovery and CO₂ purity. Vacuum pump size and cost of adsorbent were also considered in selecting these adsorbents. After further review of safety issues, one adsorbent was dropped leaving two adsorbents for pilot testing. Along with testing the adsorbents in cyclic mode, breakthrough curves were also measured on the bench-scale test unit in preparation for milestone M13.

This milestone was finished two months ahead of the schedule in Q3 2010.

Milestone M10 - Pilot Test Unit Operational

A pilot scale test unit with 12 adsorber vessels was built. This provided us with options to test various process cycles. Each vessel is ~ 11 feet long and has an internal diameter ~ 2.5 inch. Due to early completion of bench scale test unit, the resources assigned to bench unit were diverted toward construction of the continuous operation unit in Q4 2009. Continuous operation unit was commissioned two months ahead of schedule in Q3 2010.

Milestone M13 - High CO₂ Recovery Process Definition

Three different process options based on four, five and six bed systems were tested in the pilot unit. One VPSA process with eight beds was also considered theoretically. Test data were used in performing process simulations for the entire CO₂ processing unit that included coldbox-VPSA hybrid purification process. Projected process performances from simulations and capital cost estimates for the VPSA unit were used to optimize number of beds, number of vacuum pump stages, purification costs with different adsorbents and CO₂ purity from VPSA unit. The optimized process parameters were as follows: six bed VPSA unit, one stage vacuum pump, adsorbent Q and CO₂ purity of $\geq 80\%$. In addition, adsorbent Q was found to be tolerant to SO_x and NO_x in the exposure tests carried out in bench unit.

Milestone M13 was completed in Q4 2011.

Task 5 – Commercial Viability Assessment***Milestone M5 – Power Plant Performance Report***

Foster Wheeler used a real plant that was built by them as a reference plant for performing oxyfuel retrofit evaluations. A major conclusion from their study was that oxyfuel retrofit is technically feasible for both low and high sulfur coals. They also identified following limitations of existing boiler design for SO_x levels in circulating flue gas. A portion of the recirculated flue gas that is used in place of primary air must be free of SO_x. The maximum SO_x level in the flue gas cannot exceed 4,000 ppm. These constraints lowered the value of NZE technology somewhat due to necessity of having at least a small FGD unit in the boiler island.

Milestone M5 was delayed significantly due to a delay in signing subcontract with Foster Wheeler. With agreement from the DOE project manager, the milestone date was reset for completion in Q2 2010. This revision did not impact the overall project schedule or cost. Milestone M5 by Foster Wheeler was completed and a draft report was issued in July 2010 within three weeks of the scheduled completion date. The cost estimates for oxyfuel retrofits in the boiler island were also completed in July 2010 two months ahead of the schedule.

Milestone M14 – Cost of Electricity Targets Achieved

The value of technology was evaluated for different retrofit and greenfield scenarios. The costs of electricity and CO₂ capture were estimated for conventional and near zero emissions CPUs. The highest value of the NZE technology was found to be for the existing plants with high air ingress. In this situation, NZE CPU achieved significantly higher CO₂ recovery compared to the conventional CPU. The NZE technology was also found more valuable when existing plant did not have either FGD or SCR and CO₂ purity specifications were stringent with respect to SO_x and NO_x. In this scenario, NZE CPU minimized additional capex required for achieving desired CO₂ purity.

The cost of electricity for oxycombustion plants with NZE CPU was \$2 - \$4/MWh lower than that for oxycombustion plants using conventional CPU. The CO₂ avoided costs were \$8/ton to \$21/ton lower for NZE CPU when compared to conventional CPU.

Milestone M14 was completed in Q4 2011 as planned.

Milestone M15 – Pilot Demonstration Plan

Based on the favorable results in Tasks 3 and 4, efforts for pilot demonstration were kicked off in Q3 2010 three Quarters ahead of the schedule. By then it had become apparent that one near zero emissions technology option was technically feasible. University of Utah was found to be a suitable site due to existing infrastructure for oxycombustion tests. The capacity for pilot scale demonstration was fixed at 2 MW thermal boiler and 20 tpd CO₂ CPU. The total cost of building and operating the unit for three years was estimated to be ~ \$31MM.

Milestone M15 was completed in Q4 2011 as planned.

Cost Status

The final cost status is reported in Table 1.4. The cumulative incurred costs exceeded the budget in Q4 2011. After federal share of the budget was exhausted, all the expenses over the budget were borne by Praxair. The final cost was ~7% higher than the budget forecasted in the continuation application (Q4 2010) for budget year 3. The main reasons for the budget overruns were changes in labor rates implemented in middle of 2011 and delay in completion of Task 3 by two quarters beyond the planned completion date.

Table 1.4 Final Cost Status

Reporting Quarter in 2009	Q1	Q2	Q3	Q4
Baseline cost plan (SF-424A)				
Federal Share	\$474,864	\$505,163	\$372,504	\$352,032
Non-Federal Share	\$316,576	\$336,775	\$248,336	\$234,689
Total Planned	\$791,440	\$841,938	\$620,840	\$586,721
Cumulative Baseline Cost	\$791,440	\$1,633,378	\$2,254,218	\$2,840,939
Actual Incurred Costs				
Federal Share	\$292,340	\$401,350	\$309,159	\$334,656
Non-Federal Share	\$194,894	\$267,567	\$206,106	\$223,104
Total Incurred Costs	\$487,234	\$668,916	\$515,265	\$557,760
Cumulative Incurred Costs	\$487,234	\$1,156,150	\$1,671,415	\$2,229,175
Variance				
Federal Share	-\$182,524	-\$103,813	-\$63,345	-\$17,376
Non-Federal Share	-\$121,682	-\$69,208	-\$42,230	-\$11,585
Total Variance Quarterly	-\$304,206	-\$173,022	-\$105,575	-\$28,961
Cumulative Variance Quarterly	-\$304,206	-\$477,228	-\$582,803	-\$611,764
Reporting Quarter in 2010	Q1	Q2	Q3	Q4
Baseline cost plan (SF-424A)				
Federal Share	\$227,569	\$229,207	\$229,207	\$257,607
Non-Federal Share	\$151,712	\$152,805	\$152,805	\$171,738
Total Planned	\$379,281	\$382,012	\$382,012	\$429,345
Cumulative Baseline Cost	\$3,220,220	\$3,602,232	\$3,984,244	\$4,413,589
Actual Incurred Costs				
Federal Share	\$236,416	\$189,410	\$280,377	\$244,656
Non-Federal Share	\$157,611	\$126,274	\$186,918	\$163,104
Total Incurred Costs	\$394,026	\$315,684	\$467,295	\$407,760
Cumulative Incurred Costs	\$2,623,202	\$2,938,886	\$3,406,181	\$3,813,941
Variance				
Federal Share	\$8,847	-\$39,797	\$51,170	-\$12,951
Non-Federal Share	\$5,899	-\$26,531	\$34,113	-\$8,634
Total Variance Quarterly	\$14,745	-\$66,328	\$85,283	-\$21,585
Cumulative Variance Quarterly	-\$597,018	-\$663,346	-\$578,063	-\$599,648

Table 1.4 (cont.)

Reporting Quarter in 2011	Q1	Q2	Q3	Q4
Baseline cost plan (SF-424A)				
Federal Share	\$181,579	\$161,107	\$181,190	\$68,416
Non-Federal Share	\$121,053	\$107,405	\$120,794	\$45,611
Total Planned	\$302,632	\$268,512	\$301,984	\$114,027
Cumulative Baseline Cost	\$4,716,221	\$4,984,733	\$5,286,717	\$5,400,745
Actual Incurred Costs				
Federal Share	\$374,831	\$216,696	\$259,624	\$183,519
Non-Federal Share	\$249,887	\$144,464	\$173,083	\$122,346
Total Incurred Costs	\$624,718	\$361,160	\$432,707	\$305,864
Cumulative Incurred Costs	\$4,438,659	\$4,799,818	\$5,232,525	\$5,538,390
Variance				
Federal Share	\$193,252	\$55,589	\$78,434	\$115,102
Non-Federal Share	\$128,834	\$37,059	\$52,289	\$76,735
Total Variance Quarterly	\$322,086	\$92,648	\$130,723	\$191,837
Cumulative Variance Quarterly	-\$277,563	-\$184,915	-\$54,192	\$137,645
Reporting Quarter in 2012	Q1	Q2		
Baseline cost plan (SF-424A)				
Federal Share	\$0	\$0		
Non-Federal Share	\$0	\$0		
Total Planned	\$0	\$0		
Cumulative Baseline Cost	\$5,400,745	\$5,400,745		
Actual Incurred Costs				
Federal Share	\$127,062	\$29,639		
Non-Federal Share	\$84,708	\$19,759		
Total Incurred Costs	\$211,771	\$49,398		
Cumulative Incurred Costs	\$5,750,160	\$5,799,559		
Variance				
Federal Share	\$127,062	\$29,639		
Non-Federal Share	\$84,708	\$19,759		
Total Variance Quarterly	\$211,771	\$49,398		
Cumulative Variance Quarterly	\$349,416	\$398,814		

Key Accomplishments

As a result of this project, one near zero emissions oxycombustion flue gas purification technology option has been developed. This technology is based on the activated carbon process for SOx/NOx removal and coldbox-VPSA hybrid process for achieving high CO₂ recovery. This technology will produce high purity CO₂ relatively free of trace impurities, achieve high CO₂ capture rate even from plants with high air ingress and achieve near zero stack emissions.

Environmental Performance

Environmental performance for this process is shown in Table 1.5. The activated carbon process met or exceeded the environmental performance targets for low sulfur coal plants. Although this process was proposed for only low sulfur coal plants, it met or exceeded performance targets for the high sulfur coal as well as shown in Table 1.5 for case 26.

Table 1.5 Environmental Performance

Component	CO ₂ Quality	% Distribution of components Among CO ₂ and vent			Disposition of impurities
		Purified CO ₂ Stream	Vent to Atmosphere	% Removal/Reduction	
Targets for Activated Carbon Based Process for Low Sulfur Coal					
CO ₂	> 96%	96%	4%	96%	
SO _x	<100 ppm	<5%	Negligible	>95%	Gypsum waste
NO _x	<20 ppm	<5%	<5%	>90%	Dilute HNO ₃ waste
Hg	Negligible	Negligible	Negligible	>99%	On disposable carbon
Projected performance of Activated Carbon Based Process for Low Sulfur Coal (Case 14)					
CO ₂	95.5%	99.3%	0.7%	99.3%	
SO _x	2 ppm	<0.1%	Negligible	>99.9%	47% as Gypsum waste
NO _x	11 ppm	4.7%	0.5%	94.8%	Dilute acid waste
Hg	Negligible	Negligible	Negligible	>99.9%	On disposable carbon
Projected performance of Activated Carbon Based Process w/Distillation-Based Cold Box (Case 19)					
CO ₂	>99.9%	99.0%	1%	99.0%	
SO _x	2 ppm	<0.1%	Negligible	>99.9%	47% as Gypsum waste
NO _x	12 ppm	4.5%	0.7%	94.8%	Dilute acid waste
Hg	Negligible	Negligible	Negligible	>99%	On disposable carbon
Projected performance of Activated Carbon Based Process for High Sulfur Coal (Case 26)					
CO ₂	95.3%	99.3%	0.7%	99.3%	
SO _x	4 ppm	<0.1%	Negligible	>99.9%	60% as Gypsum waste
NO _x	27 ppm	4.7%	0.5%	94.8%	Dilute acid waste
Hg	Negligible	Negligible	Negligible	>99%	On disposable carbon

Cost of Electricity

For retrofitting existing coal plants with oxycombustion, the NZE CPU technology will actually increase the cost of electricity by \$2 - \$5/MWh in comparison to a conventional CPU technology. However, the benefit of the NZE CPU is only apparent when CO₂ capture costs are compared as this technology dramatically increases the capture rates. The cost of avoided CO₂ and capture CO₂ are about 18% to 24% lower using the NZE CPU. The cost difference is due to higher CO₂ capture rate of the NZE CPU and capex reduction for SO_x/NO_x removal equipment.

For greenfield oxycombustion plants, the NZE CPU will lower COE by \$2 to \$3.5/MWh compared to conventional CPU. The cost of CO₂ capture for the NZE CPU is 11 – 12% lower compared to a conventional CPU. The relative contributions for lower capture costs achieved by NZE CPU are estimated to be ~67% from the activated carbon process and ~33% from the VPSA process.

The COE for retrofitting CCS to an existing subcritical plant is only 11% - 18% higher than the COE for a new ultrasupercritical plant without CCS.

Path to Commercialization

Current technology readiness level (TRL) defined by DOE for this project is 3. In the NZE CPU, there are two new unit operations – activated carbon process and VPSA. Other unit operations such as flue gas cooler, flue gas compressor, dryer and coldbox do not need technology development. Activated carbon

process needs about one year of further testing at bench-scale to optimize the adsorption-regeneration cycle for maintaining the activity of activated carbon at high level. The VPSA was tested in a continuous pilot-scale unit. Praxair is currently commercializing VPSA technology in a different application at 100 tpd scale. Based on that experience, VPSA is ready for commercial scale deployment even today.

After activated carbon process is optimized, next step for this technology towards commercialization is to integrate all the unit operations in a pilot-scale process development unit and test it in a real environment by connecting it to an oxy-coal boiler. Pilot demonstration plan proposed under Task 5 includes a 2 MWth oxycoal boiler and a 20 tpd NZE CPU. Cost estimation for this demonstration was estimated with U. of Utah as a potential host site. The total capital cost for a demonstration unit was estimated to be ~\$15 MM and the operating costs for a three year operation were estimated to be ~\$16 MM. Successful pilot scale demonstration will take this technology to TRL 6. At that point, Praxair will undertake a detailed engineering design of a NZE CPU for a 200+ MW power plant. If this design effort projects that the technology will meet Praxair's standards for reliability, operability and safety, then it will be considered as ready for commercial scale deployment.

Task 2 – SO_x/NO_x/Hg Removal for High Sulfur Coal

Approach

Efforts for technical and commercial feasibility assessments were divided into multiple different tasks involving experimental testing and process simulations by Praxair, power plant performance assessment by Foster Wheeler and commercial viability assessment by WorleyParsons, Canada. These activities were conducted in parallel. Initial process simulations of the sulfuric acid process were carried out with the assumption that all the sulfur in coal is converted to SO_x in the boiler and the entire amount of SO_x is present in the flue gas being sent to the CPU. Performance parameters of various unit operations in the sulfuric acid process were fixed by extrapolating literature data. The resulting process design package was used by WorleyParsons, Canada, to develop an initial commercial viability assessment.

In parallel, Praxair carried out experiments on a bench-scale system to develop performance data for various unit operations and Foster Wheeler conducted power plant simulations to define flue gas composition from an oxy-combustion power plant burning high sulfur coal. Based on these new test and simulation data, a revised process design was developed for WorleyParsons. The following paragraphs provide the detailed approach used for various tasks. In addition, technology, process and chemistry are described as background information.

Technology Description

The purpose of the Task 2 project was to investigate an alternative method of SO_x and NO_x removal from flue gas produced by burning high sulfur coal in oxy-coal power plants. The process applies to oxy-combustion flue gas which is to be further compressed and processed for CO₂ capture and sequestration (CCS). Figure 2.1 shows a high level diagram of an oxy-combustion boiler for this application where two streams of recirculated flue gas are used to moderate boiler temperature. This figure shows the primary 'air' being treated in an FGD due to material of construction issues in the coal pulverizing and conveying equipment. Secondary air is shown here as not treated, but it may be partially treated for SO_x removal depending on the allowable SO_x levels in the boiler. Combustion energy is used to generate steam and a turbine is used for power generation. The flue gas produced from the boiler island is then treated in the CO₂ processing unit (CPU) for CO₂ compression and purification.

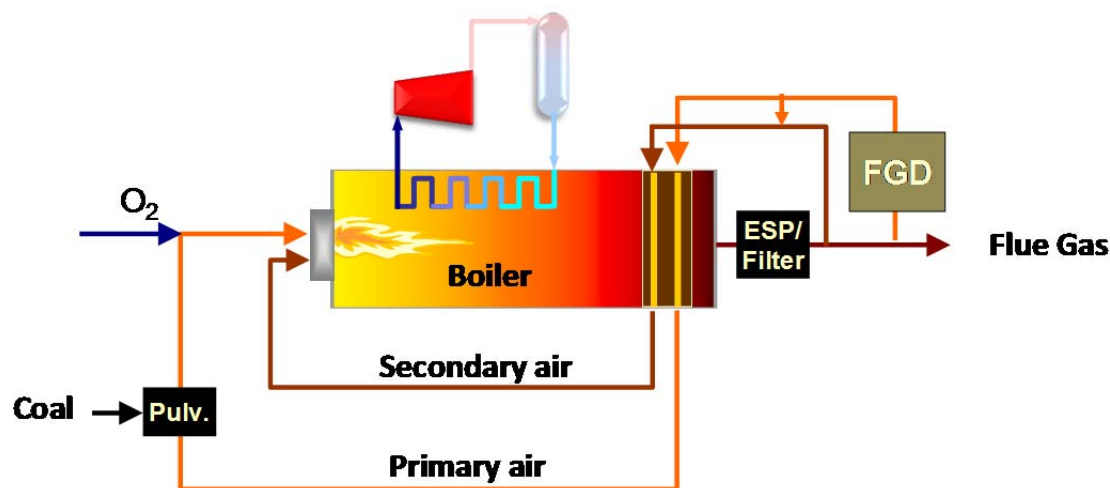


Figure 2.1 Schematic of the Oxy-coal Boiler Island

In a typical power plant SO_x is removed by reaction with lime or limestone, producing disposable gypsum using a wet or dry-FGD at atmospheric pressure. The lime/limestone reagent cost, gypsum

disposal cost, parasitic power plant load and equipment capital costs can be substantial especially in the case of high sulfur coal where all the flue gas must be treated for SO_x removal. NO_x removal is typically achieved in an SCR which requires substantial capital investment and also requires ammonia reagent.

The goal of this project was to develop a process which converts SO_x and NO_x to useful products in the compression train of an oxy-coal CPU to reduce reagent cost and parasitic power loss. Figure 2.2 shows high level diagram of the entire CPU process. Raw boiler flue gas enters the process and is cooled before a raw gas compression stage. Next the flue gas is treated in the proposed Task 2 process for SO_x and NO_x removal. Following the Task 2 process the flue gas is treated in a Cold Box cycle for CO₂ concentration into a CO₂ product which is further compressed to the final product pressure. The 'Cold Box Vent' stream is processed in a vacuum pressure swing adsorption (VPSA) process to recover CO₂ which is recycled to the raw gas compressor. The process vent gas, mostly composed of O₂, N₂ and Ar is heated and expanded for power recovery.

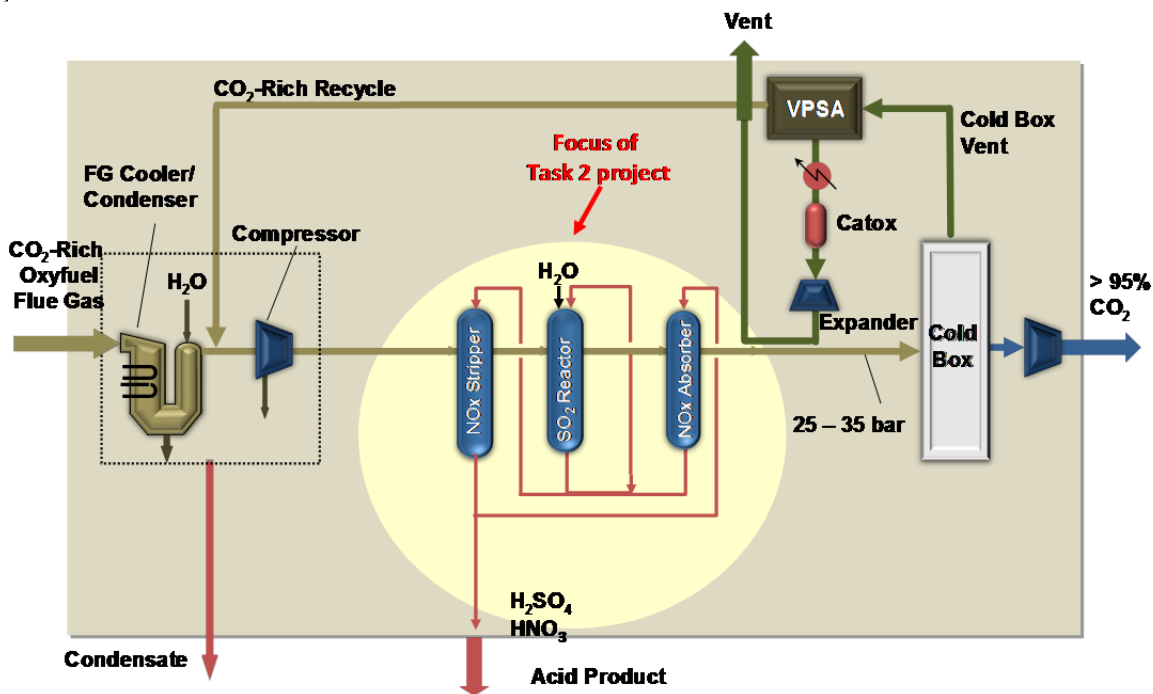


Figure 2.2 A CPU Process Using the Task 2 Process for SO_x/NO_x Removal

Process Description

Figure 2.3 below shows the configuration of the Task 2 process for flue gas purification and conversion of SO_x and NO_x to concentrated acids. The process consists of three main vessels: the NO_x stripper, the SO₂ reactor and the NO_x absorber. Flue gas enters the process on the right after leaving the raw gas compressor, typically hot or warm without going through a compressor aftercooler, because hot or warm gas is needed in the NO_x stripper. The original purpose of the NO_x stripper was to thermally desorb NO_x from NO_x laden acid, to produce a sulfuric acid product which is substantially free of absorbed NO_x. As experimental results show thermal desorption of NO_x from sulfuric acid was not achieved and it was not possible to remove NO_x from sulfuric acid to the extent needed for production of directly saleable sulfuric acid.

The second vessel is the SO_x reactor with the primary purpose of SO₂ conversion to SO₃ and sulfuric acid. The operating temperature of this vessel is lower than the operating temperature of the NO_x stripper,

further energy needs to be removed from this vessel because the acid production reactions are exothermic. In this vessel water is added to control the concentration of the product acid and to ensure that no free SO₃ is formed (oleum).

Following the SO₂ reactor the last vessel is the NO_x absorber. The purpose of this vessel is to absorb gas phase NO_x from the flue gas stream into the liquid acid stream for 1) low NO_x emissions and 2) to recycle NO_x back to the front of the process for NO_x concentration within the Task 2 cycle. Sulfuric acid has a high absorption capacity for gas phase NO_x; this vessel operates at as low temperature as is allowed by the available cooling utility for maximum NO_x capture. Following the NO_x absorber the Task 2-treated flue gas would proceed to the cryogenic processing unit of the CPU.

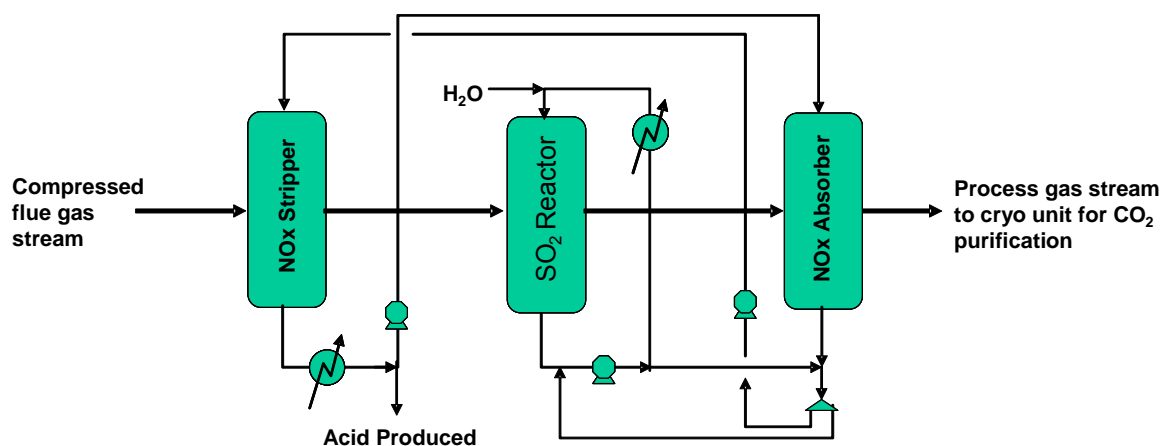


Figure 2.3 Schematic of the Task 2 Process for SO_x and NO_x Removal

Chemistry Description

In the Task 2 process a number of heterogeneous and homogeneous reactions are important for conversion of NO_x and SO_x to acids. The elevated pressure which would be present in the CPU is another key feature which increases the rates of important reactions.

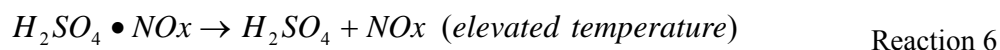
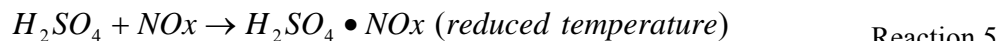
NO_x in the flue gas is primarily NO (nitric oxide) with small amounts of NO₂. Conversion of NO to NO₂ occurs homogeneously in the gas phase (Reaction 1) due to the presence of excess oxygen in the flue gas.



The formation of NO₂ is primarily important because it catalyzes SO₂ oxidation to SO₃ which in turn reforms NO, Reaction 2. This reaction largely occurs in the liquid phase (involving some intermediate steps which are not shown) followed by the hydrolysis of SO₃ to form sulfuric acid, Reaction 3. Nitric acid may also be formed when NO₂ combines with water, however in this process NO is constantly re-formed, Reaction 4, making complete NO_x containment difficult in a standard process (with water contact alone).



The important aspect of the proposed process is how these reactions are managed for production of concentrated acids. The proposed process used a scheme for NO_x recycle which absorbs and desorbs NO_x from sulfuric acid (Reactions 5 and 6) for NO_x concentration in a central vessel where the Reaction 2 takes place. The process for NO_x absorption and desorption is comparable to that used in the historic Lead Chamber Process for sulfuric acid manufacture. Various sulfuric acid production methods can be found in the references cited here [4 – 7].



Some valuable co-benefit can also be expected in this process: 1) sulfuric acid may be effective for Hg⁰ capture in the form of HgSO₄ precipitate from gas streams 2) the gas leaving the entire process has already been dehydrated due to contact with the hygroscopic concentrated sulfuric acid product. This produces flue gas that is in theory dried to an appropriate level which can directly proceed to a cold box. This could simplify the process by eliminating the need for water and Hg beds, however Hg and water adsorbent beds would likely be required to protect against the possibility of getting any Hg or Water into the cryogenic CO₂ purification process due to the potential extreme consequences if there was any carryover into the coldbox.

Subtasks 2.1, 2.2 and 2.3 - Experimental Work

In the overall process, three separate gas/liquid contacting vessels are used to carry out the required reactions. The original proposal included an additional, catalytic reaction vessel to removing NO_x from the product acid (no effective catalyst material was found and this vessel was removed from the process). The conditions inside each vessel differ in terms of process temperature and level of SO_x/NO_x impurities. Each of the vessels were tested separately in a single bench scale unit using preheated cylinder feed gases and preheated metered liquid acid (Task 2.2). The single gas/liquid contacting vessel consisted of a packed column monitored for temperature and pressure. The packed column contains roughly one equilibrium mass transfer stage. The effluent gas was analyzed for composition to determine reaction conversion, adsorption, desorption and reaction rates.

In Task 2.2 each of the three main contacting vessels were tested independently by reproducing the conditions around each vessel in terms of feed gas composition and fluid temperatures. Because the conditions inside the vessels can vary depending on the experimental results, the experimental data was collected for a range of NO_x, and SO_x levels. Gases were delivered from cylinders and were heated to an appropriate inlet temperature. Reaction conversion and reaction kinetics were determined from the collected data for the conditions in each vessel. Figure 2.4 shows the general concept of this bench scale gas/liquid contacting system.

As mentioned above potential NO_x removal catalysts were tested in a second small bench scale experimental system (Subtask 2.3).

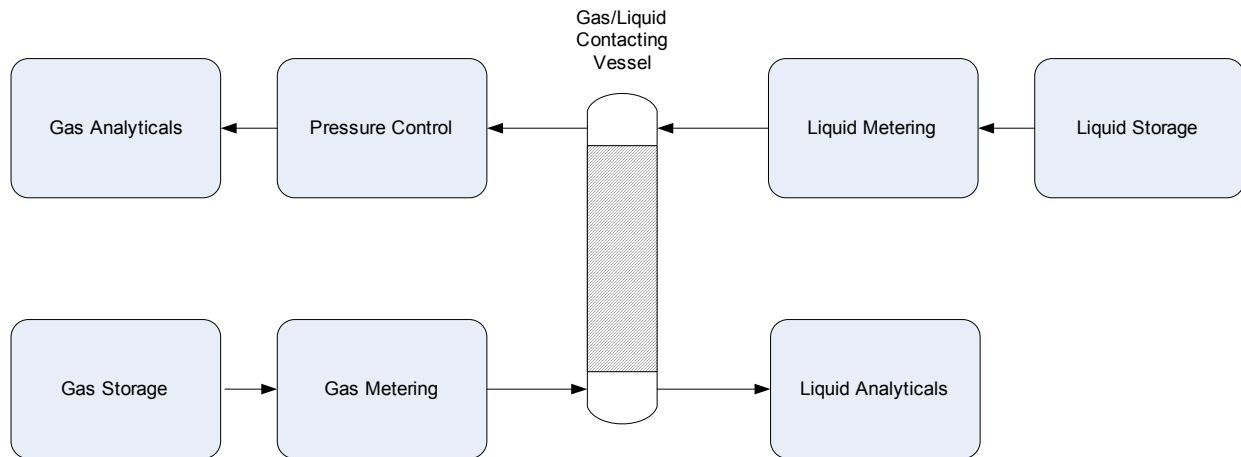


Figure 2.4 Schematic of the Task 2 Bench-Scale Unit



Figure 2.5 Photograph of the Task 2 Bench-Scale Unit

Subtask 5.1 - Process Simulation

Process simulations were completed for feed to the WorleyParsons subcontractor for comment on commercial viability, value of product acid, and Task 2 capex cost estimation. Two main process simulation iterations were completed: 1) at the beginning of the project (before experimental data was collected which was based on the limited literature data available) and 2) at the end of the project after the experimental data was collected and after feedback was received from Foster Wheeler and Task 5 activities on the expected on the flue gas composition.

Subtask 5.3 - Commercial Viability of H₂SO₄ Process

The WorleyParsons Toronto office has experience in the sulfuric acid industry designing sulfuric acid plants. Because WorleyParsons is involved in the sulfuric acid industry they have experience to provide feedback on the Task 2 process with respect to: 1) technical feasibility and commercial viability of the process, 2) assistance in developing a budgetary cost estimate, 3) commercial acid product viability based on the current acid market and logistical considerations.

Results and Discussion

Subtask 2.1: Experimental Apparatus Design and Construction

Safety and corrosion were very important in physical design of the experimental system because the experiments involve contact of toxic gases with sulfuric acid, at elevated pressure and at elevated temperature. The heated sulfuric acid stream made for a unique challenge in terms of materials compatibility due to increased corrosion rates associated with high temperature sulfuric acid. Due to these unique considerations considerable time was spent on the design of certain pieces of equipment including the acid heater, acid cooler and reactor.

From a safety standpoint a decision was made to automate system shutdowns and to provide for remote system control due to the sulfuric acid and toxic gases used in the experiment. A programmable logic controller (PLC) was used to control the system which has added some system complexity to the project.

Due to a strong emphasis on safety at Praxair, significant efforts were spent to evaluate potential failure modes and to ensure that adequate protection existed for personnel and property during the commissioning and experimentation phase of the program. Due to the toxic nature of the gases involved in this experimentation (SO_2 , NO and NO_2), it was deemed necessary to perform a dispersion analysis of a toxic gas release to make sure that the gas discharge plume from the fume hood exhauster is sufficiently dilute to ensure that there was not potential for injury in the worst case scenario.

Refer to Figure 2.6 for a dispersion analysis case showing the hood exhauster plume following an NO_2 cylinder leak. The plume shows the gas concentration in the area surrounding the hood exhauster and the extent of vertical and transverse movement of the plume. This analysis was performed for all toxic gases (SO_2 , NO_2 and NO) spanning a variety of potential cylinder leak/rupture scenarios. The plume analysis results showed that there was adequate dispersion of NO_2 and NO due to the relatively small cylinder contents but that the dispersion of SO_2 was not as complete. As a result of the plume analysis the SO_2 cylinder size was decreased.

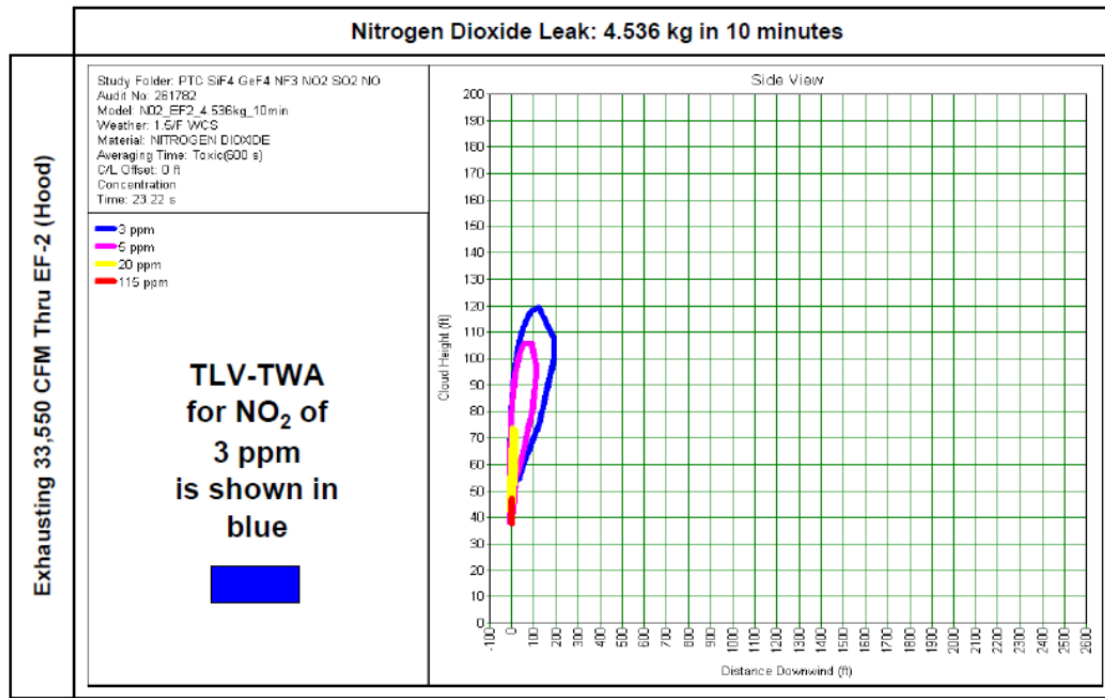


Figure 2.6 Plume Analysis for a 10 Minute Release of NO₂ through the Fume Hood Exhauster

Figure 2.7 shows the bench scale test unit constructed in subtask 2.1. The electrical and control connections are shown on the left along with an emergency spill containment kit. The experimental equipment is located in a fume hood, shown on the right. Sulfuric acid was stored in the fume hood while the toxic feed gases (SO₂, NO, NO₂) were stored in a dedicated vented gas cabinet (not shown). Figure 2.8 shows the computerized interface panel used to control the Task 2 experimental apparatus. From this interface gas flows, liquid flows, and process temperatures were controlled and monitored. Warnings, alarm conditions and analyzer readings were monitored and process data was recorded for later analysis.

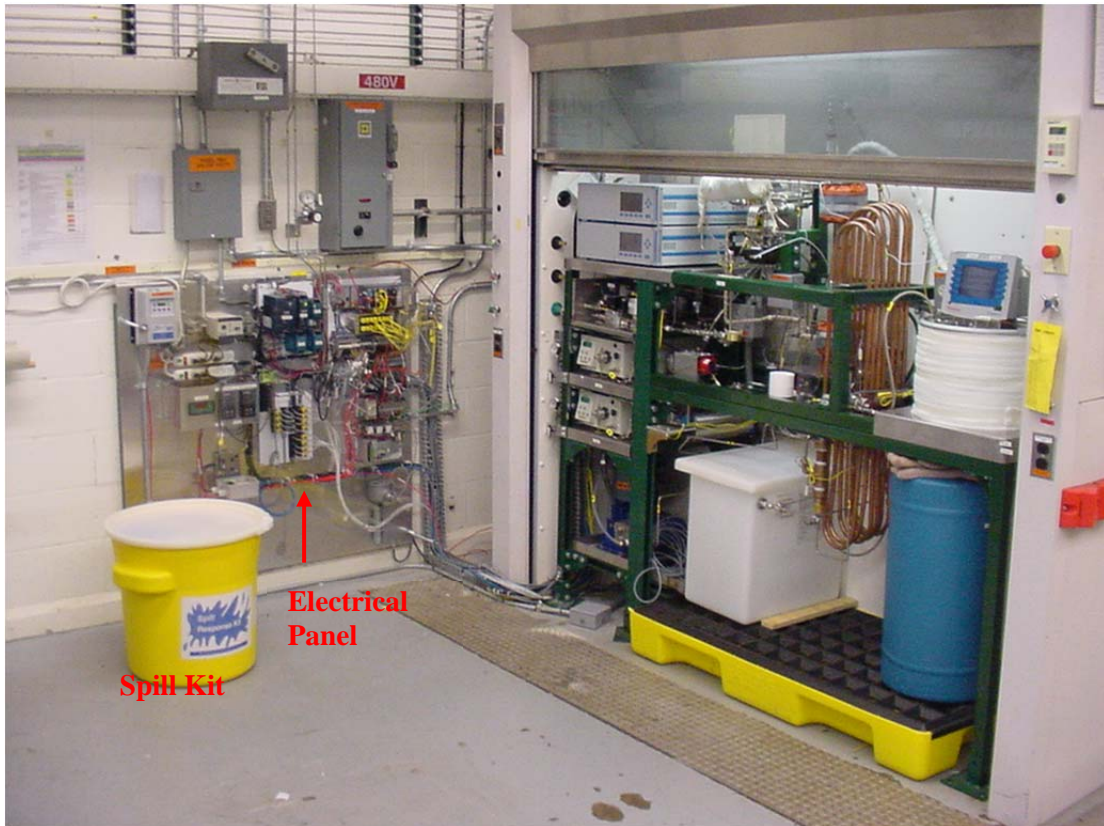


Figure 2.7 Bench Scale Unit Constructed as Part of Subtask 2.1

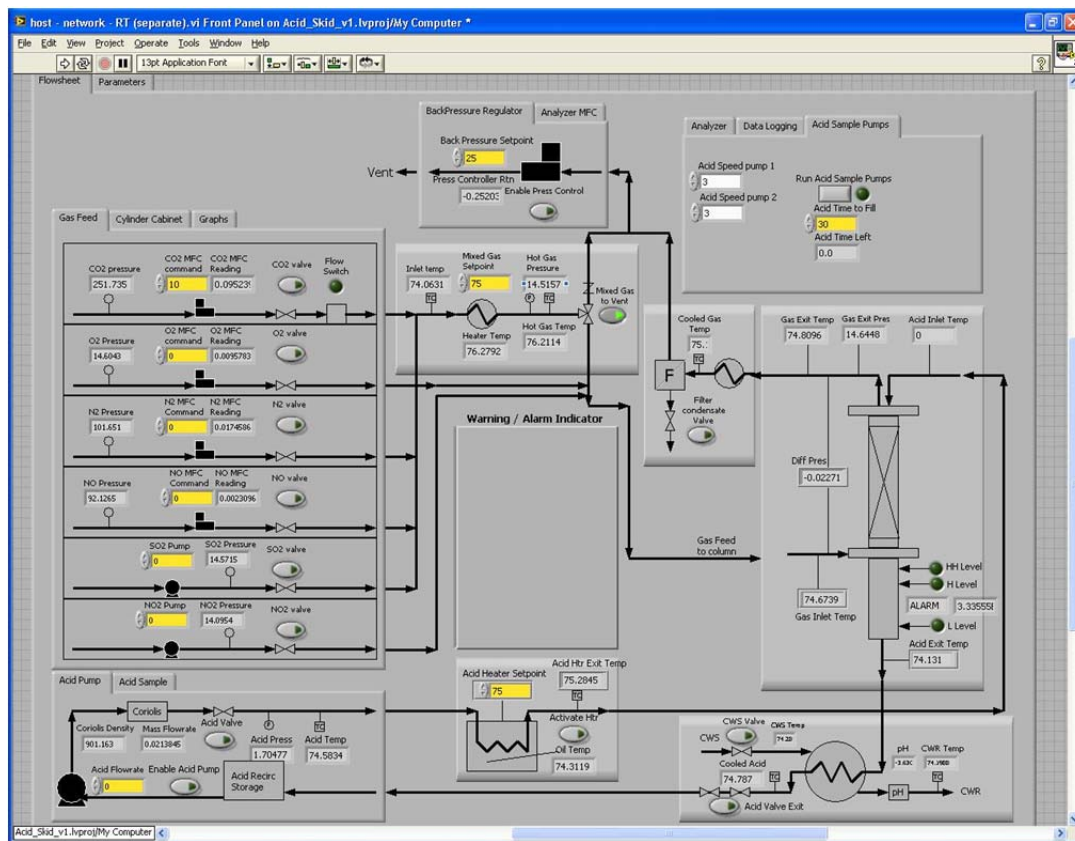


Figure 2.8 Computer Interface Control and Monitoring Panel for the Task 2 Equipment

Subtask 2.2 Data Collection in the Gas/Liquid Contactor

General experimental, commissioning and NO oxidation reactions

The initial tests conducted in the bench scale experimental apparatus included:

- tests to understand the flooding behavior of the column
- tests to quantify the mass transfer performance of the gas/liquid contactor
- experiments to investigate the NO oxidation reaction kinetics in comparison to literature-reported data

The flooding behavior of the column was tested at atmospheric pressure and at elevated pressure with water to determine the operating limits of the system needed to avoid flooding during experimentation. Figure 2.9 shows the column limits at a fixed pressure as a function of gas flowrate. The column is less likely to flood at higher pressures due to the decreased superficial gas velocity through the column. These experimental results were used to calculate the flooding limits of sulfuric acid by accounting for the higher density and viscosity of this liquid.

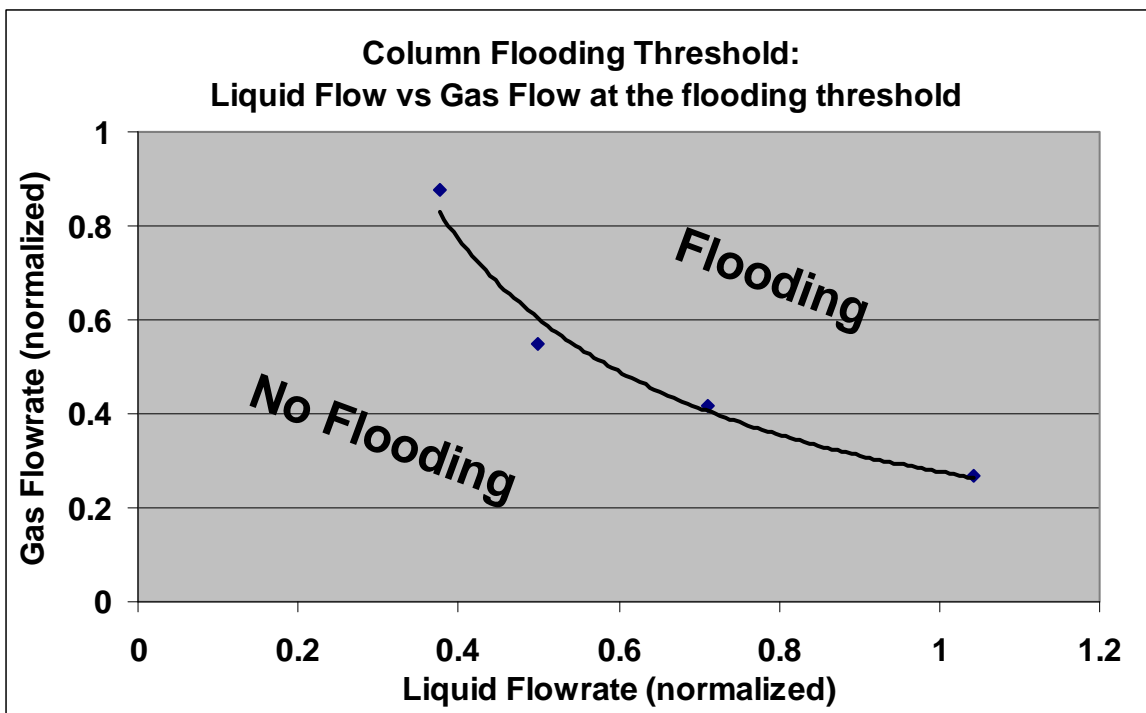


Figure 2.9 Experimental Column Flooding Threshold

To determine the number of equilibrium column stages, a stream consisting of SO₂, CO₂, N₂ and O₂ was passed through the column counter current to water at various water flow rates. The uptake of SO₂ was determined by measuring the concentration of the exhaust gas. The same process has been simulated using a process simulator (Aspen Plus) for estimation of number of equilibrium stages vs. water flowrate. Process simulations include electrolyte interactions and the formation of acid species from CO₂ and SO₂ that enable accurate simulation of the system chemistry. In the laboratory and simulated contactor SO₂ and CO₂ are absorbed into the water, forming sulfurous acid and carbonic acid that affects the pH of the water exit stream as well as the ability of the water to absorb acid gas components.

Comparing experimental data and simulation data allows for the estimation of the number of equilibrium stages in the column. See Figure 2.10 showing the relationship between number of column stages (normalized) and liquid flowrate (normalized) for a fixed gas flowrate. The results of the commissioning testing of the gas/liquid contactor confirmed column that at the number of equilibrium stages in the column was roughly 1.0 at the average expected operating conditions during the SO_x/NO_x testing.

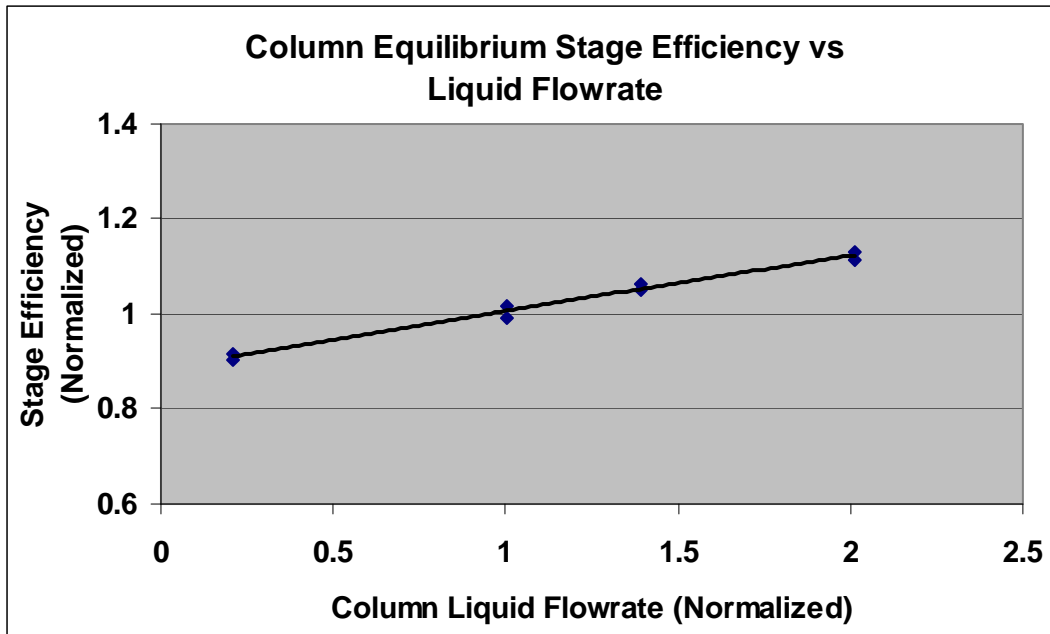


Figure 2.10 Experimental Column Stage Efficiency

The bench scale apparatus had an empty chamber having a well-known volume that was used to determine the reaction rate of the NO oxidation reaction ($\text{NO} + \frac{1}{2} \text{O}_2 \rightarrow \text{NO}_2$), Reaction 1. This reaction is well known to occur in the gas phase at the temperatures and pressures of interest in the carbon dioxide processing unit. The rate of the NO oxidation reaction was measured in the bench scale system for comparison against the literature-predicted reaction rate.

Figure 2.11 shows the conversion of NO due to the NO oxidation reaction for two flowrates. Nitric Oxide conversion depends on the flowrate and reaction pressure because these factors change the gas residence time and reactant concentrations (partial pressures) in the experimental apparatus. Figure 2.11 shows the experimentally observed reaction conversion vs. the literature-predicted reaction conversion at various pressures. Good agreement is shown between the laboratory measured conversions and kinetic rate law-predicted conversions. The cause of the larger discrepancy between experiment and prediction for the lower flowrate is likely due to the increased residence time in the tubing before and after the reaction volume. The ability to accurately predict the rate of NO oxidation is very important in the Task 2 effort because NO_2 is required to catalyze SO_2 oxidation for SO_2 removal from the compressed flue gas stream.

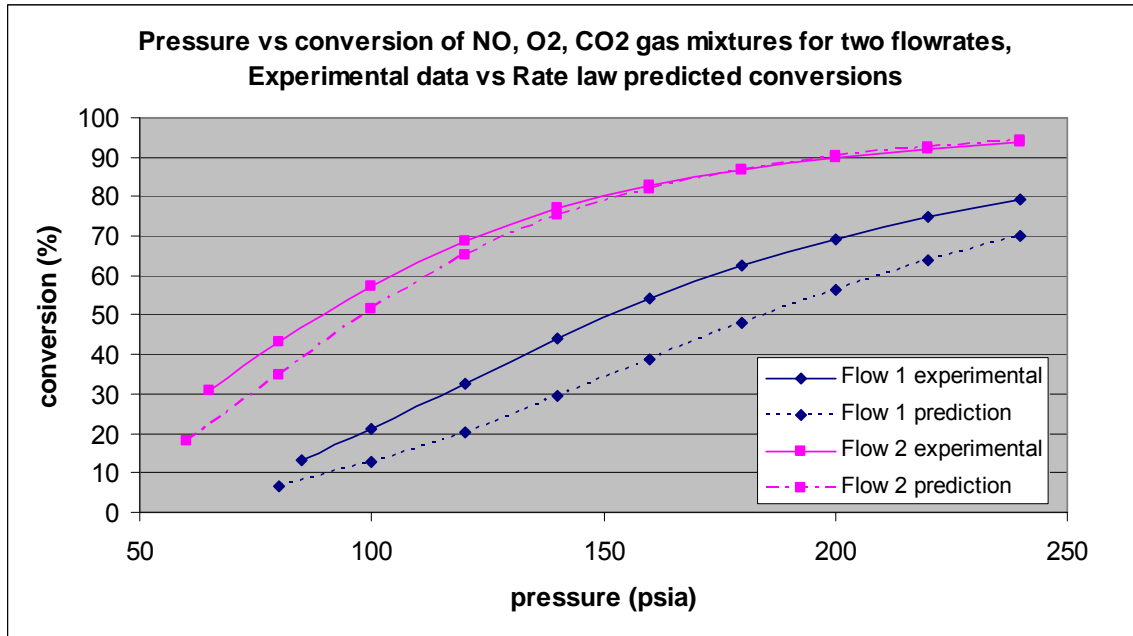


Figure 2.11 Percent Conversion of NO to NO₂ at Various Pressures and Flowrates

NO_x Absorption and Desorption with Sulfuric Acid

A number of tests were conducted to quantify the uptake of NO_x into sulfuric acid. NO_x – sulfuric acid interactions was very important in determining the feasibility of the proposed process. A number of tests were conducted to quantify NO_x absorption behavior at various conditions:

- NO_x absorption into sulfuric acid for various levels of NO_x (800 - 6600ppmv total NO_x)
- NO_x absorption into sulfuric acid for various relative amounts of NO and NO₂
- NO_x absorption into sulfuric acid at various temperatures and pressures

Figure 2.12 and Figure 2.13 below show typical data collected for NO_x absorption tests. In these particular tests various levels of NO_x (1600-6600 ppm) are contacted with sulfuric acid. The absorption behavior of NO_x into sulfuric acid is highly dependent on the ratio of NO to NO₂. Maximum NO_x absorption is observed when NO:NO₂ is around 1:1. At higher pressures (200 psia) maximum NO_x absorption is observed when there is a slight excess of NO at the reactor inlet because the homogeneous reaction just described converts NO to NO₂ inside the gas/liquid contactor. This reaction pushes the NO:NO₂ ratio close to 1:1 when the gas is in actual contact with the column packing and liquid acid.

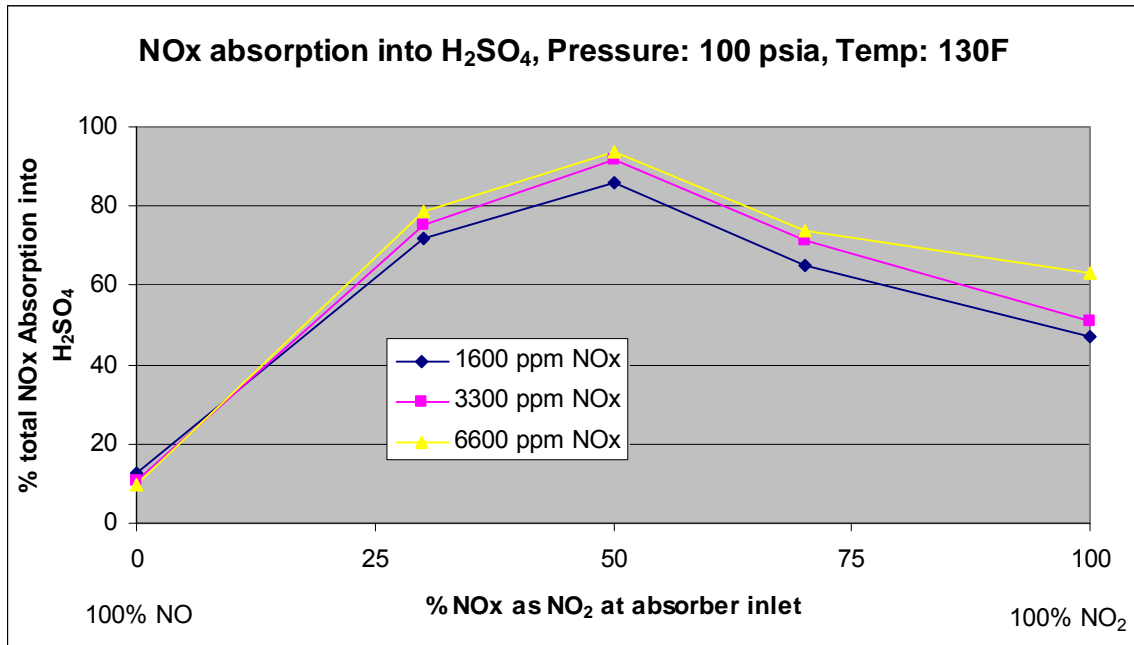


Figure 2.12 NOx Absorption by H₂SO₄; 100 psia and 130 °F

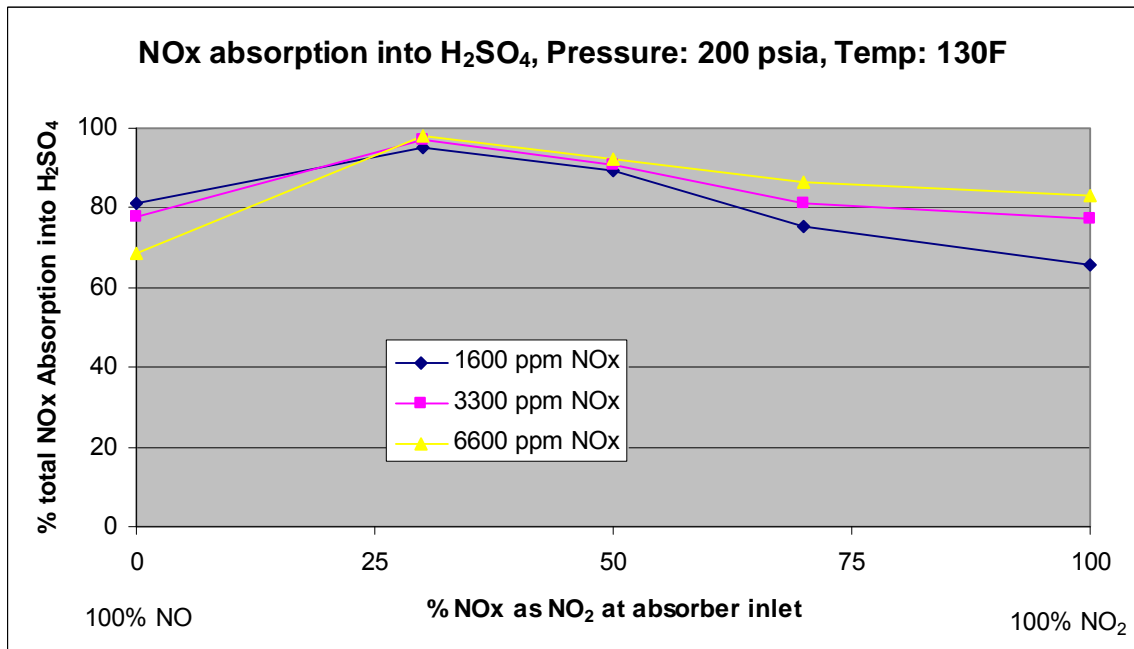


Figure 2.13 NOx Absorption by H₂SO₄; 200 psia and 130 °F

Absorption/desorption experiments were conducted at increasingly higher temperatures of up to 235°F; see Figure 2.12 to Figure 2.16. The main important result that was determined from these graphs is that NOx absorption into 93wt% sulfuric acid remains high even at temperatures of up to 235°F at a relatively low pressure of 100 psia (Figure 2.16). The limited amount of literature information available near these conditions which was consulted during the proposal phase of this program suggested that acid containing

NOx would not absorb NOx and would even begin to desorb from acid at these temperatures. Because the sulfuric acid used in these experiments contained a substantial amount of dissolved NOx the gas leaving the gas/liquid contactor should have showed a gain in NOx if there was any net NOx desorbed from the acid.

The experiments that we conducted showed that sulfuric acid continued to absorb NOx at fairly high rates even at elevated temperatures of up to 235°F. NOx desorption from sulfuric acid is an important and necessary feature for production of relatively pure sulfuric acid and is also needed so too high of levels of NOx are not build up in the re-circulating acid stream. An inability to desorb NOx from sulfuric acid, as demonstrated experimentally, means that the sulfuric acid product will likely have very high levels of dissolved NOx and further there are implications on the ability of the Task 2 process to achieve a high NOx capture rate.

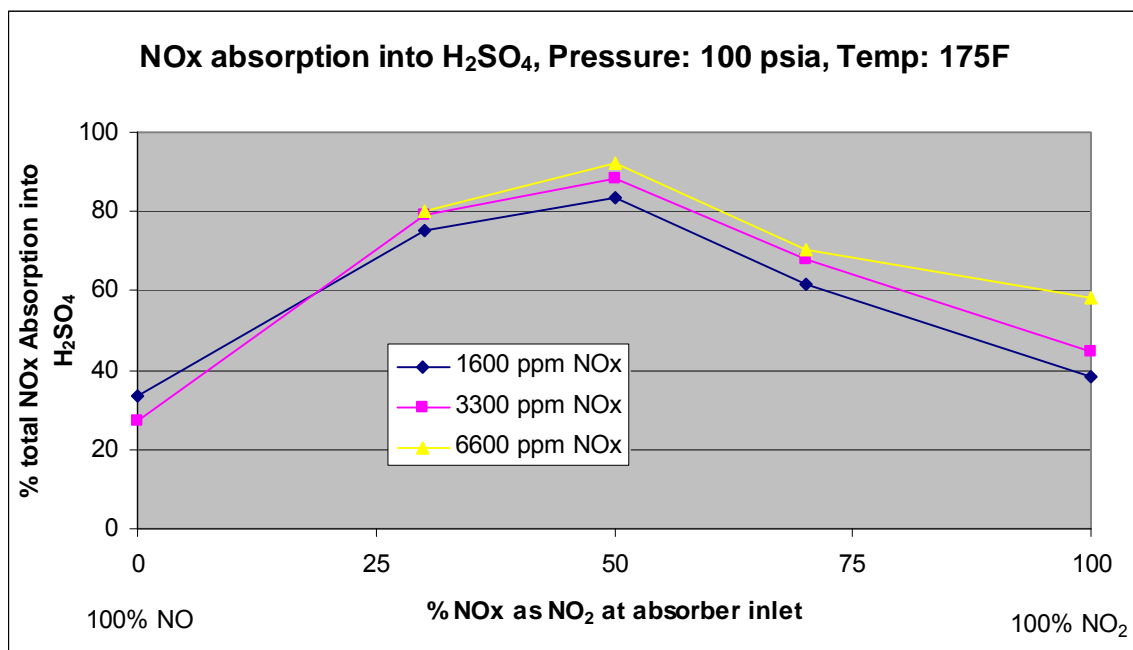


Figure 2.14 NOx Absorption by H₂SO₄; 100 psia and 175 °F

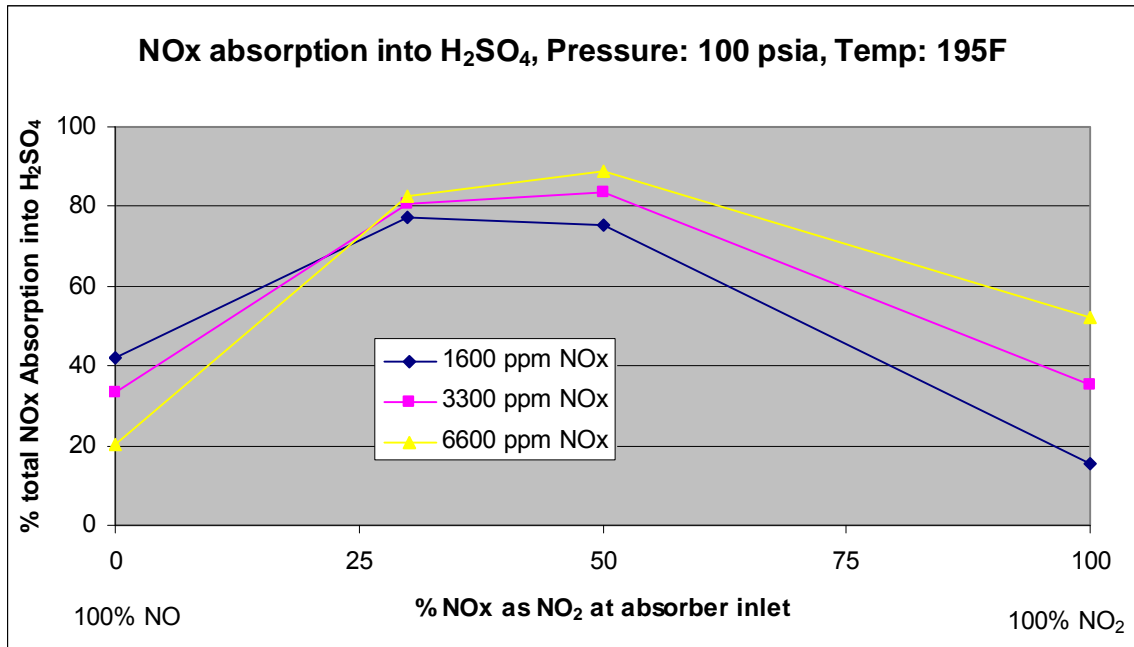


Figure 2.15 NOx Absorption by H₂SO₄; 100 psia and 195 °F

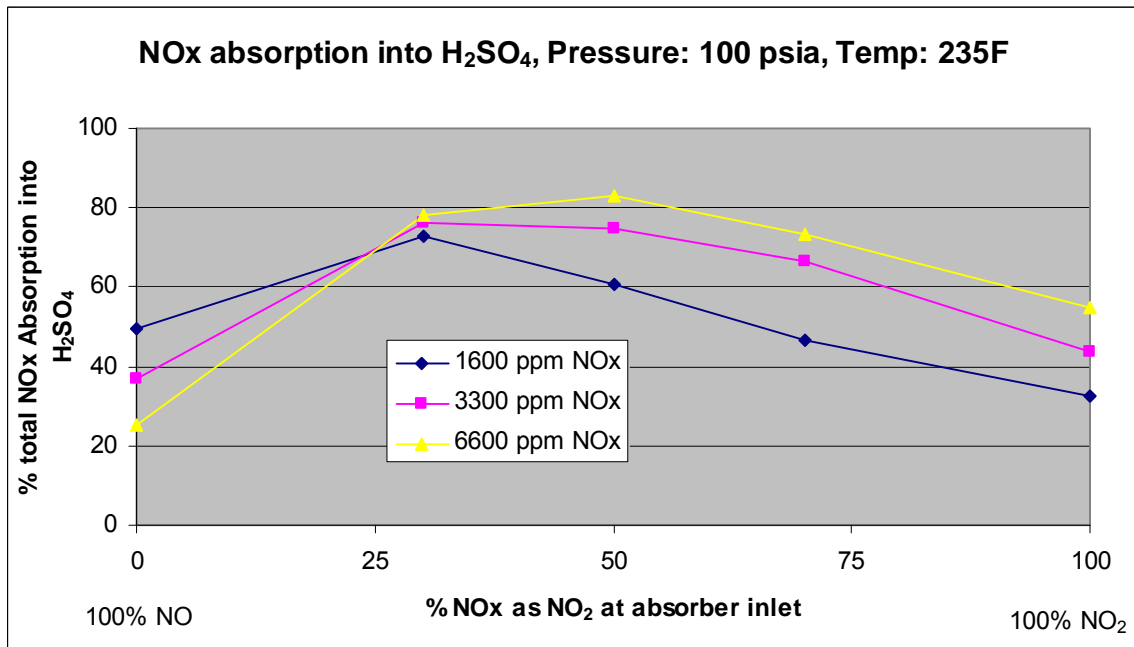


Figure 2.16 NOx Absorption by H₂SO₄; 100 psia and 235 °F

As NOx absorption experiments were conducted at progressively higher temperatures it was expected that a significant amount of NOx would thermally desorb from the liquid acid. As described above the experimental data actually showed no ability of the acid to release NOx as it is heated at the conditions investigated experimentally. As an increasing number of experiments were conducted with the same batch of acid the NOx concentration in the acid batch continued to steadily rise according to the sulfuric acid

nitrite tests, see below in Figure 2.17. This again reinforces the observation that there is significant difficulty in removing NO_x from sulfuric acid.

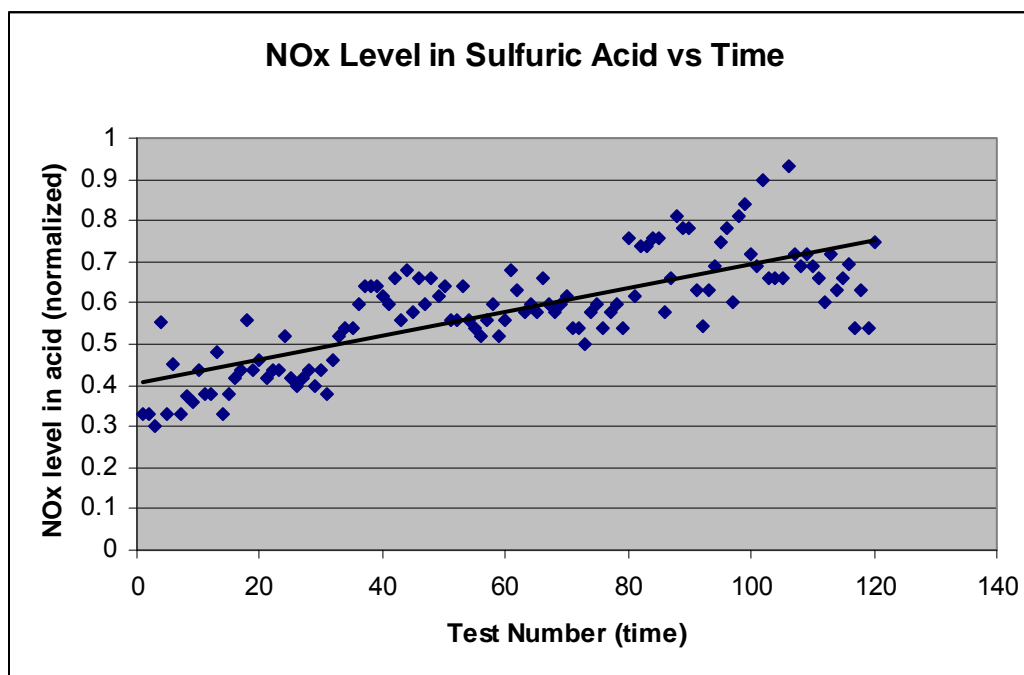


Figure 2.17 Accumulation of NO_x in H₂SO₄ during the Test Campaign

For some process conditions, generally at lower temperatures < 110°F, the gas/liquid contactor exhibited very significant pressure drop (>1psi), it was later determined that a solid substance was forming (H₂SO₄ + NO_x) and plugging up the column packing. Information from the literature regarding the Lead Chamber Process for sulfuric acid manufacture predicts the formation of a NO_x-sulfuric acid mushy solid under certain process conditions (high acid concentration and high NO_x levels). An experiment was conducted at atmospheric pressure under these conditions in clear glassware. The formation of a solid substance was visually observed confirming potential column plugging by these deposits. The pressure drop difficulties due to this solid formation was generally more frequently noticed at lower operation temperatures and higher NO_x concentrations which would be similar to conditions in the NO_x absorber vessel.

SO_x conversion and SO_x/NO_x reactions

When designing a SO₂ reactor system for the Task 2 process there are a number of variables that could be manipulated to affect SO_x containment, including temperature, NO_x levels, SO_x levels, residence time, acid flowrate, gas flowrate, etc. These variables can be adjusted by changing process parameters related to the SO₂ reactor, NO_x absorber and NO_x desorber to try to achieve high conversion of NO_x and SO₂ to acids in the final process.

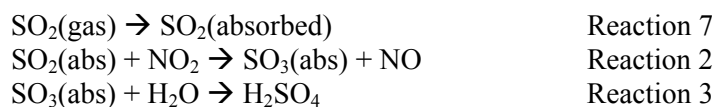
A number of key parameters were investigated as they relate to the SO_x reactor to 1) determine their impact on the SO₂ oxidation/absorption performance and 2) to aid in the estimate of process conditions and physical dimensions of an SO₂ reactor in a commercial size CPU system.

Process characteristics experimentally investigated in Q4 2010 as they relate to the SO₂ reactor:

- SO₂ level in the gas feed
- Residence time (through varied vessel pressure and gas flowrate)

- Liquid acid flowrate
- NO₂ and NO levels
- Temperature

The conversion of SO₂ to SO₃ depends on the absorption of gas phase SO₂ into the sulfuric acid liquid (Reaction 1) followed by SO₂ reaction to SO₃ and hydration to sulfuric acid (Reactions 2 and 3). The relevant SO₂ conversion reactions responsible for sulfuric acid production are shown below.



Besides any kinetic limitations of Reaction 2 the rate of SO₂ oxidation also depends on the mass transport limitations of absorbing gas phase SO₂ into the liquid as well as solubility limits of SO₂ in sulfuric acid. Based on the results of the NO_x experimentation it is expected that mass transfer resistance is not limiting in these experiments because some NO_x experiments were able to achieve up to 98% NO_x absorption at similar gas and liquid flow conditions (roughly one equilibrium mass transfer stage).

SO₂ Solubility in Sulfuric Acid

According to literature, the solubility of SO₂ in sulfuric acid can be predicted using a simple Henry's law relationship: $P_{SO_2, Gas} * H = C_{SO_2, Liq}$ [5]. At a fixed temperature and acid concentration the maximum solubility of SO₂ in sulfuric acid is determined by the partial pressure of SO₂ in the gas phase (for the binary system involving SO₂ and acid). Experimental data has been collected in our system with high partial pressures of CO₂ and high levels of NO_x in the acid. Experimental results indicate that the solubility of SO₂ in sulfuric acid is decreased by a factor of about 10 over the ideal binary case. The specific reason for this substantial decrease in SO₂ solubility is not clear however it is believed to be due to the high partial pressure of CO₂ and/or the high levels of NO_x in acid. Figure 2.18 shows the estimated maximum solubility of SO₂ in concentrated 95wt% sulfuric acid as a function of SO₂ partial pressures for the model binary system (blue line). The estimated solubility limits in our system with a high CO₂ partial pressure and NO_x dissolved in acid is shown by the pink line.

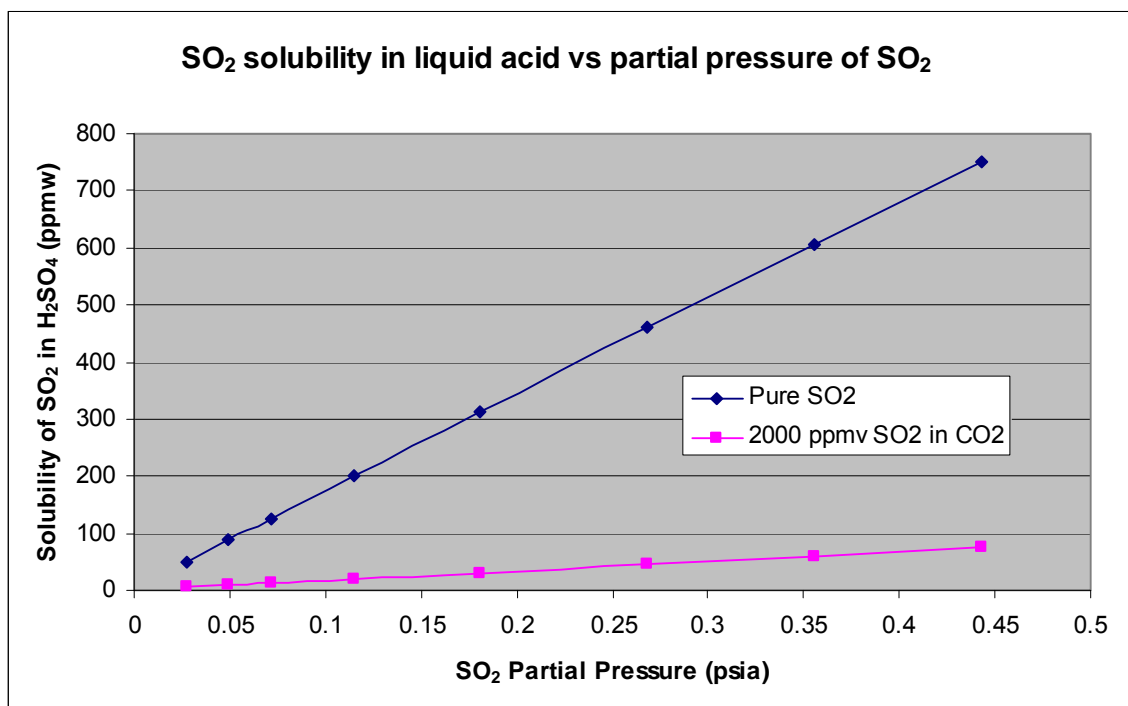


Figure 2.18 Equilibrium Solubility of SO₂ in 95wt% Sulfuric Acid vs. Partial Pressure of SO₂

It is important to note that when SO₂-containing gas is contacted with sulfuric acid SO₂ will be absorbed even in the absence of Reaction 2 due to SO₂'s solubility in sulfuric acid. Therefore removal of SO₂ from the gas phase may not necessarily be attributed to SO₂ conversion to SO₃ (Reaction 2). Direct measurement of SO₂ content of the liquid sulfuric acid was not possible in our experimental apparatus because as soon as the liquid pressure is reduced much of the SO₂ desorbs from the acid. For this reason SO₂ reaction and absorption must be measured indirectly by changing gas/liquid contactor conditions such as (flowrate, pressure, SO₂ and NO_x levels, etc.) and monitoring the gas SO₂ levels.

Effect of SO₂ Level on SO₂ Absorption and Reaction

Experiments were conducted at constant pressure, temperature, total gas flowrate, NO_x gas level and liquid flowrate with varying SO₂ level to estimate the SO₂ reaction rate in our system. Figure 2.19 shows the experimental total absorption result for the experiments (in blue) along with the vapor liquid equilibrium (VLE) predicted absorption of SO₂ into sulfuric acid (in pink) for concentrations of SO₂ of up to about 2200 ppm.

At low inlet gas concentrations of SO₂ the total absorption of SO₂ as denoted by the experimental blue line approaches that which is predicted by VLE absorption because the low concentration of liquid phase SO₂ limits the actual SO₂ oxidation rate (Reaction 2). At higher concentrations of gas inlet SO₂ the liquid concentration of SO₂ is higher and the SO₂ reaction rate (Reaction 2) is faster; this increases the spread between the blue and pink lines.

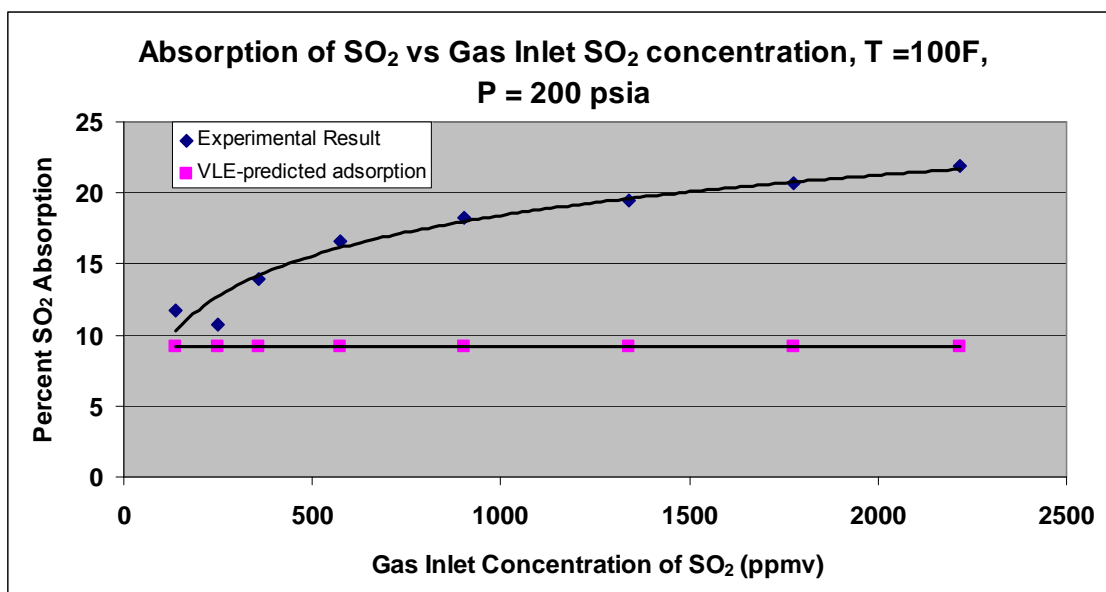


Figure 2.19 Percent SO₂ Absorption vs. Inlet Gas Concentration of SO₂

Effect of Residence Time on SO₂ Absorption

Experiments were conducted in the gas/liquid contactor at 100°F with a CO₂ gas feed containing about 2100 ppm SO₂ and a liquid sulfuric acid feed containing an excess of dissolved NO_x. Data was collected for various gas feed rates (10, 20 or 30 slpm) and various pressures (100, 150 and 200 psia) to investigate the effect of residence time on SO₂ absorption. In all experiments the liquid flowrate was kept constant. Figure 2.20 shows the effect of residence time on the absorption of SO₂. An increase in residence time has a nearly linear effect on increasing SO₂ absorption. A decrease in reaction rate is observed at high SO₂ conversions, which is believed to be due to a decrease in the rate of Reaction 2 as the SO₂(abs) concentration decreases ($Rate_{rxn2} \sim k \cdot Conc_{SO_2} \cdot Conc_{NO_2}$), as was shown above in Figure 2.19. The concentration of absorbed NO₂ is in excess and should not limit the reaction rate at the conditions investigated here.

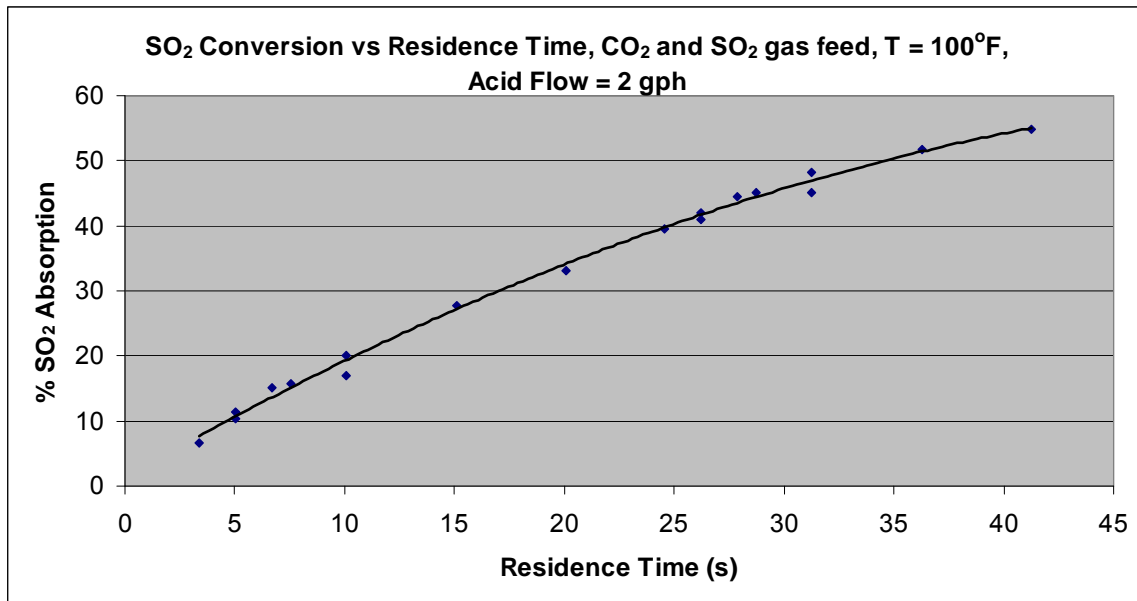


Figure 2.20 Impact of Residence Time on SO₂ Absorption in H₂SO₄ in Absence of NO_x

A second set of data was collected with roughly 800 ppm of NO_x added to the contactor feed gas, the results are shown below in Figure 2.21. The experimental data shows that the addition of 800ppm of gas phase NO_x serves to increase the rate of SO₂ absorption by roughly 10%. Gas phase NO_x is readily absorbed by sulfuric acid, as previously shown, the added gas phase NO_x increases liquid phase NO_x resulting in an increased reaction rate.

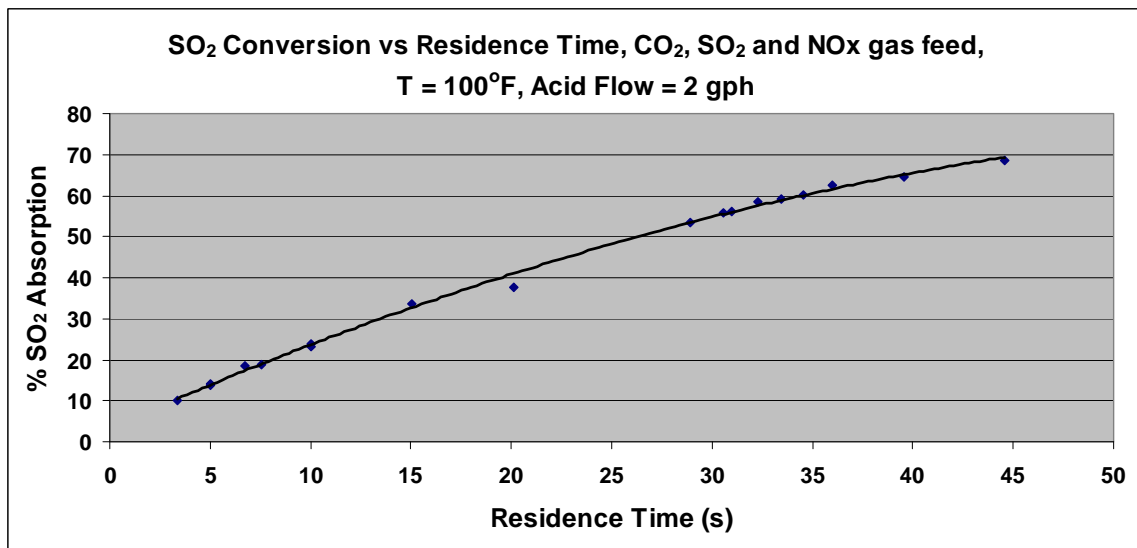


Figure 2.21 Impact of Residence Time on SO₂ Absorption in H₂SO₄ in Presence of NO_x

In Figure 2.22 some of the data from Figure 2.20 and Figure 2.21 are shown together with the VLE predicted contribution to SO₂ Absorption. The VLE-predicted absorption is calculated based on the inlet gas composition, gas flowrate, acid flowrate and system pressure and is not residence time dependent. It is, however, plotted versus residence time for comparison with the corresponding experimental data points (shown in green and blue). The difference between the blue and pink data and the green and pink

data corresponds to the amount of SO₂ oxidation (Reaction 2) taking place; the presence of gas phase NO_x allows for a faster reaction rate. As residence time is increased SO₂ absorption also increases due to Reaction 2.

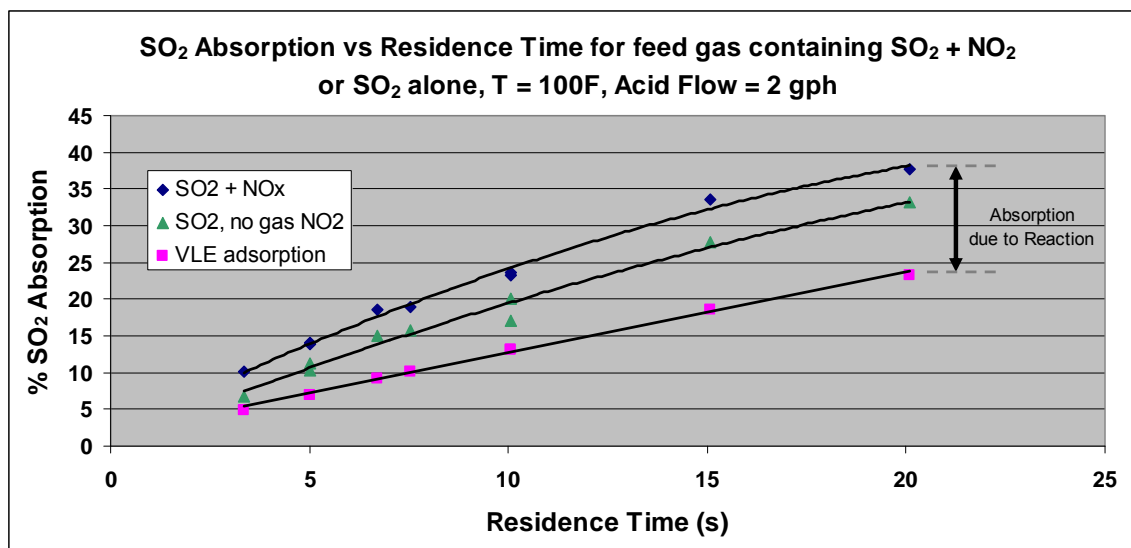


Figure 2.22 Increase in SO₂ Absorption in H₂SO₄ by Reaction with NO₂

Effect of Liquid Flowrate on SO₂ Absorption Rate

Most of the SO₂ oxidation experiments were performed using a constant acid flowrate of 2.0gph to try to fix the gas/liquid mass transport performance of the reactor (Reaction 1). Fixing the liquid flowrate essentially fixes the gas/liquid interfacial area inside the gas/liquid contactor available to absorb SO₂ (Reaction 7); this helps to remove the mass transport effects as pressure or flowrate and residence time are changed (at constant temperature). The area available for gas/liquid contact can be changed by altering the liquid flowrate, or by changing the column packing material (which was not an option in our system).

Figure 2.23 shows the effect of varying acid flowrate on SO₂ adsorption. The distance between the experimental data (blue line) and the VLE adsorption line (pink) indicates the amount of SO₂ converted to SO₃ via Reaction 2. A decrease in acid flowrate from 2.0 gph to 1.0 gph reduces the SO₂ absorption capacity and results in a roughly linear decrease in SO₂ absorption (blue curve) which follows the VLE-prediction. For an acid flowrate of 1.0 and 2.0 gph the liquid’s SO₂ capacity is relatively low, meaning that the SO₂ concentration in the liquid is very similar and the resulting SO₂ reaction rate is similar.

As acid flowrate is increased above 2.0 gph the increase in liquid SO₂ capacity starts to appreciably reduce the gas and liquid phase SO₂ concentrations resulting in a reduced rate of SO₂ reaction. This means it is expected that the distance between the blue and pink curve starts to close at higher acid flowrates, which is observed in Figure 2.23.

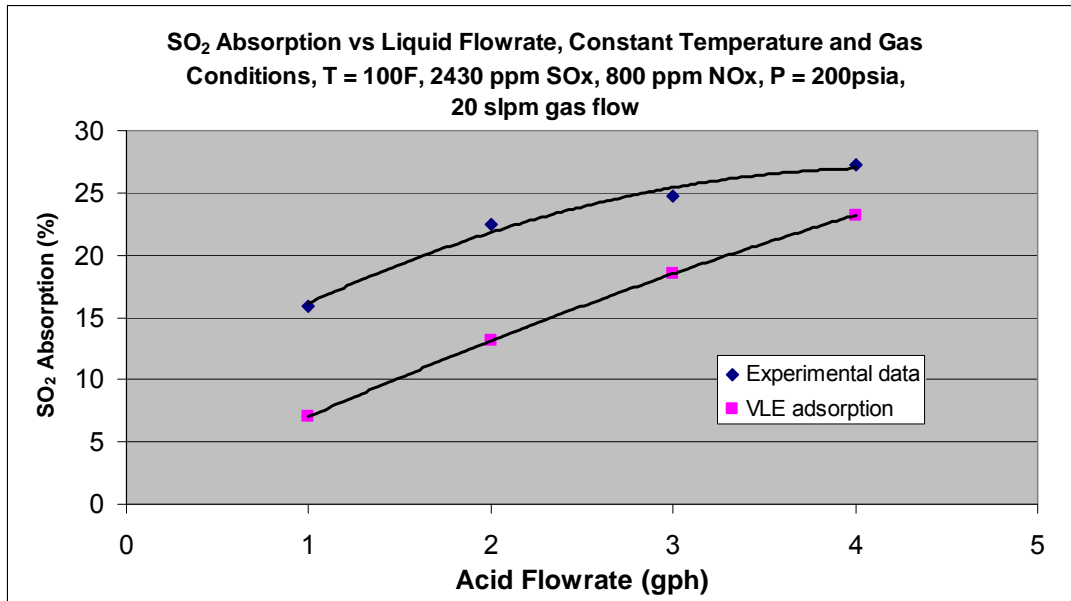


Figure 2.23 Effect of acid flowrate on SO₂ absorption.

Effect of NO_x Level on SO₂ Adsorption and Oxidation Rate

Experiments were also performed to determine the effect of increasing NO_x content in the gas feed on SO₂ reaction rate. Experiments were conducted at constant temperature (100°F), constant gas flowrate, constant pressure (200 psia or 150 psia) and constant liquid feed rate. At each pressure two sets of data were collected for feed gases containing NO₂ and NO + NO₂. Figure 2.24 and Figure 2.25 show the impact of increasing NO_x level on SO₂ adsorption rate. A relative NO_x level of 1 corresponds to about 800ppm of NO_x. As NO_x feed to the reactor is increased with other factors held constant the increase in SO₂ adsorption is directly attributable to an increase in SO₂ oxidation rate, Reaction 2. The presence of NO_x is expected to increase the rate of SO₂ reaction because NO_x is required for SO₂ oxidation. Furthermore if NO_x feed to the reactor is composed of a mixture of NO and NO₂ the reaction rate is enhanced further. Figure 2.24 shows that the NO_x enhancement is significantly greater in the higher pressure case.

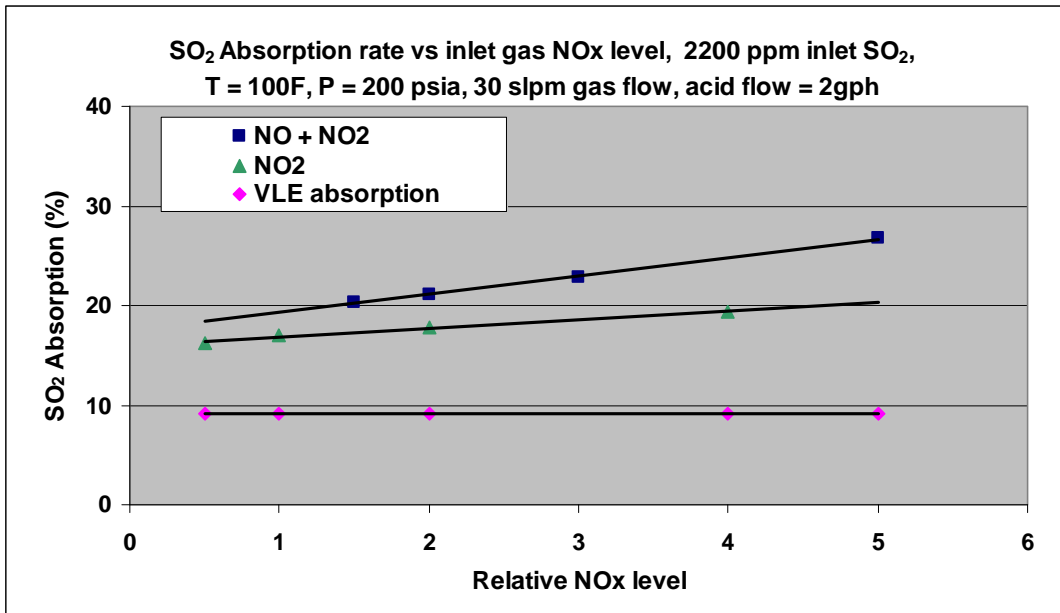


Figure 2.24 SO₂ Absorption in H₂SO₄ vs. NO_x Concentration in Feed at 200 psia.

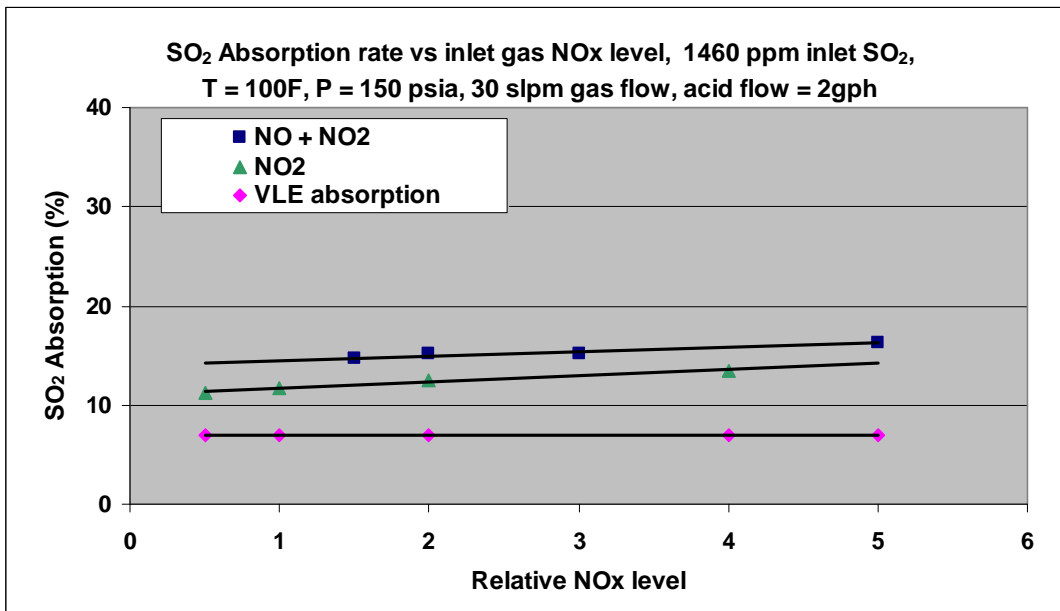


Figure 2.25 Absorption in H₂SO₄ vs. NO_x Concentration in Feed at 150 psia

Effect of Reaction Temperature on SO₂ Reaction Rate

With a fixed reaction volume and a fixed liquid flowrate an increased reaction temperature changes residence time, NO_x oxidation kinetics, reduced SO₂ solubility, and potentially the SO₂ oxidation kinetics, etc. As reaction temperature changes in the bench scale system any change in these properties is observed as a changed SO₂ reactor outlet conversion.

An increase in reaction temperature is observed to modestly decrease the SO₂ reaction rate, as shown below in Figure 2.26. The reduced SO₂ reaction rate is expected to be due to a reduced SO₂ solubility in

H₂SO₄ which is predicted in the literature. Between 100°F and 180°F about a 3 fold decrease is expected based on a decrease the Henry’s law constant.

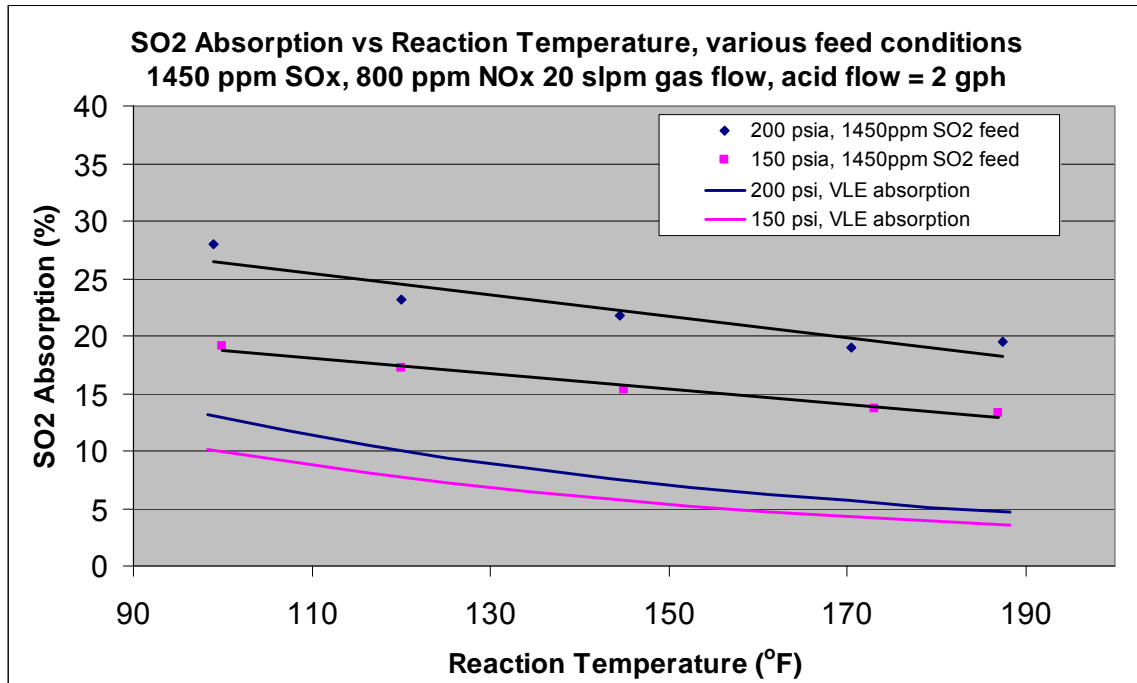


Figure 2.26 Impact of Temperature on SO₂ Absorption in H₂SO₄

Subtask 2.3 NO_x Removal with Activated Carbon

Carbon Testing for NO_x Removal from Sulfuric Acid

In Project Year 1 (2009) a number of activated carbons were tested for their effectiveness to catalyze NO_x removal from NO_x contaminated sulfuric acid at atmospheric pressure. The carbons were tested for NO_x removal by bubbling N₂ or air through a vessel containing carbon and sulfuric acid spiked with NO_x. A sulfuric acid sample was taken periodically and tested for NO_x concentration to determine the rate of NO_x removal.

The purpose of the experiment was to determine if a particular carbon in the presence of oxygen can catalyze NO_x removal from the acid at a faster rate than is observed with simple stripping of the NO_x, when an inert gas, N₂, is bubbled through the sulfuric acid.

Figure 2.27 shows a plot of NO_x concentration vs. time using Carbon 1. This set of data shows the results of trying to remove NO_x by stripping with N₂ and air. The rate of NO_x removal is shown to be significantly faster when N₂ is used for NO_x removal as opposed to air.

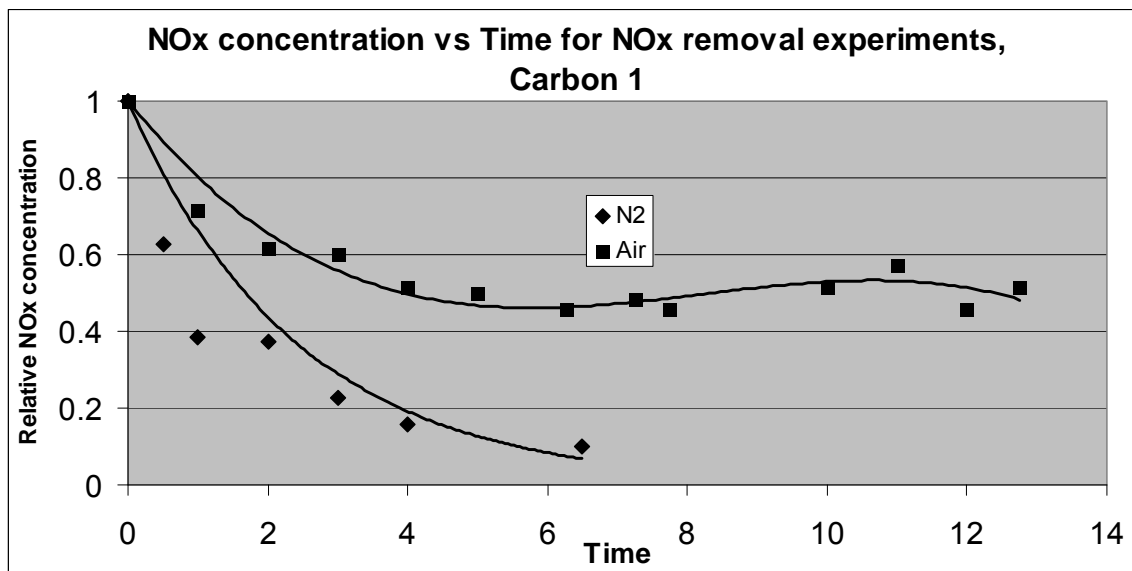


Figure 2.27 Stripping Performance of N₂ and Air for NO_x Removal from Sulfuric Acid

The results of all 5 tested carbons show the same result in which NO_x removal is slower in the presence of carbon and oxygen. The presence and type of the carbon does however impact the rate of NO_x removal because there are significant differences in the rate of NO_x removal between the carbons tested. See Figure 2.28 which shows the relative rate of NO_x removal for the different carbons.

The identity of the carbon has a significant effect on the rate of NO_x removal in the presence of N₂ and Air. Some carbons had significantly better performance than others with carbons 1 and 2 having the best performance. Carbons 4 and 5 show little effectiveness for NO_x removal using N₂ as the stripping gas; even less ability is observed for NO_x removal in the presence of air. In all cases the rate of NO_x removal is slower in the presence of O₂ indicating that NO_x removal may be somehow slowed by some type of oxidative chemistry. This result is opposite of what was expected and means that this method of NO_x removal from the circulating acid and/or the product acid is not viable as a method for selective NO_x removal.

	Relative NO _x removal rate	
	N ₂	Air
Carbon 1	1.00	0.65
Carbon 2	0.92	0.13
Carbon 3	0.29	0.14
Carbon 4	0.04	0.00
Carbon 5	0.15	0.00

Figure 2.28 Relative rate of NO_x removal for various carbons using N₂ and air

Subtask 2.4 Byproduct Purification

At the completion of Subtask 2.3, and associated Milestone M4, it was concluded that the candidate catalysts for the NO_x stripping reactor would not be able to remove NO_x from concentrated sulfuric acid to produce acid of appropriate purity for sale in the standard industrial market. The NO_x removal was much too slow to be of any value in the proposed process. Based on these results it was decided that the

NOx stripping reactor should be removed from the process and that other technologies should be evaluated for NOx removal from the product sulfuric acid.

In the proposal the performance of the NOx stripping reactor was identified as the most likely Task 2 process risk. This possibility was considered when the proposal was written and Task 2.4 was included in the original proposal to address this possibility through evaluation of alternative NOx removal methods. In this scenario the evaluation of the alternative NOx removal methods is required by Subtask 2.4 to satisfy Milestone M7. The approach taken was to evaluate methods of NOx removal used in the contact-process-based sulfuric acid industry and to rule out those methods that are not appropriate due to the Task 2 process reliance on lead chamber based chemistry.

NOx absorption into sulfuric acid occurs most substantially when NO and NO₂ are in a 1:1 ratio, forming nitrosylsulfuric acid (NO•HSO₄), see Reaction 8. The absorption behavior of NOx mixtures at various temperatures and pressures has been the subject of the much of the experimental data collected in Task 2 and was discussed above. Absorbed NOx is very important to the Task 2 process because it is required for SO₂ conversion to sulfuric acid in the process. However nitrosylsulfuric acid is also a contaminant to the final product sulfuric acid and should be removed to the extent possible, ideally down to a level of < 5ppmw, to ensure the product sulfuric acid is useful, and hopefully saleable, to sulfuric acid consumers.



Nitrosylsulfuric acid contaminant in sulfuric acid is commonly referred to as ‘nitrates’ and has a limit in typical sulfuric acid of 5 to 10 ppmw. The presence of nitrates discolors sulfuric acid and can accelerate corrosion of steel equipment. High NOx levels have also been suspected of attacking the protective coating in tank cars.

In the past, NOx levels as high as 30 ppmw (as NO₃) have been acceptable in product sulfuric acid. Current requirements are much lower at 5 ppmw or less. Sulfuric acid destined for use in the sulphonation industry requires low nitrate levels. If the acid contains high nitrate concentrations a dark black, rather than honey colored, acid slurry is formed which is cause for rejection of the acid.

High concentrations of NOx in the product acid may pose an occupational health problem if NOx is subsequently released in the process, usually as a result of diluting the acid. The reaction of NOx and dissolved iron can impart a purple color to the acid which gives the impression that the acid is otherwise off-spec.

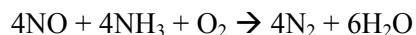
There is an expectation from acid distributors and customers that NOx levels need to be below 5 ppm even if the presence of NOx does not have any impact on the process in which the acid is used. This acid will probably go into a common storage tank with acid from other sources. Customers or acid distributors would not want to risk contaminating their entire inventory of acid because of one off-spec shipment. Acid with high NOx concentrations can be utilized in the phosphate fertilizer industry, the largest consumer of acid, with potential for no impact on the fertilizer production process.

NOx Control Strategies

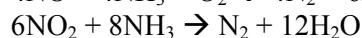
NOx control strategies for traditional contact sulfuric acid plants are broadly divided into two categories: 1) NOx removal from the feed gas prior to entering the contact plant and 2) NOx removal from the liquid acid. In a traditional sulfuric acid plant NOx is not involved in the desirable chemistry of the plant because SO₂ is directly oxidized to SO₃ on a solid catalyst in the gas phase. Therefore it is typically advantageous and less expensive to remove NOx to the extent possible before it enters the process and has the opportunity to contaminate the product sulfuric acid.

Gas Phase NOx Removal

In the context of a contact sulfuric acid plant the most desirable location to remove NOx is before the flue gas enters the contact plant, this is done with the use of a selective catalytic reduction (SCR) unit or a selective non-catalytic reduction (SNCR) unit [4]. The SCR process involves the reaction of NO and NO₂ with ammonia or urea in the presence of a catalyst to form nitrogen and water, reactions 2 and 3. The approach and equipment are essentially the same as in a power plant's SCR.



Reaction 9



Reaction 10

Traditional SCR and SNCR technologies are not of interest in the context of the Near Zero Emission Oxy-Combustion Flue Gas Purification program because the goal of the program is to evaluate other more cost effective technologies for flue gas purification. Furthermore NOx cannot be removed before the Task 2 flue gas purification scheme because the Task 2 process relies on NOx for SO₂ conversion to H₂SO₄.

NOx Removal from Liquid Acid

One approach for NOx treatment in the liquid phase processes is to reduce NOx in the product acid by the addition of strong reducing reagents to destroy NOx compounds in the acid. The most common reducing agent used is hydrazine (H₂N₄), hydrazine hydrate (N₂H₄·H₂O) or dihydrazine sulfate ((N₂H₂)₂H₂SO₄) because they are the most effective reducing agents. Other reducing agents are urea (NH₂CONH₂), hydroxyl-ammonium sulfate ((NH₂OH)·H₂SO₄) and hydroxylamine (NH₂OH). Reagents that are non-hydrazine based are typically not used with concentrated sulfuric acid because their reaction rate is too slow to be practical. The reaction between hydrazine hydrate and nitrosylsulfuric acid is as follows:



Reaction 11

The elimination of NOx using hydrazine is affected by several factors:

- Acid Strength – reaction rate is higher in 93% H₂SO₄ than 98% H₂SO₄
- Acid Temperature – reaction rate increases with increasing temperature
- Excess Hydrazine – the reaction rate is roughly proportional to % excess hydrazine
- Sulfur Dioxide – the presence of SO₂ reduces the reaction rate
- Residence time

Hydrazine chemicals are the most common and effective chemicals for NOx destruction in sulfuric acid but these chemicals are extremely toxic and are possible carcinogens. Hydrazine compounds are used to remove similar levels of NOx from sulfuric acid in contact plants as would be seen in the Task 2 process, however the total flowrate of acid requiring treatment is typically small because NOx concentrates in a very specific location in contact sulfuric acid plants where the rate of acid accumulation is low (candle filter drains in mist eliminators). In a traditional contact sulfuric acid plant only a small stream of acid is treated and added back to the process.

When hydrazine is used some amount of excess hydrazine is typically needed to achieve adequate destruction of NOx, however it is important that no excess hydrazine remains in the product acid. Typically a secondary hydrogen peroxide addition is used to consume the excess hydrazine. Treatment of sulfuric acid using hydrazine or hydrazine related compounds is expensive due to the cost of the reagent, the cost of installing an engineered hydrazine storage and delivery system, and the cost of the ozone supply and treatment system. In the context of the Task 2 process these costs are expected to be prohibitively expensive (hydrazine for example is more expensive and more toxic than ammonia).

A second approach for removal of NO_x from liquid sulfuric acid involves the dilution of concentrated sulfuric acid containing nitrosylsulfuric acid. Nitrosylsulfuric acid has a very high solubility in concentrated 93wt% sulfuric acid but has a fairly low solubility in sulfuric acid of 60wt% concentration and below. Nitrosylsulfuric acid concentrations in the candle filters of a traditional contact sulfuric acid plant is typically 5wt% to 20wt%.

When sulfuric acid containing NO_x is diluted the nitrosylsulfuric acid is hydrolyzed and NO_x fumes are released. In sulfuric acid the heat of dilution is substantial and enhances the NO_x removal effect when NO_x containing sulfuric acid is diluted because the diluted acid is substantially warmed. The released NO and NO₂ is of very high concentration and must be captured, for example by contact with water to make a dilute nitric/nitrous acid solution. Low concentration sulfuric acid has no value and is typically prohibitively expensive to concentrate to a saleable concentration of 93wt% or greater.

Subtask 2.5: Mercury Removal Research

The Near Zero Emission Oxy-Combustion Flue Gas Purification proposal included the use of a wet scrubbing process for the removal of mercury from the process gas stream. The scrubbing process uses sulfuric acid at concentrations greater than 80 wt.% H₂SO₄. The mercury in the process gas reacts to form mercury sulfate which precipitates and would be removed from solution by clarification and filtration. There is some risk involved with the process since it was not originally designed as a high pressure process gas containing mercury.

Moderate levels of mercury containment, about 90%, are typically seen in mercury removal technologies for the sulfuric acid industry. This level of Hg containment may be adequate prior to the Task 2 process in the case that any sulfuric acid product needs to be saleable from a mercury impurity standpoint. However in a CPU process a very high level of mercury containment (> 99.9%) is absolutely essential prior to the flue gas entering the coldbox due to the potential severe consequences of mercury in the coldbox. This extremely high level of mercury containment is likely not possible through mercury containment that is designed for sulfuric acid manufacture. Two main scenarios exist:

- 1) If the acid product from the Task 2 process is saleable some Hg removal may needed upstream of the Task 2 process. A mercury guard bed would also be needed downstream of the Task 2 process to ensure that no mercury makes it to the CO₂ purification coldbox.
- 2) If the acid product is not saleable the sulfuric acid product will likely be neutralized, in which case it is likely that the neutralization product will be landfilled and the mercury content will not be an issue. In this scenario a single Hg adsorbent bed would be used prior to the cold box.

Worley Parsons has offered some mercury control alternatives to the wet scrubbing method in the proposal since this method is not widely used in the sulfuric acid industry. The mercury containment methods described below [8] are alternatives to mercury containment that would be needed upstream of the Task 2 process for control of mercury in the potential sulfuric acid product.

Alternative processes such as adsorption of mercury on activated carbon or selenium filters are used in the traditional sulfuric acid industry for control of mercury in the sulfuric acid product. These processes do not involve circulating scrubbing solutions and only passing the process gas through a fixed bed of material. Two parallel units are recommended to allow one unit to taken out of service for servicing and replacement of the materials while the other unit remains on line. There is an ongoing operating cost associated with replacing the material and disposing or recycling of the spent material. The design of the

equipment is simply a pressure vessel designed to hold the required material. Little in the way of ancillary equipment would be required.

Activated Carbon

The adsorption properties of activated carbon have been used for removal of heavy metals (among them mercury), organic pollutants (such as dioxin and furans) and acid gases (HCl, SO₂). Three filter designs are typically utilized and are categorized based on the flow configuration as follows: cross flow, counter-cross flow and cross-current flow. However, the cross-flow carbon filters are most common. The adsorption capacity of the carbon filter is sensitive to humidity in the gas stream and is limited by temperature. Tight control over temperature is needed to avoid volatilization and release of mercury and to avoid creation of “hot spots”. The cross-flow design is used to minimize this risk by distributing the gas equally. Carbon monoxide sensors are installed to detect the formation of fires in the bed. The typical values reported in literature of mercury adsorption efficiency for activated carbon range between 12% and 20% of the carbon weight. Research is always geared towards increasing the porosity of the carbon to increase this efficiency. The pressure drop across the filter depends on the size of the filter bed and the amount of carbon used. If the gas contains particulate the pressure drop will increase eventually requiring replacement and renewal of the bed.

The spent carbon can be thermally treated in rotary kilns to re-establish its adsorption features. Steam is used to create a reducing environment in the activating kilns and avoid oxidation of carbon. Alternatively, the spent carbon can be disposed of in an appropriate landfill. The technology is widely used in the power industry and to remove organic material and heavy metals from off-gas streams at incineration sites in Europe. The main advantages and disadvantages of the activated carbon filter are listed in Figure 2.29.

Advantages	Disadvantages
<ul style="list-style-type: none"> ▶ Modular construction ▶ Minimum ancillary equipment ▶ High removal efficiency and low mercury output ▶ Common reagent ▶ Simple to operate and maintain 	<ul style="list-style-type: none"> ▶ Relatively low loading value ▶ Disposal of contaminated carbon ▶ Sensitivity to temperature and humidity ▶ Side reactions

Mercury removal efficiency is >90%.

Figure 2.29 Advantages and Disadvantages of the Activated Carbon Filter

The cost for activated carbon is approximately \$2100/tonne of carbon. The replacement of the carbon bed will depend on the gas flow and mercury content of the gas. Sizing the unit in terms of carbon loading will take into account the frequency of carbon replacement and maintenance cost. A typical mercury adsorption system would consist of parallel columns such that a column could be taken out of service to replace carbon when it becomes fully loaded (Figure 2.30). Sufficient isolation would be provided to enable the work to be done safely while the other column remains in operation. For this application an activated carbon loading of 10,000 lb would be loaded into a 1900 mm (6.3 ft) diameter column with a carbon bed height of about 3050 mm (10 ft) high. The activated carbon would be able to adsorb about 1500 lb of mercury before needing to be replaced.

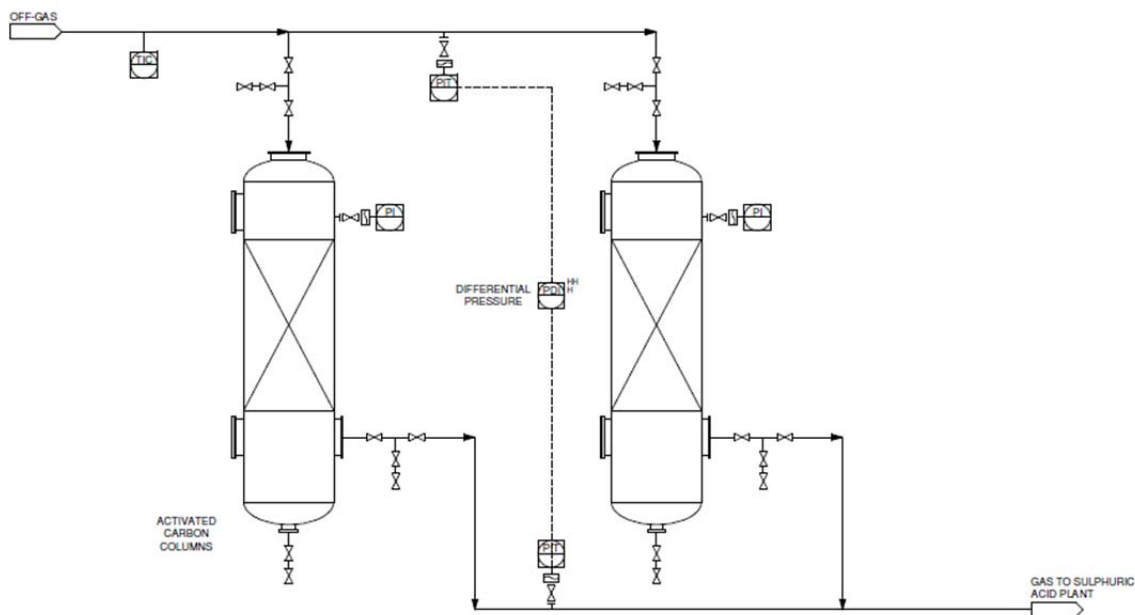
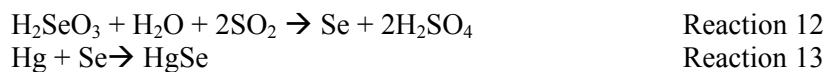


Figure 2.30 Activated Carbon Mercury Removal System

Selenium Filter

Selenium filters were developed by Boliden (currently Outotec) to target and remove elemental Hg from metallurgical off-gases based on the affinity between selenium (Se) and Hg. The filter consists of porous inert material (stainless steel or ceramic grains impregnated with metallic Se) soaked with selenious acid that reacts with water vapor and sulfur dioxide in the process gas to precipitate selenium (Reaction 12). Consequently, Se reacts with elemental Hg vapor in the gas to form mercury selenide, HgSe, (Reaction 13). The Hg removal process is summarized by the following reactions:



The key to the operation of the selenium filter is the speciation of the mercury in the gas. Mercury must be present as elemental mercury for the selenium filter to be effective. Once the mercury and selenium react, the resulting compound has a much lower vapor pressure than either elemental mercury or HgS which ensures low residual mercury levels in the gas as shown in Figure 2.31.

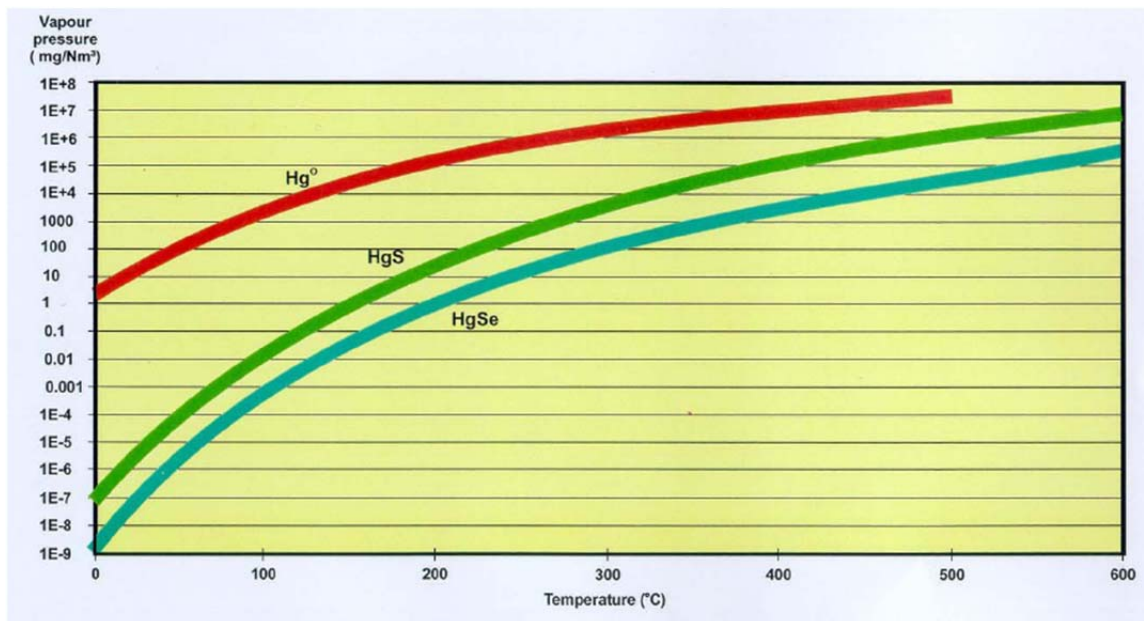


Figure 2.31 Vapor Pressure for Hg, HgS and HgSe

The filter generally consists of two layers or beds. The first layer acts as a dust filter while the second filter is the active medium in which the above reactions take place and HgSe is formed. A schematic of the selenium filter is shown in Figure 2.34.

The selenium filter continues to be effective until the level of mercury in the filter reaches 10-15%wt. The filter can then be treated to recover Hg and regenerate Se. The selenium filter method is suited for low to medium Hg concentrations in the process gas. The filter operates efficiently up to 9 mg/m³. Higher Hg concentration decreases the lifetime of the filter requiring more frequent regeneration of Se, making its operation costly. At lower Hg concentrations, the removal efficiency is decreased because of reduced molecular collisions between Hg and Se.

The temperature of the gases entering the selenium filter is limited to 120°C to avoid decomposition of HgSe in the filter and to enhance the rate of formation for HgSe. Dust loading below 9 mg/m³ is recommended to avoid frequent filter washing and reduce downtime. Water degrades active selenium and the relative humidity in the off-gas needs to be controlled to avoid formation of water droplets.

The selenium filter has been used in metallurgical off-gas applications as well as from geothermal off-gases. In geothermal applications, the steam generated underground contains non-condensable gases such as CO₂ and contaminants such as mercury and hydrogen sulfide (H₂S). The off-gases are treated in a selenium filter to remove mercury which would otherwise be vented to atmosphere. Typical operational parameters for a selenium filter are listed in Figure 2.32. A summary of advantages and disadvantages of the selenium filter method is presented in Figure 2.33.

Item	Operating Parameter
Flow rates through standard filter sizes	535 to 53500 m ³ /h
Effective Hg removal range	Up to 9 mg/m ³
Recommended residence time	2 seconds or more
Operating temperature	120 °C
Removal efficiency	>90 %
Pressure drop	50 mmH ₂ O
Dust contamination	Up to 9 mg/m ³ for feasible operation
Typical filter material usage	1 m ³ of filter material to convert 50 kg of Hg to HgSe
Average lifetime	5 years (depending on mechanical construction of filter, Hg content in flue gases and pressure drop)
Mercury Selenide disposal	Landfilled or processed for Hg recovery and Se regeneration

Figure 2.32 Typical Operational Parameters for a Selenium Filter

Advantages	Disadvantages
<ul style="list-style-type: none"> ▶ Modular construction ▶ No liquids to pump, spill or treat ▶ High mercury removal efficiency ▶ Easy regeneration and recovery processes ▶ Selective for mercury, no side reactions or catalytic activity 	<ul style="list-style-type: none"> ▶ Selenium cost is expensive ▶ Disposal or regeneration of the selenium filter ▶ High mercury loading may require frequent filter washing ▶ Lowering the relative humidity involves higher costs by addition of heat exchanger, fan for compression ▶ Low dust loading required ▶ Low temperature required ▶ There is a possibility of forming other selenium compounds in the filter that would reduce the Hg removal effectiveness

Figure 2.33 Advantages and Disadvantages of the Selenium Filter

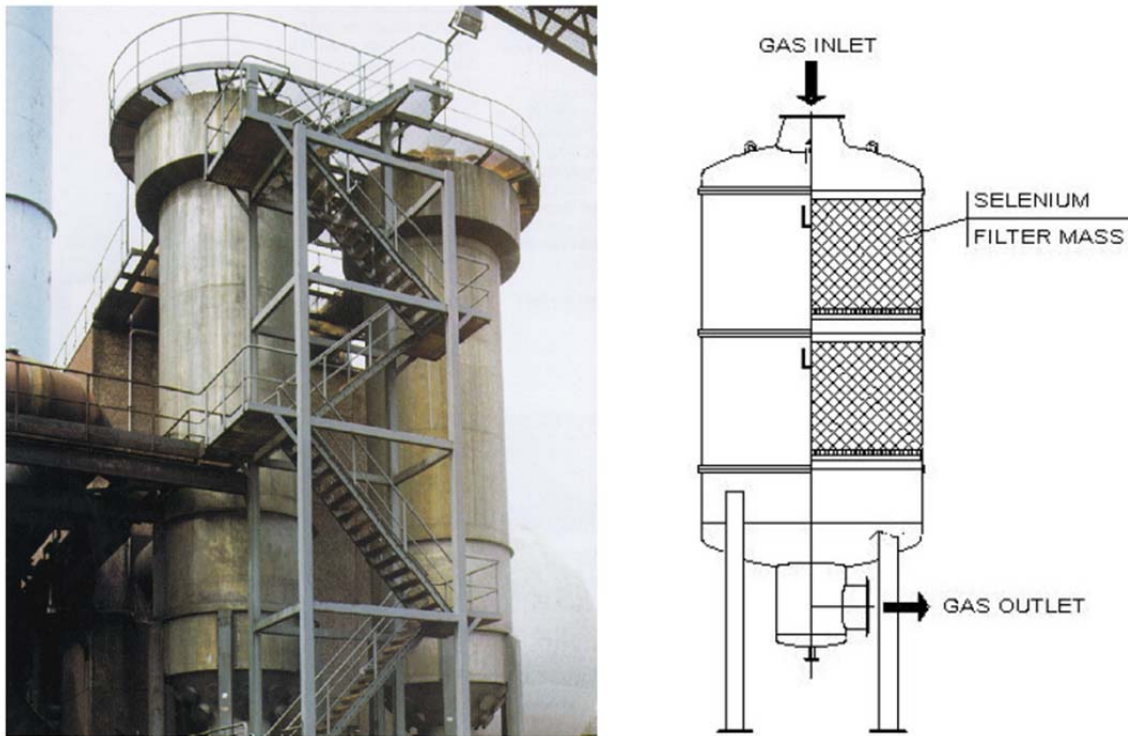


Figure 2.34 Typical Selenium Filter Arrangements

In addition to the operational Selenium disadvantages described above the selenium filter approach would likely not be possible in an Oxycoal CPU because of any potential interactions of selenium with the materials in the CPU coldbox. For example heavy metals in general are known to react destructively with aluminum metal.

Subtask 5.1 Process Simulation

Process simulation of the final Task 2 process scheme required manual iteration using different simulation tools and experimental data due to the complexity of the process simulation and the inability of any available single process simulation tool (e.g. Unisim, AspenPlus, etc.) to accurately predict the thermodynamics, chemistry and reaction behavior of the Task 2 process. The main difficulties in simulating the Task 2 process are related to 1) gas and liquid phase reactions occurring in mass transfer columns (reaction-distillation type problem), 2) general sulfuric acid adsorptive characteristics (e.g., moisture and CO₂), 3) the unique chemistry that occurs between sulfuric acid and NO_x (with this third item being the most complex and sensitive aspect of the system).

The procedure used for simulating the system was to first use a standard process simulation software (Honeywell Unisim) for high level mass and energy balance of the system. In this mass and energy balance simulation simple reactors and component splitters were used to look at the process at a high level. The main purposes being to 1) estimate the required acid recirculation rates needed to manage the system temperatures (for thermal management and for rough vessel sizing), 2) investigate the acid concentrations in the system (moisture management), and 3) in the case of the final simulation iteration, to determine the need for any process changes from a high level mass and energy balance perspective.

Following the mass and energy balance simulation some more detailed reaction modeling was performed to model the NO oxidation behavior of the system to fine tune the NOx conversion assumptions in the various vessels. Next experimental data is used to update the assumed NOx absorption and desorption behavior as well as the SO₂ oxidation behavior. These revised assumptions were then used to update the mass and energy balance simulation for the next iteration.

The low pressure flue gas conditions and composition used in the final Task 2 process simulation was taken from the Foster Wheeler report High Sulfur Bituminous Coal case. Specifically the flue gas for the “Reduced SOx” case was used because it represents the case which is most commercially relevant at this time. In the two high sulfur bituminous coal cases a traditional FGD has been used to remove SOx from the primary air stream. In the “Reduced SOx” case a portion of the secondary air stream has also been treated for SOx removal. The “Reduced SOx” case addresses potential corrosion issues on the superheater/reheater that are possible with a SOx content of above 4000ppm SOx, as described in more detail in the Foster Wheeler report. The “Reduced SOx” case represents the highest levels of SOx that Foster Wheeler would be comfortable with in this oxy-combustion scenario given the corrosion issues and their boiler experience.

The Flue gas from the “Reduced SOx” case leaves the boiler island and is compressed in 5 intercooled-centrifugal compressors (no aftercooler is needed) to an appropriate pressure for treatment in the Task 2 process and subsequently in the cold box portion of the CPU process. The gas conditions entering the Task 2 process are shown below in Figure 2.35. In the compression train a negligible amount of SO₂ is lost through NO₂ catalyzed-oxidation because the residence time in the intercoolers is low. However, roughly 15% of the NOx is lost in the last 2 intercoolers through NO oxidation and contact with water. From Figure 2.35 it is notable that the inlet gas concentration has only 12 times more SO₂ than NOx, on a molar basis, which reflects the much lower SOx levels in the gas stream as compared to the gas composition assumed in the proposal. It is also important to note that in this ‘Reduced SOx’ case the SOx levels fed to the Task 2 process are not very different from the SOx level expected in the flue gas from the low sulfur coal case.

Temperature (F)	203.7
Pressure (psia)	377.6
Mole flow (lbmol/hr)	23373
mass flow (lb/hr)	980940

Mole Fraction	
CO2	0.831545
O2	0.040943
Ar	0.031863
N2	0.086433
SO2	0.004198
NO	0.000335
NO2	0.000067
H2O	0.004260
SO3	0.000000
CO	0.000356

Figure 2.35 Pressurized Flue Gas Composition for Feed to the Task 2 Process

As discussed above the Task 2 related experimentation and literature review has found no method for selective removal of NO_x from the Task 2 process (appropriate to maintain the ability to produce concentrated sulfuric acid as was assumed in the proposal process). With no method to remove NO_x from concentrated sulfuric acid the “NO_x Stripping Reactor” has been removed from the process. In this final process design every mole of product sulfuric acid could contain up to about 0.08 mole NO_x (assuming 100% NO_x capture). This is an extremely high level of NO_x that would introduce significant safety considerations related to depressurization and handling of the product acid.

The best possible yield of sulfuric acid, and maximum possible benefit of the Task 2 process, would be achieved if all the coal sulfur could be sent to the CPU in the form of SO₂ and if all the SO₂ was converted to concentrated, pure, saleable sulfuric acid in the Task 2 process, however as described this is not feasible given the input from FW (this was the assumption in the proposal). In the other extreme, the Task 2 process, as currently configured, cannot produce concentrated acid if the SO₂ concentration to the CPU is too low because the water vapor in the CPU leaving the raw gas compression train would be more than is necessary to produce 93wt% sulfuric acid and the acid product would be too dilute (sulfuric acid concentration is typically too energy intensive to be viable).

As described above a mass and energy balance simulation was first completed with Honeywell Unisim. The mass and energy balance simulation alone was able to identify a necessary minor process change that is due to a significantly lower SO_x concentration (and higher water concentration relative to the SO_x level) in the flue gas. The inlet gas contains roughly equivalent molar amounts of SO₂ and water; this amount of moisture is already enough to make 100wt% sulfuric acid; only about 30% more water is required to make 93wt% sulfuric acid. This small amount water is added to the ‘SO_x Reactor’ however it is not enough to hydrolyze all the SO₃ that is formed in the ‘SO_x Reactor’ vessel. A stream of the circulating ~93wt% sulfuric acid going to the ‘NO_x Stripper’ is added to the ‘SO_x Reactor’ vessel to supply the extra water required to ensure the sulfuric acid concentration in the ‘SO_x Reactor’ vessel does not exceed 100%. Sulfuric acid exceeding 100% concentration (oleum) contains un-hydrolyzed SO₃, which would introduce significant additional safety considerations and material of construction issues. The updated process configuration is shown in Figure 2.36.

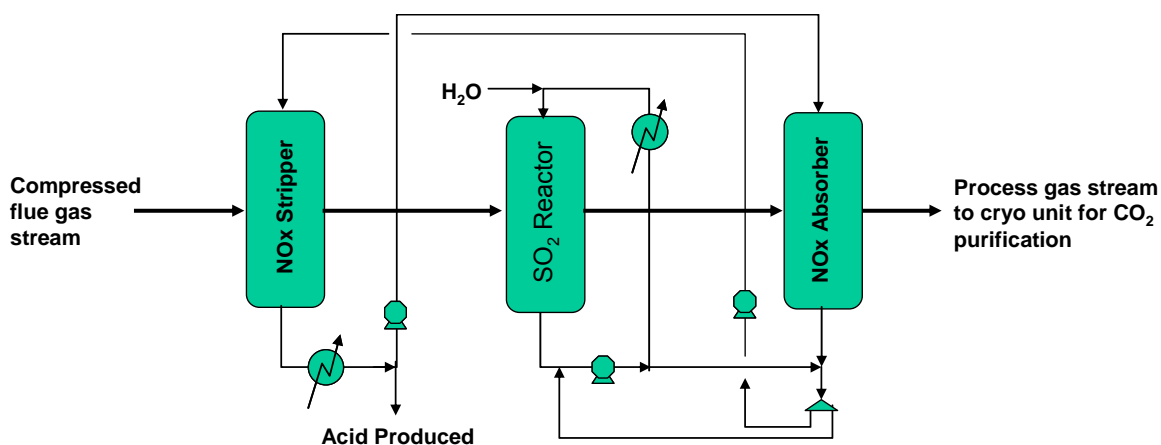
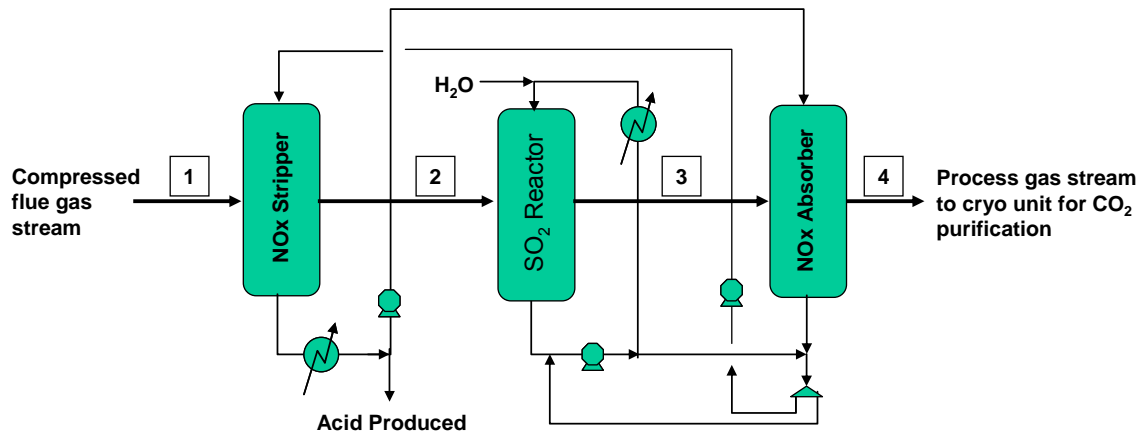


Figure 2.36 Process Schematic of the Final Task 2 Process

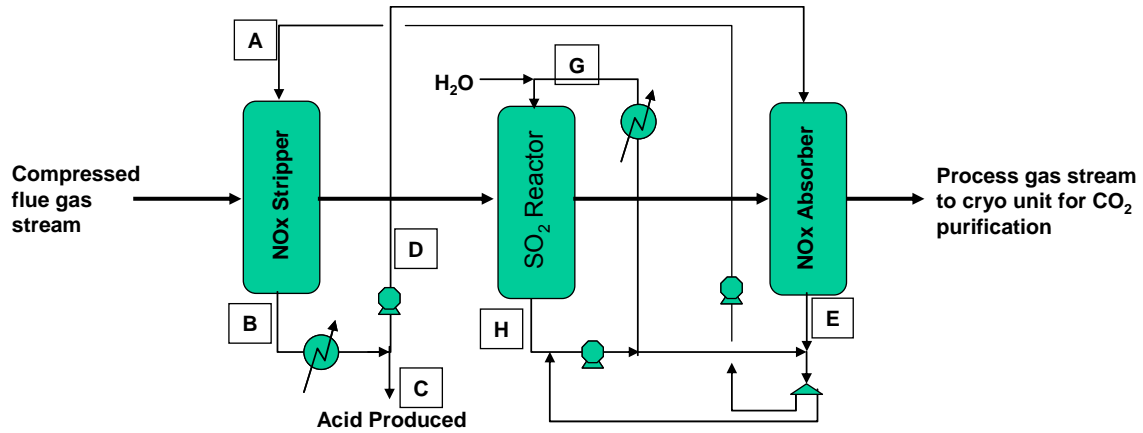
With this updated flowsheet configuration iterations were made between the simulation tools and experimental data to estimate the performance of each of the three vessels. Acid recirculation rates and gas flowrates are used to estimate vessel size and reaction residence times. A high level stream summary of the gas and liquid streams is given in Figure 2.37 and Figure 2.38.



Gas Stream	1	2	3	4
Temperature (F)	203.7	170.3	109.7	104.7
Pressure (psia)	377.6	374.6	371.6	368.6
Mole flow (lbmol/hr)	23373	23422	23321	23117
mass flow (lb/hr)	980940	985852	979574	971063

Mole Fraction	1	2	3	4
CO ₂	0.831545	0.829799	0.833402	0.840744
O ₂	0.040943	0.040522	0.038798	0.039129
Ar	0.031863	0.031797	0.031935	0.032216
N ₂	0.086433	0.086251	0.086626	0.087389
SO ₂	0.004198	0.003770	0.000038	0.000038
NO	0.000335	0.000282	0.000244	0.000001
NO ₂	0.000067	0.007087	0.007428	0.000121
H ₂ O	0.004260	0.000138	0.001172	0.000003
SO ₃	-	-	-	-
CO	0.000356	0.000355	0.000357	0.000360

Figure 2.37 Stream Summary for Gas Streams of Final Process Simulation



Liquid Stream	A	B	C	D	E	G	H
Temperature (F)	122	199	100	100	112	100	145
Pressure (psia)	390.0	377.6	377.6	377.6	371.6	374.6	374.6
Mole flow (lbmol/hr)	2773	2705	135	2570	2773	10692	10692
mass flow (lb/hr)	212554	207594	10380	197214	205726	881225	888043

Mass Fraction	A	B	C	D	E	G	H
H2SO4	0.893	0.919	0.919	0.919	0.881	0.918	0.921
H2O	0.047	0.056	0.056	0.056	0.056	0.029	0.027
NOx	0.060	0.025	0.025	0.025	0.063	0.053	0.052

Figure 2.38 Stream Summary for Liquid Streams of Final Process Simulation

The gas stream conditions for the process are shown in Figure 2.37 and the liquid stream conditions are shown in Figure 2.38. The simulated stream results show that in the ‘NOx Stripper’ a large amount of NOx is desorbed from the NOx-loaded acid. The gas leaving the NOx stripper contains about 7300 ppm of NOx with about 96% of the gas phase NOx being NO₂. A small amount of SO₂ is reacted in the ‘NOx Stripper’ with the majority of SO₂ being reacted in the SO₂ reactor. The acid produced from the ‘NOx Stripper’ has the lowest concentration of NOx in the process at about 2.5wt%.

The majority of gas SO₂ reacts in the ‘SO₂ Reactor’ because this vessel is larger and has much more circulating acid. The rate of SO₂ conversion to SO₃ is dependent on the amount of NOx containing acid present. In the ‘NOx Absorber’ NOx is absorbed by sulfuric acid for recirculation. The gas phase NOx leaving the ‘SO₂ Reactor’ contains roughly 7600ppm NOx. Roughly 98.5% of gas phase NOx is absorbed into the liquid acid in the ‘NOx Absorber’. The absorption rate of NOx is not higher because the concentration of NOx in the acid is very high and because most of the gas phase NOx here is NO₂. Although 98.5% NOx absorption seems fairly high, 98.5% absorption of 7600ppm NOx means that roughly 120ppm of NOx is leaving the Task 2 process. This means that the NOx capture rate for the Task 2 process is only about 70%.

Literature and experimental data show that maximum absorption rates for NOx are achieved when equal molar amounts of NO and NO₂ are contacted with acid that is substantially free of absorbed NOx. In the ‘NOx Absorber,’ and in the rest of the process, gas phase NOx is mostly composed of NO₂ due to the size of the 3 vessels (large residence time) and due to the fast gas phase reaction rate of NO to NO₂ at the process conditions. The vessels size cannot be decreased to reduce the amount of gas phase NO₂ because vessel size is determined by the acid and gas flowrates in the process.

For these reasons the NOx capture rate of the Task 2 process actually ends up being fairly low. The relatively high levels of NOx leaving the Task 2 process would likely present other material of construction and process issues in the downstream equipment such as the cold box and VPSA unit. The NO₂ present in the treated gas from the acid process can be scrubbed by water to improve the overall NOx removal efficiency to > 90%, while protecting the downstream equipment. This will require additional capital investment and it will also generate additional acidic waste water.

Subtask 5.3 Commercial Viability of H₂SO₄ Process

Sulfuric acid market

Of all heavy industrial chemicals, sulfuric acid is said to be the one produced in the largest tonnage. As well, sulfuric acid is perhaps the most fundamentally important chemical that it plays a part in virtually all manufactured goods [9, 10].

World Production

In 2008, the world sulfuric acid production was estimated to be 205 million tonnes. The breakdown in terms of sources is as follows:

- Elemental sulfur 64%
- Smelter gas 28%
- Pyrites 7%
- Other 1%

Sulfuric acid produced from the oxy-combustion flue gas purification process falls in to the ‘Other’ category.

Consumption

The breakdown in terms of consumption worldwide is as follows:

- Phosphate Fertilizer 48%
- Single Super Phosphate (SSP) 8%
- Ammonium Sulfate 7%
- Copper Leaching 4%
- Titanium Dioxide Production 3%
- Animal Feed 3%
- Technical Uses 2%
- Nickel Leaching 1%
- Other 24%

World Trade

The majority of sulfuric acid is produced and consumed in relative close proximity to each other. In 2007, only 16 million tonnes of acid was traded on the international markets. This is only about 8% of the total world production. Some of this world trade in sulfuric acid does enter the USA market mainly to meet demand in the fertilizer industry.

Prices

Historically, the price for sulfuric acid has remained fairly constant, particularly through the 1980's and 1990's (Figure 2.39). In the late 1990's, there is a slight drop in prices because of the world recession. As the world came out of the recession we see the price of sulfuric acid increasing in-line with the general increase in manufacturing and country GDP.

The run up in the price of elemental sulfur and sulfuric acid beginning in 2007 saw the price for these commodities reach unprecedented levels which were unsustainable. When the world-wide recession hit at the end of 2008, prices collapsed to below the levels prior to the run up in prices. Figure 2.39 shows the Producer Price Index (PPI) for sulfuric acid to the end of 2008 and the sudden downturn in prices.

Sulfuric acid prices for May-June 2009 were \$0 to \$30 per tonne, US Gulf ex-terminal (Figure 2.40). The traded market for sulfuric acid remains essentially stalled. Suppliers are focusing on balancing the market in terms of supply and demand. In early 2009, involuntary producers of sulfuric acid announced cutbacks in metals production because consumption of the by-product sulfuric acid had declined. In late 2009, some idle production has come back on-line but there still remain producers that are shut down due to labor issues and supply of concentrate.

The prices reported in the press are generally spot market prices which are subject to fluctuations based on supply and demand. Most producers and consumers of sulfuric acid have entered into 'long-term' contracts where the price of sulfuric acid is fixed and not subject to a lot of volatility. It is assumed that acid produced from flue gas purification plants will be marketed and sold according to the terms of long term contracts that are negotiated considering the current cost of acid.

For the purposes of this study, a price of \$50 per tonne of acid (100% basis) is assumed.

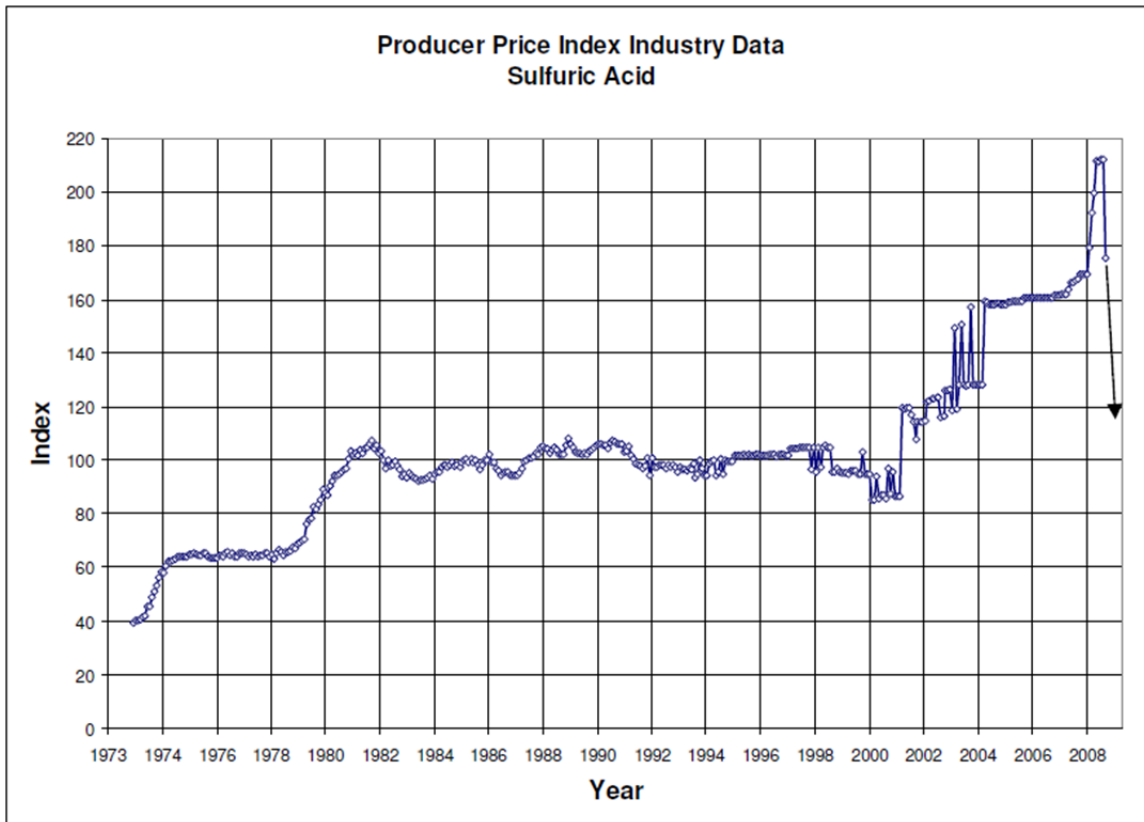


Figure 2.39 US Bureau of Labor statistics – Producer Price Index for Sulfuric Acid

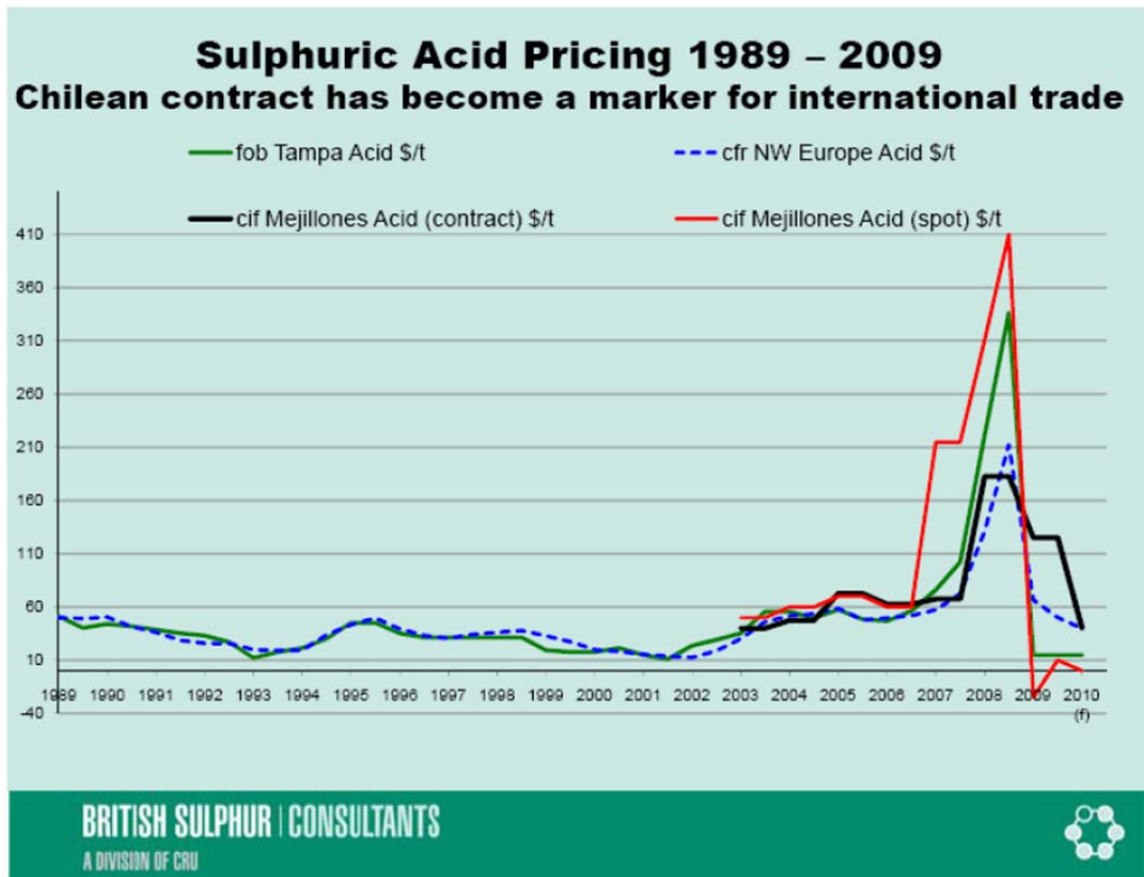


Figure 2.40 Sulfuric Acid Pricing 1989-2009

USA and North American Market

In 2008, the breakdown of the USA sulfuric acid market is as follows:

<u>Production</u>	Smelters	2,300,000 tonnes
	Sulfur Burning	28,000,000 tonnes
<u>Recycled</u>		3,150,000 tonnes
<u>Net Imports</u>		2,500,000 tonnes
<u>Total Supply</u>		35,950,000 tonnes

The USA does import sulfuric acid primarily into the Florida region to meet demand of the phosphate fertilizer industry. This excludes the acid that is imported from Canadian producers.

The production from the proposed facility is 325 MTPD or 118,625 tonnes per year (365 days/year). This represents 0.3% of the total supply of acid in the USA market for 2008.

Figure 2.41 shows the sulfuric acid producers for North America. Most production and hence consumption is located in the eastern USA with concentrations in the Florida and Gulf Coast areas. Production and consumption of acid in the western USA is centered on the mining and metals, fertilizer, and petroleum (acid regeneration) industries.

New Production

The following new production is scheduled to come on line in the next year or two in the USA:

Freeport McMoran (Safford):	420,000 MTPA
Martin Midstream (Beaumont):	150,000 MTPA
Southern States Chemicals (Wilmington):	150,000 MTPA

The new sulfuric acid plant for Freeport McMoran supplies an acid leach project in Arizona. The Martin Midstream plant is being built to supply local demand and consumption of sulfuric acid. Southern States Chemicals supplies sulfuric acid along the east coast and is building a new plant to replace two smaller older plants while increasing production two-fold.

Outlook

The long-term outlook for sulfuric acid production and consumption in the USA is flat. One consulting firm anticipates a 1.5 million tonnes per year increase in acid consumption through to 2020. During the same period production is predicted to increase only 0.15 million tonnes per year. The difference between overall production and consumption is made up by acid imports. Current acid import is approximately 2.5 million tonnes per year.

Long term predictions of acid production, consumption and prices should be used with caution since they are essentially guesses. This problem with these predictions is illustrated by the fact that no one foresaw the run-up in prices and shortages that were seen in 2007 and 2008.

If this technology is widely adopted in the USA, there is the potential to produce 350,000 to 1,800,000 tonnes per year of acid if 10 to 50 plants are built over the next 10 years. This additional production will partially reduce the amount of acid imported into the USA each year. The degree to which this occurs will depend on many factors such as the location of the plant, transportation cost, the cost of imports, etc.

The remaining acid production will simply displace ‘voluntary’ acid produced by burning sulfur. The market will set the ‘involuntary’ acid price such that producers that burn sulfur to produce acid will be forced to cut-back production.

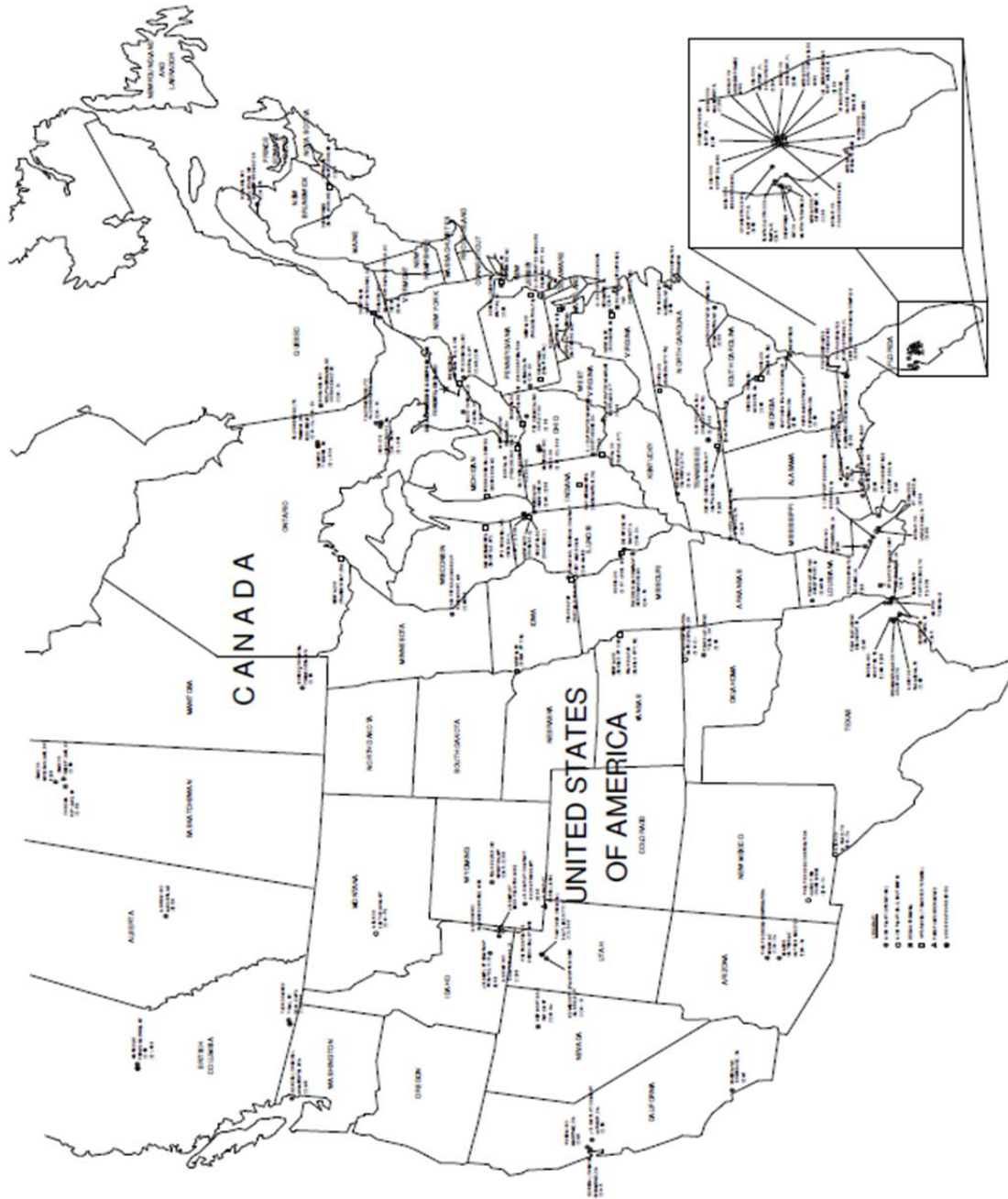


Figure 2.41 North American Sulfuric Acid Producers

Pennsylvania and Illinois Acid Markets

Norfalco, a North American supplier and distributor of sulfuric acid were contacted to obtain information on the sulfuric acid markets in the Pennsylvania and Illinois markets. Figure 2.42 shows Norfalco’s North American Distribution network.

There is plenty of competition in the Pennsylvania and Illinois markets so it would not be difficult to sell the entire production of sulfuric acid from a number of potential Oxy-Combustion power plants that could be using the Task 2 technology. The ‘local market’ refers to the sulfuric acid market that can be served by truck transportation. Variations in the local market can be overcome by shipping the acid by rail tank car which opens up a larger market area. The cost of providing loading facilities for both truck and rail is more but provides more flexibility and options for disposing of the acid.

Norfalco recommend that a producing facility maintain 3 to 4 weeks of acid storage capacity. This amount of storage helps to mitigate risks related to market and production fluctuations. This study has currently assumed a 5000 MT storage tank giving ~10 days storage capacity. The amount of storage that will be required will depend on many factors which at this stage are based on very loose assumption about the plant size, location, market, etc.

Norfalco indicate that it is extremely difficult to predict pricing one year to the next and predicting prices 4 to 5 years from now is nearly impossible.

Companies that starting up acid production facilities that are not already acid producers often choose not to market the acid themselves due to the resources required to do it properly. Many companies instead opt to sell to specialist such as Norfalco that already have the infrastructure in place, market knowledge/awareness, transportation emergency response capabilities and a large customer base to spread out supply risks. The income from the sale of product acid is more consistent and predictable when this approach is used.

Norfalco offer a free service to sulfuric acid producers/suppliers where they share information on the sulfuric acid market, distribution business and market projections. This service can be used in the future when the technology is being proposed for a specific customer or site.

Transportation and Logistics

As stated earlier, the majority of sulfuric acid is produced and consumed in close proximity to each other. The majority of the acid imported into the USA is from Canada. The acid is produced from the various smelters in northern Ontario and Quebec. This ‘involuntary’ acid is transported in large quantities by rail tank car into the markets in the northeast USA.

The primary restriction on the distribution of sulfuric acid is the high cost of transportation. The importation of Canadian smelter acid is a bit of an exception but it works because the acid is produced at low cost and large quantities of acid are transported.

In the eastern USA, there are two main importers of acid; Norfalco and Chemtrade Logistics. Both companies have extensive infrastructure for the storage, handling, transportation and distribution of sulfuric acid.

Over long distances, sulfuric acid is shipped by tank car in unit trains from the producers to terminals where it is stored and distributed to local customers by tank car or tank truck. Rail-to-truck transfer facilities avoid the need for storage facilities.

In North America, there are many producers and distributors of sulfuric acid. Some producers market their acid directly into the local market while others utilize distributors/traders. Some of the main producers and traders in the sulfuric acid market are:

<u>Company</u>	<u>Region</u>
Norfalco	Eastern USA
Chemtrade Logistics	Eastern USA
Southern States Chemicals	Eastern USA
Martin Midstream	Texas, US Gulf Coast
SATCO Florida,	US Gulf Coast, South-East USA
Rhodia	Across the USA (Acid Regeneration)
DuPont Chemical Solutions	Across the USA (Acid Regeneration)
PVS Chemicals	North, North-East USA



Figure 2.42 Norfalco Supply and Distribution Network for Sulfuric Acid

Acid Production and Marketing

The acid produced from the purification of oxy-combustion flue gases is small in comparison to the entire USA market for sulfuric acid. The acid produced is considered ‘involuntary’ acid because it is a byproduct of another process and the operator has little choice but to continue to produce the acid.

There should be no problem in ‘disposing’ of the acid produced from a typical facility in the local market. Factors that will impact on the ability to market the acid are:

- Acid is produced at a marketable concentration (i.e. 93 to 98% H₂SO₄). The market for lower acid concentrations is smaller and the acid may need to be shipped further to consumers who can use the acid.
- Acid is produced free of impurities that may limit consumers who can use the acid.
- Location of the plant relative to consumers and other producers

If Praxair's technology is applied to a facility located in the eastern USA, there should be no problem in marketing and selling the acid, if it is of appropriate purity. The acid produced would likely displace the production of 'voluntary' acid or acid that is shipped into the area from more distant producers.

The production and marketing of sulfuric will not be part of the core business of the owner and operator of a power generating plant. Therefore, it is unlikely that the owner will spend the time and resources to market, sell and distribute sulfuric acid to local consumers.

The most likely scenario, with acid of appropriate purity, is that an established sulfuric acid trader and marketing company will be engaged to remove and distribute the acid under a long term contract. As mentioned above in the byproduct purification section, if the acid is not of appropriate purity (with acid containing high levels of NO_x, for instance) an acid distributor would be unwilling to accept the acid because the acid would typically have to be mixed in storage vessels with other high purity acid. The distributor would not want to risk contaminating their entire inventory of acid because of one off-spec shipment.

Commercial Byproduct Viability

The high level of NO_x in the sulfuric acid product makes the acid unmarketable to conventional customers. The only potential customers for acid containing these levels of extremely high NO_x are customers dealing with nitration reactions this segment of the sulfuric acid market is a very small share and the demand for acid from these industries is small, such that the quantity of acid produced here would certainly overwhelm this limited market.

The high NO_x levels in the potential sulfuric acid also introduces corrosion and safety issues making any potential customers for this acid more unlikely to accept the product. Any dilution of acid will liberate NO_x which becomes a safety and hygiene issue.

Disposal (neutralization) of the product acid with limestone is the most likely possibility however when diluting and neutralizing the acid stream NO_x would be released and would have to be captured in a closed system process containing an elaborate vent and scrubbing system. Disposing of the product sulfuric acid defeats the purpose of Task 2 concept because this arrangement would still require limestone purchase and gypsum disposal,

Capex Estimate

WorleyParsons completed an initial capex estimate in year 2 of the project based on the proposal process where it was assumed that the maximum level of SO_x could be sent to the CPU and that concentrated saleable (high purity) sulfuric acid could be produced with a very high conversion of SO_x to sulfuric acid. The details of this capex estimate are shown in Appendix A. This initial capex estimate for the idealized proposal scenario showed a relatively low capex.

A second capex estimate was not performed due to the technical process issues as well as the commercial byproduct viability issues discussed above related to purity, small potential market size, and acid product safety.

Commercial Process Viability

The investigated Task 2 concept does not constitute a commercially viable process given the program goals of producing concentrated saleable sulfuric acid from oxy-combustion flue gas. Due to acid purity issues the produced acid would need to be neutralized on site with careful attention given to the disposition of NO_x. Other better alternatives for SO_x and NO_x removal include traditional removal

options via wet-FGD and SCR or the Task 3 process. Foster Wheeler feedback on the high sulfur coal case indicates that a substantial FGD must already be included in the boiler island so there is not potential for a large capex or opex benefit as compared to the traditional SO_x, NO_x removal options.

Aside from the assumed performance of the process simulation there are still questions related to the viability of the process in a scaled up version related to potential corrosion of process equipment given the very high levels of NO_x and safety issues related to NO_x. Other technical issues include: The relatively low simulated NO_x capture rate and potential column plugging given the plugging issues experienced during experimental testing.

Conclusions

The Task 2 experimental apparatus performed as designed and the experiments involving SO_x, NO_x and sulfuric acid were conducted in a safe manner without incident. The NO_x absorption experiments showed a good ability of sulfuric acid to absorb NO_x. The best absorption performance was seen when the NO:NO₂ ratio was 1:1, as is predicted in literature. For some NO_x absorption experiments, formation of a solid white material was observed. This white substance is predicted in lead chamber process literature and was known as ‘chamber crystals’.

Higher temperature NO_x desorption experiments up to 235°F showed that instead of desorption high levels of NO_x would still absorb into sulfuric acid that already contained thousands of ppm of dissolved NO_x. An inability to remove NO_x from sulfuric acid by thermal desorption (or any other method) means that NO_x would continue to build up to very high levels in the re-circulating sulfuric acid in the process. Very high NO_x levels in the acid would limit the NO_x removal efficiency of the Task 2 process. Collection of this experimental data was necessary to arrive at these conclusions because there was no experimental data in the literature collected at relevant conditions.

As part of Subtask 2.3 activated carbons were investigated as NO_x removal catalysts. The activated carbons showed a poor ability to catalytically remove NO_x from sulfuric acid. Some literature data indicated that an oxygen containing gas would help strip NO_x from sulfuric acid. However experimentally it was found that the presence of oxygen actually made NO_x removal from sulfuric acid more difficult as compared to the comparison case where N₂ was used to strip NO_x from acid.

In Subtask 2.4 other traditional methods of NO_x removal from sulfuric acid were studied for product purification. The candidate methods were taken from the sulfuric acid industry. Two methods for liquid phase NO_x removal from sulfuric acid were explored. Gas phase NO_x removal prior to the Task 2 process (via a typical SCR unit) is not an option for this project because the Task 2 concept depends on NO_x for conversion of SO₂ to sulfuric acid.

The relevant liquid phase removal options are: NO_x destruction with hydrazine (or a hydrazine related reagent) and NO_x removal through acid dilution. NO_x destruction with hydrazine may be a technically feasible option for NO_x removal from concentrated sulfuric acid. However, treatment of acid with hydrazine would add significant complexity, safety, operating cost and capex requirements to the process. A second method of liquid phase NO_x removal involves dilution of the concentrated sulfuric acid, from about 93wt%, to roughly 60wt% sulfuric acid. Re-concentration of acid is energy intensive and would add significant complexity, capital and operating cost to the process.

Because no suitable method was identified for high efficiency removal of NO_x from sulfuric acid within the Task 2 process (in Subtask 2.3 or 2.4), the process design has been changed to reflect the scenario

where all the captured NO_x is produced with the ‘product’ sulfuric acid. Due to this process change the ‘product’ sulfuric acid contains very high (percent levels) of NO_x dissolved in the sulfuric acid. The produced acid will have to be neutralized for disposal as a waste stream. Extra capital equipment would still be required from a safety standpoint to capture NO_x fumes generated during neutralization, for example.

Feedback from WorleyParsons has indicated that the sulfuric acid trade is active in the region of the US where high sulfur coal is mined and typically used (Illinois and western Pennsylvania). The acid market in these locations could easily absorb the volume of acid which would be produced from a number of power plants equipped with a hypothetical Task 2 process; however the purity of the acid would be a problem due to the high NO_x levels in the acid. Acid distributors and customers would be unwilling to accept acid having high levels of impurities, regardless of the price (or credit), because they would not want to risk contaminating their storage and transport equipment.

Process Simulation

Flue gas flow and composition from Foster Wheeler’s high-sulfur-coal boiler simulations has been used with Task 2 experimental data to complete an updated process simulation of the Task 2 SO_x/NO_x purification equipment. The SO_x content of the flue gas is significantly lower than the proposal process due to boiler constraints. The process configuration has changed to deal with the lower SO_x concentration.

While the SO_x removal efficiency of the simulated process is high, >99%, the simulated removal efficiency of NO_x from the compressed flue gas is only about 70%, meaning that roughly 120 ppm of NO_x leaves the Task 2 purification process. This high level of NO_x leaving the ‘NO_x Absorber’ is attributed to the high concentration of NO₂ in the process and the relatively low effectiveness of sulfuric acid to absorb NO_x when the NO₂:NO ratio is much greater than 1. The high levels of NO₂, and corresponding low levels of NO seen in the process simulation stream results, are due to contactor vessel size, the speed of the NO oxidation reaction, and the inability to selectively remove NO_x from the product sulfuric acid. The overall NO_x removal efficiency can be improved to >90% by installing a water scrubber downstream of the acid process.

Sulfuric acid produced from the Task 2 process is still simulated to be ~93wt% (with respect to water and H₂SO₄), The acid produced from the process is predicted to contain roughly 2.5wt% NO_x, which is a very high level of NO_x impurity compared to the NO_x impurity spec in commercial grade acid of <5ppmw.

In summary, the sulfuric acid process can remove >99% SO_x and >90% NO_x from the oxy-combustion flue gas. However, the acid produced would not meet commercial specs and it must be disposed of by neutralization. As a result, overall value of this technology is lower than the activated carbon process being developed under Task 3. Therefore, Praxair has decided not to continue further development on this technology at this time.

Task 3 – SO_x/NO_x/Hg Removal for Low Sulfur Coal

Approach

Task 3 was composed of 5 subtasks. In an initial stage, Task 3.1 focused on screening of commercially available catalytic carbon materials for their performance to remove SO₂ from concentrated CO₂ stream. A bench-unit was designed and built as scope of subtask T3.2. A comprehensive experimental investigation was carried out under subtask T3.3. A paper study for mercury removal was completed as part of subtask T3.4. The aim of subtask 3.5 followed the successful demonstration of excellent simultaneous SO_x and NO_x removal in previous tasks, and had as main objective designing, building, and operation of a dual bed continuous unit. The latter was used to assess the activated carbon longevity and its performance change over time.

The following paragraphs provide the detailed approach used for each subtasks. In addition, technology, process and chemistry are described as background information.

Technology Description

The purpose of Task 3 project was to investigate an alternative method of SO_x and NO_x removal from flue gas produced by burning low sulfur coal in oxy-coal power plants. The process applies to oxy-combustion flue gas which is to be further compressed and processed for CO₂ capture and sequestration (CCS). Figure 3.1 shows a high level diagram of an oxy-combustion boiler for this application where two streams of recirculated flue gas are used to moderate boiler temperature. Figure 3.1 shows the primary ‘air’ being treated in an FGD due to material of construction issues in the coal pulverizing and conveying equipment. Secondary air is not required to be treated. Combustion energy is used to generate steam and a turbine is used for power generation. The flue gas produced from the boiler island is then treated in the CO₂ processing unit (CPU) for CO₂ compression and purification.

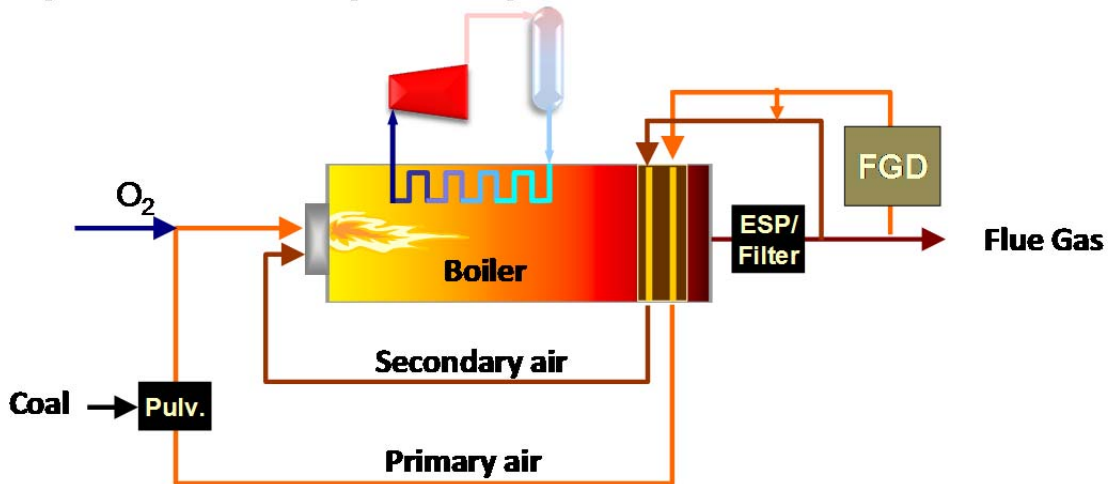


Figure 3.1 Schematic of the Oxy-coal boiler island

In a typical power plant SO_x is removed by reaction with lime or limestone, producing disposable gypsum using a wet or dry-FGD at atmospheric pressure. The lime/limestone reagent cost, gypsum disposal cost, parasitic power plant load and equipment capital costs can be substantial. NO_x removal is typically achieved in an SCR which requires substantial capital investment and also requires ammonia reagent.

The goal of this project was to develop a process, which simultaneously removes SO_x and NO_x within an oxy-coal CPU. Figure 3.2 shows a high level diagram of the entire CPU process. Raw boiler flue gas enters the process and is cooled before a raw gas compression stage. Next the flue gas is treated in the

proposed Task 3 process for SO_x and NO_x removal. Following the Task 3 process the flue gas is treated in a Cold Box cycle to concentrate the CO₂, and further compress it to the final product pressure. The ‘Cold Box Vent’ stream is processed in a vacuum pressure swing adsorption (VPSA) process to recover CO₂ which is recycled to the raw gas compressor. The process vent gas, mostly composed of O₂, N₂ and Ar is heated and expanded for power recovery.

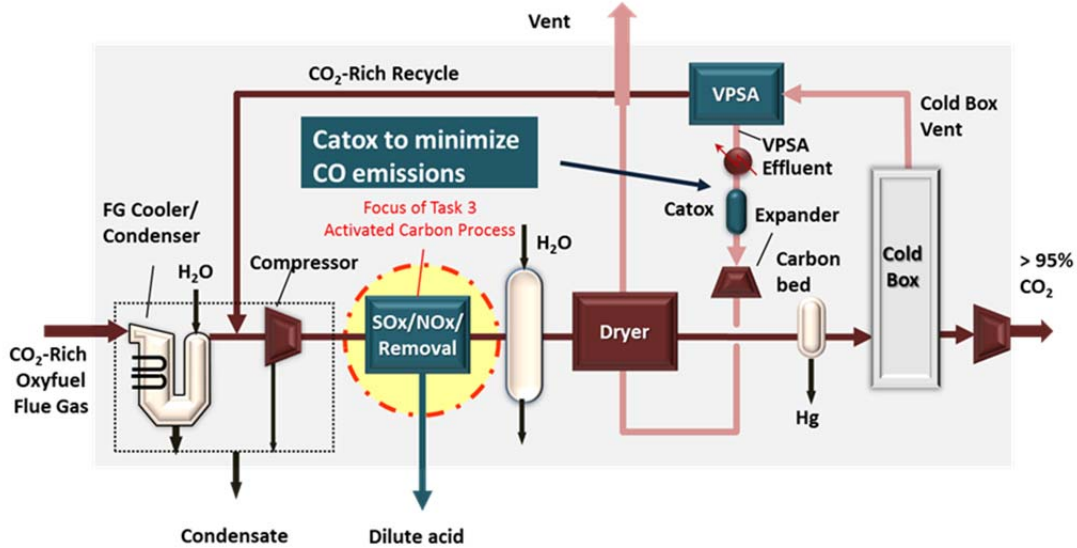


Figure 3.2 A CPU with Activated Carbon Process for SO_x/NO_x Removal

Process Description

Figure 3.3 below shows the configuration of the Task 3 process for flue gas purification by simultaneously removing SO_x and NO_x at high pressure. In order to ensure continuous operation, the process must consist of at least two activated carbon beds alternatively operated in adsorption and regeneration modes. Typically the flue gas containing SO_x and NO_x passes through the carbon bed from bottom to top. Once the carbon bed in service is almost saturated with contaminants a valve system switches the flue gas feed to the second bed, while regeneration starts for the saturated bed. Regeneration of the carbon material is achieved by passing a stream of water from top to bottom. The waste water can be recycled in order to minimize the waste water generated. A drying step is required to remove the water adsorbed on the active sites in order to complete the regeneration stage. The nitrogen can be used for drying. The Task 3- treated flue gas would be further processed in the CPU to produce purified CO₂ stream.

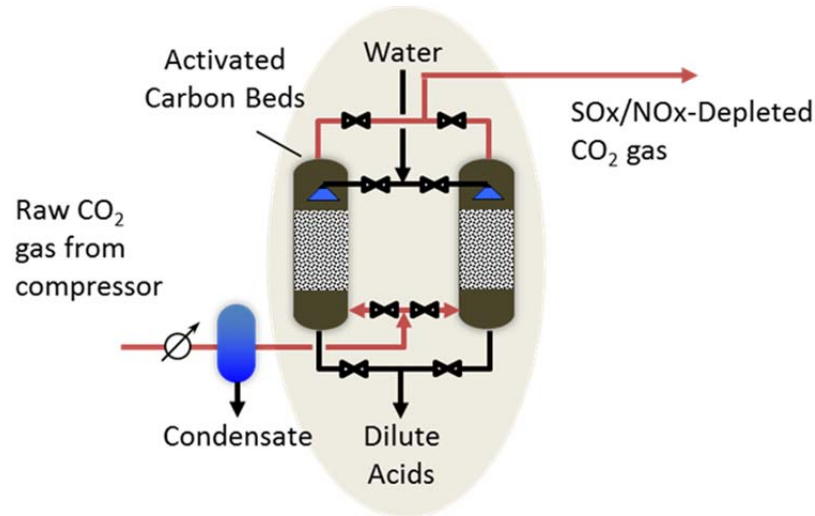
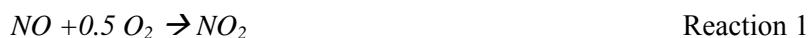


Figure 3.3 Task 3 Activated Carbon Process for SO_x/NO_x Removal

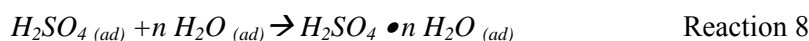
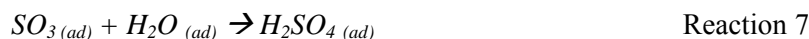
Chemistry Description

In the Task 3 process a number of heterogeneous and homogeneous reactions take place for NO_x and SO_x oxidation, and formation of the sulfuric and nitric acids. The elevated pressure which would be present in the CPU is another key feature which increases the rates of adsorption related reactions and mass transfer fluxes.

Adsorption stage involves homogeneous and catalytic oxidation of the contaminants and adsorption of the oxidation products on the activated carbon material. The inferior oxides of sulfur and nitrogen are oxidized to their superior oxides by oxygen through the flowing reactions:



Reaction 1 takes place homogeneously in the gas phase and is enhanced by high pressure and low temperature [11]. Reaction 2 is heterogeneously catalyzed by the activated carbon. NO₂ and SO₃ are the species that are adsorbed on the carbon. Water presence in the vapor phase significantly affects the reaction mechanism for SO₂ removal. One of the proposed mechanisms [12] for SO₂ adsorption onto activated carbon in the presence of oxygen and water vapor is given below:

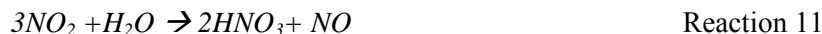


This mechanism suggests that once the H_2SO_4 is produced the active sites occupied by water and sulfur trioxide are freed and the activated carbon retention capacity increases. In addition the hygroscopic nature of the sulfuric acid makes possible to fix the water molecules from the gas stream. NO_2 can react with SO_2 in homogeneous phase and can act as a catalyst for oxidation of SO_2 .



Reaction 9 indicates that the presence of NO_2 enhances the oxidation of SO_2 . If O_2 is present in excess, the NO formed in Reaction 9 can be easily re-oxidized.

Once the activated carbon is saturated, the SO_x and NO_x components breakthrough and their presence in reactor gas effluent can be detected. The adsorption capacity of the activated carbon can be restored by passing a water stream over the carbon bed. In this manner water reacts with SO_3 and NO_2 forming the corresponding acids.



The regeneration stage consists of washing the activated carbon bed with water followed by drying with an inert gas stream (i.e. N_2 or CO_2). Consequently, most of the sulfur oxides can be captured as sulfuric acid. However, due to the stoichiometry of Reaction 11, a third of the NO_x adsorbed on the activated carbon are produced back as NO during the regeneration stage.

Subtasks 3.1 – SO_x and NO_x Removal Material Selection

The subtask 3.1 addressed selection of adequate activated carbon materials. Material selection was based on testing commercially available materials for SO_2 removal. Since SO_2 is typically the contaminant with a higher concentration, performance of its removal was considered as a first requirement for a preliminary material performance screening.

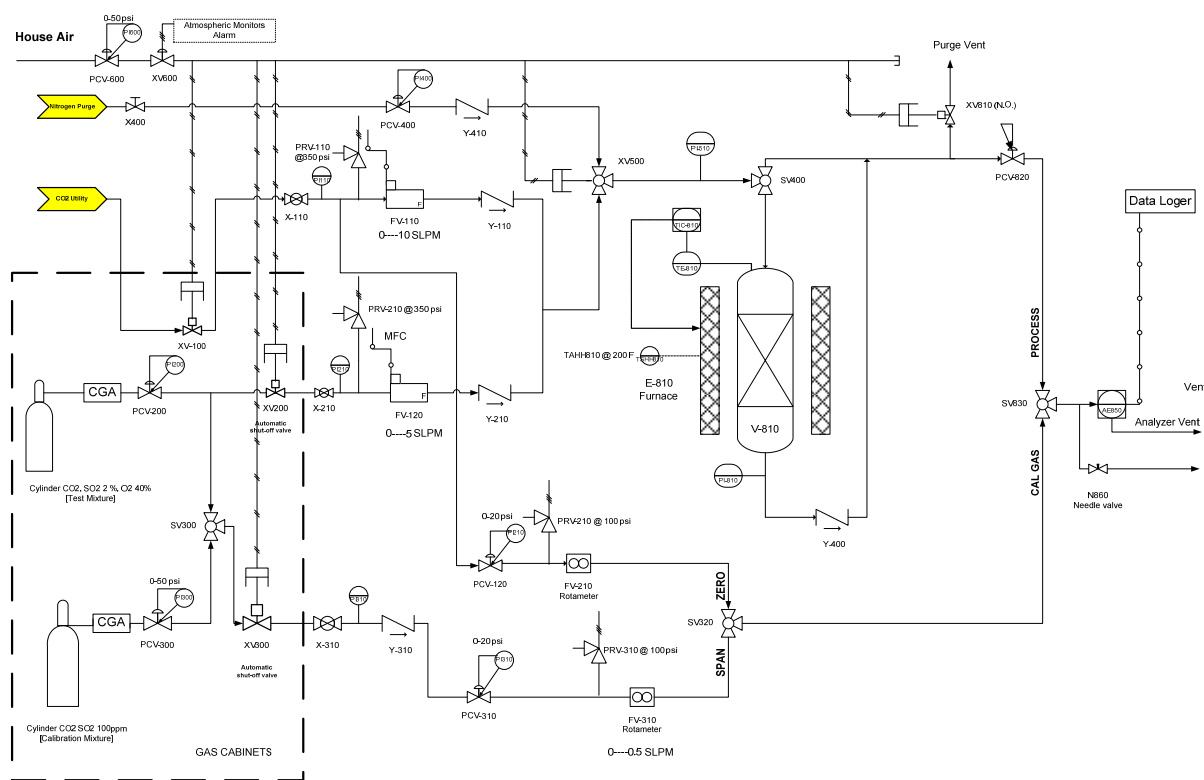


Figure 3.4 PI&D of the Experimental Set-up for Material Testing

The PI&D of the experimental set-up for material screening is given in Figure 3.4. Each material was loaded as a fixed bed in a $\frac{3}{4}$ " tube with a length of 12". A flow of process gas of 3 SLPM was passed over the fixed bed, ensuring at least 6s residence time. The process gas source was obtained by blending a mixture of 2% SO₂, 40 % O₂ in CO₂ from a gas cylinder, with pure CO₂ delivered directly from a service tank. The typical composition of the process gas fed to the activated carbon bed was about 2000 ppm SO₂, 4% O₂ in CO₂. For tests to be performed at 80 C (176 F), the $\frac{3}{4}$ " tube was placed in a furnace, which was controlled based on the temperature measurement taken by a thermocouple inserted axially in the middle of the bed. The process gas pressure was maintained at about 15 bar (221 psia).

The test procedure consisted of three consecutive steps. First, a break-through test for SO₂ was carried out by passing the process gas containing SO₂ over the activated carbon bed. The SO₂ concentration was monitored continuously by means of a PG250 Horiba Analyzer. The test was completed when the SO₂ concentration in the effluent stream reaches 100 ppm. In the second step, the bed saturated with SO₂ was regenerated by water washing. In the last step, a small amount of inert gas, more specifically N₂, was passed through the bed to remove free water. The materials were tested for at least three consecutive cycles. The performance index utilized to compare various activated carbon materials was calculated as the amount of SO₂ removed per unit weight of carbon in the bed. Six different materials were tested. The material that had the capacity to retain the highest amount of SO₂ was selected for further testing of simultaneous removal of SO_x and NO_x.

Subtask 3.2 – Design and Construction of the Bench Unit

The scope of this subtask was to build a bench-scale unit operated in batch mode for a comprehensive experimental investigation of simultaneously SO_x and NO_x removal over a wide range of operating conditions and feed compositions. The PI&D of the bench-unit is given in Figure 3.5. A fixed bed test

reactor containing about 100 g of activated carbon, and a simulated flue gas flow of 10 SLPM were used. The test reactor had a diameter of 1", while the length of the carbon bed was about 18". The simulated gas flow mixtures flows from top to bottom. A high precision high pressure water pump was used to provide the amount of process water so that the feed composition achieved up to 1800 ppm of water vapors. On top of the activated carbon bed, 6" height of inert ceramic beads were used to ensure mixing of the process gas with process water, and water vaporization.

Typical flue gas composition used during the investigation was:

85-90 % (vol.) CO₂
4-6 % (vol.) N₂
2-6 % (vol.) O₂
200-750 ppmv NO
1000-3000 ppmv SO₂

The source of SO₂ component was provided by gas cylinders of 6 % SO₂ in N₂, while the source for NO component was provided from 3% NO in N₂ gas cylinders. High purity O₂ gas cylinders were used to deliver the required O₂, while pure CO₂ was delivered directly from a service tank. Mixtures with various compositions and humidity levels were prepared by adjusting the mass flow controllers used to deliver each gas stream and the high precision high pressure water metering pump for water delivery.

In order to maintain the test bed at constant temperature, up to 80 C (176 F), the 1" test reactor was placed in a heating blanket, which was controlled based on the temperature measurement taken by a thermocouple inserted axially in the middle of the activated carbon bed. The process gas pressure of up to 15 bar (221 psia) was maintained by means of a back-pressure regulator. The experimental-set up was provided with capabilities for regeneration by washing it with water, and drying with nitrogen.

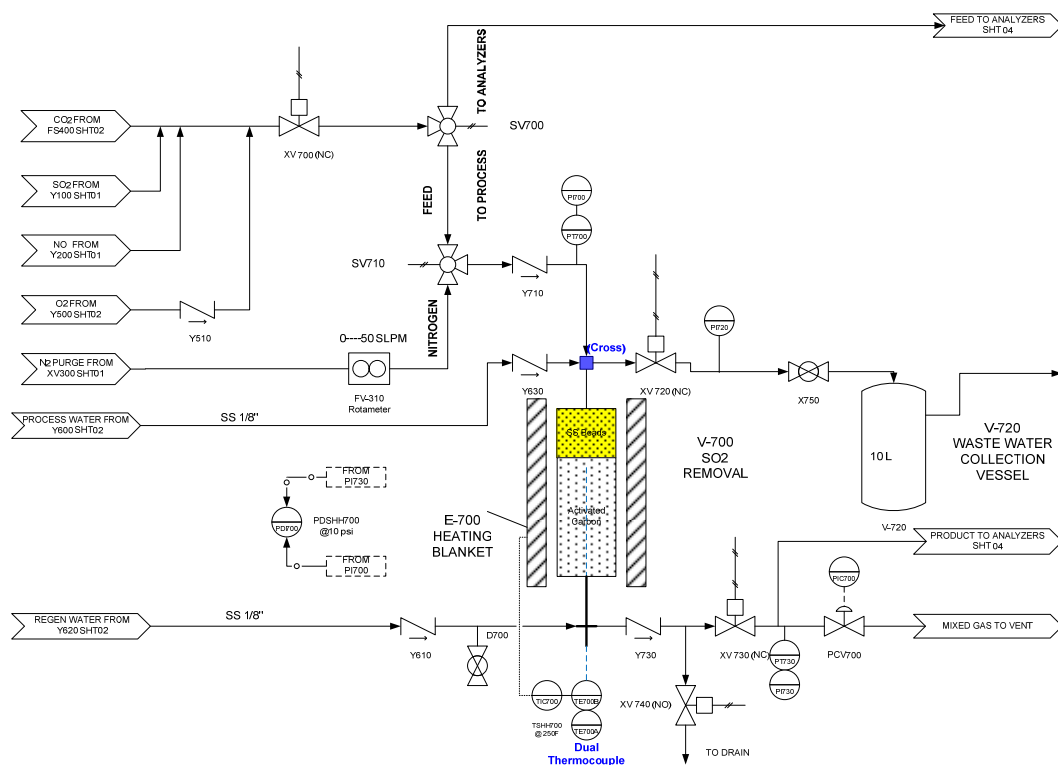


Figure 3.5 P&ID of the Bench Unit for Simultaneous SO_x/NO_x Removal

The SO₂, NO, and NO₂ concentrations of the gas stream exiting the test reactor were monitored continuously by the Emerson Analyzer. A sample conditioning system based on Nafion membrane was utilized to remove the water contained in the process gas stream before sending it to the analyzers.

A fairly high degree of automation was included to comply with safety requirements, to allow remote control, and acquire relevant experimental data. For this purpose a Programmable Logic Controller (PLC) and a user interface design in LabView was used. Due to high toxicity of the gaseous components involved, precautions were taken to ensure safety measures and protection of operators. The feed and calibration gases containing SO₂ and NO were placed in a secured gas cabinet provided with appropriate vents. Continuous atmospheric monitors for the toxic components were installed. Any detection of the toxic gases initiated the automatic shut-down of the system. Automatic shut-off valves, for the feed gases and water used for process and regeneration, were provided in the system for this purpose. In case of emergency shut-down, a flow of nitrogen purged the entire system.

The bed was regenerated by flowing water from bottom to top such that the total volume of regeneration water flown was at least 6 times the carbon volume. The waste water was collected in a vessel, neutralized with sodium bicarbonate and discharged. Waste water samples were collected for selected experiments and analyzed for their content of the following ions: *Sulfates* (SO₄²⁻), *Nitrates* (NO₃⁻), *Nitrite* (NO₂⁻). A Hach 890 colorimeter was used for this purpose.

Subtask 3.3 – SO_x/NO_x Removal Tests

An experimental plan was designed to investigate the influence of several key operating parameters on process efficiency and carbon capacity to retain the SO_x and NO_x. The investigated operating parameters

were: temperature, pressure, inlet composition (NO / SO₂ molar ratio), presence of water in the inlet flue gas stream, and total inlet flowrate (residence time). A two-level factorial design was employed to screen the impact of key process variables for simultaneous removal of SO_x and NO_x on activated carbon. The values for the high-low levels considered for each parameter are given in Table 3.1.

Table 3.1 Ranges for the Two Level Factorial Design for Selected Parameters

Parameter	Low	High
Temperature, C	20	80
Pressure, bar	3.4	15
Feed Humidification	No (Dry)	Yes (Saturation)
Total Feed Gas Flow, SLPM	10	25
SO ₂ Concentration, ppm	2000	4000
NO Concentration, ppm	0	750

A total of 24 carbon beds were tested for selected conditions. For each bed the adsorption-regeneration cycle was repeated 3-5 times. During each breakthrough test the reactor gas effluent composition was continuously monitored. The breakthrough completion was considered at the time when either contaminant (SO_x or NO_x) achieved 30 ppm in the reactor gas effluent. For the adsorption stage, the process performance was determined by calculating the amounts of contaminants retained on the activated carbon, as well as the efficiency of their removal from the gas stream. The retention of each contaminant is calculated as:

$$\text{Retention}_i = \frac{\left[\int_0^{\text{BT}} (F_i \cdot y_i^{\text{in}}) dt - \int_0^{\text{BT}} (F_T \cdot y_i^{\text{out}}) dt \right] \cdot \frac{1}{V_0}}{m_{\text{carbon}}}, \frac{\text{moles of SO}_2 \text{ or NO}}{\text{g Carbon}} \quad (1)$$

Where:

- i NO, or SO₂
- F_i gas flow of fed contaminant from source, SLPM
- y_iⁱⁿ molar fraction of contaminant i from source
- F_T total gas flow rate at the reactor outlet, SLPM
- y_i^{out} molar fraction of contaminant i at reactor outlet
- t time, min
- BT breakthrough time (to 30 ppm of SO₂ or NO), min
- V₀ molar volume in standard conditions, l/mole

A cumulative molar retention can be calculated as:

$$\text{Retention}_{\text{SO}_2+\text{NO}} = \text{Retention}_{\text{SO}_2} + \text{Retention}_{\text{NO}} \quad (2)$$

The removal efficiency for each component is calculated as

$$Efficiency_i = \frac{\left[\int_0^{BT} (F_i \cdot y_i^{in}) dt - \int_0^{BT} (F_T \cdot y_i^{out}) dt \right]}{\int_0^{BT} (F_i \cdot y_i^{in}) dt} \cdot 100 \quad (3)$$

Subtask 3.4 – Mercury and Residual NO_x Removal Research

In any conventional coal fired power plant, mercury emission is an environmental issue, wherein current regulations in several countries require its removal down to less than 5-10 mg/MWh. However, in any oxy-coal combustion power plant with CO₂ capture, mercury is not only an environmental issue but also an operational issue specifically to any aluminum based heat exchangers (BAHX) used in the CO₂ clean-up and processing unit. It may be expected that mercury should be removed down to 0.01 µg/Nm³ (this is the current standard applied in any NG/LNG plant) [13]. A literature survey was conducted to assess the current state of art for mercury removal options.

Subtask 3.5 – Continuous Operation Unit

A continuous unit was designed and built to address the scalability of the process, to prove continuous operation 24 h x 7 days per week, and to test the activated carbon material longevity.

The system was designed to fit in a walk-in hood. It was assembled on three removable skids: *gases and water supply skid*, *reactor skid*, and *analytical skid*. This modularity ensured easy access for maintenance and potential modifications. The supply skid contained the mass flow controllers for the source gases, the water pumps for process water and regeneration water, and a high pressure high precision pump for liquid SO₂ delivery. The gas supply system delivered CO₂, specialty gases and N₂. The CO₂ was delivered from a six-ton bulk tank located outside the building. SO₂ source was either a 6 % SO₂ in N₂ mixture delivered from a gas cylinders or liquid SO₂. NO source was a 3 % NO in N₂ mixture delivered from a gas cylinder. The cylinders of toxic gases were placed in gas cabinets adjacent to the hood.

The P&ID of the reactor skid is given in Figure 3.6. It consisted of two fixed bed reactors holding activated carbon. Each bed had a diameter of 2” and a length of 20”. To ensure good flow distribution a segment of inert packing was placed above and below the carbon bed. The flue gas containing SO_x and NO_x passed through the carbon bed from bottom to top. Once the carbon bed in service was saturated with contaminants, a valve system switched the flue gas feed to the second bed; and regeneration started for the saturated bed. Regeneration of the carbon material was achieved by flooding the carbon beds with water from bottom to top. A pair of electronic level indicators was used to show the water level in the reactor vessel and signal when the water covered the height of the carbon bed. Once flooded, the reactor held the water for 10 min, then the water was drained at the bottom of the bed by slightly pressurizing the reactor with nitrogen. This flooding sequence was repeated at least 6 times to ensure removal of the sulfuric and nitric acid formed during the regeneration stage. After washing with water, the carbon bed was dried using nitrogen at 180 °F. The dried bed was cooled by passing nitrogen at ambient temperature.

The simulated flue gas contained 450 ppm SO₂, 200 ppm NO, 4 % O₂, 94 % CO₂, water vapor of about 1725 ppm (saturation level), and N₂ as balance. The gas flow was delivered at 250 psia and ambient temperature. The unit was designed for continuous operation. For this purpose full automation was implemented to meet safety standards and allow it to run unattended. The reactor outlet gas composition was continuously monitored using an MLT Rosemount/Emerson analyzer. During the regeneration stage, potential gases degassing from the carbon beds were redirected towards a second analyzer (Horiba PG-

250) by using a secondary flow of carbon dioxide. This was done to quantify the amount of contaminants that were not captured in the liquid phase during the regeneration stage.

Adsorption/regeneration cycles were carried out 24/7 for 40 days. The waste water was neutralized before discharging. Occasionally, the waste water was sampled and its content of SO_4^{2-} , SO_3^{2-} , NO_3^- , and NO_2^- was analyzed in order to determine the amount of SO_x and NO_x converted to sulfuric and nitric acid. Standard colorimetric methods for waste water analysis were used.

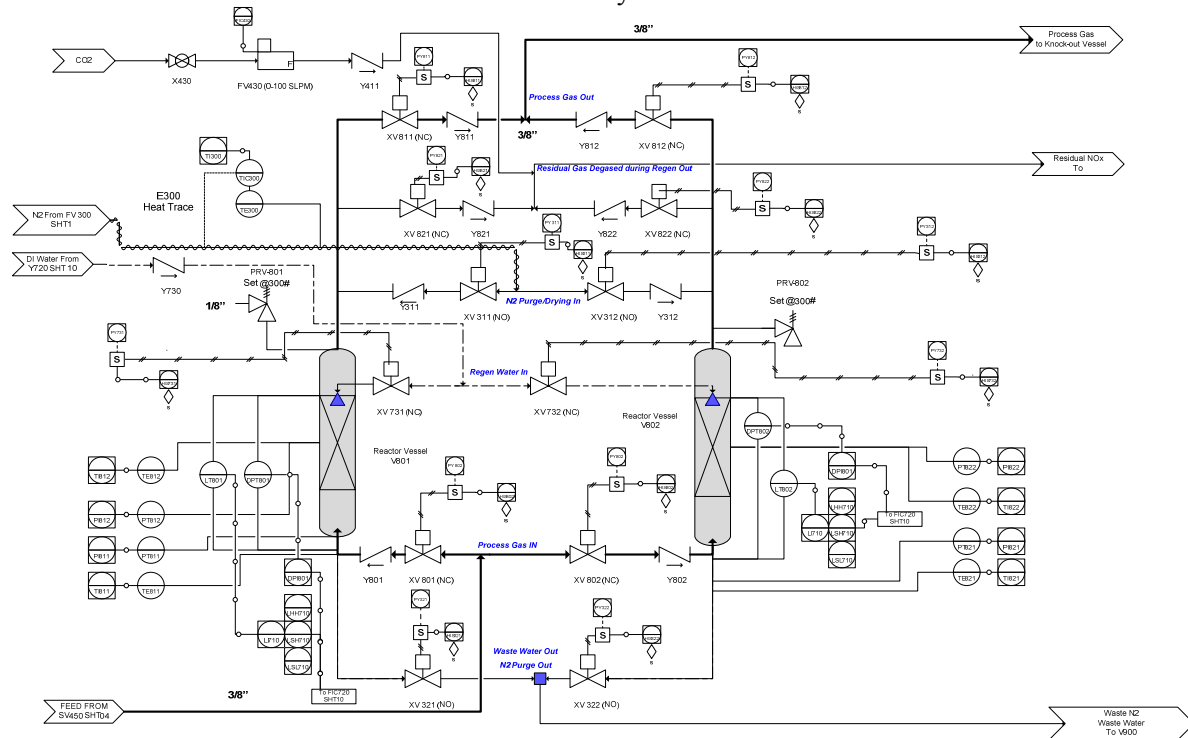


Figure 3.6 Dual Bed Reactor System for Simultaneous SO_x/NO_x Removal

The main goal of the experimental investigation is to understand how the carbon material capability to simultaneously remove traces of SO_x and NO_x evolve during a period of two months of continuous operation. The workflow for the proposed experimental program is given in Figure 3.7.

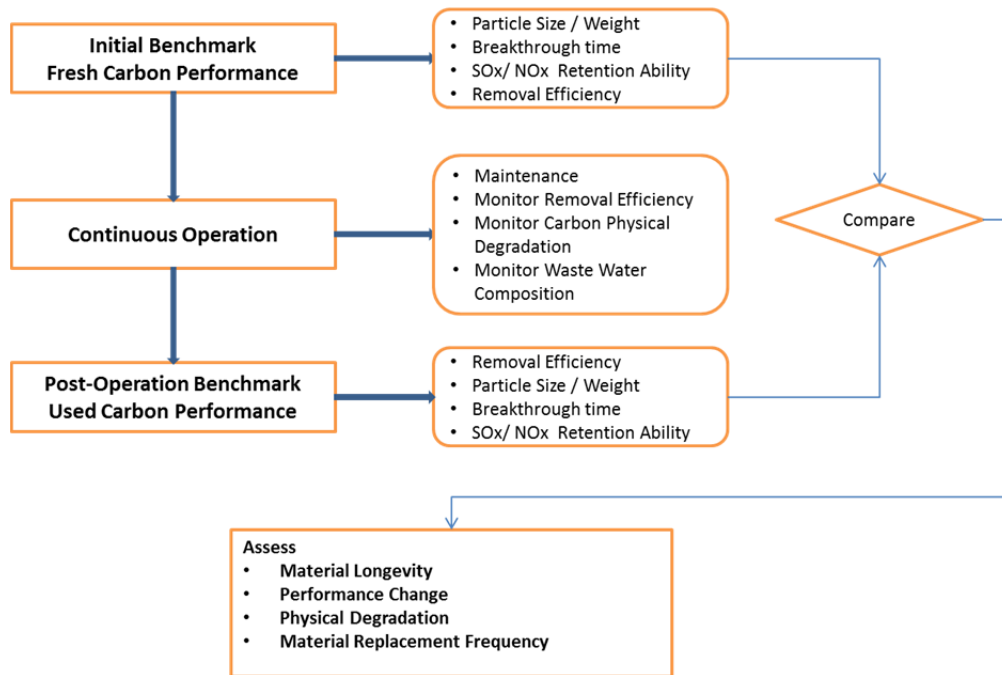


Figure 3.7 Workflow to Assess the Activated Carbon Material Longevity

First a benchmark is established for the fresh carbon. More specifically, the breakthrough time and consequently the initial amount of SO₂ and NO retained per unit mass of activated carbon, was determined for a set of inlet conditions for both beds. For the benchmarking purpose, the adsorption stage was conducted till breakthrough of any of the contaminants occurred. In this particular study, the breakthrough time is considered to take place when any of the contaminants: SO₂ or NO_x concentration reaches 30 ppm in the gas stream leaving the reactor skid.

After the benchmarking was defined, the unit operated almost continuously for 40 days. The advanced automation and safety features allowed the unit to run 24 h/day with minimum supervision and unattended during weekends. The outlet concentration of all components was monitored continuously. It was sought to understand primarily if continuous operation altered the carbon material performance. In order to ensure the process continuity, two parallel beds were used. While one bed operated in adsorption mode, the second bed was regenerated. A generic operating schedule is given in Table 3.2.

Table 3.2 Dual Bed Activated Carbon Unit Cycle Steps

Cycle	1			2		
Bed A	Adsorption			Washing	Drying	Hold
Bed B	Washing	Drying	Hold	Adsorption		

Continuous operation was configured so that the adsorption stage duration was at least equal or higher than the duration of the regeneration (washing and drying of the other carbon bed). A continuous and smooth transition from the bed in service to the regenerated bed was achieved.

At the end of continuous operation period, a similar systematic evaluation of the breakthrough time, and SO_x/NO_x removal efficiency and capacity was reassessed. The results were compared with the initial benchmarking in order to conclude how the activated carbon material changed its capability to simultaneously remove SO_x and NO_x.

Results and Discussion

Subtask 3.1: SO_x and NO_x Removal Material Selection

Six samples of commercially available activated carbon were tested. Figure 3.8 compares the SO₂ removal performance of these samples. The SO₂ retention is calculated using equation (1) and then is scaled based to the best performance among all experiments. Figure 3.8 gives a comparison on relative bases for all samples investigated, and each cycle.

For the first cycle, the sample was loaded as received from the suppliers, while the following cycles are performed after the materials had undergone regeneration by water washing. No extensive drying was applied; therefore the moisture content in the bed in subsequent cycles was significantly higher as compared to the first cycle. This explains lower SO₂ retention by the carbon bed in the first cycle as compared to the following 2 cycles.

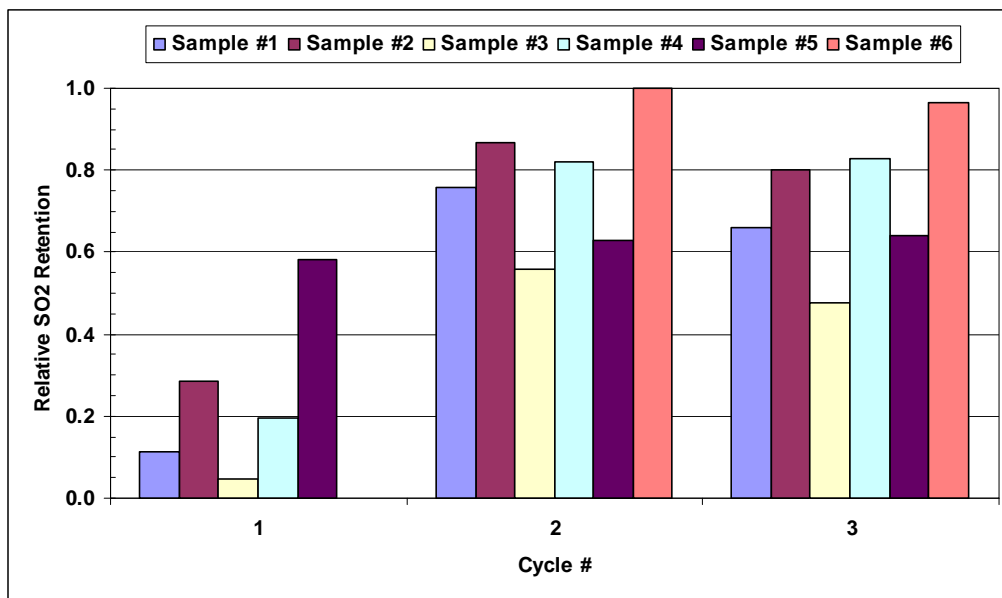


Figure 3.8 Relative Retention of SO₂ for Different Activated Carbon Samples

The relative SO₂ retention on the tested samples ranged from 0.55 – 1 (excluding cycle 1 results). Considering the variations in test conditions, measurement errors and limited number of tests, the performance of these samples are considered comparable. Material represented by Sample #2 was selected for simultaneous SO_x and NO_x removal in the bench unit designed and assembled as part of subtask 3.2.

Subtask 3.2: Design and Construction of the Bench Unit

The bench unit for simultaneously SO_x and NO_x removal is shown in Figure 3.9. It had a compact lay-out to fit all the components in a designated hood. Easy access to all manual valves and instrumentation was available in order to maintain safe and efficient operation. The gas cabinets containing the cylinders with toxic gases for process investigation and calibration are shown in Figure 3.10. Also, Figure 3.10 shows on the right hand side the PLC box.

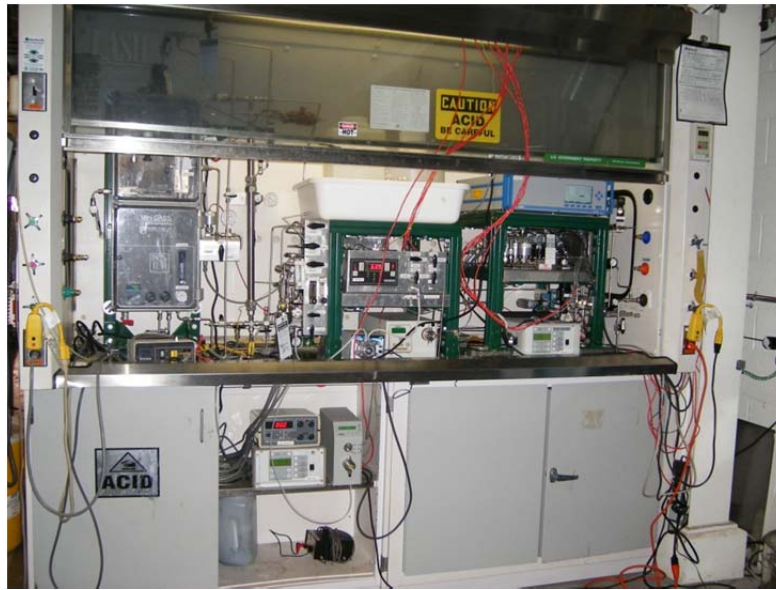


Figure 3.9 Bench Unit for Batch Mode Operation



Figure 3.10 Gas Cabinet for Toxic Gas Cylinders Storage and PLC Box

One of the challenges encountered during operation of the experimental set-up was related to the humidification of the feed stream. The initial solution was to inject a small amount of water to the main gas stream before entering the reactor. It was observed that the process water delivery and its vaporization prior to entering the reactor bed did not provide a constant flow and composition in the feed stream of the water vapors. To avoid this shortcoming, the system was modified to include a humidifier vessel. This enabled the CO₂ stream to pass through a column of water and to saturate with water vapors. The humidifier vessel concept is shown in Figure 3.11. The vessel consists of pipe with 4" diameter and 3' height, and contains 0.5 l water. The CO₂ stream with flows in the range of 10-25 SLPM is fed through a 1/4" pipe and directed towards the bottom of the vessel. A sparger delivers the gas flow across the vessel cross-section. Steel wool is used as packing to ensure enhanced gas-liquid interfacial area. In this manner

the gas bubbles through the liquid water from bottom to top, leaving the vessel close to saturation conditions. A baffle was provided to minimize the possibility of carrying liquid water along with the gas stream.

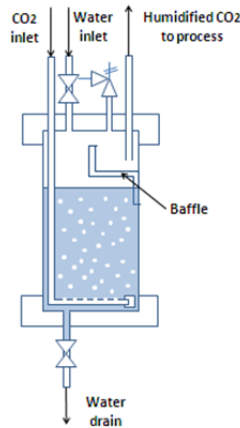


Figure 3.11 Schematic of CO₂ humidifier

The water content in the CO₂ stream was confirmed by performing humidity measurements using a Moisture Monitor Series 35 from Panametrics. The measurements showed good correlation with the theoretical saturation levels. This design was used for a more in-depth investigation of the water content impact on the process performance.

Subtask 3.3: SO_x/NO_x Removal Tests

The results of a typical breakthrough test are shown in Figure 3.12 as time dependence of measured reactor outlet concentration for SO₂ and NO. Usually the NO breaks through first and exhibits a gradual increase of outlet concentration as compared with SO₂ which shows a sharper breakthrough. These breakthrough curves were used to calculate the retention and contaminants removal efficiency using the equations (1) – (3).

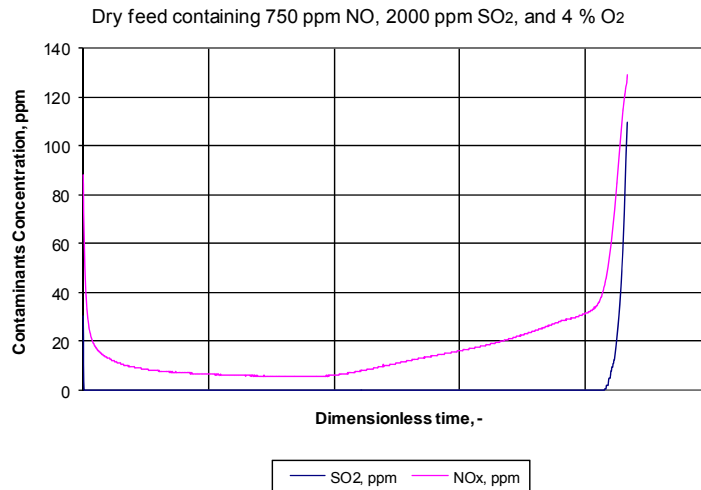


Figure 3.12 Reactor Outlet SO₂ and NO_x Concentrations as a Function of Time

The experimental results for each bed reported on relative bases are given in Table 3.3. The retention values reported in Table 3.3 are scaled using the bed number 9 as benchmark. The molar retention considered is an average for the number of adsorption-regeneration cycles completed for each bed. In Table 3.3, columns I and J contain individual relative retentions of NO and SO₂ respectively, while column K shows the combined relative retention. Columns L and M display the removal efficiency as calculated by equation (14). Overall the results obtained indicate a good simultaneous removal of SO_x and NO_x with efficiency higher than 99% for SO₂ and 93% for NO_x. The influence of the operating conditions investigated is discussed below.

Table 3.3 Activated Carbon Process – Bench Unit Results

Bed Index	Total Flow SLPM	Inlet Composition			H ₂ O in Feed	Temp C	Press. psig	Relative Retention (Benchmark Bed 9)			Efficiency	
		SO ₂ , ppm	NO, ppm	O ₂ , %				NO	SO ₂	NO+SO ₂	NO, %	SO ₂ , %
A	B	C	D	E	F	G	H	I	J	K	L	M
1	10	0	750	0	No	20	220	0.0	NA	0.0	0.00	NA
2	10	0	750	4	No	20	220	1.7	NA	0.4	99.30	NA
3	10	2000	750	4	No	20	220	1.0	0.9	0.9	97.33	99.99
4	10	0	750	6	No	20	220	2.0	NA	0.5	97.20	NA
5	10	2000	750	4	No	80	220	0.6	0.6	0.6	97.30	99.99
6	10	0	750	6	No	80	220	1.1	NA	0.3	99.33	NA
7	10	2000	0	4	No	20	220	NA	0.6	0.4	NA	99.99
8	10	2000	750	4	Yes	20	220	1.6	1.6	1.6	97.30	99.99
9	10	2000	750	4	No	20	220	1.0	1.0	1.0	97.50	99.99
10	10	2000	0	4	Yes	20	220	NA	1.3	0.9	NA	99.99
11	10	2000	0	4	Yes	20	220	NA	1.3	1.0	NA	99.99
12	10	2000	750	4	No	20	220	1.0	0.9	0.9	99.80	99.99
13	10	2000	0	4	No	20	220	NA	0.4	0.3	NA	99.99
14	10	2000	750	4	Yes	20	220	1.0	1.0	1.0	97.60	99.99
15	10	2000	750	4	Yes	20	220	1.8	1.8	1.8	98.05	99.98
16	25	2000	750	4	Yes	20	220	1.0	1.0	1.0	96.95	99.97
17	10	2000	750	4	Yes	20	50	0.3	0.3	0.3	93.04	99.97
18	10	4000	210	4	Yes	20	220	0.1	0.9	0.7	93.90	99.99
19	10	4000	510	4	Yes	20	220	0.4	1.1	0.9	96.94	99.98
20	18	2000	750	4	Yes	20	220	0.9	0.9	0.9	94.72	99.97
21	10	2000	750	4	Yes	20	150	0.7	0.8	0.8	97.45	99.98
22	10	3000	510	4	Yes	20	220	0.4	0.9	0.8	97.55	99.98
23	10	2000	750	4	Yes	20	100	0.6	0.6	0.6	96.70	99.97

Influence of Temperature

Experiments were conducted at two different temperatures 80 °C and 20 °C respectively. It was observed that the activated carbon capacity to adsorb SO_x and/ or NO_x is almost doubled at ambient temperature than at 80 °C (see Figure 3.13). The removal efficiencies were higher than 97 % for NO_x and higher than 99 % for SO_x for both temperatures.

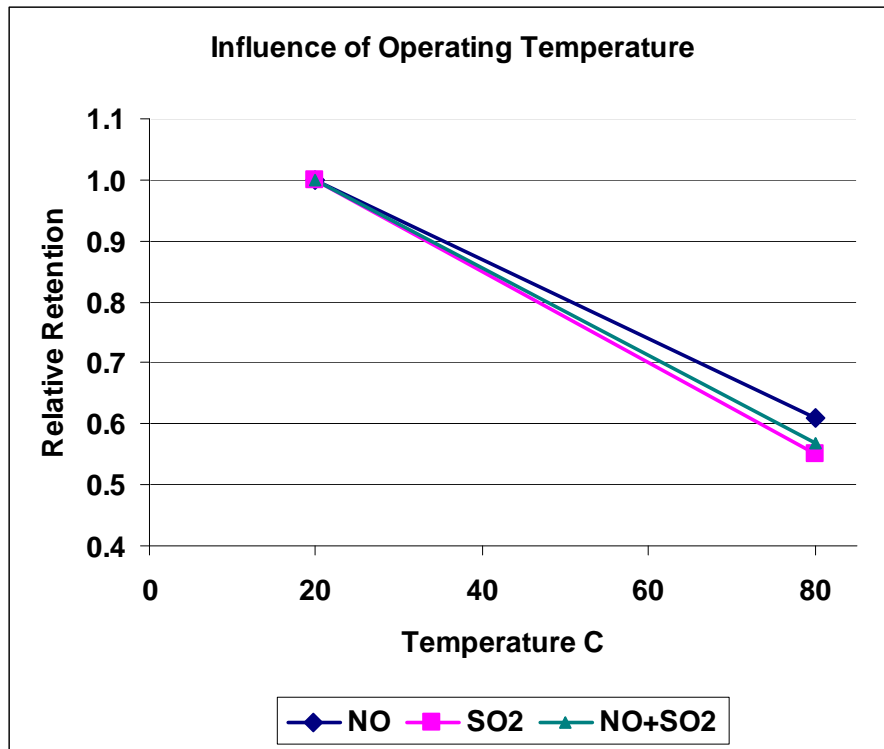


Figure 3.13 Influence of Temperature on Relative Retention of SO_x and NO_x

Influence of Pressure

Experiments were conducted at four different pressures 50, 100, 150, and 220 psig respectively. The activated carbon capacity to adsorb SO_x and NO_x significantly decreases with the decrease of pressure (see Figure 3.14). The SO₂ removal efficiency is less impacted by the decrease in pressure. Removal efficiency higher than 99 % is obtained for all pressures. The NO removal efficiency on the other hand is somehow more visible influenced by the decrease in pressure (see Figure 3.15). The NO removal efficiency is about 93 % at 50 psig and it increases to 97.3 % at 220 psig. This is a consequence of pressure influence on Reaction 1.

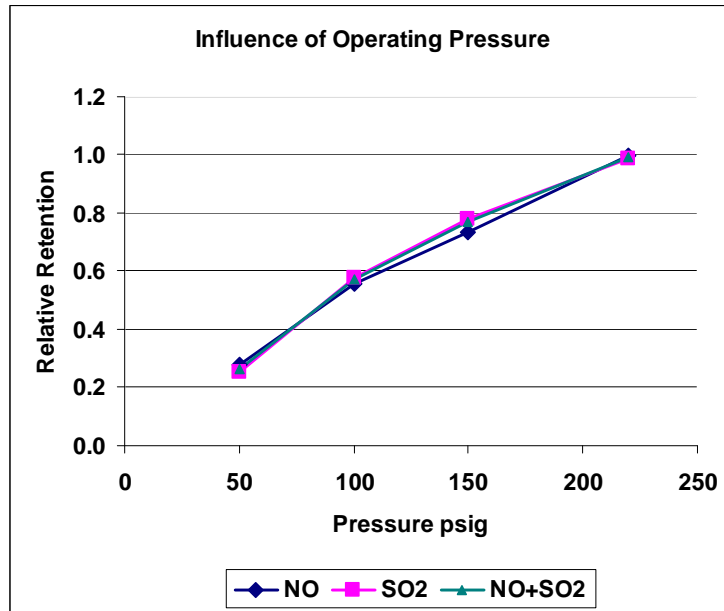


Figure 3.14 Influence of Operating Pressure on Relative Retention of SOx and NOx

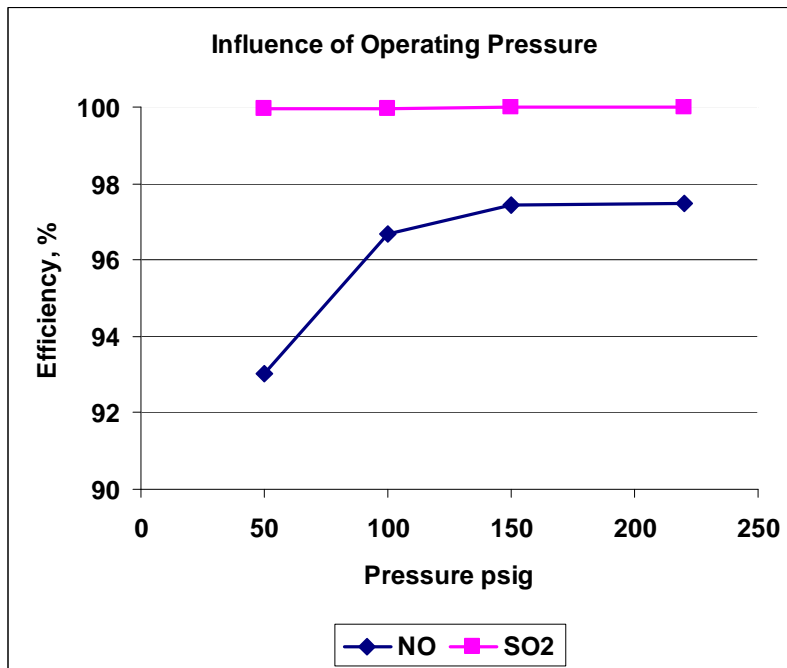


Figure 3.15 Influence of Operating Pressure on SOx and NOx Removal Efficiencies

Influence of Inlet Composition

Experiments were conducted at different NO/ SO₂ inlet molar ratio in the range of 0 - 0.4 (see Figure 3.16). It was concluded that within this range a higher NO/ SO₂ molar ratio is beneficial for individual and overall retention capacity of contaminants on activated carbon. This can be attributed to Reaction 9 which shows that there is an enhancement of SO₂ oxidation in the presence of NO₂, while the NO oxidation and adsorption is inhibited by SO₂ presence. The NO/ SO₂ inlet molar has little effect on SO₂

removal efficiency. A lower NO/ SO₂ inlet molar leads to slightly lower removal efficiency of the NO (see Figure 3.17).

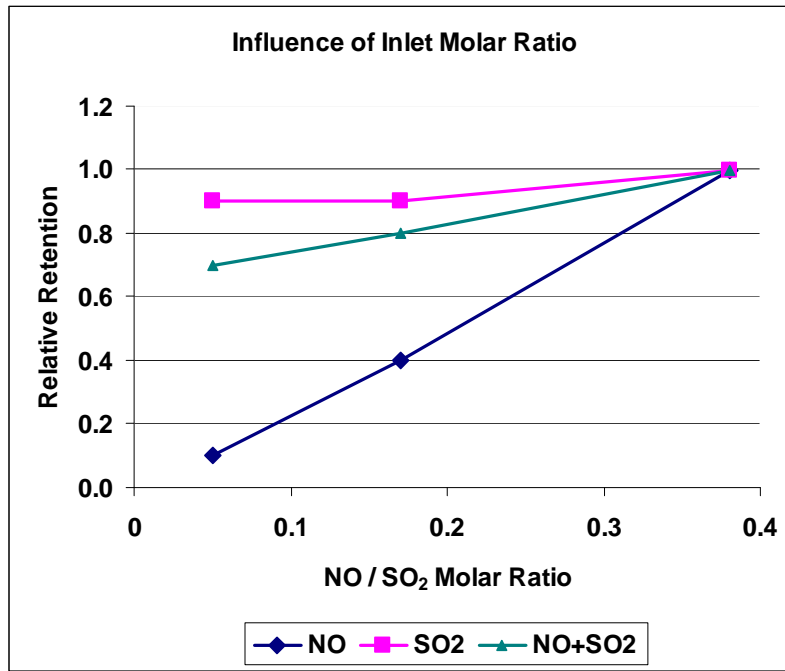


Figure 3.16 Influence of NO/SO₂ Molar Ratio in Feed on Relative Retention

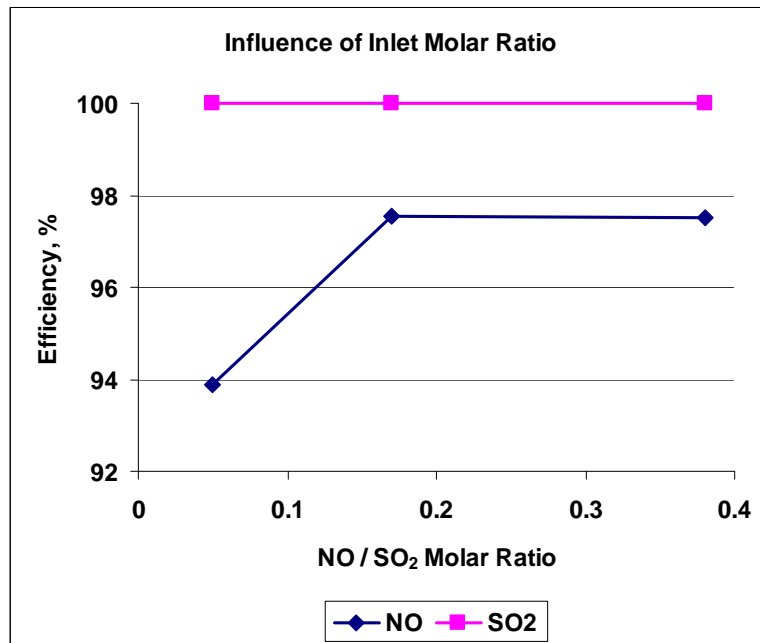


Figure 3.17 Influence of NO/SO₂ Molar Ratio in Feed on Removal Efficiency

Influence of Water

Water presence in the simulated flue gas stream enhances SO₂ removal through Reactions 3-8. Based on the experimental results obtained, it can be concluded that as long as water vapors are present in the feed at a concentration lower or closed to SO₂ concentration, they have a positive effect on simultaneous SO_x / NO_x removal. Excess water concentration in the gas phase may initiate Reaction 11 which can inhibit the removal of NO_x during the adsorption stage.

Influence of residence time

The effect of residence time on the overall retention of the contaminants on the activated carbon bed is not significant. The results indicate that the differences between the retentions for different gas flowrates, and similar temperature, pressure and inlet composition are within the experimental error (see Figure 18).

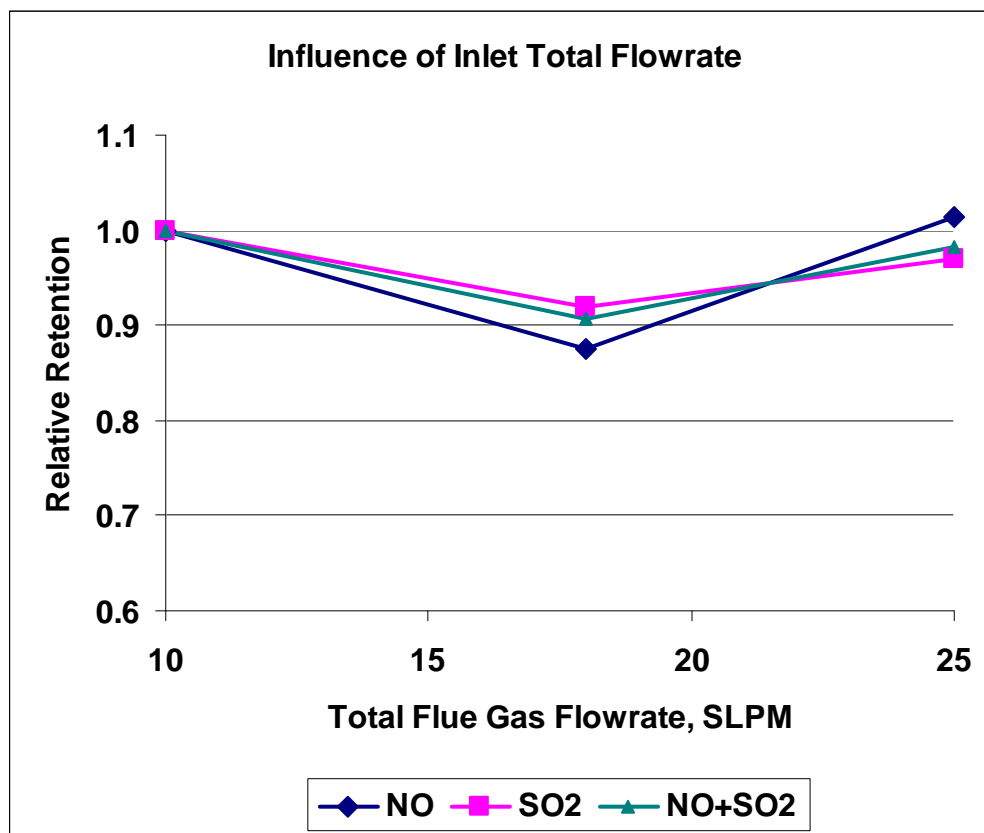


Figure 3.18 Influence of Total Feed Flowrate on Relative Retention

Waste Water Analysis

Waste water analysis was contracted to IsleChem LLC to determine the content of sulfate, sulfite, nitrate and nitrite for selected experiments using ion chromatography. The results indicate that most of the SO_x species (more than 99 %) adsorbed on the activated carbon were found in the waste water stream in the form of sulfates and sulfites. The nitrogen species found in the waste water stream are nitrates and nitrites and correspond to less than 60 % of the NO adsorbed on carbon. This supports the findings previously discussed that during the regeneration period part of the NO₂ is converted back to NO.

Material Longevity Investigation

The bench unit was used to briefly investigate material longevity in batch mode operation, by repeating the adsorption regeneration cycles. For this purpose, a carbon bed was exposed to the conditions given for bed 9 in Table 3.3. After about 20 cycles of adsorption – regeneration, material performance remained unaltered.

Subtask 3.4: Mercury and Residual NO_x Removal Research

Mercury in the flue gas usually exists in three forms: oxidized (Hg²⁺, usually as HgCl, HgO, and HgS), elemental (Hg⁰) and particle-bound (Hg^p). Due to its high volatility, mercury usually exists in vapor form. Oxidized mercury is soluble in water and can be removed through its dissolution in water [14]. Relative amount of different mercury forms present in the flue gas depends on coal type and combustion systems. Studies done on pilot and full-scale systems indicated that amount of oxidized mercury ranges from 10-80% of the total vapor phase mercury [15, 16 and 17].

There are three locations where mercury can be captured in the CPU: compression stage, moisture removal stage, and within the activated carbon process stage during the regeneration stage, when the acidic waste water can dissolve most of the mercury left in the gas stream. Additionally, a polishing step using sulfur impregnated activated carbon can be used before the cold box for final mercury removal.

Subtask 3.5: Continuous Operation Unit

Continuous Unit Construction

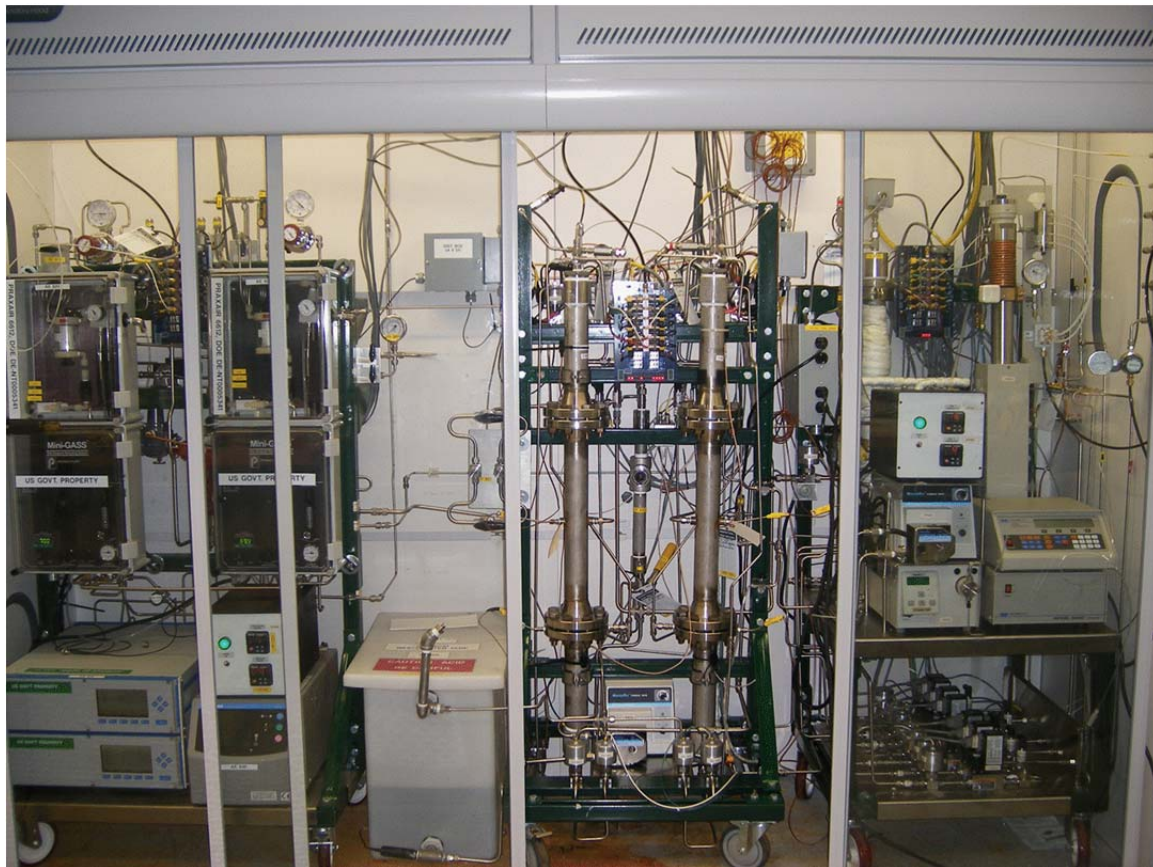


Figure 3.19 Continuous Unit experimental set-up

The continuous unit is shown in Figure 3.19. The reactor skid was located in the center of the hood; the supply skid was located at the right end, while the analytical skid is shown at the left end.

The MFCs for gas metering were located at the bottom of the skid, while the liquid SO₂ pump, the water process pump, and water pump for regeneration were mounted at the top of the supply skid. This also contained the humidifier. The water pump for the discharge of the waste water vessel, which can be seen between the analytical and the reactor skid, was mounted at the bottom of the reactor skid. The analyzers were located at the bottom of the analytical skid, while the sample conditioning units for drying the gas samples before sending them to the analyzers can be seen mounted on the upper side of the skid.

Continuous Unit Commissioning

Testing of Regeneration Stage

Regeneration consisted of washing the carbon material with water, to remove the contaminants in the form of their corresponding acids: H₂SO₄, and HNO₃, followed by a drying step to remove the water from the carbon material. The water was fed from bottom to top to avoid channeling and to ensure complete filling of the vessel's volume. The water was kept in the vessel for 10 min to allow enough time for acids formation and their dissolution in the washing water. The waste water was drained pressurizing with nitrogen. Initial tests were conducted to understand the functionality of the regeneration sequence and the required time to complete one regeneration stage.

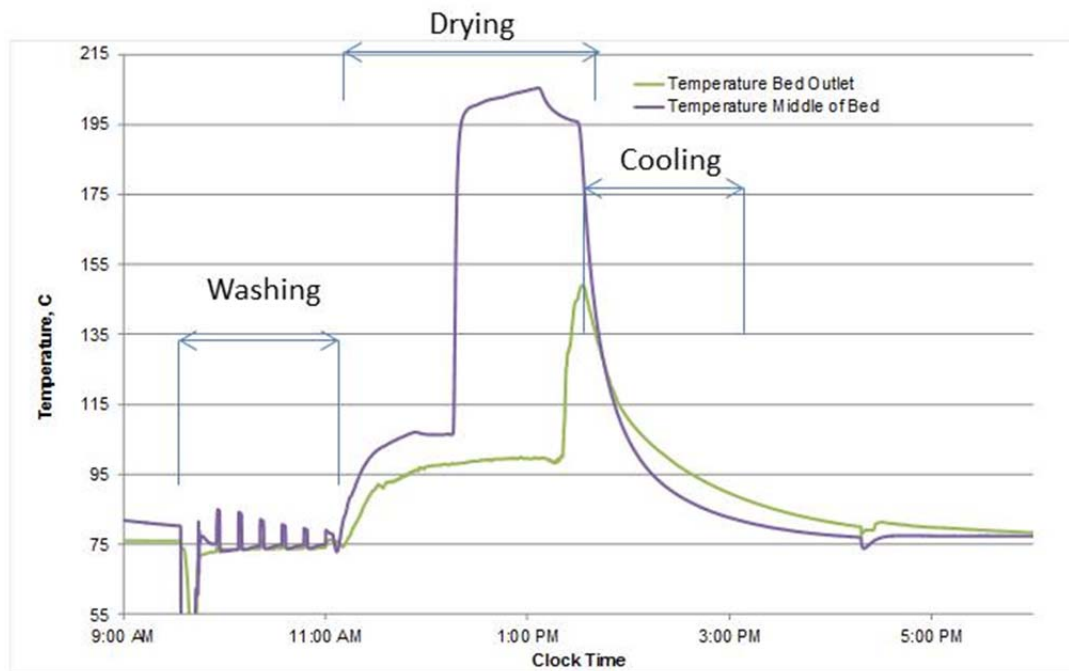


Figure 3.20 Temperature Profiles During the Regeneration Stage

Figure 3.20 shows the temperature profile during the regeneration stage. It can be seen that first, due to the depressurization of the bed, the temperature dropped below the ambient. For each water washing step, a slight increase in temperature is observed. This corresponds to the formation of sulfuric and nitric acids which are exothermic reactions. After the washing was completed, nitrogen was flown through the bed for drying. A heating tape was used to preheat nitrogen to 300F before entering the reactor. The

temperature profiles depicted in Figure 3.20 indicate that as water was evaporated the carbon bed started to heat up gradually. A spike in temperature occurred when most of the water was removed. About 3-4 hours are required for the bed to dry. A cooling period was allowed to avoid starting the adsorption stage with the activated carbon material at temperatures above ambient.

Samples of waste water were collected for each six discharges. Each sample was analyzed for its content in SO_4^{2-} , and NO_3^- ions in order to understand the efficiency of regeneration. Semi-quantitative colorimetric methods based on a HACH 890 colorimeter (methods 8051, 10020, and 8153) were used.

Figure 3.21 shows for example the depletion of the sulfate ion concentration with the number of washes. A two order of magnitude decrease was observed. This is an indication of almost complete removal of sulfates through six consecutive washes.

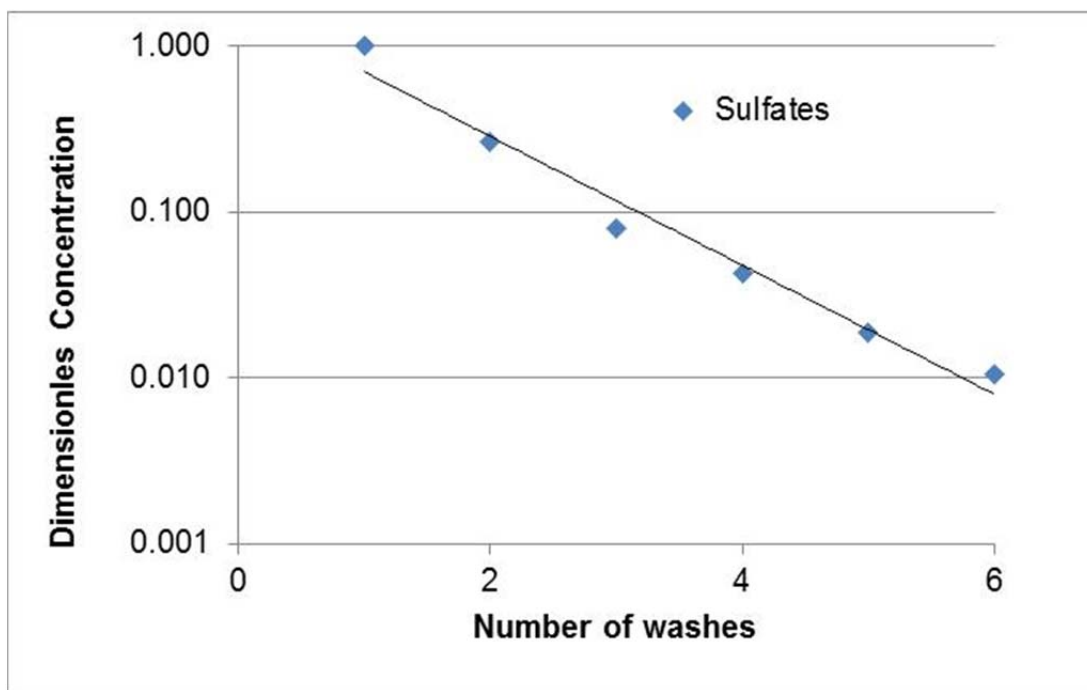


Figure 3.21 Depletion of Sulfate Ions in Waste Water with the Number of Washes

Testing of Adsorption Stage

The simulated flue gas stream was obtained by mixing the following components: 100% CO_2 (gas), 3% NO in Nitrogen (gas), O_2 100 % (gas) and 100 % SO_2 (liquid). A Teledyne ISCO 500 high pressure high precision pump was used for liquid SO_2 delivery. Several runs using liquid SO_2 as source showed that pumping and vaporizing the SO_2 into the simulated flue gas mixture was challenging. Although the pump had good accuracy, SO_2 flashes within the pump itself leading to uneven flow supply and misleading metering of the amount of SO_2 delivered. Modifications were made to use a gas source of 3% SO_2 in N_2 , which gave a more stable feed delivery and composition.

The benchmark evaluation was performed for a simulated flue gas containing: 450 ppm SO_2 , 200 ppm NO , 4 % O_2 , 94 % CO_2 and N_2 as balance, operating at 220 psig and close to the ambient temperature. The gaseous feed was saturated with water. First adsorption cycle on each bed was carried out for 30 hours each. No breakthrough was observed in this time indicated high level of retention capacity of the

carbon. Outlet concentrations of the main components from bed 801 during second adsorption cycle are shown in Figure 3.22 as a function of running time.

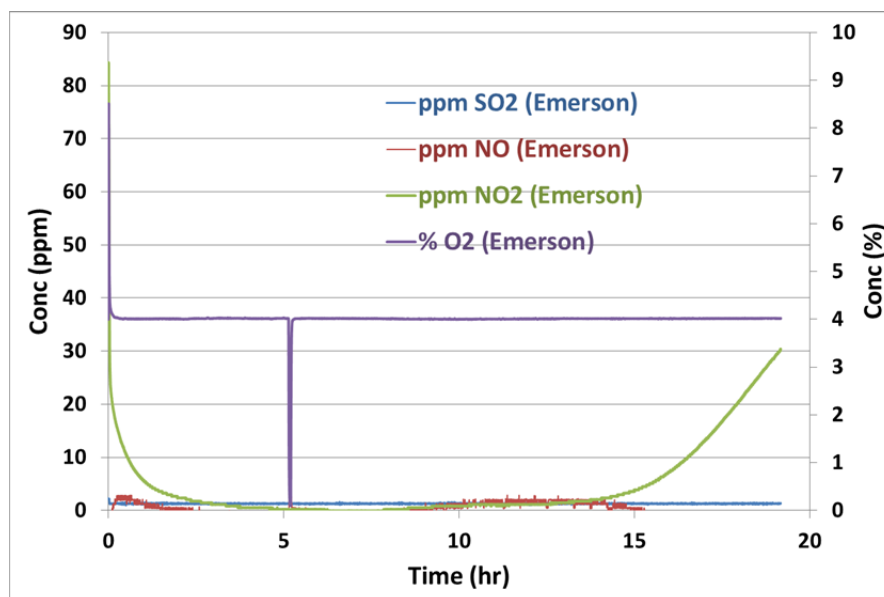


Figure 3.22 Reactor Effluent Concentrations as a Function of Time

It can be seen that for the selected conditions the breakthrough time is about 19 hours. The SO₂ and NO concentrations in flue gas exiting the reactor remained low below 5 ppm for the whole run, while NO₂ stayed below 5 ppm for ~ 14 hours after which it started to appear at the reactor exit. Thus NO₂ is the first contaminant to breakthrough. For the entire run, SO₂ and NO_x (NO + NO₂) removal efficiency was ~100% and ~98% respectively.

During the commissioning and initial experimental tests other operating issues were identified. One important aspect was related to beds depressurization. Sudden pressure release had a severe impact on the activated carbon. Material dusting was observed, most probably induced by gas-solid friction and sudden temperature drop. Modifications were implemented to achieve a gradual change in pressure when the feed was switched between beds, or for shut-down.

Continuous Unit Operation and Material Longevity Testing

In order to study the longevity of the carbon material, adsorption / regeneration cycles (as shown in table 1) were repeated 24/7 for 40 days. A log of outlet concentrations of main components was maintained to see the impact of repeated cycles on breakthrough time and thus on retention capacity of the carbon. Cycle times were set such that a clear breakthrough of contaminant was observed and beds were switched only after breakthrough occurred. For the purpose of analyzing bed’s retention capacity, 30ppm of NO₂ at the reactor exit was used to mark the end of adsorption cycle.

During the entire run of 40 days, SO₂ and NO removal efficiency of ~100% and 97-98% was observed respectively. Figure 3.23 shows breakthrough time for bed 801 after several repeated adsorption / regeneration cycles. For the first adsorption cycle breakthrough was not seen even after 30hrs of adsorption time (not shown in Figure 3.23). In the second cycle, breakthrough time decreased to ~19 hours. It can be observed that during the course of 40 days breakthrough time gradually dropped down

from 20 hr to ~10 hr. The drop was steep till 12th cycle after which it was more gradual. Similar results were observed for bed 802.

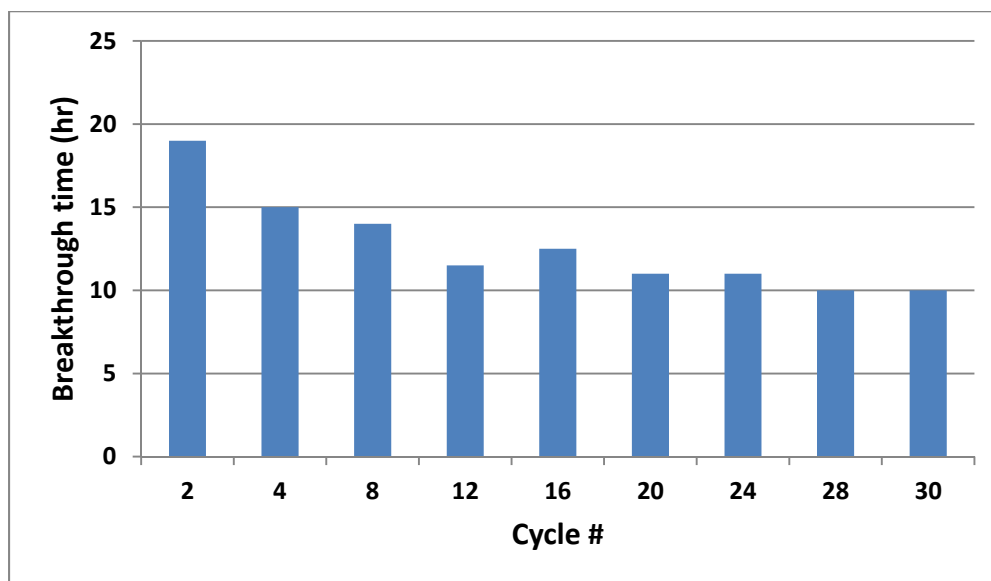


Figure 3.23 Breakthrough Time for Bed 801

Table 3.4 shows the removal efficiency of SO_x and NO_x during adsorption cycles for bed 801. Over 40 day period, removal efficiency of SO_x and NO_x was >99% and >98% respectively. Similar efficiencies were observed for bed 802.

Table 3.4. Removal efficiency for bed 801 over 40 days of continuous operation

Cycle #	Removal efficiency	
	SO _x	NO _x
2	99.8	99.1
4	99.9	98.2
8	100	98.5
12	100	97.4
16	100	98.1
20	99.6	98.8
24	99.6	98.9
28	99.4	99.0
30	99.6	98.8

Outlet concentrations of the main components from bed 801 during 30th adsorption cycle (last cycle) are shown in Figure 3.24 as a function of running time. Breakthrough time dropped to ~10 hours indicating significantly reduced retention capacity of the activated carbon compared to benchmark. During the entire run SO₂ and NO concentrations in flue gas exiting the reactor remained low below 5 ppm. As seen in the benchmark, NO₂ was the first contaminant to breakthrough and it started to appear at the reactor exit only after ~6 hours but stayed below 10ppm until 9.5 hours. This suggests that despite the reduced retention capacity removal efficiency of the bed was unchanged. SO₂ and NO_x removal efficiency was ~100% and ~98% respectively.

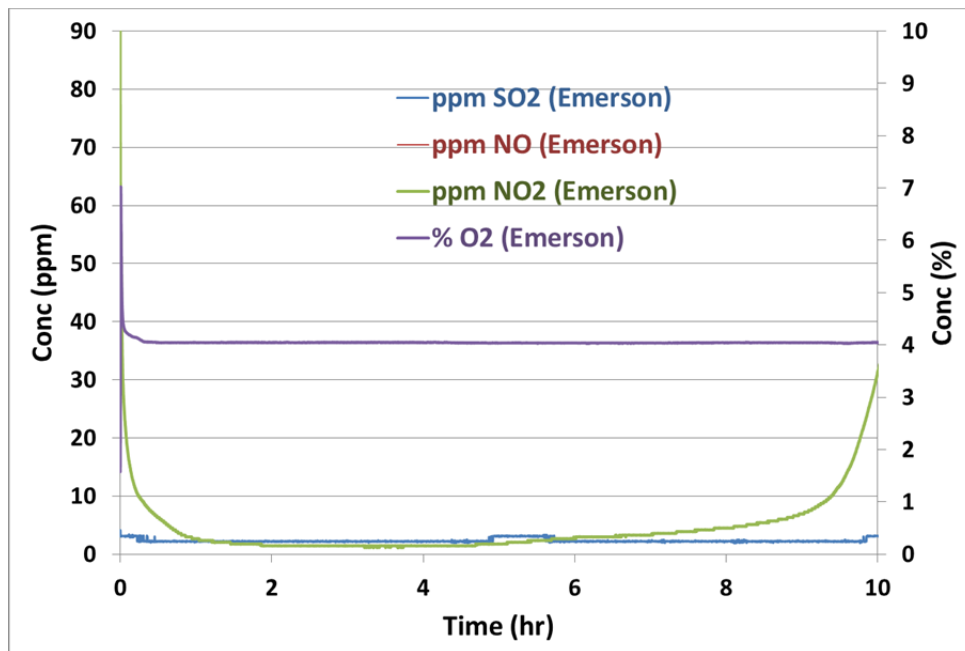


Figure 3.24 Reactor effluent concentration profiles for 30th adsorption cycle

Such drop in breakthrough time was not observed for a feed with 2000ppm SO₂ and 750ppm NO when it was tested on a bench unit for 20 cycles. For each cycle, breakthrough time was ~7.5 hours. When continuous run is compared against the bench scale study, there were several differences in the adsorption and regeneration steps due to differences in relative flow rates, bed volumes and regeneration times. In continuous run, during initial cycles of adsorption carbon bed was exposed to contaminants for very long time. This over exposure might have led to irreversible adsorption of contaminants leading to reduced active sites per unit volume of bed. In the regeneration step, much higher heating temperatures were used in the continuous unit compared to those in the bench scale testing.

In order to verify the structural stability of carbon, a BET analysis was performed. BET analysis provides precise specific surface area evaluation of materials by nitrogen multilayer adsorption measured as a function of relative pressure using a fully automated analyzer. The technique encompasses external area and pore area evaluations to determine the total specific surface area. The BET surface areas of carbon before and after continuous run were 745 m²/g and 677 m²/g, respectively. Within the experimental errors this small drop in surface area is negligible. This indicates that the pore structure of carbon was intact during the repeated adsorption-regeneration cycles.

In order to check any irreversible adsorption of contaminants on the carbon surface, ion chromatography was performed on spent carbon. Spent carbon was combusted in a pressurized decomposition vessel with oxygen atmosphere. The combustion gases are scrubbed using a gas washing bottle containing a solution of NaHCO₃/Na₂CO₃. The scrubber solution is then analyzed for nitrate and sulfate by ion chromatography. The nitrate and sulfate content of the scrubber solution is used to calculate total nitrate and sulfate content of the carbon sample. It was found that total nitrate and sulfate content of the spent carbon was 3.7% and 2.3% by weight respectively. This indicates that some of the nitrates and sulfates were not removed by water regeneration cycles and ultimately led to drop in retention capacity of the carbon.

Since simple water wash was unable to completely regenerate the carbon sample it was studied that if a thermal re-activation can be used for complete regeneration. In this test, spent carbon was placed in a furnace at 950 °C under inert atmosphere in order to remove any strongly bound contaminants. It was then subjected to ion exchange chromatography as described above. It was found that even after the thermal reactivation at 950 °C nitrate and sulfate ions were not removed from the carbon surface. This clearly indicates that the drop in retention capacity of the carbon is due to the irreversible adsorption of nitrates and sulfates and such irreversible adsorption must be avoided.

Hence, further work is needed to optimize adsorption/regeneration cycle in order to maintain carbon bed's high retention capacity for SO_x/NO_x over a long period of time. This includes:

1. Reduce the cycle time to < 7 hours by increasing feed gas flow or decreasing the amount of carbon. This will reduce the total time of exposure and will limit the adsorption to the surface level.
2. Increase regeneration efficiency by achieving a continuous flow of water through the carbon bed. This will help to remove strongly bound contaminants from the carbon.
3. Eliminate/minimize heating during regeneration step.

Conclusions

A near-zero emissions flue gas purification technology, for existing PC power plants that are retrofitted with oxy-combustion technology, was developed and demonstrated. As proposed, the potential advantages of the Task 3 process is the ability to simultaneously remove SO_x and NO_x impurities, with high efficiency and eliminate or reduce the need for traditional flue gas purification technologies (FGD and SCR). The following major conclusions can be made: 1) Activated carbon material is suitable for simultaneous SO_x and NO_x removal at elevated pressures and ambient temperatures; 2) Continuity and scalability of the process is achievable through a multi-bed reactor design 3) Good purification performance can be achieved, more specifically the contaminant content in the stream exiting the purification stage is: SO_x <10 ppm, NO_x <20 ppm.

The dual bed system was successfully tested with continuous operation for investigating carbon bed's longevity. The overall SO_x and NO_x removal efficiencies of >99.9% and >98%, respectively, were achieved. The retention capacity of activated carbon material for SO_x and NO_x was significantly reduced over a long term test period of 40 days. Optimization of adsorption-regeneration cycle is needed to maintain long term activity of activated carbon material at a higher level and thus minimize the capital cost of the system. Minimization of acidic waste water is also required to reduce disposal costs.

Task 4 – High CO₂ Recovery

Approach

High CO₂ recovery was achieved by using a cold-box VPSA hybrid process with the focus of the technology development on the VPSA process. An adsorption based process is proposed to capture CO₂ from the cold box vent gas. The vent gas from the cold box is dry and is at high pressure. The entire process will achieve > 95 % CO₂ recovery.

To maintain high CO₂ recovery, a VPSA unit was used to recover CO₂ from the cold box vent. The VPSA unit adsorbs CO₂ while letting other gases pass through. The CO₂-rich stream (>75% CO₂) from the VPSA is recovered at low pressure and is sent to the front end of the purification process, where it is mixed with the flue gas from the boiler. The VPSA unit consists of a multi-bed system with one bed always on the feed while other beds are going through regeneration steps. Figure 4.1 schematic shows the various steps during a cycle. It is designed to ensure a continuous mode of operation for feed entering the VPSA unit and products withdrawn from it while operation of each bed is in a cyclic steady state. The use of multiple beds allows efficient use of pressure energy and achieves high CO₂ recovery.

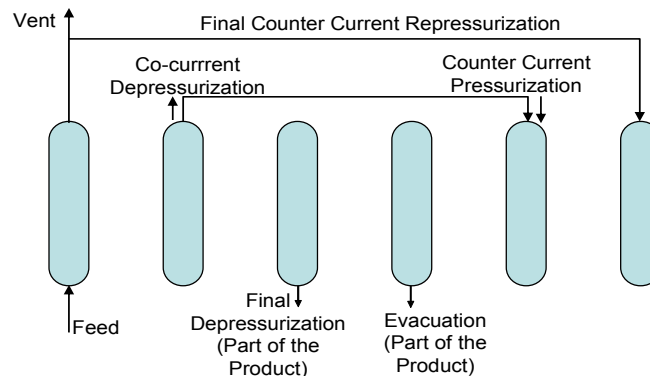


Figure 4.1 VPSA Process Cycle Steps

This work was directed towards a process innovation and *not* towards an adsorbent innovation. Our goal was to develop a process using commercially available adsorbents. The CO₂ VPSA process was developed in several steps according to the schedule shown in Table 4.1. Typical process steps chosen were:

1. Counter-current (opposite to feed flow direction) repressurization from the high pressure gas generated by a column on its feed step.
2. Co-current feed the gas mixture to be separated.
3. Co-current (same direction as the feed flow) depressurize the column to a lower pressure. Complete depressurization could happen in multiple steps,
4. Equalize the pressure in the other columns by the gas being generated in Step 3. Pressure equalization in the receiving column is in counter-current direction. This will correspond to multiple depressurization(s) during step 3,
5. Final depressurization close to ambient pressure in counter current direction. This constitutes part of the final product.
6. Evacuate the vessel to a sub ambient pressure in counter current direction. This constitutes the remaining part of the final product. Store the product gas in a storage tank.
7. Go back to Step 1 and repeat the cycle.

Since this was an adsorption based process, the first step was to identify commercial adsorbents capable of carrying out the separation. The list was narrowed down to 6 adsorbents. This was done by measurement and/or compilation of relevant separation properties followed by, theoretical calculations and our know-how to select proper separation adsorbents.

Table 4.1 Task 4 Schedule

		2009				2010				2011			
		Q1	Q2	Q3	Q4	Q1	Q2	Q3	Q4	Q1	Q2	Q3	Q4
4	High CO ₂ Recovery												
4.1	Separation Agent Identification												
4.2	Simulation Tool												
4.3	Bench-Scale Tests												
4.4	Continuous Operation Tests												

The second step was to test the best possible adsorbent candidates, identified in the first step, in a small “bench unit”. This experimental unit was a small diameter, short length, and had a single column. The dimensions were chosen such that the quantity of adsorbent required is less than 0.5 kg (one pound). All the process steps were performed on the bench unit. However, experiments on this unit were carried out in a discontinuous manner. The results from this unit were analyzed to estimate the performance of a continuous process cycle. Based upon this data three adsorbents were chosen for testing on the continuous operation test unit.

At the same time, data gathered from the first step was used to put together a detailed simulator. Experimental data collected in the second step was simulated. Comparison of the simulator and the bench unit results was used to upgrade the simulator.

The third step was to test the best possible adsorbent candidates identified in the second step in a continuous operation test unit. Each column was of approximately plant column length but had a smaller diameter column to minimize gas consumption but still get relevant data for design scale-up. The dimensions were chosen such that the quantity of adsorbent required was ~ 3.5 – 4.5 Kg (8-10 pound) per column. The process cycle was run in a continuous manner in this unit till the process reached cyclic steady state. Process simulator developed in the prior step was tested against the data collected in this step. The continuous operation test unit was well-instrumented and the data was collected for different process options. This unit was controlled by a PLC (Programmable Logic Control). The data was analyzed such that it can be used for design scale-up. Three process options on different adsorbents were tested. The data collected in the third step was used to design a system for commercial viability assessment in Task 5. Overall process optimization was done to find out the most economic option.

Results and Discussion

The project proceeded in the steps as outlined in Table 4.1. However, the results will be discussed in a different sequence:

- Task 4.1: Separation Agent Identification,
- Task 4.3: Bench-Scale Tests,
- Task 4.2.1: Simulation Tool: First part - Bench Scale Test Simulation
- Task 4.4: Continuous Operation Tests
- Task 4.2.2: Simulation Tool: Second part - Continuous Operation Test Simulation

Task 4.1: Separation Agent Identification

The VPSA process selected was as outlined in section on Approach above and listed in Praxair Patents [18, 19 and 20].

We collected pure component equilibrium data for the key components in the gas mixture: CO₂ and N₂, for various adsorbents as identified in literature search on Adsorbents. Pure component CO₂ equilibrium data is shown in Figure 4.2 and pure component N₂ equilibrium data is shown in Figure 4.3. Based upon this information, we theoretically calculated expected performance of these adsorbents for the separation process as outlined above. The following six adsorbents were selected for best “expected” performance for screening in the bench unit in cyclic mode:

1. Adsorbent A,
2. Adsorbent D,
3. Adsorbent G,
4. Adsorbent P,
5. Adsorbent Q, and
6. Adsorbent S.

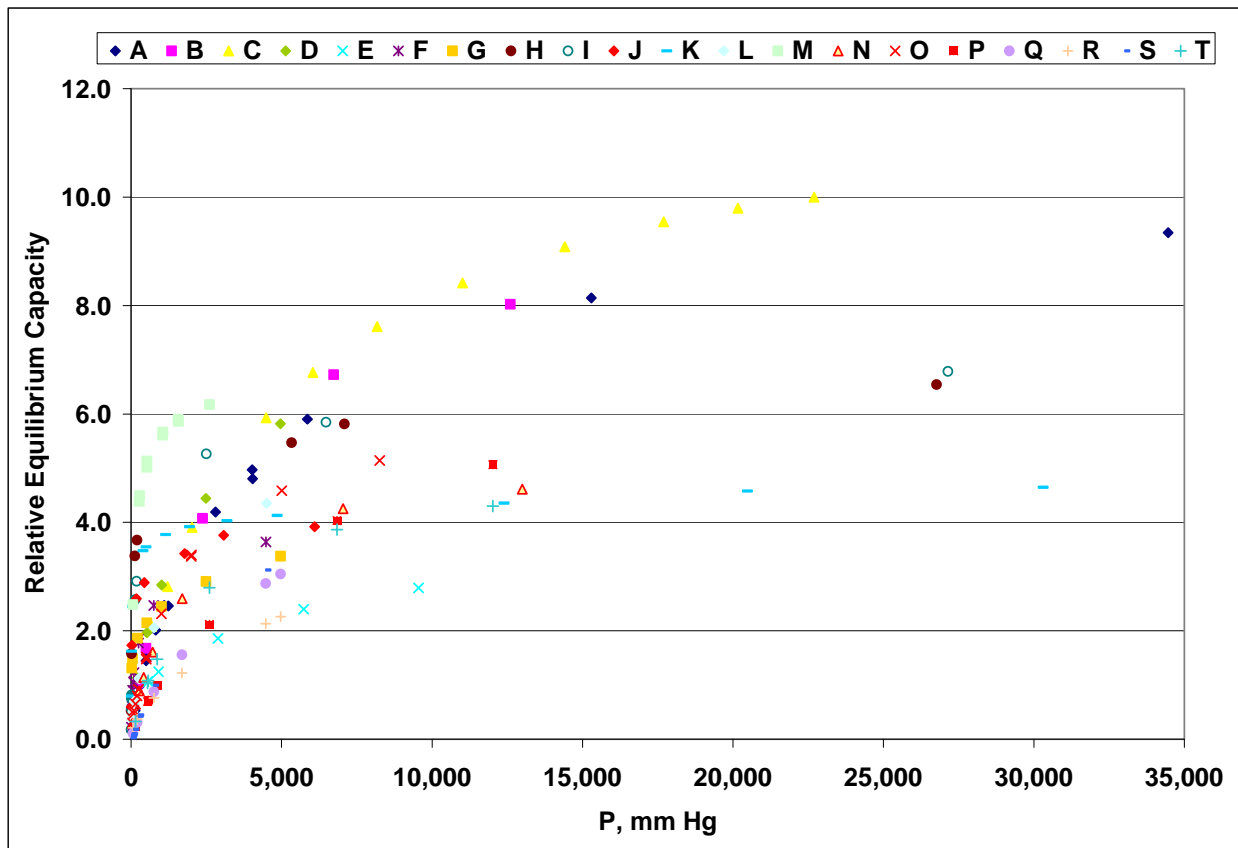


Figure 4.2 Pure Component CO₂ Equilibrium Data

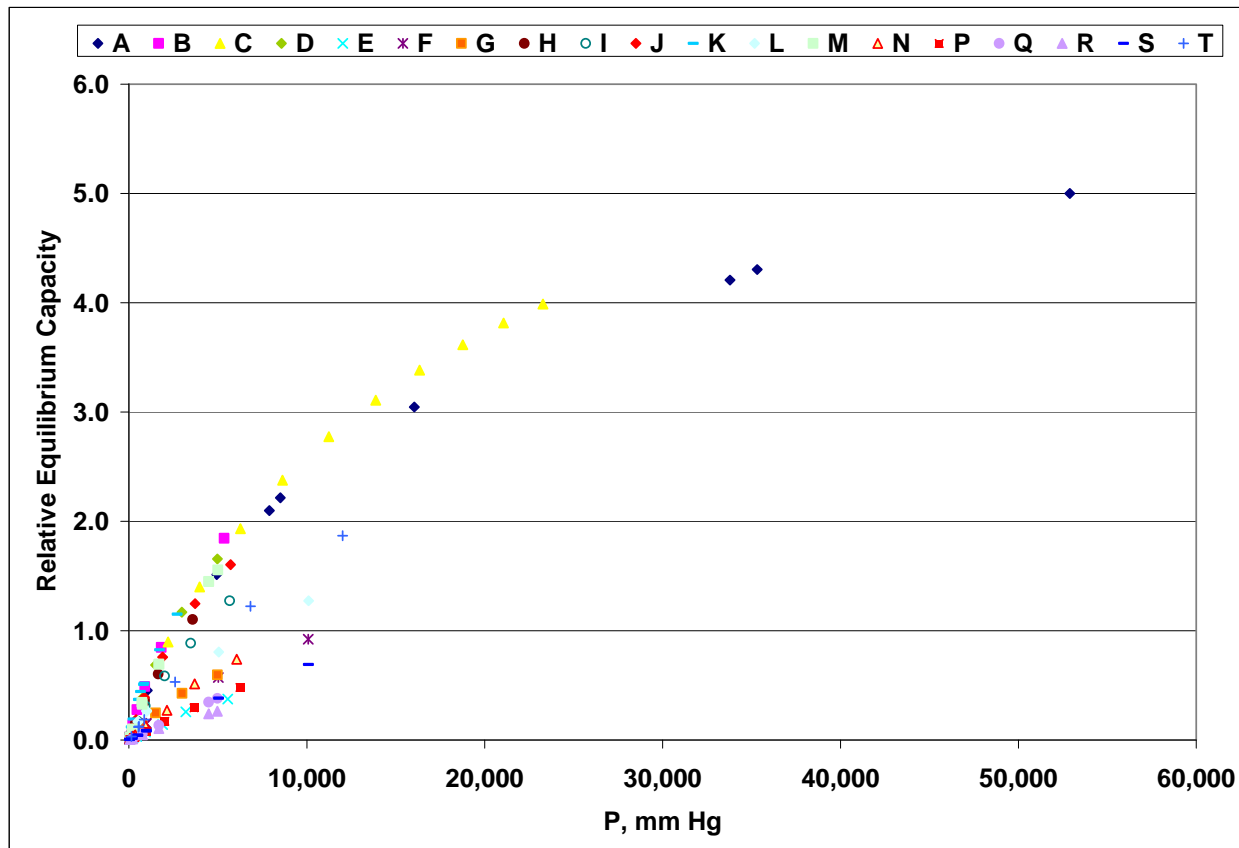


Figure 4.3 Pure Component N₂ Equilibrium Data

Physical properties, particle size and packed density for the chosen adsorbents were measured and are listed in Table 4.2.

Table 4.2. Physical Properties of the VPSA Adsorbents

Name	Particle Size mm	Packed Density gm/cc
A	1.923	0.48
D	2.268	0.54
G	1.787	0.80
P	1.615	0.70
Q	1.983	0.83
S	2.415	0.67

Task 4.3 Bench-Scale Tests

The bench unit was built with a small diameter (17.5 mm) short length (1524 mm) single column. The dimensions were such that the quantity of adsorbent required is less than 0.5 kg (one pound). This helps to speed up the experiments and test several adsorbents in a timely manner. Photograph of the bench unit is given in Figure 4.4.

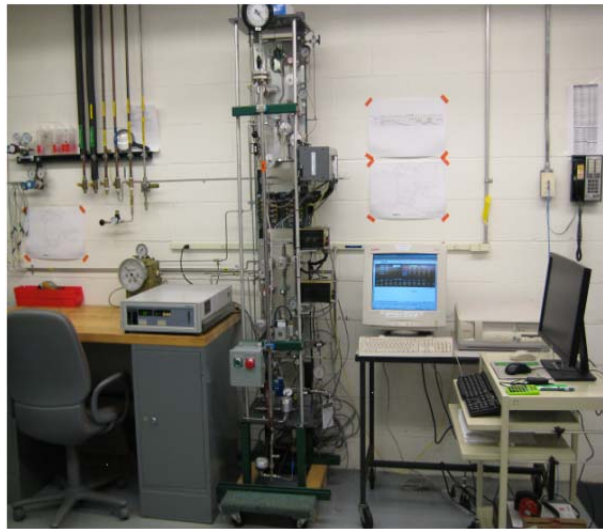


Figure 4.4 VPSA Bench Unit

Two types of experiments were carried out on the bench-scale unit. The first set of experiments was to measure equilibrium capacity and length of the unused bed (LUB) by a dynamic technique. A mixture of CO₂ and N₂ is flowed through the column packed with the adsorbent. CO₂ breakthrough curve in the effluent gas is measured. Mass balance around the column provides CO₂ equilibrium capacity. Length of the unused bed (LUB) is calculated from the spread of the breakthrough curve. This experiment is done at different flow rates. Table 4.3 lists the summary of breakthrough data on the above selected six adsorbents. The purpose of these experiments was to calculate equilibrium parameters and mass transfer coefficients for the simulator as will be discussed in the next section.

Table 4.3 Breakthrough Data from the VPSA Bench Unit

Feed Conditions: CO ₂ 38%, N ₂ 62%, pressure ~24 bara, temperature ~ 21 °C				
Adsorbent	Relative Particle Size	Relative Feed Flow Rate	Relative LUB	Relative Equilibrium Capacity
A	1	1	1	1
A		1.33	0.94	1.02
A		1.67	1.08	1.05
D	1.17	0.93	0.98	1.09
D		1.40	1.13	1.19
D		1.87	1.62	1.06
G	0.92	0.94	0.96	0.37
G		1.86	1.22	0.49
P	0.83	0.91	1.05	0.67
P		1.37	1.19	0.67
P		1.83	1.40	0.71
Q	1	0.93	1.25	0.63
Q		1.40	1.36	0.65
Q		1.87	1.84	0.67
S	1.25	0.93	1.40	0.78
S		1.40	1.72	0.80
S		1.87	1.82	0.83

A larger particle will have lower pressure drop in the adsorbent vessel. This is a desirable property for the process. However, a larger particle size is likely to have longer mass transfer zone (2 times LUB), which is undesirable from process performance point of view. Higher working capacity is desirable for an adsorbent. Higher working capacity depends upon the combination of higher equilibrium capacity and shape of the equilibrium isotherm. Due to this multi-interaction of various adsorbent parameters, the second set of experiments on the bench unit was cyclic in nature. These experiments were carried out in the following manner:

1. Counter-current (opposite to feed flow direction) repressurization from a premixed gas cylinder,
2. Co-current feed flow from a premixed gas cylinder. Record feed and outlet gas pressure, concentration and flow rate,
3. Depressurize the vessel to a medium pressure in Co-current (same direction as feed flow) direction. Record outlet gas pressure, concentration and flow rate,
4. Depressurize the vessel to ~ ambient pressure in counter-current direction. Record outlet gas pressure, concentration and flow rate,
5. Evacuate the vessel to a sub ambient pressure in counter-current direction. Record outlet gas pressure, concentration and flow rate,
6. Go back to Step 1 and repeat the experiment till cyclic steady state is reached.

For a given process condition, the cyclic experiment was repeated continuously many times at least for eight hours. Comparative results are shown in Table 4.4 for all the six adsorbents A, D, G, P, Q and S. It is clear from the table that no single adsorbent is the best in all the key categories:

Adsorbent D: based upon adsorbent cost per unit of production is the best but it will have a larger vacuum pump.

Table 4.4 Results from Cyclic Experiments on the VPSA Bench Unit

Adsorbent	Relative CO ₂ Recovery	Relative CO ₂ Purity	Relative Total Product		Relative Vacuum Pump Size	\$ Adsorbent for unit Production
			Weight Basis	Volume Basis		
	(Higher is better)	(Higher is better)	(Higher is better)	(Higher is better)	(Lower is better)	(Lower is better)
A (Base)	1.00	1.00	1.00	1.00	1.00	1.00
D	1.07	1.01	1.06	1.20	1.20	0.34
G	0.70	0.97	0.32	0.51	1.03	1.43
P	1.07	1.03	0.66	1.02	0.97	1.09
Q	1.05	1.04	0.65	1.14	1.07	1.16
S	1.05	1.03	0.73	0.99	1.13	2.09

Adsorbent G: is high in adsorbent cost per unit of production, will require a larger vessel and has low CO₂ recovery. So it may be removed from further considerations.

Adsorbent P: has smallest vacuum train and all the other parameters are “reasonable”.

Adsorbent Q: has maximum CO₂ recovery and CO₂ product purity, it is somewhat high on adsorbent cost per unit of production, but all the other parameters are “reasonable”.

Adsorbent S: is highest in adsorbent cost per unit of production, will require a larger vacuum pump and somewhat larger vessel so it may be removed from further consideration.

Adsorbent A: The base adsorbent is middle of the road as compared with all the six adsorbents tested. Therefore, detailed design data and economics are needed to select the final best adsorbent. However, from the above relative results three adsorbents (D, P and Q), are chosen to move forward for testing in the continuous test unit. A safety concern for Adsorbent D was identified in the overall process scheme. Adsorbent D has tendency to form dust, which can enter vacuum pump and regeneration heater and create a potential fire hazard. Therefore, it was partially dropped for the time being.

Task 4.2.1: Simulation Tool: First Part- Bench Scale Test Simulation

We contracted an outside vendor (PSe) to develop a CO₂ VPSA Simulation Model using gPROMS, mathematical modeling software. They divided the work into 4 stages for the two adsorbents P & Q:

- Stage 1- Equilibrium isotherm model
- Stage 2- Mass transfer model – i.e. fitting breakthrough curves
- Stage 3- Four Bed CO₂ VPSA Process Simulation
- Stage 4- Six Bed CO₂ VPSA Process Simulation

Stage 1 - Praxair provided PSe single-component isotherm data for CO₂, N₂ and CO at 2 temperatures each. PSe fitted the equilibrium using Langmuir isotherm model for CO₂ and linear isotherm model for N₂ and CO. They used Heteroscedastic variance model, combination of constant and constant relative variance, for statistical analysis. Summary of equilibrium parameters for adsorbent P and Q is in Table 4.5.

Table 4.5 Equilibrium Parameters for Adsorbent P and Q

	Adsorbent P			Adsorbent Q		
	CO ₂	CO	N ₂	CO ₂	CO	N ₂
b ₁ (atm ⁻¹)	0.16574	-	-	0.2335	-	-
b ₂ (mK)	2.7453	1.4958	1.4629	3.0224	2.3183	1.6679
q _{0_b1} (Henry's const for CO and N ₂)	1.067	0.073427	0.047345	0.99826	0.075892	0.041275
q ₀ (mmol/g)	6.437	-	-	4.275	-	-
ΔH _{ads} (J/mol)	22824	12436	12163	25128	19274	13867

Stage 2 - Praxair provided 3 Breakthrough curves at different flow rates for each adsorbent- P and Q. Feed was 38% CO₂; balance was N₂ at 350 psia. PSe used Ideal Adsorbed Solution Theory (IAST) to describe multi-component adsorption. They used standard heat transfer correlations. Ergun equation was used for momentum balance. They estimated mass transfer coefficient (MTC) for CO₂ and N₂ for each adsorbent using Linear Driving Force (LDF) model. It was assumed that CO₂ and N₂ MTCs are same. To match the concentration and temperature breakthrough curves, PSe adjusted the feed flow rates by ~ 3-7%. This is within experimental error. Also, since we do not have independent binary equilibrium isotherm data, a small binary adjustment parameter (α) was needed for CO₂ on adsorbent P. The results from the updated parameter estimation provide a much better fit to both the breakthrough and the temperature curves. Statistical analysis on the estimated parameters shows good confidence. The estimated additional metal mass between the bed and thermocouple is in good agreement with the

expected mass based on the flange and additional mass. Mass transfer coefficients for adsorbent P and Q are summarized in Table 4.6.

Table 4.6 Mass transfer coefficients for adsorbent P and Q

Parameter	Adsorbent P	Adsorbent Q
MTC CO ₂ and N ₂	0.1445± 0.0017	0.0558 ±0.00042
α	0.0415 ± 0.00029	0

Task 4.4: Continuous Operation Tests

We built a continuous operation test unit with 12 adsorber vessels. This provided us with options to test various process cycles. Each vessel is ~ 11 ft long and has an internal diameter ~ 2.5 inch. Photograph of the Continuous Operation Test unit is given in Figure 4.5. Praxair safety department approved the operation of the unit. Three process options with one, two or three pressure equalizations were done. One pressure equalization option had 4 adsorber vessels (beds), two pressure equalization options had 5 adsorber vessels (beds) and three pressure equalization options had 6 adsorber vessels (beds). The process cycles are listed in Tables 4.7 (4 Beds), Table 4.8 (5 Beds) and Table 4.9 (6 Beds). Table 4.10 outlines a cycle with four pressure equalizations and 8 beds. This process option was also evaluated by theoretical calculations.



Figure 4.5 Photograph of the VPSA Continuous Operation Unit

Table 4.7 VPSA Process Cycle for Four Beds – One Pressure Equalization

	Time, sec →	CO ₂ VPSA - 4 Beds					
A1		FEED	DP1	BD	Evacuation	PE1	FeRP
A2		PE1	FeRP	FEED	DP1	BD	Evacuation
A3		Evacuation	PE1	FeRP	FEED	DP1	BD
A4		DP1	BD	Evacuation	PE1	FeRP	FEED
Feed		Feed to CO ₂ VPSA → Product is High Pressure Feed Effluent					
DP1		CoC DP1 to PE1 with a bed.					
BD		Blow Down- CcC DP Gas mixed with Evacuated Gas.					
Evac.		CcC Evacuation gas is mixed with BD gas. Mixed gas is Total CO₂ product					
PE1		CCC PE1 with the Bed on DP1					
FeRP		CcC RP by high pressure Feed Effluent					

Table 4.8 VPSA Process Cycle for Five Beds – Two Pressure Equalizations

	Time, sec →	CO ₂ VPSA - 5 Beds							
A1		FEED	DP1	DP2	BD	Evacuation	PE2	PE1	FeRP
A2		PE1	FeRP	FEED	DP1	DP2	BD	Evacuation	PE2
A3		Evacuation	PE2	PE1	FeRP	FEED	DP1	DP2	BD
A4		BD	Evacuation	PE2	PE1	FeRP	FEED	DP1	DP2
A5		DP1	DP2	BD	Evacuation	PE2	PE1	FeRP	FEED
Feed		Feed to CO ₂ VPSA → Product is High Pressure Feed Effluent							
DP1		CoC DP1 to PE1 with a bed.							
DP2		CoC DP2 to PE2 with another bed.							
BD		Blow Down- CcC DP Gas mixed with Evacuated Gas.							
Evac.		CcC Evacuation gas is mixed with BD gas. Mixed gas is Total CO₂ product							
PE2		CCC PE2 with the Bed on DP2							
PE1		CCC PE1 with the Bed on DP1							
FeRP		CcC RP by high pressure Feed Effluent							

Table 4.9 VPSA Process Cycle for Six Beds – Three Pressure Equalizations

	Time, sec	CO ₂ VPSA - 6 Beds									
A1		FEED	DP1	DP2	DP3	BD	Evacuation	PE3	PE2	PE1	FeRP
A2		PE1	FeRP	FEED	DP1	DP2	DP3	BD	Evacuation	PE3	PE2
A3		PE3	PE2	PE1	FeRP	FEED	DP1	DP2	DP3	BD	Evacuation
A4		Evacuation	PE3	PE2	PE1	FeRP	FEED	DP1	DP2	DP3	BD
A5		DP3	BD	Evacuation	PE3	PE2	PE1	FeRP	FEED	DP1	DP2
A6		DP1	DP2	DP3	BD	Evacuation	PE3	PE2	PE1	FeRP	FEED
Feed		Feed to CO ₂ VPSA → Product is High Pressure Feed Effluent									
DP1		CoC DP1 to PE1 with a bed.									
DP2		CoC DP2 to PE2 with another bed.									
DP3		CoC DP3 to PE3 with another bed.									
BD		Blow Down- CcC DP Gas mixed with Evacuated Gas.									
Evac.		CcC Evacuation gas is mixed with BD gas. This is Total CO₂ product									
PE3		CCC PE3 with the Bed on DP3									
PE2		CCC PE2 with the Bed on DP2									
PE1		CCC PE1 with the Bed on DP1									
FeRP		CcC RP by high pressure Feed Effluent									

Table 4.10 VPSA Process Cycle for Eight Beds - Four Pressure Equalizations

	Time, sec	CO ₂ VPSA - 8 Beds													
A1		FEED	DP1	DP2	DP3	DP4	DP5	BD/Mix	Evacuation	PE5	PE4	PE3	PE2	PE1	FeRP
A2		PE1	FeRP	FEED	DP1	DP2	DP3	DP4	DP5	BD/Mix	Evacuation	PE5	PE4	PE3	PE2
A3		PE3	PE2	PE1	FeRP	FEED	DP1	DP2	DP3	DP4	DP5	BD/Mix	Evacuation	PE5	PE4
A4		PE5	PE4	PE3	PE2	PE1	FeRP	FEED	DP1	DP2	DP3	DP4	DP5	BD/Mix	Evacuation
A5		Evacuation	PE5	PE4	PE3	PE2	PE1	FeRP	FEED	DP1	DP2	DP3	DP4	DP5	BD/Mix
A6		DP5	BD/Mix	Evacuation	PE5	PE4	PE3	PE2	PE1	FeRP	FEED	DP1	DP2	DP3	DP4
A7		DP3	DP4	DP5	BD/Mix	Evacuation	PE5	PE4	PE3	PE2	PE1	FeRP	FEED	DP1	DP2
A8		DP1	DP2	DP3	DP4	DP5	BD/Mix	Evacuation	PE5	PE4	PE3	PE2	PE1	FeRP	FEED
Feed		Feed to CO ₂ VPSA → Product is High Pressure Feed Effluent													
DP1		CoC DP1 to PE1 with a bed.													
DP2		CoC DP2 to PE2 with another bed.													
DP3		CoC DP3 to PE3 with another bed.													
DP4		CoC DP4 to PE4 with another bed.													
DP5		CoC DP5 to PE5 with another bed.													
BD		Blow Down- CcC DP Gas mixed with Evacuated Gas.													
Evac.		CcC Evacuation gas is mixed with BD gas. This is Total CO₂ product													
PE5		CCC PE5 with the Bed on DP5													
PE4		CCC PE4 with the Bed on DP4													
PE3		CCC PE3 with the Bed on DP3													
PE2		CCC PE2 with the Bed on DP2													
PE1		CCC PE1 with the Bed on DP1													
FeRP		CcC RP by high pressure Feed Effluent													

First series of experiments had the following operating conditions:

Adsorbent: P
 Feed Pressure ~ 24.5 bara
 Feed Temperature ~ 24 °C
 Feed Composition:
 CO₂ ~ 31%
 CO ~ 0.2%
 N₂ ~ 68.8%

The results are summarized in Table 4.11 on a relative basis. Similar series of experiments were done with adsorbent Q. These are summarized in Table 4.12 on a relative basis.

Table 4.11 VPSA Pilot Unit Results – Adsorbent P

# of Pressure Equalizations	1							
# of Adsorber Vessels	4							
Sr. No.	1	2	3	4	5	6	7	13
Date	7/29/2010	8/3/2010	8/3/2010	8/27/2010	9/10/2010	8/31/2010	9/1/2010	9/9/2010
Experiment Name	4B1_SPT	4B2_SPT	4B2B_SPT	4B3_SPT	4B7_SPT	4B4_IT	4B5_IT	4B6_IT-PT
Feed Pressure	24.1	24.1	24.1	24.1	24.2	24.1	24.1	24.2
Feed Temperature	23.4	24.6	25.2	20.9	20.2	23.9	25.9	20.5
Feed CO ₂	31.0%	30.3%	30.8%	31.4%	30.7%	30.7%	30.7%	30.6%
CO ₂ Product Purity, %	78.8%	79.9%	79.9%	81.5%	80.1%	82.4%	79.8%	78.0%
CO ₂ Recovery, %	98.1%	97.7%	94.5%	93.7%	94.5%	96.0%	97.6%	94.8%
Relative Bed size factor	1	0.980	0.993	1.023	0.977	1.027	1.014	1.046
# of Pressure Equalizations	2		3					
# of Adsorber Vessels	5		6					
Sr. No.	8	9	10	11	12	14	15	
Date	9/15/2010	9/16/2010	9/22/2010	9/23/2010	9/24/2010	10/21/2010	10/29/2010	
Experiment Name	5B1_IT	5B2_SPT	6B1_SPT	6B2_SPT	6B3_IT	6B4_IT	6B5_IT_TP T	
Feed Pressure	24.1	24.1	24.1	24.1	24.1	24.0	24.1	
Feed Temperature	22.8	20.0	22.3	21.1	23.1	18.3	16.5	
Feed CO ₂	30.6%	30.6%	30.6%	30.6%	30.3%	30.7%	30.9%	
CO ₂ Product Purity, %	78.9%	80.2%	79.5%	80.3%	80.0%	80.7%	88.1%	
CO ₂ Recovery, %	98.9%	97.4%	97.7%	98.0%	98.4%	99.7%	96.7%	
Relative Bed size factor	1.370	1.315	2.118	2.069	2.080	2.021	1.629	

Table 4.12 VPSA Pilot Unit Results – Adsorbent Q

# of Pressure Equalizations	1					
# of Adsorber Vessels	4					
Sr. No.	1 (Base)	16	17	18	19	20
Date	7/29/2010	12/8/2010	12/10/2010	12/14/2010	12/15/2010	1/5/2011
Experiment Name	4B1_SPT	4B1_IT	4B2_IT	4B3_IT	4B4_IT	4B5_IT
Feed Pressure	24.1	24.1	24.1	24.3	24.3	24.1
Feed Temperature	23.4	26.8	27.6	27.1	27.3	27.9
Feed CO ₂	31.0%	30.4%	30.3%	30.2%	30.2%	30.2%
CO ₂ Product Purity, %	78.8%	81.6%	80.1%	87.4%	87.6%	74.6%
CO ₂ Recovery, %	98.1%	95.5%	96.3%	69.0%	58.6%	97.6%
Relative Bed size factor	1	1.031	1.085	1.319	1.554	1.055
# of Pressure Equalizations	1	3				
# of Adsorber Vessels	4	6				
Sr. No.	21	22	23	24	26	27
Date	1/6/2011	12/2/2010	12/3/2010	1/11/2011	1/19/2011	1/20/2011
Experiment Name	4B6_IT	6B1_IT_TP T	6B2_IT_TP T	6B3_IT_TP T	6B4_IT_TP	6B5_IT
Feed Pressure	24.3	24.0	24.0	23.9	24.0	24.1
Feed Temperature	28.0	18.2	17.9	26.2	27.3	27.1
Feed CO ₂	30.1%	30.5%	30.4%	29.8%	29.9%	30.6%
CO ₂ Product Purity, %	85.6%	80.2%	80.1%	75.6%	84.3%	90.9%
CO ₂ Recovery, %	85.6%	98.9%	99.1%	99.5%	97.5%	94.9%
Relative Bed size factor	1.076	2.134	2.142	2.602	2.014	1.673
# of Pressure Equalizations	3		3			
# of Adsorber Vessels	6		6 (Shallower vacuum)			
Sr. No.	28	29	30	31	32	
Date	1/25/2011	1/26/2011	2/18/2011	3/1/2011	3/2/2011	
Experiment Name	6B6_IT	6B7_IT	6B8_IT	6B9_IT	6B10_IT	
Feed Pressure	24.1	24.1	24.1	24.0	24.0	
Feed Temperature	27.9	28.2	30.6	27.9	27.9	
Feed CO ₂	33.7%	34.0%	29.7%	29.9%	30.1%	
CO ₂ Product Purity, %	94.1%	96.9%	89.2%	87.9%	87.6%	
CO ₂ Recovery, %	91.9%	70.3%	86.2%	89.6%	90.8%	
Relative Bed size factor	1.503	1.981	1.888	1.953	1.985	

Adsorbent Choice:

Figure 4.6 compares the Recovery vs. Purity performance of Adsorbent P and Q for two process options: 6 Bed and 4 Bed. It is observed that as CO₂ purity increases CO₂ recovery decreases. This drop occurs earlier (in purity) and is sharper for the 4 Bed Option than for the 6 bed process option.

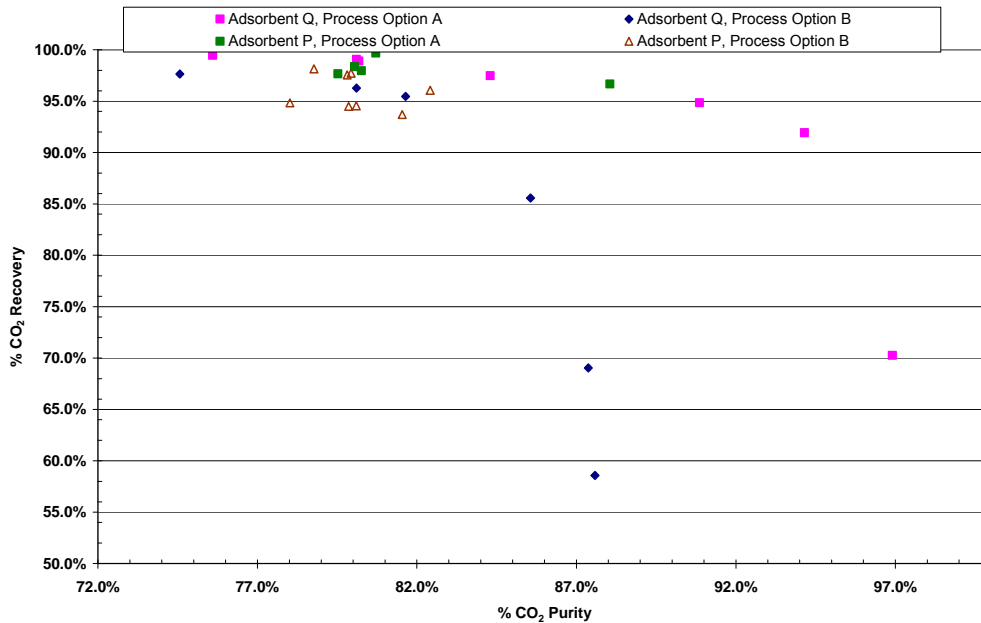


Figure 4.6 VPSA Adsorbents P and Q – CO₂ Recovery vs. Purity

Figure 4.7 compares relative bed sizing factor (BSF) against the product of product (CO₂) recovery and product (CO₂) purity. It is observed that BSF for the 4 bed option is lower than for the 6 bed option. A lower BSF will result in lower plant cost.

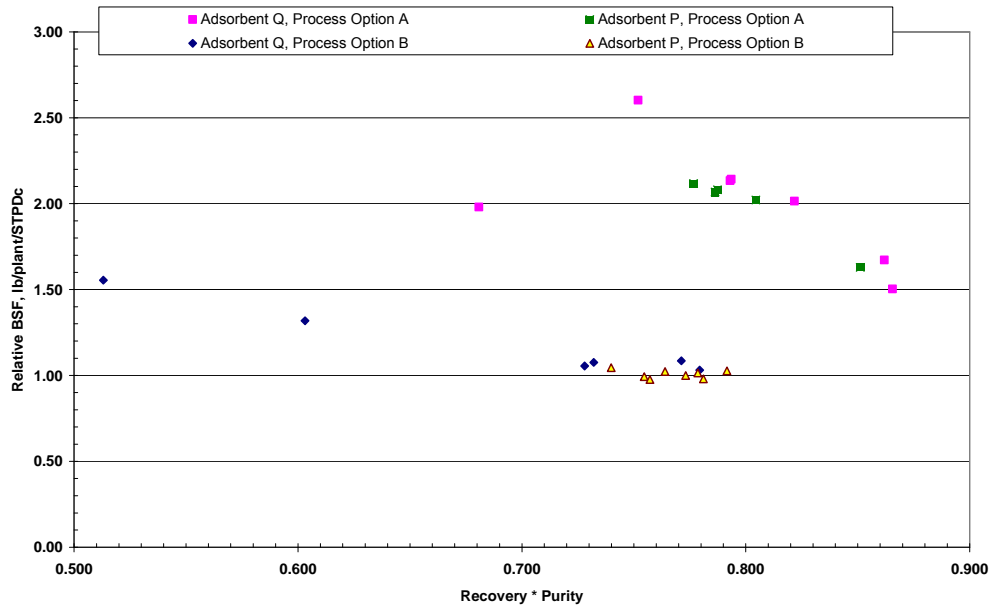


Figure 4.7 P and Q - Relative BSF vs. CO2 Recovery * Purity

Figures 4.8 and 4.9 compare the vacuum pump performance for 6 and 4 bed process options, respectively for adsorbent P and Q. It is observed that the vacuum pump performance for adsorbent P and Q is identical for either of the process options. This implies that the vacuum pump will be identical for adsorbents P and Q in either of the process options.

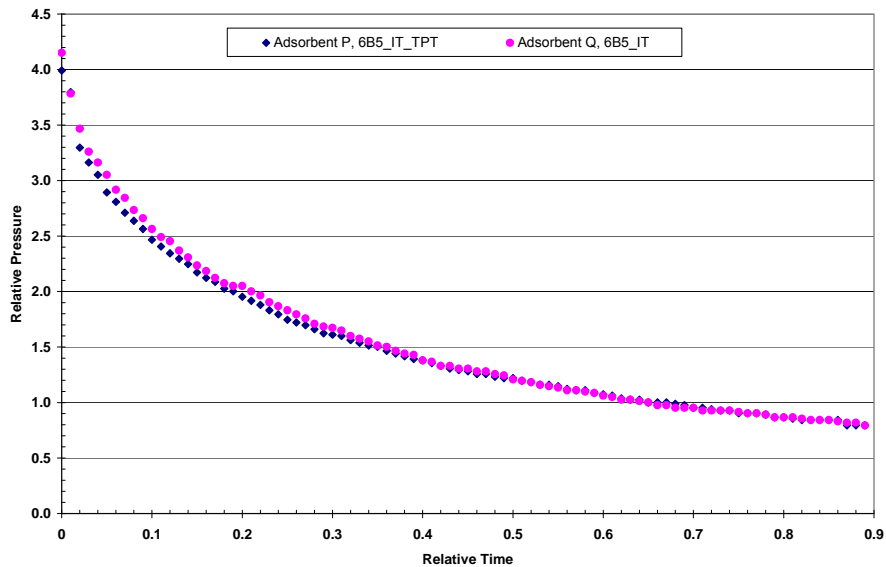


Figure 4.8 Process Option A: Vacuum Pump Comparison P vs. Q

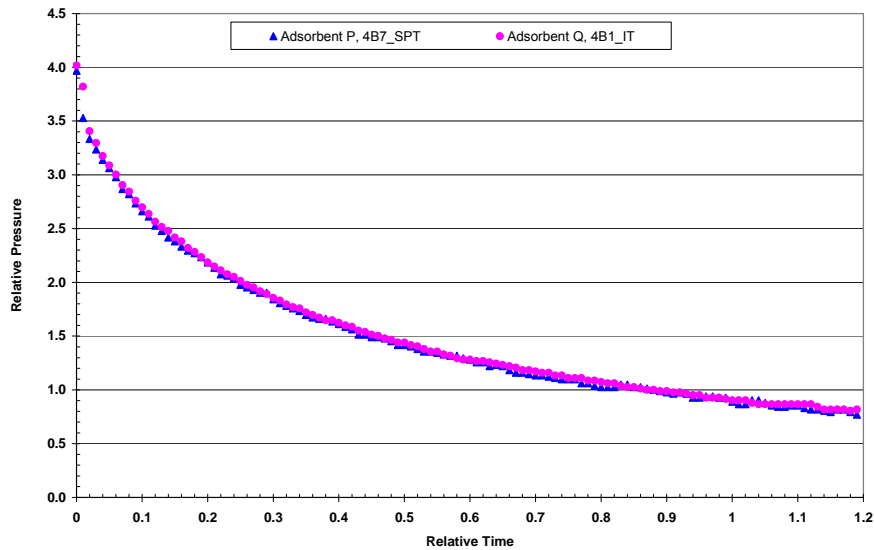


Figure 4.9 Process Option B: Vacuum Pump Comparison P vs. Q

So the performance of these two adsorbents is quite similar with some advantage to adsorbent Q at higher product purity. Adsorbent Q is ~ 30 % less expensive than Adsorbent P; Adsorbent Q is beaded vs. granules for Adsorbent P; Adsorbent Q is less dusty than Adsorbent P. Particle size of Adsorbent Q is larger than adsorbent P (Adsorbent Q: dp = 1.98 mm vs. Adsorbent P: dp = 1.62 mm, Table 4.2). Therefore, out of these two adsorbents, adsorbent P is dropped from further consideration.

We do not have design data for Adsorbent D from the pilot unit, but we have information to design the process based upon data from the bench-scale tests (Table 4.4). It shows:

- BSF ~ 60% lower for Adsorbent D vs. Adsorbent Q
- Vacuum Train Size is ~ 24% bigger for Adsorbent D vs. Adsorbent Q
- Price/lb Adsorbent D ~ 45% of Adsorbent Q

Adsorbent D is very dusty material so it is possible to get dust in the vacuum pump and regeneration gas heater. This causes safety concerns in the plant. We estimated that installed cost of a process based upon Adsorbent D will be about \$300 K more than based upon Adsorbent Q. Higher cost combined with the safety concerns forced us to drop Adsorbent D from further consideration. So going forward we have only one Adsorbent Q for process designs.

Purity Choice

For about the same Carbon-Dioxide Purification Unit (CPU) power, high purity VPSA process has ~ \$1 million lower installed cost than a lower purity VPSA case. This implies that we should design for high CO₂ product purity from VPSA. Based upon further simulation studies for the entire CPU listed in Section 5.1 it is concluded that we should design for a VPSA process at highest CO₂ product purity at ≥90% CO₂ recovery.

However, based upon the practical consideration of operating the continuous operation test unit, it was decided not to constraint the design data on CO₂ recovery from VPSA *but* on product purity. Desired CO₂ product purity from VPSA is ≥ 80%.

Process Choice

Keeping the above constraint, it was concluded in Section 5.1 that for high purity cases, installed cost of VPSA Process with 4 beds should be ~ \$2 million less than for VPSA Process with 6 beds for us to choose VPSA Process with 4 beds over VPSA Process with 6 beds. However, economic calculations on design cases showed that installed cost of VPSA Process with 4 beds is *only* ~ \$1 million less than for VPSA Process with 6 beds. This shows that moving forward we should choose VPSA Process Option with 6 beds.

CPU Simulations in Section 5.1 showed that if installed capital difference for VPSA Process with 8 beds is more than \$430 K than VPSA Process with 6 beds than we should use VPSA Process with 6 beds. We estimated that installed capital cost difference for VPSA Process with 8 beds is ~ \$ 1 million more than VPSA Process with 6 beds. Therefore, moving forward we chose VPSA Process Option with 6 beds.

Evacuation Level Choice

Three design experiments were carried out on the continuous operation test unit on adsorbent Q at a shallower vacuum level. These are listed as experiments # 30, 31 and 32 in Table 4.12.

Based upon simulations performed under Task 5, it was concluded that for a large scale power plant, if the capital cost of one stage vacuum pump (shallower vacuum level) VPSA is higher by up to \$357,000 compared to a two stage vacuum pump (deeper vacuum level) VPSA, one stage vacuum pump VPSA will be preferable. Cost estimation showed that the one stage vacuum pump VPSA is actually *lower* by ~ \$400,000 than a two stage vacuum pump VPSA. Therefore, future experiments will be carried out such that we will need only one stage vacuum pump (shallower vacuum level) in the plant.

Based upon the above cost optimization analysis, along with Section 5.1, the final operating conditions for VPSA design data were chosen. These are listed in Table 4.13.

Table 4.13 VPSA Pilot Test Plan

Feed Pressure	% CO ₂	% CO	%N ₂	New Case No.
psia			N ₂ +O ₂ +Ar	
268	36%	0.12%	63.88%	1
298	35%	0.16%	64.84%	2
329	32.5%	0.16%	67.34%	3
348	30%	0.13%	69.87%	4
358	34%	0.17%	65.83%	5
371	29%	0.13%	70.87%	6
399	33%	0.17%	66.83%	7
450	29%	0.19%	70.81%	8
500	31.5%	0.17%	68.33%	9
550	35%	0.12%	64.88%	10
Feed temperature – 70 °F, CO ₂ recovery > 90%				

Table 4.14 summarizes all the data at these operating conditions. This will be used for plant design in the future.

Table 4.14 The VPSA Pilot Data – Process A, Adsorbent Q, Shallower Vacuum

Date:	8/18/2011	8/26/2011	9/20/2011	2/18/2011	3/1/2011
New Case Number:	# 1	# 2	# 3	# 4	# 4
Experiment Name:	6B1 IT	6B2 IT	6B3 IT	6B8 IT	6B9 IT
Feed Pressure, psia	267.7	297.0	328.9	349.6	348.8
Feed Temperature, F	82.1	73.2	78.8	87.1	82.2
Feed CO ₂ , %	36.26%	34.68%	32.70%	29.74%	29.94%
CO ₂ Recovery, %	97.1%	98.2%	97.6%	86.2%	89.6%
CO ₂ Product Purity, %	86.9%	84.4%	83.7%	89.2%	87.9%
Relative Bed Size Factor, lb adsorbent/STPD CO ₂ capacity	1	0.98	0.92	0.77	0.80
Date:	3/2/2011	9/28/2011	9/30/2011	10/4/2011	10/5/2011
New Case Number:	# 4	# 5	# 6	# 7	# 8
Experiment Name:	6B10 IT	6B5 IT	6B6 IT	6B7 IT	6B8 IT
Feed Pressure, psia	348.7	357.7	371.5	399.8	450.8
Feed Temperature, F	82.2	79.6	78.3	77.80	78.10
Feed CO ₂ , %	30.09%	33.40%	29.80%	33.27%	29.03%
CO ₂ Recovery, %	90.8%	96.5%	95.6%	94.2%	94.5%
CO ₂ Product Purity, %	87.6%	85.9%	83.5%	87.3%	83.2%
Relative Bed Size Factor, lb adsorbent/STPD CO ₂ capacity	0.81	0.82	0.85	0.72	0.75
Date:	10/7/2011	10/11/2011	10/13/2011		
New Case Number:	# 8 B	# 9	# 10		
Experiment Name:	6B8B IT	6B9 IT	6B10 IT		
Feed Pressure, psia	450.8	500.7	550.7		
Feed Temperature, F	77.90	78.90	77.40		
Feed CO ₂ , %	29.03%	31.42%	35.35%		
CO ₂ Recovery, %	94.6%	93.5%	94.9%		
CO ₂ Product Purity, %	83.8%	85.9%	87.2%		
Relative Bed Size Factor, lb adsorbent/STPD CO ₂ capacity	0.74	0.65	0.57		

From Table 4.14 it is observed that small amount of CO in feed has no impact on process performance. Only difference between experiments (S. No. 8: # 6B8_IT and # 6B8b_IT) is that the feed in experiment # 6B8_IT had no CO, whereas feed in experiment # 6B8b_IT had 0.23% CO. The process performance

from these two experiments (# 6B8_IT and # 6B8b_IT) is identical; confirming that small amount of CO in the feed has no impact on process performance.

Effect of SO₂ and NO_x on adsorbent performance in CO₂ VPSA

The bench scale unit as described in Task 4.3 was used for these experiments. This unit was modified by installing NO_x (NO₂ and NO) and SO₂ analyzers and corresponding safety devices. The cyclic experiments as described in Task 4.3 were followed:

1. Counter-current (opposite to feed flow direction) repressurization from a premixed gas cylinder.
2. Co-current feed flow from a premixed gas cylinder. Record feed and outlet gas pressure, concentration and flow rate.
3. Depressurize the vessel to a medium pressure in Co-current (same direction as feed flow) direction. Record outlet gas pressure, concentration and flow rate.
4. Depressurize the vessel to ~ ambient pressure in counter-current direction. Record outlet gas pressure, concentration and flow rate.
5. Evacuate the vessel to a sub ambient pressure in counter-current direction. Record outlet gas pressure, concentration and flow rate.
6. Go back to Step 1 and repeat the experiment till cyclic steady state is reached.

Overall approach of the experiments was as follows:

1. Start with fresh adsorbent sample (Q).
2. First run a base case cycle experiment: Feed = 40% CO₂ plus 60% N₂. Run Cycles. Collect base data.
3. NO₂ (or SO₂) exposure experiments: Feed= 100 ppm NO₂ (or SO₂) plus 40% CO₂, balance N₂. Run Cycles as described above. Collect NO₂ (or SO₂) cyclic data and compare with the base data obtained in Step 2.
4. Repeat experiment in Step 3 for several days. Due to safety concerns, these experiments were not run unattended. The unit was shut down after working hours and restarted again in the morning from the same place as last evening’s shut down.
5. After the adsorbent exposure is finished, collect adsorbent samples from the exposed adsorbent column for analysis.
6. Change to fresh adsorbent between NO₂ and SO₂ experiments and repeat the above procedure (Steps 1 to 5) for the next gas mixture.

Six cyclic experiments using Adsorbent Q were carried out on the bench unit with 100 ppm NO₂ in the feed gas. Adsorbent Q was exposed. CO₂ product purity and recovery did NOT change within the six bench cyclic experiments as shown in Table 4.15. Total NO_x exposure was 0.103 mlbmole per lb of the adsorbent. For various size plant designs this is equivalent to 15 to 30 days of plant exposure at 10 ppm NO₂ concentration in the feed.

Table 4.15 Bench-Scale NO₂ Exposure Experiments for Adsorbent Q

Experiment	Base Case	Day 2	Day 3	Day 4	Day 5	Day 6
Feed NO ₂ , ppm	0	98	101	101	101	100
CO ₂ Product Purity, %	88.39%	89.55%	87.51%	87.81%	87.60%	88.35%
CO ₂ Product Recovery, %	80.9%	81.1%	82.0%	81.2%	82.2%	81.7%

Seven adsorbent samples were collected from the exposed adsorbent Q at various lengths of the adsorbent column. TGA (Thermo Gravimetric Analysis) were done on these samples to estimate effect of NO₂ exposure on CO₂ capacity on the exposed samples. The results are listed in Table 4.16. The first row lists the performance of a fresh, never exposed adsorbent (Q) sample. Second column shows the total weight loss from the sample. This is primarily moisture loss from the fresh sample. The third column lists the CO₂ capacity of the adsorbent after one cycle of adsorption and desorption by N₂ on the TGA unit. The fourth column lists the CO₂ capacity of the adsorbent after fifth cycle of adsorption and desorption by N₂ on the TGA unit. The next two columns show CO₂ capacity of the adsorbent after it has been activated under N₂ purge @ 150 °C. The other rows show similar data from different sample locations in the exposed column.

Table 4.16 TGA Analysis after Exposure of Adsorbent Q to NO₂

Sample Position Inlet to Outlet	Total wt. loss (%)	As Received		After 150 C Activation	
		CO ₂ Cap. Cycle 1 (%)	CO ₂ Cap. Cycle 5 (%)	CO ₂ Cap. Cycle 1 (%)	CO ₂ Cap. Cycle 5 (%)
Fresh Sample	3.72	3.22	3.67	4.58	4.59
0 "	6.84	2.47	2.92	4.35	4.36
1.75 "	4.37	2.98	3.40	4.45	4.45
15 "	3.96	3.03	3.46	4.43	4.43
29.5 "	3.69	3.27	3.76	4.59	4.60
44.5 "	3.71	3.23	3.71	4.60	4.60
57.25 "	3.16	3.34	3.73	4.57	4.57
60 "	2.42	3.51	3.81	4.56	4.57

It is concluded from this data:

- The CO₂ capacity in the adsorbent towards the feed end is more affected than CO₂ capacity in the adsorbent towards the feed effluent end (rows 1 to 8, columns 2 and 3). This is to be expected since NO₂ exposure in the adsorbent sample is highest in the column towards the feed end (0") than towards the feed effluent end (60").
- After about five N₂ purges, the sample above ~ 30" from the feed inlet, retains the CO₂ capacity same as in the fresh sample. Row 1, column 4 vs. row 5, column 4.
- After 150 °C activation the samples recover all the CO₂ capacity of the fresh sample (last two columns).

After the NO₂ exposure experiments, the bench scale unit was re-packed with fresh Adsorbent Q. Five cyclic experiments were carried out on the bench unit with 100 ppm SO₂ in the feed gas. CO₂ product purity and recovery did NOT change within the five bench cyclic experiments as shown in Table 4.17. Total SO₂ exposure was 0.081 mlbmole per lb of the adsorbent. For various size plant designs this is equivalent to 100 to 240 days of plant exposure at 1 ppm SO₂ concentration in the feed.

Table 4.17 Bench-Scale SO₂ Exposure Experiments for Adsorbent Q

Experiment	Base Case	Day 1	Day 2	Day 4	Day 5
Feed NO ₂ , ppm	0	100	100	102	102
CO ₂ Purity, %	90.45%	88.92%	89.06%	89.85%	89.53%
CO ₂ Recovery, %	71.4%	70.7%	70.9%	69.6%	71.0%

Seven adsorbent samples were collected from the exposed adsorbent at various lengths of the adsorbent column. TGA (Thermo Gravimetric Analysis) were done on these samples to estimate effect of SO₂ exposure on CO₂ capacity on the exposed samples. The results are listed in Table 4.18. The first row lists the performance of a fresh, never exposed adsorbent (Q) sample. Second column shows the total weight loss from the sample. This is primarily moisture loss from the fresh sample. The third column lists the CO₂ capacity of the adsorbent after one cycle of adsorption and desorption by N₂ on the TGA unit. The fourth column lists the CO₂ capacity of the adsorbent after fifth cycle of adsorption and desorption by N₂ on the TGA unit. The next two columns show CO₂ capacity of the adsorbent after it has been activated under N₂ purge @ 150 °C. The other rows show similar data from different sample locations in the exposed column.

Table 4.18 TGA Analysis after Exposure of Adsorbent Q to SO₂

Sample Position Inlet to Outlet	Total wt. loss (%)	As Received		After 150 C Activation	
		CO ₂ Cap. Cycle 1 (%)	CO ₂ Cap. Cycle 5 (%)	CO ₂ Cap. Cycle 1 (%)	CO ₂ Cap. Cycle 5 (%)
Fresh Sample	3.72	3.22	3.67	4.58	4.59
0 "	1.46	3.48	3.66	4.18	4.19
1.75 "	2.44	3.34	3.65	4.33	4.33
15 "	3.47	3.15	3.60	4.37	4.37
29.5 "	3.79	3.50	3.72	4.62	4.62
44.5 "	3.77	3.21	3.69	4.56	4.57
57.25 "	4.07	3.13	3.64	4.56	4.56
60 "	1.47	3.55	3.73	4.27	4.27

It is concluded from this data:

- CO₂ capacity on the adsorbent is not affected by SO₂ exposure on adsorbent Q ,
- After about five N₂ purges, CO₂ capacity on the adsorbent further increases on adsorbent Q.

Ion chromatography (IC) analysis was performed on samples of adsorbent Q from the individual columns to look for evidence of NO_x and SO_x retention by the adsorbent. The analysis method employed water extraction procedure to convert any retained NO_x or SO_x species to nitrate or sulfate, respectively. These were, individually quantified by the IC technique which was calibrated against appropriate NIST standards. Results are shown in Figure 4.10.

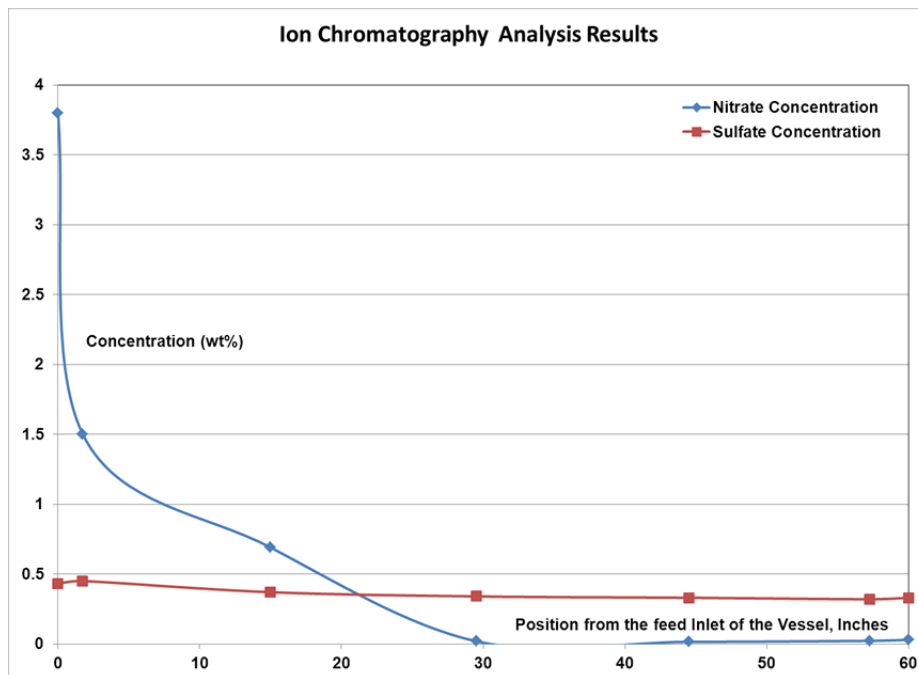


Figure 4.10 SO_x and NO_x Retention on Adsorbent Q

This plot shows:

- Nitrates are retained up to ~ 30” in the adsorbent (Q) column. This implies that NO₂/NO affect the column up to ~ 30” of the height from feed end. However, it should be noted that the process performance is not affected,
- Sulfate retention in the column is very low. This implies that SO₂ does not affect adsorbent Q in this process. This is also supported by the process performance data in Table 4.17 and information in Table 4.18.

Overall conclusions from these experiments and this analysis are:

- NO₂/NO affect ~ ½ the column height from the feed end. However, the process performance is not affected,
- Sulfate formation in the column is very low. This implies that SO₂ does not affect adsorbent Q in this process. The process performance is also not affected.

Task 4.2.2: Simulation Tool: Second Part - Continuous Operation Test Simulation

During Stages 3 and 4 of the simulation effort, external consultant decided to simulate 4 and 6 Bed CO₂ VPSA processes with adsorbents Q and P. The results for 4 Bed CO₂ VPSA with adsorbent Q is shown in Table 4.19.

The first column lists data from the Continuous Operation Test unit for adsorbent Q on 4 Bed CO₂ VPSA process as the basis. The second column (Simulation Run 7) compares the simulation results on a relative basis to Continuous Operation Test unit data. These simulation results are in predictive mode i.e. equilibrium and mass transfer coefficients calculated beforehand were used (First part- Bench Scale Test Simulation). This simulation did not consider Carbon Monoxide (CO) in the feed gas mixture. The third column (Simulation Run 12) includes Carbon Monoxide (CO) in the feed gas mixture. Addition of

Carbon Monoxide (CO) in the feed gas mixture *did not* improve the predictions. This was also observed from the data from the Continuous Operation Test Unit in Task 4.4, Section d (Table 4.14). Therefore, for future simulation runs Carbon Monoxide (CO) is not included in the feed gas mixture. For the first two simulations, runs in the predictive mode, CO₂ product purity and recovery are ~ 10% to 12% lower, bed sizing factor (BSF) is ~ 10% higher and average CO₂ in the high pressure waste gas is almost two times higher. Equilibrium parameters (b1, b2 and qob1) were calculated within ± 95% confidence interval. For the next simulation (Simulation Run 38 - Column 4), pellet void volume as measured by mercury intrusion, b1 CO₂, b2 CO₂ to the lower range of ± 95% confidence interval, and qo_b1 CO₂ to the higher range of ± 95% confidence interval along with heat transfer coefficient as a function of flow rate are used. This brought the simulation results closer to the data. Next (Simulation Run 39 – Column 5), the calculated value of mass transfer coefficient (First part- Bench Scale Test Simulation) is arbitrarily increased by a factor of two. Simulation results are now closer to the data. However, it should be appreciated that the simulation is no longer in *predictive* mode. It is in calibration mode.

Table 4.19 Comparison of VPSA Pilot Data vs. Simulation

Process Option	Pilot Data	B w/o CO	B with CO	B w/o CO	B w/o CO
Pilot Run #	4B1_IT	Simulation Run 7	Simulation Run 12	Simulation Run 38	Simulation Run 39
Relative Feed Flow Rate	1.0	1.0	1.0	1.0	1.0
Feed Temperature					
Average CO ₂ in HP Waste	1.0	2.3	2.2	1.8	1.1
CO ₂ Product Recovery	1.0	0.88	0.89	0.92	0.95
CO ₂ Product Purity	1.0	0.90	0.89	0.99	1.01
Relative Bed Sizing Factor (BSF)	1.0	1.1	1.1	1.1	1.0

Simulated pressure profiles are close to the measured pressure profiles but the simulated temperature profiles are far from the measured temperature profiles. Therefore, we provided the measured temperature profiles to the consultant. Simulation Runs # 33 and # 34 changed other parameters in an attempt to match base Continuous Operation Test data, first column in Table 4.20. The match between data and simulation prediction did not improve.

Table 4.20 Comparison of Pilot Data vs. Simulation for Process B and Adsorbent P

Process and Adsorbent	Process B and Adsorbent P		
	Pilot Data	Simulation	
Run #	4B5_IT	Run 4	Run 5
Feed Flow Rate, scfh	1.0	1.0	1.0
CO ₂ Product Purity, %	1.0	0.90	0.90
CO ₂ Product Recovery, %	1.0	0.90	0.92
Average CO ₂ in HP Waste, %	1.0	2.4	2.0
Bed Sizing Factor (BSF), lb/STPD CO ₂ capacity	1.0	1.18	1.2

Table 4.20 compares the Simulation results against data from the Continuous Operation Test unit for Adsorbent P, 4 Bed CO₂ VPSA process with similar conclusions as above. Tables 4.21 and 4.22 provide

similar comparisons for a 6-Bed CO₂ VPSA process with similar conclusions as above for a 4-bed CO₂ VPSA process.

Table 4.21 Comparison of Pilot Data vs. Simulation for Process A and Adsorbent Q

Process and Adsorbent	Process A and Adsorbent Q		
	Pilot Data	Simulation	
Run #	6B5 IT	Run 33	Run 34
Feed Flow Rate, scfh	1.0	1.0	1.0
CO ₂ Product Purity, %	1.0	0.92	0.92
CO ₂ Product Recovery, %	1.0	0.97	0.98
Average CO ₂ in HP Waste, %	1.0	0.9	0.7
Bed Sizing Factor (BSF), lb/STPD CO ₂ capacity	1.0	0.90	0.9

Table 4.22 Comparison of Pilot Data vs. Simulation for Process A and Adsorbent P

Process and Adsorbent	Process A and Adsorbent P		
	Pilot Data	Simulation	
Run #	6B5 IT TPT	Run 1	Run 2
Feed Flow Rate, scfh	1.0	1.0	1.0
CO ₂ Product Purity, %	1.0	0.91	0.91
CO ₂ Product Recovery, %	1.0	0.88	0.90
Average CO ₂ in HP Waste, %	1.0	3.5	2.8
Bed Sizing Factor (BSF), lb/STPD CO ₂ capacity	1.0	1.08	1.1

For all these tables (4.19, 4.20, 4.21 and 4.22) the first column lists Continuous Operation Test unit data on a relative basis. The second and third columns list the simulation results for the best cases, on a relative basis to Continuous Operation Test unit data. These simulation results are in predictive mode i.e. equilibrium and mass transfer coefficients calculated beforehand were used and no other parameters were changed to match the data. These simulations did not consider Carbon Monoxide (CO) in the feed gas mixture. On average, based upon results from Tables 4.19, 4.20, 4.21 and 4.22, runs in the predictive mode, CO₂ product purities are 5-10% lower than the data; CO₂ product recoveries are also 5-10% lower than the data and the bed sizing factor (BSF) is ~ 10% lower to 20% higher than the data from the continuous operation test unit.

Simulated pressure profiles are close to the measured pressure profiles but the simulated temperature profiles are far from the measured temperature profiles. This is despite the fact that Praxair had provided the measured temperature profiles to the consultant.

Conclusions

In Task 4 we accomplished the following:

1. An exhaustive literature search was done for adsorbents and adsorption based processes. Physical and thermodynamic properties of the adsorbents were measured. Six adsorbents and one process were selected for further testing,
2. A single column bench test unit was built for testing the adsorbents and process in a rapid manner,
3. Breakthrough curves were collected on the six adsorbents to collect fundamental data for simulations,
4. Cyclic experiments were performed to choose the adsorbents for testing on the continuous test unit to collect design data,
5. 12 bed continuous test unit to collect design data was built with extensive process control,
6. Exhaustive design data was collected on two adsorbents (Adsorbents P and Q) for the chosen VPSA process,
7. Based upon techno-economic analysis, the process was optimized and the following were chosen for final design:
 - a) Adsorbent Q,
 - b) 6 Bed VPSA process,
 - c) Desired CO₂ product purity of $\geq 80\%$,
 - d) Shallower (Single Stage) vacuum level.
8. Based upon limited data on the bench-scale unit, it was concluded that NO_x/SO_x did not affect the performance of adsorbent Q,
9. Simulations were used to calculate mass transfer coefficients from the breakthrough data,
10. Simulations were used to predict the performance of process design data from the continuous test unit in a predictive mode (only information used was from conclusion # 9), product purities are 5-10% lower than the data; CO₂ product recoveries are 5-10% lower than the data and the bed sizing factor (BSF) is ~ 10% lower to 20% higher than the data from the continuous operation test unit.

Task 5 – Commercial Viability Assessment

Approach

Commercial viability was assessed for incorporating oxyfuel combustion and near zero emissions flue gas purification technology into pulverized coal power plants. Fuels included both a high sulfur coal and a low sulfur coal. Technoeconomic evaluations were performed for retrofit and greenfield scenarios.

Subtask 5.1 - Process and Systems Engineering

Process Modeling for Foster Wheeler Study in Subtask 5.2

The objective of this subtask activity was to estimate utilities for ASU and CPU for Foster Wheeler's study on power plant performance assessment. The environmental performance of NZE CPU was also estimated. The ASU estimates were scaled from other studies involving oxy-coal power plants. The CPU utilities were estimated based on detailed simulations. Power consumption numbers were based on technologies available today.

Praxair performed process simulations of CO₂ processing units for 460 MW (gross) oxycoal plants burning high sulfur and low sulfur coals. Flue gas compositions were estimated by Foster Wheeler under subtask 5.2. Unisim was used to model CPUs and to generate heat and mass balances. Utility requirements were estimated based on vendor quotes for the compressors and Praxair's experience for designing other CPU components. Values of utility extractions from the boiler island for ASU and CPU were used by Foster Wheeler to finalize their boiler island models. Reductions in atmospheric emissions were calculated using the emissions from the air-fired boilers as the basis for comparison.

Process Modeling for Economic Feasibility Evaluation in Subtask 5.4

Praxair performed economic feasibility analysis using DOE's design basis guidelines and 550 MW net power output for both the air-fired and oxy-fired cases. Foster Wheeler's oxyfuel power plant design for 460 MW gross plant was used as a basis to develop scaled up cases for the economic feasibility analysis. This approach was agreed to in a teleconference with the DOE manager and DOE's system analysis expert.

Thermoflex was used to match the results from Foster Wheeler's 460 MW (gross) boiler island models. These models provided the starting point for developing 550 MW (net) Thermoflex models with ambient conditions and steam cycles typically used in DOE boiler island studies. An iterative work process was used to develop the 550 MW (net) models. An initial boiler island model was created. Unisim was then used to model the CPUs to capture CO₂ from the flue gases predicted by the Thermoflex model. Boiler island utility extractions for the CPU, including power, were calculated from the Unisim model. A spreadsheet model was used to calculate utility extractions for the ASU. The boiler island model was run again using the new values for utility extractions. Several iterations using this procedure were usually needed until net power of 550 MW was obtained. Final modeling results were used as input for the Subtask 5.4 economic feasibility evaluation. Power consumption values for ASU and CPU were based on technologies that are expected to be available in next five years. As a result, parasitic load for the CCS cases was lower than estimated in the Foster Wheeler efforts in Subtask 5.2.

Design basis and assumptions for the process models are listed in Tables 5.1, 5.2, 5.3, 5.4, 5.5, 5.6 and 5.7. They were developed based on the DOE's guidelines. Case definitions are listed in Tables 5.8 and 5.9.

Table 5.1 Ambient Conditions

Elevation, ft	0
Barometric Pressure, psia	14.696
Dry Bulb Temperature, °F	59
Wet Bulb Temperature, °F	51.5
Relative Humidity	60%

Table 5.2 Cooling Water

Cooling Water Temperature, °F	60
Temperature Rise, °F	20
Cooling Water Return Temperature, °F	80

Table 5.3 Oxygen Specification

O ₂ purity, mol%	97%
O ₂ Delivery Pressure at ASU Battery Limits, psia	25
O ₂ Delivery Temperature, °F	120

Table 5.4 Coal Specification

Fuel	Low S	High S
Coal Name	Montana PRB	Illinois No. 6
ASTM D388 Rank	Subbituminous	High Volatile A Bituminous
<i>Proximate Analysis, wt.%</i>		
Moisture	25.77%	11.12%
Volatile Matter	30.34%	34.99%
Ash	8.19%	9.70%
Fixed Carbon	35.70%	44.19%
Total	100.00%	100.00%
<i>Ultimate Analysis</i>		
Carbon	50.07%	63.75%
Hydrogen	3.38%	4.50%
Nitrogen	0.71%	1.25%
Sulfur	0.73%	2.51%
Chlorine	0.01%	0.29%
Ash	8.19%	9.70%
Moisture	25.77%	11.12%
<u>Oxygen</u>	<u>11.14%</u>	<u>6.88%</u>
Total	100.00%	100.00%
<i>Heating Value</i>		
HHV, Btu/lb	8564	11666
LHV, Btu/lb	8252	11252
Hardgrove Grindability Index	57	60

Table 5.5 Steam Cycle Definition

Cycle	Subcritical	SC	USC
Main Steam Pressure, psia	2415	3515	4015
Main Steam Temperature, °F	1050	1110	1350
Reheat Steam Pressure, psia	615	655	1145
Reheat Steam Temperature, °F	1050	1150	1400
Condensing Pressure, in Hg	2	2	2

Table 5.6 Boiler Island Environmental Controls

Boiler Environmental Controls	Low S - Air Fired	Low S - Oxy Fired w/Conv CPU	Low S - Air Fired w/Near Zero Emissions CPU	High S - Air Fired	High S - Oxy Fired w/Conv CPU	High S - Oxy Fired w/Near Zero Emissions CPU
NOx Removal by SCR	72.0%	72.0%	0.0%	72.0%	72.0%	0.0%
SO2 Removal by FGD	98.0%	98.0%	98.0%	98.0%	98.0%	98.0%
PM Removal by Baghouse	99.7%	99.7%	99.7%	99.7%	99.7%	99.7%

Table 5.7 CO₂ to Pipeline Specification

Pressure, psia	2215
Temperature, °F	95
Minimum Purity, mol %	95%

Process Modeling for Task 4 VPSA

VPSA Feed Conditions

CPU process modeling was done, using Unisim, to determine the range of VPSA feed conditions that would be most appropriate for the continuous VPSA pilot tests (Subtask 4.4). CO₂ purity in the CPU feed stream was set at 80% vol. and 88% vol. (dry basis). Both low purity (partial condensation) and high purity (distillation) cold boxes were modeled. For the low purity cases, the purity of the CO₂ from the CPU was set at >95% vol. For these cases, VPSA feed pressures ranged from 350-550 psia. For the cases using a distillation-based cold box, the oxygen content of the CO₂ from the CPU was set at 10 ppmv. For these cases, VPSA feed pressures ranged 268 – 398 psia.

VPSA Process Options

CPU process modeling was done, using Unisim, as part of an effort to determine the most economical CO₂ VPSA configuration. For the VPSA configurations under consideration, experimentally derived values for VPSA CO₂ recovery and VPSA product purity were used in the Unisim process model. Economic evaluations were performed by calculating the difference in specific power (kWh/tonne) and the difference in capital cost for cases under consideration.

Subtask 5.2 - Oxyfuel Power Plant Performance

Foster Wheeler performed a technical feasibility assessment, including conceptual cost estimates for retrofitting oxy-fuel technology to an existing 460 MW power plant burning low sulfur PRB fuel and high sulfur bituminous fuel. Foster Wheeler used their proprietary FW-FIRE CFD code to determine furnace performance and the Aspen-Plus platform for the plant simulations. Results of the study are reported in detail in a final topical report [21]. A summary of the results is presented in this report.

Subtask 5.3 – By-product (Sulfuric Acid) Commercial Viability

The write-up for this subtask has been integrated in Task 2.

Subtask 5.4 – Economic Feasibility

Greenfield and retrofit scenarios were used in the economic feasibility evaluations. In the greenfield scenarios, full capital cost was used in the calculation of cost of electricity. Air ingress for the greenfield scenarios is assumed to be 2%. For the retrofit (“old plant”) scenarios, it is assumed the existing boiler island requires a capital upgrade to keep running independent of whether CCS is used. The suffix “a” is added to the case number when this assumption is used, e.g., “Case 1a”. Air ingress for the retrofit scenarios is generally assumed to be 10%. An additional scenario was evaluated to compare incremental cost of purifying CO₂ to ~99.9% vol. using a distillation process instead of purifying CO₂ to ~95% vol. using a partial condensation process. Another scenario was evaluated to estimate the potential cost savings if the boiler FGD could be eliminated. The scenarios studied are listed in Table 5.8.

Table 5.8 Economic Feasibility Scenarios

Scenario Description	Fuel	Steam Cycle	FGD in Base Case	SCR in Base Case	Air Ingress	Base Case No.	Conv Case No.	NZE Case No.
Greenfield plants w/low air ingress - low S coal	Low S	Sub	Yes	Yes	2%	3	7, 8, 10	14
Greenfield plants w/low air ingress - high S coal	High S	Sub	Yes	Yes	2%	21	22, 24	25, 26
Old plants w/high air ingress -- low S coal	Low S	Sub	No	No	10%	1a	11a	15a
Old plants w/high air ingress -- high S coal	High S	Sub	Yes	No	10%	20a	23a	27a
Greenfield plants using the SC steam cycle	Low S	SC	Yes	Yes	2%	4	12	17
Greenfield plants using the USC steam cycle	Low S	USC	Yes	Yes	2%	5	13	18
Comparison of partial condensation vs. distillation	Low S	Sub	Yes	Yes	2%	3	na	14, 19
Potential for cost reduction if FGD is eliminated	Low S	Sub	Yes	Yes	2%	3	6, 9,10	14, 16
New plant w/o CCS vs. old plant w/CCS	Low S	USC, Sub	Yes	Yes	2%, 10%	5	na	14a, 15a

To evaluate the scenarios, a set of 27 cases were defined. Process simulations were performed for each case and a DOE economic evaluation methodology was applied to calculate cost of electricity, cost of

captured CO₂ and cost of avoided CO₂. Case study definitions are shown in Tables 5.9 and 5.10. Assumptions used in the economic analysis are listed in Table 5.11.

At the time the economic feasibility study was performed, it had been concluded that the Task 2 sulfuric acid process for SO_x/NO_x removal would not be technically feasible and that SO_x/NO_x removal for high sulfur coals could be done with the Task 3 activated carbon process. A single case using the Task 2 process in the NZE CPU was included in the economic feasibility study to determine if an economic benefit might exist should the process be made technically feasible at a future time. All other cases with NZE CPU's included the Task 3 process.

Table 5.9 Low Sulfur Coal Case Definitions

Case No.	Boiler Island					CPU
	Steam Cycle	Firing Mode	Air Intrusion	SCR	FGD	
1	Sub.	Air		No	No	None
2	Sub.	Air		No	Yes	None
3	Sub.	Air		Yes	Yes	None
4	SC	Air		Yes	Yes	None
5	USC	Air		Yes	Yes	None
6	Sub.	Oxy	2%	Yes	No	Conventional
7	Sub.	Oxy	2%	Yes	PA	Conventional
8	Sub.	Oxy	2%	Yes	Entire FG	Conventional
9	Sub.	Oxy	2%	Yes	CPU Feed	Conventional
10	Sub.	Oxy	2%	Yes	PA + CPU Feed	Conventional
11	Sub.	Oxy	10%	Yes	PA + CPU Feed	Conventional
12	SC	Oxy	2%	Yes	PA + CPU Feed	Conventional
13	USC	Oxy	2%	Yes	PA + CPU Feed	Conventional
14	Sub.	Oxy	2%	No	PA	NZE - Activated Carbon
15	Sub.	Oxy	10%	No	PA	NZE - Activated Carbon
16	Sub.	Oxy	2%	No	No	NZE - Activated Carbon
17	SC	Oxy	2%	No	PA	NZE - Activated Carbon
18	USC	Oxy	2%	No	PA	NZE - Activated Carbon
19	Sub.	Oxy	2%	No	PA	NZE - Act C - Distillation

Definition of Abbreviations:

- Sub: Subcritical Steam Cycle
- SC: Supercritical Steam Cycle
- USC: Ultrasupercritical Steam Cycle
- PA: Primary Air
- SA: Secondary Air
- Act C: Activated Carbon

Table 5.10 High Sulfur Coal Case Definitions

Case No.	Boiler Island					CPU
	Steam Cycle	Firing Mode	Air Intrusion	SCR	FGD	
20	Sub.	Air	2%	No	Yes	None
21	Sub.	Air	2%	Yes	Yes	None
22	Sub.	Oxy	2%	Yes	PA + Partial SA + CPU Feed	Conventional
23	Sub.	Oxy	10%	Yes	PA + Partial SA + CPU Feed	Conventional
24	Sub.	Oxy	2%	Yes	Entire FG	Conventional
25	Sub.	Oxy	2%	No	PA + Partial SA	NZE - Sulfuric Acid
26	Sub.	Oxy	2%	No	PA + Partial SA	NZE - Activated Carbon
27	Sub.	Oxy	10%	No	PA + Partial SA	NZE - Activated Carbon

Table 5.11 Assumptions Used in Economic Feasibility Study

Cost of Low Sulfur Coal, \$/MMBtu	\$1.50
Cost of High Sulfur Coal, \$/MMBtu	\$2.50
Subcritical Power Plant Unit Capex, \$/kW, gross excl. FGD & SCR	\$1800
SC Power Plant Capital Unit Capex, \$/kW gross excl. FGD & SCR	\$1854
USC Power Plant Capital Unit Capex, \$/kW gross excl. FGD & SCR	\$1890
Old Subcritical Power Plant Unit Capex, \$/kW gross excl. FGD & SCR	\$323
FGD Unit Capex for Low Sulfur Coal, \$/kW gross	\$200
FGD Unit Capex for High Sulfur Coal, \$/kW gross	\$250
% of FGD Capex Associated with Scrubber (Low Sulfur Coal)	10%
% of FGD Capex Associated with Scrubber (High Sulfur Coal)	25%
SCR Unit Capex, \$/kW gross	\$89
Oxyfuel Retrofit of Boiler Island Unit Capex, \$/kW gross	\$150
Oxyfuel Retrofit EPC, % of Capex	10%
Base Plant Capital Charges, % of Capex/yr	16.4%
Oxyfuel Plant Capital Charges, % of Capex/yr	17.5%
Annual Utilization	85%
Property Taxes and Insurance, % of Capex/yr	1.5%
O&M Labor, % of Capex/yr	1.7%
Variable O&M, % of Capex/yr	1.0%
Ca/S Molar Ratio for SO _x Neutralization	1.08
FGD Sulfur Removal Efficiency	98%
Gypsum Waste/CaSO ₄ Ratio	1.3
Cost of Ammonia, \$/ton	\$850
Cost of Limestone, \$/ton	\$15
Cost of Gypsum Disposal, \$/ton	\$30
Cost of Ash Disposal, \$/ton	\$16
CO ₂ Pipeline Length, miles	50
CO ₂ Pipeline Unit Capex, \$MM/mile	\$2.00
CO ₂ Well Capacity, tpd/well	200
CO ₂ Well Unit Capex, \$MM/well	\$2.00
Pipeline and Storage Charges, % of Capex/yr	15%

Subtask 5.5 – Integration and Operability

AES, a global power company based in the USA provided power producers perspective on integration and operability issues for the proposed technologies. AES’s feedback was based on retrofit considerations for one of the plants in their fleet. Initial focus was on discussion around key factors that affect the reliable operation and dispatch of power plant without CO₂ capture. The focus then shifted to retrofit considerations and operability issues for the proposed technologies. AES discussed practical aspects of integrating the proposed technologies and provided feedback on desirable design parameters for operability.

Subtask 5.6 – Plan for Pilot Demonstration

Lab scale tests of Near Zero Emissions technology have been performed using blends of pure gases to simulate flue gases from oxy-coal power plants. To demonstrate the ability of Near Zero Emissions technology to process actual flue gases, a pilot facility is needed. Praxair worked with the University of Utah to estimate the capital and operating costs of an 8 MMBtu/h oxy-coal furnace which would provide flue gas to a 20 tpd CPU, which would be located at the university’s Institute for Clean and Secure Energy experimental facility. The University of Utah provided cost estimates for the furnace and Praxair engineering and R&D departments provided cost estimates for the CPU.

Results and Discussion

The results are presented by topic in the following order instead of strictly following the order in which subtasks were organized:

- Foster Wheeler study on power plant performance
- Process modeling for Task 4 VPSA process
- Technoeconomic feasibility analysis
- Integration and operability
- Plan for pilot demonstration

Subtask 5.1 – Process and Systems Engineering for Foster Wheeler Study

Process Description

The Praxair near zero emissions (NZE) CPU process schematic is shown in Figure 5.1. The unit operations of NZE CPU are described below.

Flue Gas Cooler/Condenser

The flue gas cooler condenser is used to cool the flue gas, reduce the amount of water in the flue gas, and remove HCl and HF. The cooler is a U-shaped vessel. Flue gas flows downward through the first leg of the “U” and is cooled by two sets of indirect heat exchange coils. The first coil is cooled by boiler feed water. The second coil is cooled by cooling water. The flue leaving the indirect heat exchange section of the cooler flows upward through the second leg of the “U” where it is cooled by direct contact with water. The injected water and flue gas condensate exit the bottom of the cooler/condenser.

Raw Gas Compressor

Cooled flue gas is mixed with recycled CO₂ from the CO₂ VPSA and sent to the suction of the raw gas compressor. The compressor comprises a multi-stage centrifugal compressor with inter-stage cooling, final stage after-cooling and condensate removal after each cooler.

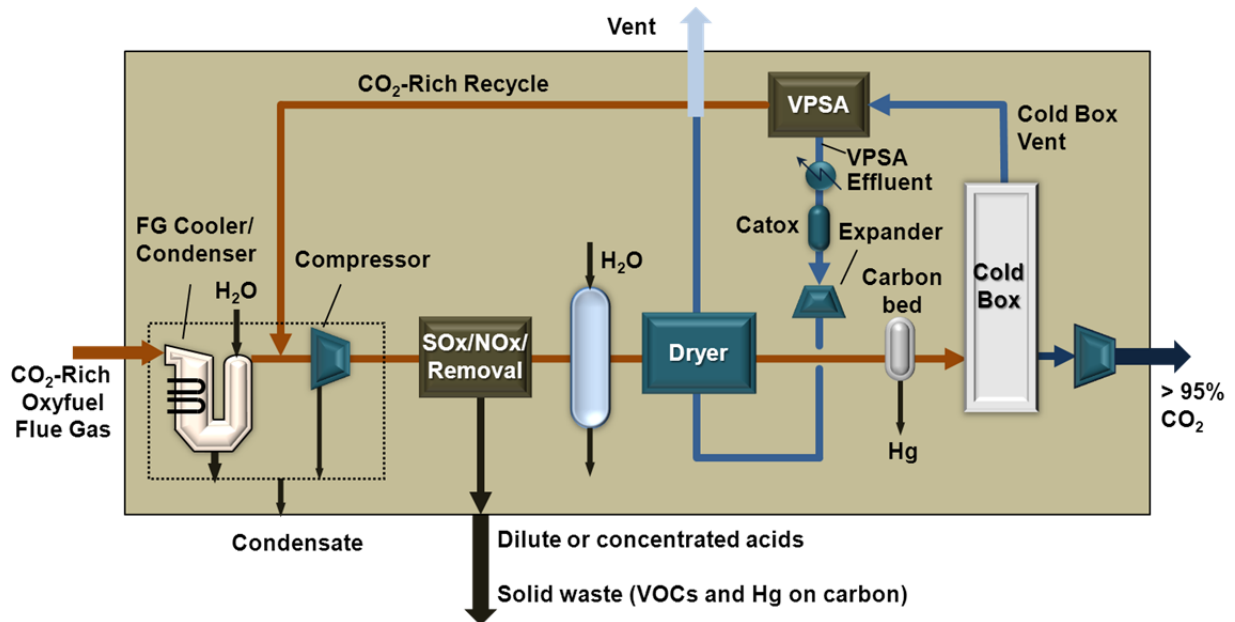


Figure 5.1 Near Zero Emissions CPU Process Schematic

SOx/NOx Removal System

Compressed flue gas is sent to the SOx/NOx removal system, consisting of either the Task 2 or Task 3 process to promote the reaction of SOx to form H₂SO₄ and the reaction of NOx to form HNO₃.

Water Wash Column

The purpose of the wash column is to reduce SOx/NOx concentration in the gas stream leaving the SOx/NOx removal system in the event a breakthrough occurs in the SOx/NOx removal process.

Dryer

The dryer reduces the moisture content of the gas to <1 ppmv and prevents freezing within the cold box. Two adsorption beds are used. One bed is used to dry the gas, while the other is thermally regenerated. Gas from the expansion turbine is heated and used to regenerate the dryer. The heater is bypassed during the cooling step of the regeneration cycle. Regeneration gas leaving the dryer is vented to atmosphere.

Mercury Guard Bed

Mercury is removed from the dry gas using a fixed bed of specialty activated carbon. Mercury removal is necessary to prevent corrosion of the brazed aluminum heat exchanger in the cold box.

Cold Box

The gas stream from the mercury guard bed is sent to a cold box which separates the raw gas into a purified CO₂ stream and a cold box vent stream which contains most of the nitrogen, oxygen, argon and CO from the flue gas.

Purified CO₂ Compressor

Purified CO₂ from the cold box is compressed and sent to a pipeline for underground sequestration.

CO₂ VPSA

The vent stream from the cold box contains significant amounts of CO₂. Rather than vent this stream directly to atmosphere, it is sent to a CO₂ VPSA where much of the CO₂ is recovered. The recovered CO₂ is blended with raw gas leaving the direct contact cooler and sent to the raw gas compressor. The CO₂ VPSA also produces a CO₂-depleted waste stream which is sent to the Catox system.

Catox

The Catox system is used to reduce emissions of CO. The waste stream from the CO₂ VPSA is heated and sent to a catalytic reactor. The catalytic reactor promotes the reaction of CO with O₂ to form CO₂.

Expansion Turbine

Hot, pressurized gas from the Catox system is sent to an expansion turbine to generate electrical power and reduce the net power consumption of the CPU. Gas from the expansion turbine is used to regenerate the dryer beds.

CPU Modeling Results for Foster Wheeler Study

The activated carbon process was used for SO_x and NO_x removal for the low sulfur CPU model. The acid process was used for SO_x and NO_x removal in the high sulfur model. CPU stream summaries are shown in Tables 5.12 and 5.13. For the low sulfur case, the purified CO₂ contains 7 ppmv SO_x and 5 ppmv NO_x. For the high sulfur case, the purified CO₂ contains 68 ppmv SO_x and 57 ppmv NO_x.

Table 5.12 Stream Summary for NZE CPU -- Low Sulfur Coal

Stream	CO ₂ Rich Oxyfuel Flue Gas	Condensate	Process Water	Dilute Acid	Vent	>95% CO ₂
Temperature, °F	145	91	70	70	50	91
Pressure, psia	12	12	50	12	12	2215
Molar Flow Rate, lbmole/hr	31,129	8,477	320.4	323	2,913	19,710
Mass Flow Rate, lb/hr	1,108,000	152,772	5,773	7,143	93,971	859,891
Composition (mole fraction)						
CO ₂	0.620485	0.000050	0	0	0.072600	0.969214
N ₂	0.056899	0	0	0	0.505382	0.015179
O ₂	0.027499	0.000001	0	0	0.226348	0.009458
Ar	0.021399	0	0	0	0.187752	0.006051
H ₂ O	0.272793	0.999804	1.000000	0.942230	0.005483	0.000001
CO	0.000280	0	0	0	0.002428	0.000083
SO ₂	0.000465	0.000052	0	0	0	0.000007
SO ₃	0.000006	0.000022	0	0	0	0
NO	0.000140	0	0	0	0.000007	0
NO ₂	0.000016	0.000005	0	0	0	0.000005
HCl	0.000018	0.000066	0	0	0	0
HNO ₃	0	0	0	0.014503	0	0
H ₂ SO ₄	0	0	0	0.043267	0	0

Table 5.13 Stream Summary for NZE CPU – High Sulfur Coal

Stream	CO ₂ Rich Oxyfuel Flue Gas	Condensate	Process Water	Conc. Acid (H ₂ SO ₄)	Dilute Acid (HNO ₃)	Vent	<95% CO ₂
Temperature, °F	145	91	100	100	100	50	91
Pressure, psia	12	12	400	20	20	12	2215
Molar Flow Rate, lbmol/hr	25,735	4,609	51	137	18	2,878	17,988
Mass Flow Rate, lb/hr	971,000	83,329	910	10,218	726	92,831	784,805
Composition (mole fraction)							
CO ₂	0.685258	0.000016	0	0	0	0.069339	0.969300
N ₂	0.068796	0	0	0	0	0.519187	0.015368
O ₂	0.033098	0	0	0	0	0.219933	0.009101
Ar	0.025398	0	0	0	0	0.189428	0.006033
H ₂ O	0.182489	0.997337	1	0.290673	0.500000	0	0.000002
CO	0.000284	0	0	0	0	0.002096	0.000071
SO ₂	0.003837	0.000136	0	0	0	0	0.000068
SO ₃	0.000047	0.000262	0	0	0	0	0
NO	0.000352	0	0	0	0	0.000017	0.000001
NO ₂	0.000039	0.000004	0	0	0	0	0.000056
HCl	0.000402	0.002244	0	0	0	0	0
HNO ₃	0	0	0	0	0.500000	0	0
H ₂ SO ₄	0	0	0	0.709327	0	0	0

Key contaminant emission rates for the air-fired and oxy-fired cases are shown in Tables 5.14 and 5.15. These early CPU process simulations were performed without catalytic oxidation of the cold box vent stream. With the addition of catalytic oxidation, CO emissions are reduced to essentially zero. Reductions in stack emissions are shown in Table 5.16. CO₂ capture is 98.9%. NO_x emissions are reduced by 99.5% (low sulfur) and 99.6% (high sulfur). Emissions of HCl, HF, VOC's and Hg are reduced by >99.9%.

Table 5.14 Emissions for Plant using Low Sulfur Coal

Fuel	Low Sulfur PRB			
	Air-Fired		Oxy-Fired	
Combustion Type	Air-Fired		Oxy-Fired	
Net Power, MW	418		301	
Location	FG to Stack		CPU Vent	
Units	lb/hr	lb/MW net	lb/hr	lb/MW net
CO (w/o Catox)	536	1.282	198	0.658
SO ₂	501	1.199	0.083	0.00028
SO ₃	15.8	0.038	0	0
NO _x (as NO ₂)	247	0.591	0.880	0.003
Hg	0.051	0.000122	0	0

Table 5.15 Emissions for Plant using High Sulfur Coal

Fuel	High Sulfur Bituminous -- Reduced SOx			
Combustion Type	Air-Fired		Oxy-Fired	
Net Power, MW	416		304	
Location	FG to Stack		CPU Vent	
Units	lb/hr	lb/MW net	lb/hr	lb/MW net
CO (w/o Cattox)	538	1.293	169	0.556
SO ₂	328	0.788	0	0
SO ₃	28	0.067	0	0
NOx (as NO ₂)	267	0.642	2.32	0.008
Hg	0.004	0.000010	0	0

Table 5.16 Reductions in Stack Emissions Compared to Air-Fired Power Plant

Process	Low Sulfur Coal	High Sulfur Coal
Component	% Reductions in stack emissions	% Reductions in stack emissions
CO ₂	98.9%	98.9%
CO (w/o Cattox)	63.1%	68.6%
SO _x	>99.9%	>99.9%
NO _x	99.5%	99.6%
HCl	>99.9%	>99.9%
VOC	>99.9%	>99.9%
Hg	>99.9%	>99.9%

Overall Utilities

Table 5.17 summarizes the overall utilities consumed in the ASU and CPU. Thermal energy extracted from the power plant is a sum of thermal energy in various steam and hot water streams supplied to the ASU and CPU.

Table 5.17 ASU and CPU Utilities

Fuel	Low S	High S
ASU + CPU Power, MW	125.9	119.7
Thermal Energy Extraction from Power Plant, MMBtu/h	47	47
Cooling Water, klb/h	31,800	29,700

Subtask 5.2 - Oxyfuel Power Plant Performance by Foster Wheeler

Results of the Foster Wheeler study are reported in detail in a final topical reported [21]. Power plant performance for both low sulfur coal and high sulfur coal is summarized in Table 5.18. For low sulfur coal, the effect of steam and water extractions for the ASU and CPU was assessed to be a plant power reduction of 4.4 MW. The extra cooling water required by the ASU/CPU results in an increase in cooling power load of 2.5 MWe. Net HHV efficiency is 25.6% compared to the air-fired net HHV efficiency of 35.8%. For high sulfur coal, the effect of steam and water extractions for the ASU and CPU was assessed to be a plant power reduction of 4.4 MW. The extra cooling water required results in a cooling power load of 2.3 MWe. Net efficiency is 26.9% (high SOx) and 26.6% (reduced SOx) compared to the air-fired net

efficiency of 36.7%. The total efficiency penalty for the CCS is ~ 10 percentage points (not 10%) for both low and high sulfur coal plants. It should be noted that this analysis was done with the assumption of power values for ASU and CPU corresponding to the currently available technologies.

Table 5.18 Power Plant Performance Summary

		Low S PRB		High S Bit	
		Air-fired	O ₂ -fired	Air-fired	O ₂ -fired
Fuel Flow	klb/h	449	452	331	334
Air Flow	klb/h	3585	0	3567	0
Oxygen Flow	klb/h	0	725	0	712
Recirc. Flue Gas	%	0.0%	67.7%	0.0%	72.5%
Limestone	klb/h	2.14	1.35	27.2	17.1
Boiler Efficiency	%	86.7	89.4	89.3	92.4
Gross Power	MWe	461	467	460	465
Aux. Power	MWe	43	38	45	40
ASU/CPU Power	MWe		126.0		119.7
Extra Cooling Water Power	MWe		2.5		2.3
Net Power	MWe	418	301	416	304
Net HHV Efficiency	%	35.8	25.6	36.7	26.6

Power plant emissions are summarized in Tables 5.19 and 5.20. For the low sulfur case, the flue gas to the CPU contains 471 ppmv SO_x and 156 ppmv NO_x (wet basis). The flue gas to the CPU from the power plant using high sulfur coal contains 3884 ppmv SO_x and 391 ppmv NO_x.

Table 5.19 Power Plant Emissions – Low Sulfur PRB

	Air-Fired at Stack			O ₂ -Fired to CPU		
	ppmv	lb/h	lb/MMBtu	Ppmv	lb/h	lb/MMBtu
CO	128	536	0.13	280	244	0.06
SO ₂	52	501	0.13	465	928	0.23
SO ₃	1.3	15.8	0.0040	5.8	14.4	0.0036
NO _x	36	247	0.062	156	223	0.056
NH ₃	0.7	1.5	0.00037	0	0	0
HCl	0.1	0.8	0.00020	18	20.9	0.0052
PM		49	0.012		49	0.012
VOC	1.8	11.9	0.0030	1.3	1.8	0.0004
	ppbv	lb/h	lb/TnBtu	Ppbv	lb/h	lb/TnBtu
Hg	1.7	0.051	12.8	10.1	0.063	15.7

Table 5.20 Power Plant Emissions – High Sulfur Bit.

	Air-Fired at Stack			O ₂ -Fired to CPU		
	ppmv	lb/h	lb/MMBtu	ppmv	lb/h	lb/MMBtu
CO	133	538	0.14	284	205	0.05
SO ₂	35	328	0.08	3837	6326	1.62
SO ₃	2.4	28.0	0.0073	47.4	97.7	0.0251
NO _x	40	267	0.069	391	496	0.127
NH ₃	0.6	1.6	0.00041	0	0	0
HCl	3.7	19.4	0.00503	402.1	377.3	0.097
PM		79	0.020		66	0.017
VOC	1.4	9.1	0.0024	1.2	1.3	0.0003
	ppbv	lb/h	lb/TnBtu	ppbv	lb/h	lb/TnBtu
Hg	0.2	0.004	1.1	1.0	0.005	1.3

Oxyfuel Retrofit Capital Cost Estimates for Boiler Island

Conceptual level cost estimates were performed for the incremental equipment and installation cost of the oxyfuel retrofit in the boiler island and steam system (covering Foster Wheeler’s scope of the plant simulation) for the reference 460 MW (gross) plant. The Foster Wheeler portion of the cost estimate included the following equipment:

- HRA lower economizer enlargement
- Low pressure economizer
- O₂ distribution
- Hot gas recirculation (1350 klb/hr at 325°F)
- Cold gas recirculation (1480 klb/hr at 102°F)
- High pressure steam extraction
- Low pressure steam extraction
- CPU vent gas heater
- Flue gas extraction to CPU (970 klb/hr at 325°F)
- Auxiliary air replacement by auxiliary CO₂
- Improved Boiler Sealing
- Primary Gas Heater (tubular, gas-to-gas)

The estimates are summarized in Tables 5.21 and 5.22. Costs for heat exchangers, piping/ducting and boiler sealing were estimated by Foster Wheeler. Costs for additional cooling tower capacity and quench towers were estimated by Praxair.

Table 5.21 O₂-Fired Retrofit Cost Estimate – Low Sulfur Coal

	\$ MM
Heat Exchangers	35.95
Piping and ducting	37.15
Boiler Sealing	7.85
Additional Cooling Tower Capacity	13.12
Quench Tower	1.35
Total	95.42

Table 5.22 O₂-Fired Retrofit Cost Estimate – High Sulfur Coal

	\$ MM
Heat Exchangers	33.87
Piping and ducting	42.70
Boiler Sealing	7.89
Additional Cooling Tower Capacity	12.92
Quench Tower	1.24
Total	98.62

Subtask 5.1 – Process and Systems Engineering for Task 4 VPSA Process

VPSA Feed Conditions

The CPU process schematic is shown in Figure 5.1. The purpose of the modeling effort was to determine the range of pressures and compositions of the cold box vent, which feeds the VPSA.

The composition of the CO₂-rich oxyfuel flue gas was based on Foster Wheeler’s prediction for low sulfur coal. In the process model, air was added or removed from this flue gas to achieve 80% and 88% CO₂ (dry basis). Flue gas conditions are shown in Table 5.23.

Constraints placed on the models include:

- For the low purity CPU, CO₂ product purity is greater than or equal to 95%.
- For the high purity CPU, O₂ concentration of the CO₂ product equals 10 ppmv.
- Temperature of the low pressure CO₂ stream in the cold box is no colder than -65 °F.

Table 5.23 CO₂ Rich Oxy-Fuel Flue Gas

CO ₂ Concentration, % vol.	80%		88%	
Temperature, °F	145		145	
Pressure, psia	12		12	
Molar Flow, lb mol/hr	32,640		30,440	
Mass Flow, lb/hr	1,152,000		1,088,000	
Basis	Wet	Dry	Wet	Dry
Composition, mole fraction				
CO ₂	0.591832	0.799979	0.634486	0.879949
N ₂	0.090347	0.122122	0.040555	0.056244
O ₂	0.035907	0.048535	0.023391	0.032440
Ar	0.020842	0.028172	0.021671	0.030055
H ₂ O	0.260190		0.278952	
CO	0.000267	0.000361	0.000286	0.000397
SO ₂	0.000444	0.000600	0.000475	0.000659
SO ₃	0.000006	0.000008	0.000006	0.000009
NO	0.000134	0.000180	0.000143	0.000199
NO ₂	0.000015	0.000021	0.000016	0.000023
HCl	0.000017	0.000023	0.000018	0.000026

Simulation results are shown in Tables 5.24 and 5.25. For both feed purities and CPU types, it was found that specific power is close to the minimum specific power over a wide range of raw gas compressor discharge pressures. CO₂ concentration of the VPSA feed ranges from about 29% vol. to 36% vol. for conditions where the relative specific power is close to the minimum. For a given raw gas compressor discharge pressure, the VPSA feed pressure for a high purity CPU is substantially lower than for a low purity CPU.

Table 5.24 VPSA Feed Using Low Purity CPU

CO ₂ Concentration in Raw Gas, vol.%	80%				
Raw Gas Compressor Discharge Pressure, psia	359	409	509	559	609
VPSA Feed Pressure, psia	350	400	500	550	600
CPU Relative Specific Power	1.132	1.122	1.110	1.129	1.196
VPSA Feed Composition, mole fraction					
CO ₂	0.349765	0.316960	0.299467	0.350557	0.446755
N ₂	0.404414	0.425803	0.438279	0.406244	0.345446
O ₂	0.152139	0.158761	0.161183	0.149581	0.128169
Ar	0.092504	0.097240	0.099805	0.092442	0.078626
CO	0.001175	0.001233	0.001262	0.001172	0.001001
NOx	0.000003	0.000003	0.000003	0.000003	0.000002
CO ₂ Concentration in Raw Gas, vol.%	88%				
Raw Gas Compressor Discharge Pressure, psia	359	409	509	559	609
VPSA Feed Pressure, psia	350	400	500	550	600
CPU Relative Specific Power	1.017	1.010	1.004	1.000	1.032
VPSA Feed Composition, mole fraction					
CO ₂	0.362894	0.335037	0.327666	0.361266	0.459504
N ₂	0.309830	0.324859	0.330708	0.314469	0.265123
O ₂	0.162159	0.167496	0.166819	0.158315	0.135364
Ar	0.162992	0.170393	0.172569	0.163819	0.138198
CO	0.002120	0.002210	0.002233	0.002125	0.001807
NOx	0.000005	0.000005	0.000005	0.000005	0.000004

Table 5.25 VPSA Feed Using High Purity CPU

CO ₂ Concentration in Raw Gas, vol.%	80%				
Raw Gas Compressor Discharge Pressure, psia	370	400	450	500	550
VPSA Feed Pressure, psia	250	268	296	323	348
CPU Relative Specific Power	1.235	1.143	1.116	1.116	1.116
VPSA Feed Composition, mole fraction					
CO ₂	0.382213	0.363725	0.338702	0.319012	0.303337
N ₂	0.379585	0.390945	0.406320	0.418418	0.428049
O ₂	0.149499	0.153973	0.160028	0.164793	0.168586
Ar	0.087578	0.090199	0.093746	0.096537	0.098759
CO	0.001122	0.001156	0.001201	0.001237	0.001265
NO _x	0.000003	0.000003	0.000003	0.000003	0.000003
CO ₂ Concentration in Raw Gas, vol.%	80%				
Raw Gas Compressor Discharge Pressure, psia	600	650	700		
VPSA Feed Pressure, psia	371	375	356		
CPU Relative Specific Power	1.119	1.124	1.145		
VPSA Feed Composition, mole fraction					
CO ₂	0.290726	0.284647	0.286471		
N ₂	0.435798	0.439532	0.438411		
O ₂	0.171638	0.173109	0.172668		
Ar	0.100547	0.101409	0.101150		
CO	0.001288	0.001299	0.001296		
NO _x	0.000003	0.000003	0.000003		
CO ₂ Concentration in Raw Gas, vol.%	88%				
Raw Gas Compressor Discharge Pressure, psia	350	400	450	500	550
VPSA Feed Pressure, psia	265	300	334	366	398
CPU Relative Specific Power	1.053	1.003	1.000	1.001	1.002
VPSA Feed Composition, mole fraction					
CO ₂	0.394856	0.360872	0.334791	0.325583	0.342483
N ₂	0.286851	0.302961	0.315323	0.319688	0.311676
O ₂	0.162978	0.172131	0.179155	0.181635	0.177084
Ar	0.153285	0.161893	0.168499	0.170832	0.166551
CO	0.002025	0.002139	0.002226	0.002257	0.002200
NO _x	0.000004	0.000005	0.000005	0.000005	0.000005
CO ₂ Concentration in Raw Gas, vol.%	88%				
Raw Gas Compressor Discharge Pressure, psia	600	650			
VPSA Feed Pressure, psia	377	353			
CPU Relative Specific Power	1.011	1.022			
VPSA Feed Composition, mole fraction					
CO ₂	0.370804	0.389063			
N ₂	0.298252	0.289597			
O ₂	0.169456	0.164539			
Ar	0.159377	0.154752			
CO	0.002106	0.002045			
NO _x	0.000005	0.000005			

Based on the CPU process simulations, a set of VPSA feed conditions were established by the Praxair adsorption group for CO₂ VPSA continuous pilot plant testing. These conditions are shown in Table 4.13 of Subtask 4.4 Results.

VPSA Process Options

The CPU process schematic is shown in Figure 5.1. Refer to Subtask 4.4 for details. The purpose of the CO₂ VPSA is to improve the recovery of CO₂ within the CPU by capturing CO₂ that would otherwise be vented and recycling it to the CPU. Since the CO₂ VPSA is a unit operation located within the recycle of a larger process (CPU), it is important to consider the performance of the entire CPU when optimizing the VPSA.

As a first step towards understanding the interaction between the CO₂ VPSA and the rest of the CPU, simulations were done in which the CO₂ recovery and CO₂ product purity of the VPSA were independently varied. Figure 5.2 shows the effect of VPSA purity on the specific power of the ASU and CPU (shown as a relative number). Higher purity of the VPSA product results in lower CPU specific power (kWh/ton CO₂).

Figure 5.3 shows the effect of the CO₂ recovery of the VPSA on the overall CO₂ recovery of the CPU. Higher CO₂ recovery from the VPSA results in higher CO₂ recovery of the CPU. To achieve about 99% CO₂ recovery in the CPU, this curve indicates the CO₂ recovery of the VPSA should be greater than about 90%.

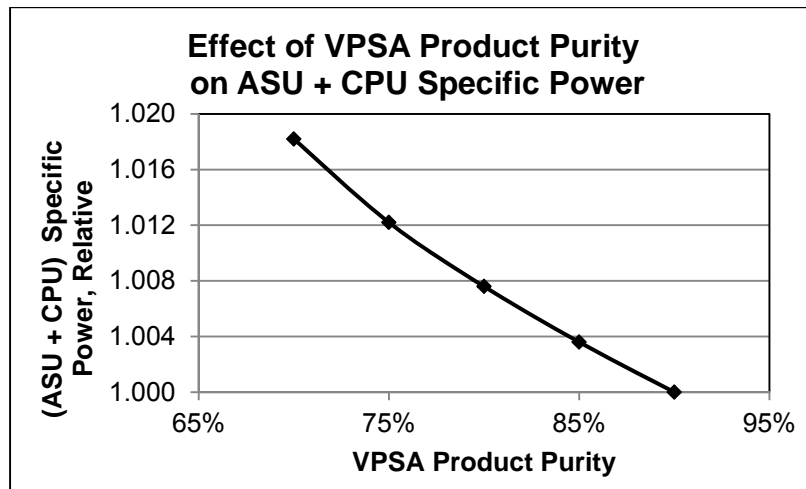


Figure 5.2 Effect of VPSA Product Purity on ASU + CPU Specific Power

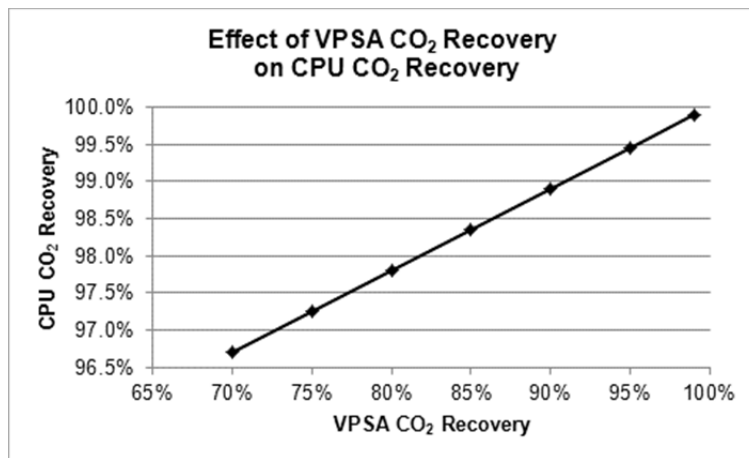


Figure 5.3 Effect of VPSA CO₂ Recovery on CPU CO₂ Recovery

The next step was to generate models needed to perform economic analysis of the various VPSA options. VPSA performance was estimated using experimental data. CPU performance, including power consumption, was estimated using process simulation.. Rather than perform cost estimates for each VPSA configuration, cost differences were estimated and evaluated against differences in power consumption. This enabled the process of selecting VPSA configuration options to be completed much more quickly than if thorough cost estimates were done for each case.

The preferred VPSA configuration was found to have the following features:

- Adsorbent Q
- 6 bed VPSA process
- Shallow vacuum (single-stage vacuum pump)

Subtask 5.1 – Process and Systems Engineering for Economic Feasibility Evaluation

Low Sulfur Coal

Overall performance of the power plant cases are listed in Tables 5.26, 5.27 and 5.28. Net HHV efficiency for air-fired plants using the subcritical steam cycle is 36.3% - 36.8%, depending on the environmental controls. Net HHV efficiency increases to 39.0% for the supercritical steam cycle and to 41.4% for the ultrasupercritical steam cycle.

Table 5.26 Overall Performance – Air Firing of Low Sulfur Coal

Case No.	1	2	3	4	5
Air or Oxy Firing	Air	Air	Air	Air	Air
Fuel	Low S	Low S	Low S	Low S	Low S
CPU Type	None	None	None	None	None
Steam Cycle	Sub	Sub	Sub	SC	USC
Air Intrusion	2%	2%	2%	2%	2%
SCR	No	No	Yes	Yes	Yes
FGD	No	Yes	Yes	Yes	Yes
Main Steam Rate, kpph	3733	3766	3779	3678	3079
Coal Rate, tpd	7151	7214	7236	6751	6356
Fuel HHV, MWth	1495	1508	1513	1411	1329
Gross Power, MWe	595.6	600.9	602.7	606.7	606.1
Aux Power, MWe	45.3	51.3	53.1	56.7	56.0
Net Power, MWe	550.3	549.5	549.6	549.9	550.1
Gross Efficiency (HHV)	39.8%	39.8%	39.8%	43.0%	45.6%
Net Efficiency (HHV)	36.8%	36.4%	36.3%	39.0%	41.4%

The conventional CPU captures ~92% of the CO₂ in the flue gas, except in Case 11 (high air intrusion), where CO₂ capture decreases to 78.2%. Net HHV efficiency for the conventional CPU is 7.5 to 7.8 percentage points less than the net HHV efficiency for the equivalent air-fired cases. Lower efficiency penalty in this analysis compared to that for the Foster Wheeler study (where it was ~ 10 percentage points) is due to lower parasitic load for the advanced ASU and CPU designs assumed in this analysis.

Cases 6-10 illustrate the effect of treating various flue gas streams with FGD for the conventional CPU's. Case 6 has no FGD and has a net HHV efficiency of 29.3%. Small decreases in net HHV efficiency (< 0.2 percentage point) occur in Case 7 (PA only), Case 9 (CPU feed only), and Case 10 (PA + CPU feed). In Case 8, the entire flue gas stream is treated by an FGD and results in a decrease in net HHV efficiency of

1 percentage point. Case 10 is considered the best case for the conventional CPU's, as it results in relatively low SOx concentration in the CPU feed without significant additional impact of the FGD on the net HHV efficiency.

A comparison of Cases 10 and 11 shows that high air ingress decreases net HHV efficiency by 0.6 percentage point for the conventional CPU's. Case 10 had an air ingress rate of 2% and Case 11 had an air ingress rate of 10%.

The NZE CPU captures >99% of the CO₂ contained in the flue gas, except in Case 15 (high air intrusion), where CO₂ capture decreases to 97.7%. The NZE CPU's higher CO₂ capture rate is due to the CO₂ VPSA which recycles a large fraction of the CO₂ that would otherwise be vented from the CPU. Net HHV efficiency for the NZE CPU is 7.8 to 8.1 percentage point less than the HHV efficiency of the equivalent air-fired cases. Net HHV efficiency of the NZE CPU is 0.1 to 1.0 percentage point less than the conventional CPU due to the energy consumption of the CO₂ VPSA and higher flue gas compressor flow rate due to recycling of CO₂, and higher purified CO₂ compressor flow rate due to higher CO₂ capture. A comparison of Cases 14 and 15 shows that high air ingress reduces net HHV efficiency by 1.2 percentage point for the NZE CPU.

Differences in net HHV efficiencies for Subtask 5.1 and Subtask 5.2 are due mostly to differences in the steam cycle, ambient conditions, and assumed performance of the ASU and CPU.

Table 5.27 Overall Performance – Oxy Firing of Low Sulfur Coal with Conventional CPU

Case No.	6	7	8	9	10	11	12	13
Air or Oxy Firing	Oxy	Oxy	Oxy	Oxy	Oxy	Oxy	Oxy	Oxy
Fuel	Low S	Low S	Low S	Low S	Low S	Low S	Low S	Low S
CPU Type	Conv	Conv	Conv	Conv	Conv	Conv.	Conv.	Conv.
Steam Cycle	Sub	Sub	Sub	Sub	Sub	Sub	SC	USC
Air Intrusion	2%	2%	2%	2%	2%	10%	2%	2%
SCR	Yes	Yes	Yes	Yes	Yes	Yes	Yes	Yes
FGD	No	PA	Entire FG	CPU Feed	PA + CPU Feed	PA + CPU Feed	PA + CPU Feed	PA + CPU Feed
Main Steam Rate, kpph	4638	4639	4772	4655	4666	4760	4545	3795
Contained O ₂ from ASU, tpd	13697	13761	14243	13902	13843	13473	12973	11973
Coal Rate, tpd	8972	9006	9278	9038	9030	9224	8454	7804
Fuel HHV, MWth	1876	1883	1939	1889	1888	1928	1767	1631
Gross Power, MWe	766.2	768.5	780.3	770.2	771.3	780.2	766.8	753.4
Boiler Island Aux Power, MWe	62.3	63.4	70.5	64.0	65.2	68.5	70.7	68.8
ASU + CPU Aux Power, MWe	154.5	155.2	160.5	156.5	156.0	162.7	146.2	134.7
Net Power, MWe	549.4	550.0	549.3	549.7	550.1	549.0	549.9	550.0
Gross Efficiency (HHV)	40.9%	40.8%	40.2%	40.8%	40.9%	40.5%	43.4%	46.2%
Net Efficiency (HHV)	29.3%	29.2%	28.3%	29.1%	29.1%	28.5%	31.1%	33.7%
CO ₂ Captured, tpd	15178	15264	15770	15327	15289	13309	14360	13252
CO ₂ Capture Rate, %	92.2%	92.2%	92.0%	91.9%	91.9%	78.2%	92.1%	92.1%

Table 5.28 Overall Performance – Oxy Firing of Low Sulfur Coal with NZE CPU

Case No.	14	15	16	17	18	19
Air or Oxy Firing	Oxy	Oxy	Oxy	Oxy	Oxy	Oxy
Fuel	Low S	Low S	Low S	Low S	Low S	Low S
CPU Type	NZE	NZE	NZE	NZE	NZE	NZE-Distil
Steam Cycle	Sub	Sub	Sub	SC	USC	Sub
Air Intrusion	2%	10%	2%	2%	2%	2%
SCR	No	No	No	No	No	No
FGD	PA	PA	No	PA	PA	PA
Main Steam Rate, kpph	4684	4933	4692	4569	3800	4779
Contained O ₂ from ASU, tpd	13950	13898	13887	12987	11978	14174
Coal Rate, tpd	9127	9551	9094	8495	7835	9265
Fuel HHV, MWth	1908	1997	1901	1776	1638	1937
Gross Power, MWe	778.3	809.5	776.8	771.2	756.5	790.0
Boiler Island Aux Power, MWe	63.3	68.0	62.4	67.3	65.0	65.0
ASU + CPU Aux Power, MWe	167.0	191.4	164.6	153.9	141.9	174.9
Net Power, MWe	547.9	550.0	549.8	549.9	549.6	550.1
Gross Efficiency (HHV)	40.8%	40.5%	40.8%	43.4%	46.2%	40.8%
Net Efficiency (HHV)	28.7%	27.5%	28.9%	31.0%	33.6%	28.4%
CO ₂ Captured, tpd	16660	17157	16569	15514	14309	16890
CO ₂ Capture Rate, %	99.3%	97.7%	99.3%	99.3%	99.3%	99.0%

CPU feed stream information is shown in Tables 5.29 and 5.30. On a dry basis, CO₂ concentration is ~85% except for the high air intrusion cases where CO₂ concentration is ~65%. For the conventional CPU, SO_x concentration varies from 38 – 3426 ppmv, depending on which streams are treated by FGD. An SCR is in place in the boiler island for all the conventional CPU cases resulting in a NO_x concentration of 16 ppmv in the CPU feed. The Thermoflex software used to model the boiler island does not have the ability to predict NO_x and CO concentrations. NO_x concentration is based on the Foster Wheeler 460 MW boiler island modeling results and the assumption of 90% removal of NO_x by the SCR. CO concentration is based on the Foster Wheeler 460 MW boiler island modeling results.

Table 5.29 CPU Feed – Low Sulfur Coal with Conventional CPU

Case No.	6	7	8	9	10	11	12	13
Air or Oxy Firing	Oxy	Oxy	Oxy	Oxy	Oxy	Oxy	Oxy	Oxy
Fuel	Low S	Low S	Low S	Low S	Low S	Low S	Low S	Low S
CPU Type	Conv	Conv	Conv	Conv	Conv	Conv.	Conv.	Conv.
Steam Cycle	Sub	Sub	Sub	Sub	Sub	Sub	SC	USC
Air Intrusion	2%	2%	2%	2%	2%	10%	2%	2%
SCR	Yes	Yes	Yes	Yes	Yes	Yes	Yes	Yes
FGD	No	PA	Entire FG	CPU Feed	PA + CPU Feed	PA + CPU Feed	PA + CPU Feed	PA + CPU Feed
Flow Rate, lb mol/hr	50200	51090	55318	50797	50881	67275	47398	43757
Contained CO ₂ , tpd	16456	16554	17137	16682	16638	17015	15596	14394
CO ₂ , vol.%	62.08%	62.17%	58.66%	62.18%	61.92%	47.89%	62.30%	62.29%
N ₂ , vol.%	5.70%	5.71%	5.37%	5.70%	5.79%	21.49%	5.65%	5.67%

Case No.	6	7	8	9	10	11	12	13
O ₂ , vol.%	2.72%	2.72%	2.73%	3.04%	2.90%	4.19%	2.90%	2.90%
Ar, vol.%	2.16%	2.17%	2.04%	2.17%	2.16%	1.80%	2.17%	2.17%
H ₂ O, vol.%	26.96%	27.01%	31.17%	26.87%	27.20%	24.60%	26.95%	26.94%
CO, ppmv	280	280	280	280	280	280	280	279
SO ₂ , ppmv	3391	1795	19	66	36	30	36	36
SO ₃ , ppmv	35	20	5	17	10	8	10	10
NO, ppmv	14	14	14	14	14	14	14	14
NO ₂ , ppmv	2	2	2	2	2	2	2	2
HCl, ppmv	34	18	0	0	0	0	0	0
NH ₃ , ppmv	1	1	1	1	1	1	1	1
CO ₂ , vol.%,(Dry Basis)	84.99%	85.18%	85.22%	85.03%	85.06%	63.15%	85.28%	85.25%

For the NZE CPU, SO_x concentration in the CPU feed varies from 1545 – 3401 ppmv, depending mostly on which streams are treated by FGD. Because the NZE CPU has the ability to remove SO_x and NO_x, the CPU feed is not treated by the FGD and no SCR is used. NO_x concentration in the CPU feed is 156 ppmv, based on the Foster Wheeler boiler island modeling results.

Table 5.30 CPU Feed – Low Sulfur Coal with NZE CPU

Case No.	14	15	16	17	18	19
Air or Oxy Firing	Oxy	Oxy	Oxy	Oxy	Oxy	Oxy
Fuel	Low S	Low S	Low S	Low S	Low S	Low S
CPU Type	NZE	NZE	NZE	NZE	NZE	NZE-Distil
Steam Cycle	Sub	Sub	Sub	USC	USC	Sub
Air Intrusion	2%	10%	2%	2%	2%	2%
SCR	No	No	No	No	No	No
FGD	PA	PA	No	PA	PA	PA
Flow Rate, lb mol/hr	51106	68409	50910	47600	43896	51934
Contained CO ₂ , tpd	16778	17556	16686	15623	14410	17053
CO ₂ , vol.%	62.17%	48.59%	62.07%	62.15%	62.16%	62.17%
N ₂ , vol.%	5.71%	21.74%	5.68%	5.68%	5.69%	5.67%
O ₂ , vol.%	2.72%	4.10%	2.72%	2.73%	2.73%	2.73%
Ar, vol.%	2.17%	1.82%	2.16%	2.16%	2.16%	2.16%
H ₂ O, vol.%	27.01%	23.55%	26.98%	27.05%	27.03%	27.04%
CO, ppmv	280	280	280	280	280	280
SO ₂ , ppmv	1794	1538	3391	1797	1795	1798
SO ₃ , ppmv	8	7	10	8	8	8
NO, ppmv	140	140	140	140	140	140
NO ₂ , ppmv	16	16	16	16	16	16
HCl, ppmv	18	15	34	18	18	18
NH ₃ , ppmv	0	0	0	0	0	0
CO ₂ , vol.%, (Dry Basis)	85.18%	63.56%	85.00%	85.19%	85.19%	85.21%

The quantities and key impurities of the purified CO₂ produced by the CPU are listed in Tables 5.31 and 5.32. The conventional CPU purifies CO₂ to 95.1 – 95.4% vol. Higher CO₂ purities can be reached, but result in lower CO₂ capture and/or higher power consumption. The range of SO_x concentration is 48 –

4426 ppmv and NOx concentration is 17 – 24 ppmv in the purified CO₂. CO concentration is 42 – 107 ppmv. The conventional CPU does not include unit operations for removal of SOx, NOx and CO.

The NZE CPU purifies CO₂ to 95.0 – 95.5% vol. In Case 19, a distillation column is used in the CPU instead of a phase separator, and purifies CO₂ to >99.9% vol. SOx concentration in the purified CO₂ is 2 – 4 ppmv and NOx concentration is 11-14 ppmv. CO concentration in the purified CO₂ is 45 – 108 ppmv. When a distillation column is used, CO concentration in the purified CO₂ is <1 ppmv. In summary, the CO₂ purity (with regards to trace impurities) achieved by the NZE CPU is better than that achieved by the conventional CPU.

Table 5.31 Purified CO₂ from Conventional CPU (Low Sulfur)

Case No.	6	7	8	9	10	11	12	13
Air or Oxy Firing	Oxy	Oxy	Oxy	Oxy	Oxy	Oxy	Oxy	Oxy
Fuel	Low S	Low S	Low S	Low S	Low S	Low S	Low S	Low S
CPU Type	Conv	Conv	Conv	Conv	Conv	Conv.	Conv.	Conv.
Steam Cycle	Sub	Sub	Sub	Sub	Sub	Sub	SC	USC
Air Intrusion	2%	2%	2%	2%	2%	10%	2%	2%
SCR	Yes	Yes	Yes	Yes	Yes	Yes	Yes	Yes
FGD	No	PA	Entire FG	CPU Feed	PA + CPU Feed	PA + CPU Feed	PA + CPU Feed	PA + CPU Feed
Contained CO ₂ , tpd	15,178	15,264	15,770	15,328	15,289	13,309	13,252	13,252
CO ₂ Capture, %	92.2%	92.2%	92.0%	91.9%	91.9%	78.2%	92.1%	92.1%
CO ₂ Purity, % vol.	95.1%	95.3%	95.5%	95.5%	95.5%	95.4%	95.5%	95.5%
SOx, ppmv	4,426	2,354	48	99	65	82	65	67
NOx, ppmv	17	17	18	17	17	24	17	17
CO, ppmv	102	102	107	99	100	42	101	101

Table 5.32 Purified CO₂ from NZE CPU (Low Sulfur)

Case No.	14	15	16	17	18	19
Air or Oxy Firing	Oxy	Oxy	Oxy	Oxy	Oxy	Oxy
Fuel	Low S	Low S	Low S	Low S	Low S	Low S
CPU Type	NZE	NZE	NZE	NZE	NZE	NZE - Distil
Steam Cycle	Sub	Sub	Sub	SC	USC	Sub
Air Intrusion	2%	10%	2%	2%	2%	2%
SCR	No	No	No	No	No	No
FGD	PA	PA	No	PA	PA	PA
Contained CO ₂ , tpd	16,661	17,156	16,570	14,309	14,309	16,890
CO ₂ Capture, %	99.3%	97.7%	99.3%	99.3%	99.3%	99.0%
CO ₂ Purity, % vol.	95.5%	95.0%	95.5%	95.5%	95.5%	99.998%
SOx, ppmv	2	2	4	2	2	2
NOx, ppmv	11	14	11	11	11	12
CO, ppmv	107	45	108	107	107	<1

Atmospheric emissions for the low sulfur cases are listed in Tables 5.33, 5.34 and 5.35. Case 1 (air fired, no FGD or SCR) is used as basis for comparing the emissions. Cases 4 and 5 indicate that modest reductions in CO₂ emissions from air-fired boilers may be achieved by improving boiler island fuel efficiency through the use of advanced steam cycles. The supercritical (SC) steam cycle reduces CO₂ emissions by 5.1% and the ultrasupercritical steam cycle reduces CO₂ emissions by 10.6%. A conventional FGD unit installed on the air-fired boilers reduces SO_x emissions by 97.6% - 97.9%. A conventional SCR unit installed on the air-fired boilers reduces NO_x emissions by 89.1% - 90.5%.

Table 5.33 Atmospheric Emissions – Air Firing of Low Sulfur Coal

Case No.	1	2	3	4	5
Air or Oxy Firing	Air	Air	Air	Air	Air
Fuel	Low S	Low S	Low S	Low S	Low S
CPU Type	na	na	na	na	na
Steam Cycle	Sub	Sub	Sub	SC	USC
Air Intrusion	2%	2%	2%	2%	2%
SCR	No	No	Yes	Yes	Yes
FGD	No	Yes	Yes	Yes	Yes
Stack/CPU Vent Composition					
CO ₂ , % vol.	13.73%	12.89%	12.87%	12.92%	12.85%
SO _x , ppmv	752	16	17	17	17
NO _x , ppmv	186	186	19	19	19
CO, ppmv	128	128	128	128	128
Stack/CPU Vent Emission Rate					
CO ₂ , kpph	1093	1109	1113	1038	977
SO _x , lb/h (as SO ₂)	8734	196	213	199	187
NO _x , lb/h (as NO ₂)	1553	1678	169	157	148
CO, lb/h	650	702	705	656	621
Emission Reduction (Compared to Case 1)					
CO ₂				5.1%	10.6%
SO _x		97.8%	97.6%	97.7%	97.9%
NO _x			89.1%	89.9%	90.5%
CO					4.5%

The conventional CPU processing flue gas from oxy-fired boilers burning low sulfur coal reduces CO₂ emissions by 89.6% - 91.3% as compared to Case 1. An exception is Case 11 (high air infiltration) which has a reduction in CO₂ emissions of 71.8%. SO_x emissions are reduced by 99.2% - 100.0% and NO_x emissions are reduced by 99.6% - 99.8%. CO emissions are reduced by 47.7% - 58.8% (except for Case 11). Reductions in SO_x and NO_x emissions are largely due to environmental controls in the boiler island and cold box VLE (vapor liquid equilibrium) resulting in sequestration of some of the SO_x and NO_x with the purified CO₂. Reduction in CO emissions is attributed mostly to cold box VLE resulting in some of the CO being sequestered with the purified CO₂.

Table 5.34 Atmospheric Emissions – Conventional CPU (Low Sulfur Coal)

Case No.	6	7	8	9	10	11	12	13
Air or Oxy Firing	Oxy	Oxy	Oxy	Oxy	Oxy	Oxy	Oxy	Oxy
Fuel	Low S	Low S	Low S	Low S	Low S	Low S	Low S	Low S
CPU Type	Conv	Conv	Conv	Conv	Conv	Conv.	Conv.	Conv.
Steam Cycle	Sub	Sub	Sub	Sub	Sub	Sub	SC	USC
Air Intrusion	2%	2%	2%	2%	2%	10%	2%	2%
SCR	Yes	Yes	Yes	Yes	Yes	Yes	Yes	Yes
FGD	No	PA	Entire FG	CPU Feed	PA + CPU Feed	PA + CPU Feed	PA + CPU Feed	PA + CPU Feed
Stack/CPU Vent Composition								
CO ₂ , % vol.	37.75%	37.82%	37.94%	37.90%	37.91%	28.88%	37.94%	37.91%
SO _x , ppmv	162	87	2	4	2	2	2	2
NO _x , ppmv	9	9	10	9	9	5	9	9
CO, ppmv	1711	1705	1780	1655	1664	729	1684	1677
Stack/CPU Vent Emission Rate								
CO ₂ , kpph	106	108	114	113	112	309	103	95
SO _x , lb/h (as SO ₂)	66.6	35.9	0.8	1.6	1.0	3.0	1.0	0.9
NO _x , lb/h (as NO ₂)	2.7	2.8	3.1	2.9	2.9	5.8	2.6	2.4
CO, lb/h	307	308	340	313	314	496	291	268
Emission Reduction (Compared to Case 1)								
CO ₂	90.3%	90.2%	89.6%	89.7%	89.7%	71.8%	90.6%	91.3%
SO _x	99.2%	99.6%	100.0%	100.0%	100.0%	100.0%	100.0%	100.0%
NO _x	99.8%	99.8%	99.8%	99.8%	99.8%	99.6%	99.8%	99.8%
CO	52.7%	52.6%	47.7%	51.8%	51.7%	23.7%	55.3%	58.8%

The NZE CPU processing flue gas from oxy-fired boilers burning low sulfur coal reduces CO₂ emissions by 98.7% - 99.1% as compared to Case 1 when air intrusion is low. The case 15 with high air infiltration reduces CO₂ emissions by 96.9%. SO_x emissions are essentially eliminated and NO_x emissions are reduced by >99.8%. CO emissions are reduced by 99.4% - 99.6%. Reductions in SO_x and NO_x emissions are largely due to the SO_x/NO_x removal processes in the CPU. Reduction in CO emissions is due to the Catox reactor. The SO_x and NO_x emission reduction achieved by the NZE CPU is similar to those achieved by the conventional CPU, while CO and CO₂ emission reduction achieved by the NZE CPU is superior.

Table 5.35 Atmospheric Emissions – NZE CPU (Low Sulfur Coal)

Case No.	14	15	16	17	18	19
Air or Oxy Firing	Oxy	Oxy	Oxy	Oxy	Oxy	Oxy
Fuel	Low S	Low S	Low S	Low S	Low S	Low S
CPU Type	NZE	NZE	NZE	NZE	NZE	NZE - Distil
Steam Cycle	Sub	Sub	Sub	SC	USC	Sub
Air Intrusion	2%	10%	2%	2%	2%	2%
SCR	No	No	No	No	No	No
FGD	PA	PA	No	PA	PA	PA
Stack/CPU Vent Composition						
CO ₂ , % vol.	5.70%	4.31%	5.70%	5.71%	5.70%	5.61%
SO _x , ppmv	0	0	0	0	0	0
NO _x , ppmv	9	5	10	9	9	10
CO, ppmv	26	10	27	26	26	25
Stack/CPU Vent Emission Rate						
CO ₂ , kpph	10.3	34.0	10.1	9.6	8.8	14.2
SO _x , lb/h (as SO ₂)	0	0	0	0	0	0
NO _x , lb/h (as NO ₂)	1.9	3.8	1.8	1.7	1.5	2.6
CO, lb/h	3.1	5.0	3.0	3.1	2.6	4.1
Emission Reduction (Compared to Case 1)						
CO ₂	99.1%	96.9%	99.1%	99.1%	99.2%	98.7%
SO _x	100.0%	100.0%	100.0%	100.0%	100.0%	100.0%
NO _x	99.9%	99.8%	99.9%	99.9%	99.9%	99.8%
CO	99.5%	99.2%	99.5%	99.5%	99.6%	99.4%

High Sulfur Coal

Overall performance of the entire plant including boiler island, ASU and CPU is listed in Tables 5.36, 5.37 and 5.38. Net HHV efficiency for air-fired plants is 37.6%. The difference between the two air-fired cases is the inclusion of an SCR in Case 2. The conventional CPU captures 91.7% of the CO₂ at 2% air intrusion. 75% of the CO₂ is captured at 10% air infiltration. Net HHV efficiency for the conventional CPU is 7.6 to 8.1 % points less than the HHV efficiency for the equivalent air-fired cases.

The NZE CPU captures 99.2% - 99.3% of the CO₂ at 2% air infiltration and 97.4% of the CO₂ at 10% air infiltration. As with the low sulfur coal cases, the higher CO₂ capture rate associated with the NZE CPU is due to the CO₂ VPSA which recycles a large fraction of the CO₂ that would otherwise be vented from the CPU. Net HHV efficiency for the NZE CPU is 8.3 to 9.1 % points less than the HHV efficiency for the equivalent air-fired cases. Net HHV efficiency of the NZE CPU is 0.1 to 1.1 % points less than the HHV efficiency of the equivalent conventional CPU due to the energy consumption of the CO₂ VPSA, higher flue gas compressor flow rate due to the recycled CO₂, and higher purified CO₂ compressor flow rate due to the higher CO₂ capture rate.

Table 5.36 Overall Performance – Air Firing of High Sulfur Coal

Case No.	20	21
Air or Oxy Firing	Air	Air
Fuel	High S	High S
CPU Type	None	None
Steam Cycle	Sub	Sub
Air Intrusion	2%	2%
SCR	No	Yes
FGD	Yes	Yes
Main Steam Rate, kpph	3733	3753
Coal Rate, tpd	5137	5143
Fuel HHV, MWth	1463	1465
Gross Power, MWe	600.3	601.1
Boiler Island Aux. Power, MWe	50.1	51.0
Net Power, MWe	550.2	550.1
Gross Efficiency (HHV)	41.0%	41.0%
Net Efficiency (HHV)	37.6%	37.6%

Table 5.37 Overall Performance – Oxy Firing of High Sulfur Coal with Conventional CPU

Case No.	22	23	24
Air or Oxy Firing	Oxy	Oxy	Oxy
Fuel	High S	High S	High S
CPU Type	Conv	Conv	Conv
Steam Cycle	Sub	Sub	Sub
Air Intrusion	2%	10%	2%
SCR	Yes	Yes	Yes
FGD	PA + Partial SA + CPU Feed	PA + Partial SA + CPU Feed	Entire FG
Main Steam Rate, kpph	4636	4721	4736
Contained O ₂ from ASU, tpd	13432	12967	13658
Coal Rate, tpd	6430	6559	6541
Fuel HHV, MWth	1831	1868	1863
Gross Power, MWe	764.0	771.7	769.8
Boiler Island Aux. Power, MWe	65.5	68.3	67.9
ASU + CPU Aux Power, MWe	149.2	153.2	151.7
Net Power, MWe	549.3	550.2	550.2
Gross Efficiency (HHV)	41.7%	41.3%	41.3%
Net Efficiency (HHV)	30.0%	29.5%	29.5%
CO ₂ Captured, TPD	14027	11694	14259
CO ₂ Capture Rate, %	91.7%	75.0%	91.7%

Table 5.38 Overall Performance – Oxy Firing of High Sulfur Coal with NZE CPU

Case No.	25	26	27
Air or Oxy Firing	Oxy	Oxy	Oxy
Fuel	High S	High S	High S
CPU Type	NZE- Sulfuric Acid	NZE - Activated Carbon	NZE - Activated Carbon
Steam Cycle	Sub	Sub	Sub
Air Intrusion	2%	2%	10%
SCR	No	No	No
FGD	PA + Partial SA	PA + Partial SA	PA + Partial SA
Main Steam Rate, kpph	4672	4672	4910
Contained O ₂ from ASU, tpd	13410	13425	13330
Coal Rate, tpd	6466	6470	6794
Fuel HHV, MWth	1841	1842	1935
Gross Power, MWe	769.9	770.0	800.1
Boiler Island Aux. Power, MWe	63.0	63.0	67.6
ASU + CPU Aux Power, MWe	156.7	157.0	182.8
Net Power, MWe	550.2	550.0	549.8
Gross Efficiency (HHV)	41.8%	41.8%	41.4%
Net Efficiency (HHV)	29.9%	29.9%	28.4%
CO ₂ Captured, tpd	15160	15182	15627
CO ₂ Capture Rate, %	99.2%	99.3%	97.4%

CPU feed stream information is shown in Tables 5.39 and 5.40. On a dry basis, CO₂ concentration is ~83% except for the high air intrusion cases where CO₂ concentration is ~60%. For the conventional CPU, SO_x concentration is 60 – 95 ppmv, depending on the amount of air intrusion and which streams are treated by the FGD. An SCR is in place in the boiler island for all the conventional CPU cases in this evaluation resulting in a NO_x concentration of 39 ppmv. The Thermoflex software used to model the boiler island does not have the ability to predict NO_x and CO concentrations. NO_x concentration is based on the Foster Wheeler 460 MW boiler island modeling results and the assumption of 90% removal of NO_x by the SCR. CO concentration is based on the Foster Wheeler 460 MW boiler island modeling results.

For the NZE CPU, SO_x concentration in the CPU is 3141 – 3695 ppmv, depending on the amount of air intrusion. No FGD treatment of the CPU feed and no SCR is used in conjunction with the NZE CPU. NO_x and CO concentrations are based on the Foster Wheeler 460 MW boiler island modeling results.

Table 5.39 CPU Feed – High Sulfur Coal with Conventional CPU

Case No.	22	23	24
Air or Oxy Firing	Oxy	Oxy	Oxy
Fuel	High S	High S	High S
CPU Type	Conv	Conv	Conv
Steam Cycle	Sub	Sub	Sub
Air Intrusion	2%	10%	2%
SCR	Yes	Yes	Yes

Case No.	22	23	24
FGD	PA + Partial SA + CPU Feed	PA + Partial SA + CPU Feed	Entire FG
Flow Rate, lb mol/h	45110	61730	49410
Contained CO ₂ , tpd	15290	15597	15550
CO ₂ , vol.%	64.18%	47.85%	59.59%
N ₂ , vol.%	6.70%	24.42%	6.27%
O ₂ , vol.%	3.77%	4.95%	3.51%
Ar, vol.%	2.37%	1.91%	2.20%
H ₂ O, vol.%	22.94%	20.84%	28.39%
CO, ppmv	280	280	280
SO ₂ , ppmv	73	61	46
SO ₃ , ppmv	22	18	14
NO, ppmv	35	35	35
NO ₂ , ppmv	4	4	4
HCl, ppmv	0	0	0
NH ₃ , ppmv	1	1	1
CO ₂ , vol.%, (Dry Basis)	83.29%	60.45%	83.22%

Table 5.40 CPU Feed – High Sulfur Coal with NZE CPU

Case No.	25	26	27
Air or Oxy Firing	Oxy	Oxy	Oxy
Fuel	High S	High S	High S
CPU Type	NZE- Sulfuric Acid	NZE - Activated Carbon	NZE - Activated Carbon
Steam Cycle	Sub	Sub	Sub
Air Intrusion	2%	2%	10%
SCR	No	No	No
FGD	PA + Partial SA	PA + Partial SA	PA + Partial SA
Flow Rate, lb mol/h	45390	45450	62860
Contained CO ₂ , tpd	15271	15291	16043
CO ₂ , vol.%	63.71%	63.71%	48.32%
N ₂ , vol.%	6.67%	6.67%	24.72%
O ₂ , vol.%	3.41%	3.40%	4.73%
Ar, vol.%	2.35%	2.35%	1.92%
H ₂ O, vol.%	23.40%	23.40%	19.90%
CO, ppmv	280	280	280
SO ₂ , ppmv	3674	3632	3123
SO ₃ , ppmv	21	21	18
NO, ppmv	347	347	347
NO ₂ , ppmv	39	39	39
HCl, ppmv	302	299	257
NH ₃ , ppmv	0	0	0
CO ₂ , vol.%, (Dry Basis)	83.17%	83.18%	60.33%

The quantities and key impurities of the purified CO₂ produced by the CPU are listed in Tables 5.41 and 5.42. The conventional CPU purifies CO₂ to 95.1% vol. - 95.3% vol. Higher CO₂ purities can be reached, but result in lower CO₂ capture and/or higher power consumption. The range of SO_x concentration is 80 – 131 ppmv, depending on the placement of the FGD and amount of air intrusion. NO_x concentration is 43 – 61 ppmv and CO concentration is 39 – 95 ppmv.

The NZE CPU purifies CO₂ to ~95.3%. In Case 25, the Task 2 sulfuric acid process used instead of the Task 3 activated carbon process for SO_x/NO_x removal. SO_x concentration is 4 - 25 ppmv, depending mostly on which SO_x/NO_x removal process is used. NO_x concentration is 10 - 35 ppmv, depending on the type of SO_x/NO_x removal process and the degree of air intrusion. CO concentration is 37 - 94 ppmv, depending on the amount of air intrusion.

Table 5.41 Purified CO₂ from Conventional CPU (High Sulfur)

Case No.	22	23	24
Air or Oxy Firing	Oxy	Oxy	Oxy
Fuel	High S	High S	High S
CPU Type	Conv	Conv	Conv
Steam Cycle	Sub	Sub	Sub
Air Intrusion	2%	10%	2%
SCR	Yes	Yes	Yes
FGD	PA + Partial SA + CPU Feed	PA + Partial SA + CPU Feed	Entire FG
Contained CO ₂ , tpd	14028	11693	1426
CO ₂ Capture, %	91.8%	75.0%	91.7%
CO ₂ Purity, % vol.	95.3%	95.1%	95.3%
SO _x , ppmv	93	131	80
NO _x , ppmv	40	61	43
CO, ppmv	88	39	95

Table 5.42 Purified CO₂ from NZE CPU (High Sulfur)

Case No.	25	26	27
Air or Oxy Firing	Oxy	Oxy	Oxy
Fuel	High S	High S	High S
CPU Type	NZE- Sulfuric Acid	NZE - Activated Carbon	NZE - Activated Carbon
Steam Cycle	Sub	Sub	Sub
Air Intrusion	2%	2%	10%
SCR	No	No	No
FGD	PA + Partial SA	PA + Partial SA	PA + Partial SA
Contained CO ₂ , tpd	15160	15182	15627
CO ₂ Capture, %	99.3%	99.3%	97.4%
CO ₂ Purity, % vol.	95.4%	95.3%	95.4%
SO _x , ppmv	42	4	5
NO _x , ppmv	10	27	35
CO, ppmv	93	94	37

Atmospheric emissions for the high sulfur cases are listed in Tables 5.43, 5.44, and 5.45. Case 20 (Air – fired, no SCR, includes FGD) is used as a basis for comparing the atmospheric emissions. The slightly higher SO_x emission shown in Case 21 compared to Case 20 is due to the conversion of some SO₂ to SO₃ in the SCR and the default setting of the Thermoflex FGD module at 50% SO₃ removal efficiency.

Table 5.43 Atmospheric Emissions – Air Firing of High Sulfur Coal

Case No.	20	21
Air or Oxy Firing	Air	Air
Fuel	High S	High S
CPU Type	0	0
Steam Cycle	Sub	Sub
Air Intrusion	2%	2%
SCR	No	Yes
FGD	Yes	Yes
Stack/CPU Vent Composition		
CO ₂ , % vol.	12.36%	12.35%
SO _x , ppmv	41	44
NO _x , ppmv	143	14
CO, ppmv	133	133
Stack/CPU Vent Emission Rate		
CO ₂ , kpph	1,018	1,019
SO _x , lb/hr (as SO ₂)	488	529
NO _x , lb/hr (as NO ₂)	1234	124
CO, lb/hr	698	700
Emission Reduction (Compared to Case 20)		
NO _x		89.9%

The conventional CPU reduces CO₂ emissions by 68% – 89.7%, depending on the amount of air infiltration. SO_x emissions are reduced by 98.9% - 99.8%. NO_x emissions are reduced by 98.9% - 99.5%. CO emissions are reduced by 34.3% - 59.1%. Reductions in SO_x and NO_x emissions are largely due to environmental controls in the boiler island and sequestration of some of the SO_x and NO_x with the purified CO₂. Reduction in CO emissions is due to sequestration of some of the CO with the purified CO₂.

Table 5.44 Atmospheric Emissions – Conventional CPU (High Sulfur Coal)

Case No.	22	23	24
Air or Oxy Firing	Oxy	Oxy	Oxy
Fuel	High S	High S	High S
CPU Type	Conv	Conv	Conv
Steam Cycle	Sub	Sub	Sub
Air Intrusion	2%	10%	2%
SCR	Yes	Yes	Yes
FGD	PA + Partial SA + CPU Feed	PA + Partial SA + CPU Feed	Entire FG

Case No.	22	23	24
Stack/CPU Vent Composition			
CO ₂ , % vol.	34.65%	28.90%	34.62%
SO _x , ppmv	3	3	3
NO _x , ppmv	20	11	22
CO, ppmv	1479	640	1592
Stack/CPU Vent Emission Rate			
CO ₂ , kpph	105	325	108
SO _x , lb/hr (as SO ₂)	1.3	5.3	1.2
NO _x , lb/hr (as NO ₂)	6.5	13.6	7.2
CO, lb/hr	286	459	314
Emission Reduction (Compared to Case 20)			
CO ₂	89.7%	68.0%	89.4%
SO _x	99.7%	98.9%	99.8%
NO _x	99.5%	98.9%	99.4%
CO	59.1%	34.3%	55.1%

The NZE CPU reduces CO₂ emissions by 96.5% - 99.1%, as compared to Case 20, depending on the degree of air infiltration. SO_x emissions are essentially eliminated and NO_x emissions are reduced by 99.3% - 99.9%. CO emissions are reduced by 99.3% - 99.6%. Reductions in SO_x and NO_x emissions are due to the SO_x/NO_x removal process in the CPU. Reductions in CO emissions are due to the Catox reactor.

Table 5.45 Atmospheric Emissions – NZE CPU (High Sulfur Coal)

Case No.	25	26	27
Air or Oxy Firing	Oxy	Oxy	Oxy
Fuel	High S	High S	High S
CPU Type	NZE- Sulfuric Acid	NZE - Activated Carbon	NZE - Activated Carbon
Steam Cycle	Sub	Sub	Sub
Air Intrusion	2%	2%	10%
SCR	No	No	No
FGD	PA + Partial SA	PA + Partial SA	PA + Partial SA
Stack/CPU Vent Composition			
CO ₂ , % vol.	5.00%	4.94%	4.23%
SO _x , ppmv	0	0	0
NO _x , ppmv	8	21	10
CO, ppmv	23	23	9
Stack/CPU Vent Emission Rate			
CO ₂ , kpph	9.7	9.5	35.4
SO _x , lb/hr (as SO ₂)	<1	<1	<1
NO _x , lb/hr (as NO ₂)	1.6	4.2	9.0
CO, lb/hr	2.8	2.8	4.6

Case No.	25	26	27
Emission Reduction (Compared to Case 20)			
CO ₂	99.1%	99.1%	96.5%
SO _x	>99.9%	>99.9%	>99.9%
NO _x	99.9%	99.7%	99.3%
CO	99.6%	99.6%	99.3%

Subtask 5.4 – Economic Feasibility

Economic feasibility was performed for the following scenarios:

- Greenfield plants with low air ingress – low sulfur coal
- Greenfield plants with low air ingress – high sulfur coal
- Relative impacts of activated carbon and VPSA process units on NZE CPU performance
- Retrofit old plants with high air ingress – low sulfur coal
- Retrofit old plants with high air ingress – high sulfur coal
- Greenfield plants using the SC steam cycle.
- Greenfield plants using the USC steam cycle
- Comparison of partial condensation vs. distillation
- Potential for cost reduction if FGD is eliminated.
- New plant without CCS vs. old plant with CCS

Greenfield Plants with Low Air Ingress – Low Sulfur Coal

Cases 3, 7, 8, 10, and 14 were used to evaluate greenfield plants burning low sulfur coal. The results are shown in Table 5.46. Case 3 is the air-fired case used as the basis of comparison. Cases 7, 8 and 10 are oxy-fired cases using conventional CPU’s. Case 14 uses a Near Zero Emissions CPU. In Case 7, an FGD is used to treat only the primary recirculated flue gas. In Case 8, the entire flue gas stream is treated by an FGD. In Case 10, only the primary recirculated flue gas and the CPU feed are treated by an FGD. Table 5.31 shows that Case 7 results in 2354 ppmv of SO_x in the purified CO₂ from the CPU, while Cases 8 and 10 result in 48 ppmv and 65 ppmv of SO_x respectively. In comparison, the NZE CPU produces purified CO₂ with only 2 ppm SO_x (Table 5.32). If there are no specifications for SO_x concentration in the purified CO₂ from the CPU, then Case 7 is the preferred conventional CPU case as it results in the lowest COE. Case 8 is the most expensive of the conventional CPU cases evaluated with a COE of \$153.9/MWh. If SO_x concentration targets are implemented, then Case 10 would be considered the preferred conventional CPU case as the COE for Case 10 is \$6.0/MWh lower than Case 8, while producing purified CO₂ with a reasonably low SO_x concentration. Case 10 is used as the conventional CPU case for comparison with the NZE CPU in the discussion below.

The impact on cost of electricity of retrofitting CCS to a new plant, burning low sulfur coal, is shown in Figure 5.4, which contains results for Cases 3, 10, and 14. The capex component in Figure 5.4 corresponds to capital in \$/MWh listed in Table 5.46 and it is estimated from capex charge of either 16.4% or 17.5% as defined in Table 5.11. The opex component includes all other charges and it is a total of operating & fixed costs and pipeline & injection well costs listed in Table 5.46. The air intrusion rate of these plants is assumed to be 2%. Compared to an air-fired plant (Case 3) COE increases by \$65.6/MWh when using a conventional CPU (Case 10), and by \$63.6/MWh when using an NZE CPU (Case 14). The NZE CPU reduces the cost of captured CO₂ by \$6.4/ton and the cost of avoided CO₂ by \$8.5/ton as compared to a conventional CPU, shown in Figure 5.5. The reduction in CO₂ capture cost is due to the capex reduction for SO_x/NO_x removal (smaller FGD and no SCR) and the higher CO₂ capture rate of the NZE CPU.

Table 5.46 Economic Estimates for Greenfield Plants with Low Air Ingress – Low Sulfur Coal

Case No.	3	7	8	10	14
Air or Oxy Firing	Air	Oxy	Oxy	Oxy	Oxy
Fuel	Low S	Low S	Low S	Low S	Low S
CPU Type	na	Conv	Conv	Conv	Praxair
Partial Condensation or Distillation CPU	na	PC	PC	PC	PC
CPU SO _x /NO _x Removal	na	None	None	None	Act C
Steam Cycle	Sub	Sub	Sub	Sub	Sub
Air Intrusion	2%	2%	2%	2%	2%
SCR	Yes	Yes	Yes	Yes	No
FGD	Yes	Yes	Yes	Yes	Yes
Stream treated by FGD	Entire FG	PA	Entire FG	PA + CPU Feed	PA
Total Capital, \$MM	1259	2125	2275	2180	2133
Capex, \$/kW (net)	2290	3860	4140	3960	3890
Total Operating & Fixed Costs, \$MM/yr	130.6	181.5	192.9	186.6	182.6
Cost of Electricity					
Capital, \$/MWh	50.4	90.7	97.3	93.1	91.4
Operating & Fixed Costs, \$/MWh	31.9	44.3	47.2	45.6	44.8
Pipeline & Injection Wells, \$/MWh		9.3	9.5	9.3	9.8
Total Cost of Electricity (COE), \$/MWh	82.3	144.3	153.9	147.9	146.0
Increase in COE Compared to Base Case, \$/MWh		62.0	71.6	65.6	63.6
CO₂ Capture Cost					
Basis of Comparison		Case 3	Case 3	Case 3	Case 3
CO ₂ Emission Before Capture, t/MWh	1.014	1.254	1.300	1.260	1.276
CO ₂ Emission After Capture, t/MWh		0.098	0.104	0.102	0.009
Capture Cost, \$/ton		53.57	59.84	56.61	50.23
Avoided Cost, \$/ton		67.60	78.61	71.88	63.34

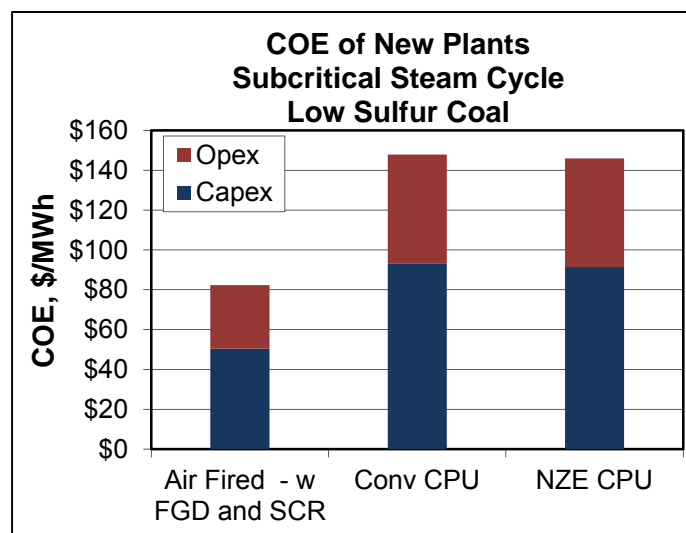


Figure 5.4 COE of New Plants using Low Sulfur Coal

In combination with the results discussed in subtask 5.1, it can be said that the NZE CPU achieves lower atmospheric emissions, higher CO₂ capture rates and higher CO₂ purity while lowering the CO₂ capture costs. It is interesting to note that the NZE CPU case 14 results in lower CO₂ capture cost even when compared to the conventional CPU case 7, which produces CO₂ with very high concentration of SO_x.

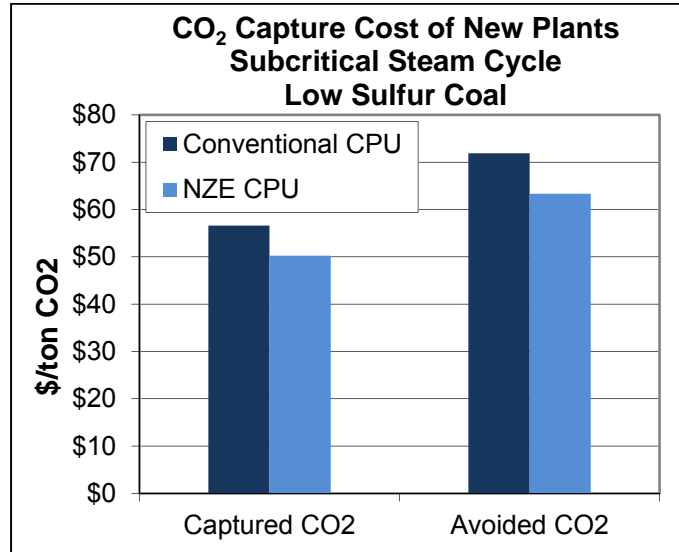


Figure 5.5 Cost of CO₂ Capture for New Plants using Low Sulfur Coal

Greenfield Plants with Low Air Ingress – High Sulfur Coal

Cases 21, 22, 24, 25, and 26 were used to evaluate greenfield plants burning high sulfur coal. The air intrusion rate of these plants is assumed to be 2%. The results are shown in Table 5.47. Case 21 is the air-fired case used as the basis of comparison. Cases 22 and 24 are oxy-fired cases using conventional CPU's. Cases 25 and 26 use Near Zero Emissions CPU's. In Case 22, the primary recirculated flue gas, a portion of the secondary recirculated flue gas and the CPU feed are treated by an FGD. In Case 24, the entire flue gas stream is treated by an FGD. Case 22 is considered the preferred conventional CPU case as the COE is \$4.1/MWh cheaper than Case 24. Case 22 is used as the conventional CPU case for comparison with the NZE CPU cases in the discussion below. The CPU for Case 25 includes the Task 2 sulfuric acid process to remove SO_x and NO_x. In Case 25, no credits are assumed for the sale of concentration H₂SO₄ byproduct. The CPU for Case 26 includes the Task 3 activated carbon process to remove SO_x and NO_x.

Table 5.47 Economic Estimates for Greenfield Plants with Low Air Ingress – High Sulfur Coal

Case No.	21	22	24	25	26
Air or Oxy Firing	Air	Oxy	Oxy	Oxy	Oxy
Fuel	High S	High S	High S	High S	High S
CPU Type	na	Conv	Conv	Praxair	Praxair
Partial Condensation or Distillation CPU	na	0	0	PC	PC
CPU SO _x /NO _x Removal	na	None	None	H ₂ SO ₄	Act C
Steam Cycle	Sub	Sub	Sub	Sub	Sub
Air Intrusion	2%	2%	2%	2%	2%
SCR	Yes	Yes	Yes	No	No
FGD	Yes	Yes	Yes	Yes	Yes

Case No.	21	22	24	25	26
Stream Treated by FGD	Entire FG	PA + Partial SA + CPU Feed	Entire FG	PA + Partial SA	PA + Partial SA
Total Capital, \$MM	1286	2197	2268	2144	2145
Capex, \$/kW (net)	2340	4000	4120	3900	3900
Total Operating & Fixed Costs, \$MM/yr	179.0	240.6	245.9	236.1	236.2
Cost of Electricity					
Capital, \$/MWh	51.5	94.0	96.8	91.7	91.7
Operating & Fixed Costs, \$/MWh	43.7	58.8	60.0	57.6	57.7
Pipeline & Injection Wells, \$/MWh		8.8	8.9	9.2	9.2
Total Cost of Electricity (COE), \$/MWh	95.2	161.6	165.7	158.5	158.5
Increase in COE Compared to Base Case, \$/MWh		66.4	70.5	63.3	63.3
CO₂ Capture Cost					
Basis of Comparison		Case 21	Case 21	Case 21	Case 21
CO ₂ Emission Before Capture, t/MWh	0.926	1.160	1.178	1.156	1.158
CO ₂ Emission After Capture, t/MWh		0.096	0.098	0.009	0.009
Capture Cost, \$/ton		62.39	65.27	55.12	55.06
Avoided Cost, \$/ton		79.93	85.07	68.93	68.97

COE estimates are shown in Figure 5.6 and CO₂ capture costs are shown in Figure 5.7. Compared to an air-fired plant (Case 21) COE increases by \$66.4/MWh when using a conventional CPU (Case 22). Compared to an air-fired plant, COE increases by \$63.3/MWh for both the sulfuric acid and activated carbon based NZE CPU cases (25 and 26). Both the NZE CPUs reduce the cost of captured CO₂ by \$7.3/ton and the cost of avoided CO₂ by \$11.0/ton compared to the conventional CPU. The reduction in CO₂ capture cost of the NZE CPU Cases 25 and 26 can be attributed to lower capex for SO_x/NO_x removal and higher CO₂ capture rates. The above results confirmed that the value of Task 2 sulfuric acid process is similar to that of Task 3 activated carbon process when credit from by-product sale is not available to the sulfuric acid process. When this conclusion was combined with the fact that Task 3 process was able to achieve the SO_x/NO_x removal performance target for high sulfur coal also, it was decided to discontinue further efforts on Task 2 process.

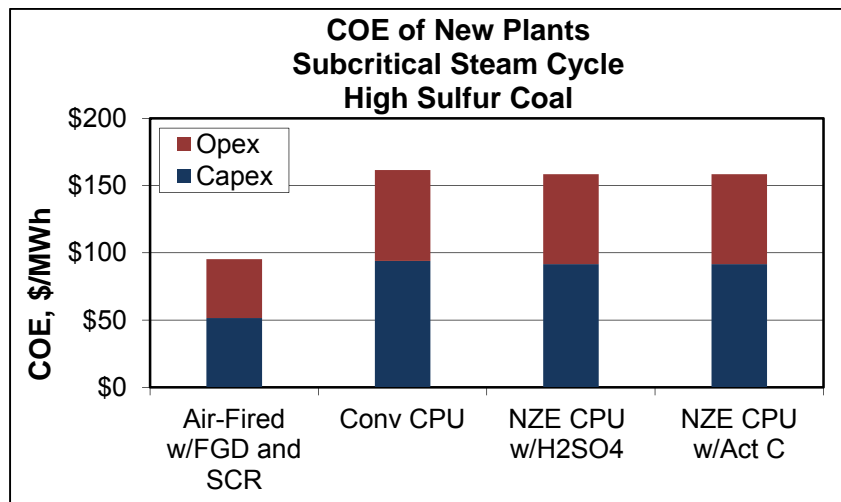


Figure 5.6 COE of New Plants using High Sulfur Coal

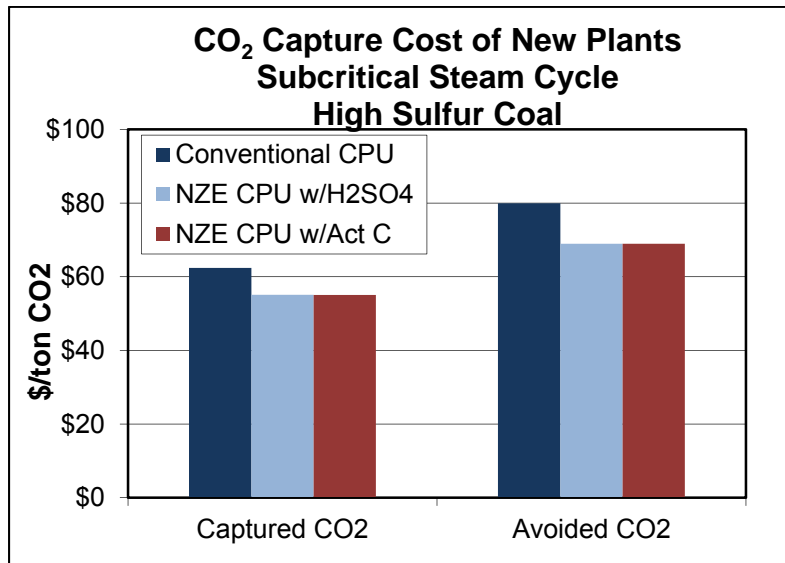


Figure 5.7 Cost of CO₂ Capture for New Plants using High Sulfur Coal

Relative Impacts of Activated Carbon and VPSA Process Units on the NZE CPU Performance

To understand the relative contributions of activated carbon process and VPSA process in lowering the CO₂ capture costs, additional cases based on the NZE CPU case 14 were developed with either of those two processes included in the CPU. Case 14c CPU included activated carbon process while Case 14v CPU included VPSA. These two cases were compared with cases 3 (air fired base case), 10 (oxy fired case with conventional CPU) and 14 (oxy fired case with NZE CPU). The results are shown in Table 5.48. First to recap the comparison between cases 10 and 14, the NZE CPU results in ~\$2/MWh lower COE and \$8.5/ton lower CO₂ avoided cost than the conventional CPU.

Comparing the COE and CO₂ capture cost data for cases 14c (CPU with activated carbon only) and 14v (CPU with VPSA only), it is clear that these two technologies create value completely differently. The COE of case 14c is ~\$5.8/MWh lower than the conventional CPU case 10 and this delta is \$3.9/MWh better than what NZE CPU case 14 achieves. The main reason for lower COE is due to savings in capex associated with smaller FGD and elimination of SCR. The CO₂ avoided cost of case 14c is \$6.3/ton lower than that of conventional CPU (case 10). When case 14v (CPU with VPSA only) is compared against case 10, the COE of case 14v increases by \$3.7/MWh, however, the CO₂ avoided cost decrease by \$3/MWh. The increase in COE is due to additional capital and operating costs associated with VPSA and the balance of CPU equipment. However, the increase in CO₂ capture rate compared to case 10 is higher than the increase in capex and opex, and hence incremental cost of CO₂ capture in case 14v is lower. The net result is decrease in CO₂ avoided cost by \$3/ton. When both activated carbon process and VPSA are included in the NZE CPU case 14, the net decrease of \$1.9/MWh compared to case 10 is slightly lower than the combined impact (\$2.05/MWh) of cases 14c and 14v. Similarly, the net reduction in CO₂ avoided cost of \$8.5/ton in case 14 against case 10 is slightly lower (~8%) than the combined reductions from cases 14c and 14v. Thus, benefits of these two technologies are not completely mutually exclusive. It is also clear that larger benefit is derived from the activated carbon process (~67%) than from the VPSA process (~33%). Figure 5.8 shows comparison of COEs and Figure 5.9 shows comparison of CO₂ capture costs for the cases discussed above.

Table 5.48 Economic Estimates for Relative Impact of NZE CPU Components

Case No.	3	10	14	14c	14v
Air or Oxy Firing	Air	Oxy	Oxy	Oxy	Oxy
Fuel	Low S	Low S	Low S	Low S	Low S
CPU Type	na	Conv	Praxair	Praxair	Praxair
Partial Condensation or Distillation CPU		PC	PC	PC	PC
CPU SO _x /NO _x Removal			Act C	Act C	No
VPSA installed?			Yes	No	Yes
Steam Cycle	Sub	Sub	Sub	Sub	Sub
Air Intrusion	2%	2%	2%	2%	2%
SCR	Yes	Yes	No	No	Yes
FGD	Yes	Yes	Yes	Yes	Yes
Stream treated by FGD	Entire FG	PA + CPU Feed	PA	PA	PA + CPU Feed
Total Capital, \$MM	1259	2180	2133	2082	2233
Capex, \$/kW (net)	2290	3960	3890	3790	4060
Total Operating & Fixed Costs, \$MM/yr	130.6	186.6	182.6	179.3	190.1
Cost of Electricity					
Capital, \$/MWh	50.44	93.07	91.42	89.07	95.42
Operating & Fixed Costs, \$/MWh	31.90	45.57	44.75	43.79	46.41
Pipeline & Injection Wells, \$/MWh		9.26	9.80	9.27	9.79
Total Cost of Electricity (COE), \$/MWh	82.34	147.90	145.98	142.13	151.62
Increase in COE Compared to Base Case, \$/MWh		65.56	63.64	59.79	69.28
CO₂ Capture Cost					
Basis of Comparison		Case 3	Case 3	Case 3	Case 3
CO ₂ Emission Before Capture, t/MWh	1.0142	1.2603	1.2763	1.2566	1.2760
CO ₂ Emission After Capture, t/MWh		0.1022	0.0094	0.1018	0.0088
Capture Cost, \$/ton		56.6	50.2	51.8	54.7
Avoided Cost, \$/ton		71.9	63.3	65.5	68.9

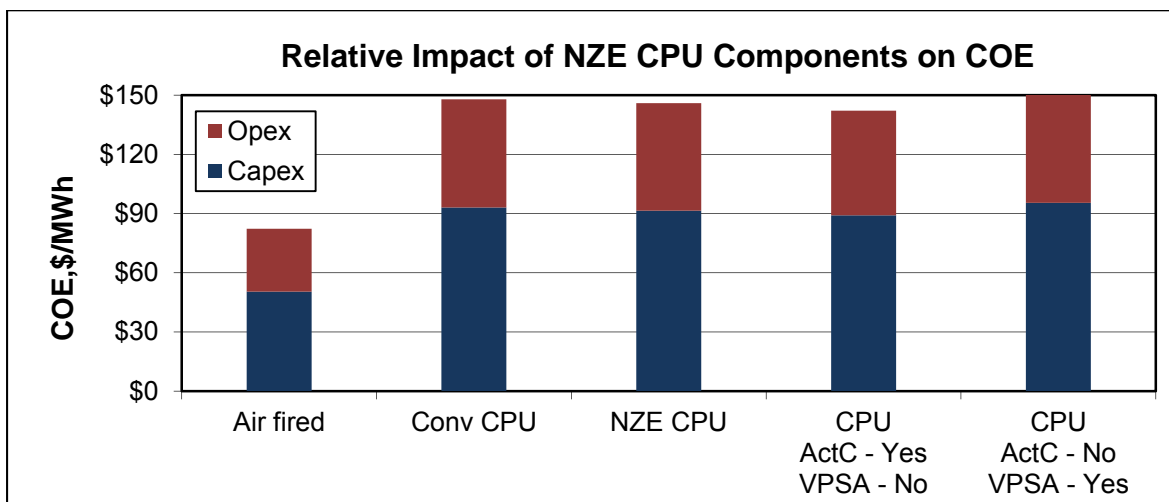


Figure 5.8 Relative Impact of NZE CPU Components on COE

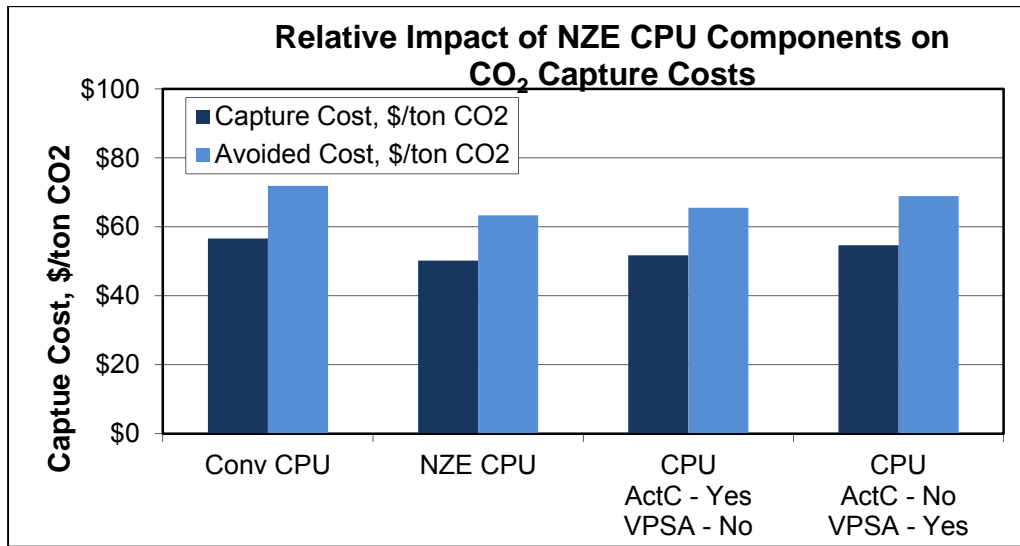


Figure 5.9 Relative Impact of NZE CPU Components on CO₂ Capture Costs

Retrofit Old Plants with High Air Ingress – Low Sulfur Coal

The impact of retrofitting CO₂ capture to an old plant, burning low sulfur coal, is shown in Figure 5.10, which contains results for Cases 1a (air-fired), 11a (conventional CPU), and 15a (NZE CPU). The air intrusion rate for these cases is assumed to be 10%. Because the boiler island requires a relatively small Capex only to keep the plant operating, the COE for the air plant is low compared to the greenfield case and the relative impact of adding CCS to the old plant is very high – almost tripling the COE. On absolute basis, the increases in COEs for the CCS cases (11a and 15a) are similar in magnitude to those for the low air intrusion CCS cases (10 and 14).

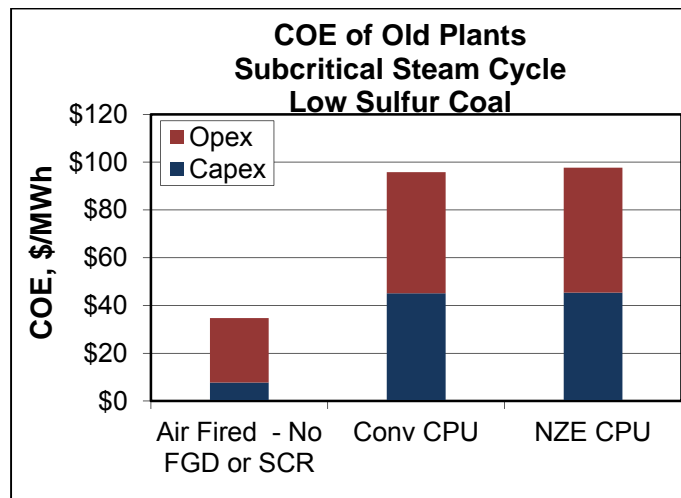


Figure 5.10 COE of Old Plants using Low Sulfur Coal

The high air intrusion rate reduces the CO₂ capture rate of the conventional CPU to about 78%, which increases the benefit of the NZE CPU for cost of captured CO₂ and avoided CO₂, as shown in Figure 5.11. Cost of captured CO₂ using the NZE CPU is \$12.0/ton less than captured CO₂ cost using the conventional CPU. Cost of avoided CO₂ for the NZE CPU is \$20.2 less than the cost using the conventional CPU. Details of the cost estimates are in Table 5.49.

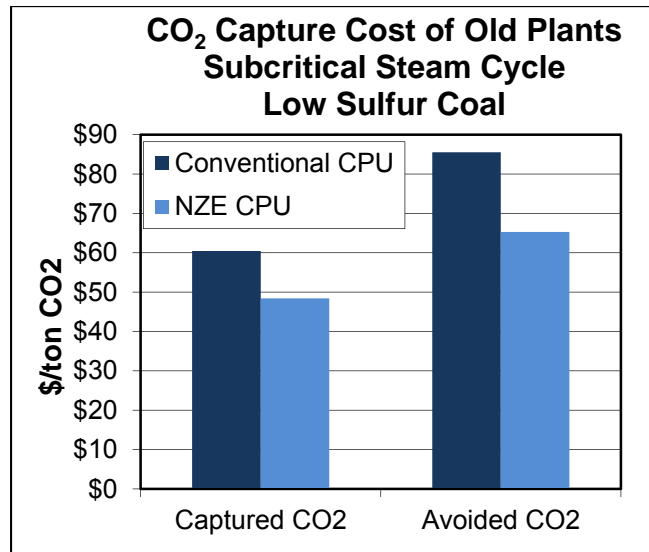


Figure 5.11 Cost of CO₂ Capture for Old Plants using Low Sulfur Coal

Table 5.49 Economic Estimates for Old Plants with High Air Ingress – Low Sulfur Coal

Case No.	1a	11a	15a
Air or Oxy Firing	Air	Oxy	Oxy
Fuel	Low S	Low S	Low S
CPU Type	na	Conv	Praxair
Partial Condensation or Distillation CPU	na	PC	PC
CPU SO _x /NO _x Removal	na	None	None
Steam Cycle	Sub	Sub	Sub
Air Intrusion	2%	10%	10%
SCR	No	Yes	No
FGD	No	Yes	Yes
Stream Treated by FGD	None	PA + CPU Feed	PA
Total Capital, \$MM	192	1054	1059
Capex, \$/kW (net)	350	1920	1930
Total Operating & Fixed Costs, \$MM/yr	110.7	172.2	173.6
Cost of Electricity			
Capital, \$/MWh	7.7	45.1	45.4
Operating & Fixed Costs, \$/MWh	27.0	42.1	42.4
Pipeline & Injection Wells, \$/MWh		8.6	9.9
Total Cost of Electricity (COE), \$/MWh	34.7	95.8	97.7
Increase in COE Compared to Base Case, \$/MWh		61.1	63.0
CO₂ Capture Cost			
Basis of Comparison		Case 1a	Case 1a
CO ₂ Emission Before Capture, t/MWh	0.996	1.292	1.331
CO ₂ Emission After Capture, t/MWh		0.281	0.031
Capture Cost, \$/ton		60.46	48.44
Avoided Cost, \$/ton		85.52	65.28

Retrofit Old Plants with High Air Ingress – High Sulfur Coal

The impact of retrofitting CO₂ capture to an old plant, burning high sulfur coal, is shown in Figure 5.12, which contains results for Cases 20a (air-fired), 23a (conventional CPU), and 27a (NZE CPU). The air intrusion rate for these cases is assumed to be 10%. The impact of CCS on COE is similar to that discussed for the low sulfur cases with high air intrusion.

The high air intrusion rate reduces the CO₂ capture rate of the conventional CPU to about 75%, which increases the benefit of the NZE CPU for cost of captured CO₂ and avoided CO₂, as shown in Figure 5.13. Cost of captured CO₂ using the NZE CPU is \$12.0/ton less than captured CO₂ cost using the conventional CPU. Cost of avoided CO₂ for the NZE CPU is \$21.1 less than the cost using the conventional CPU. Details of the cost estimates are in Table 5.50.

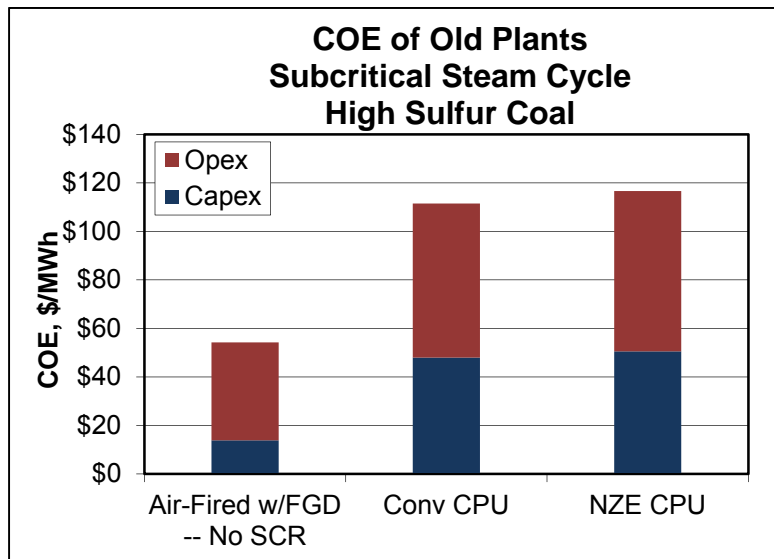


Figure 5.12 COE of Old Plants using High Sulfur Coal

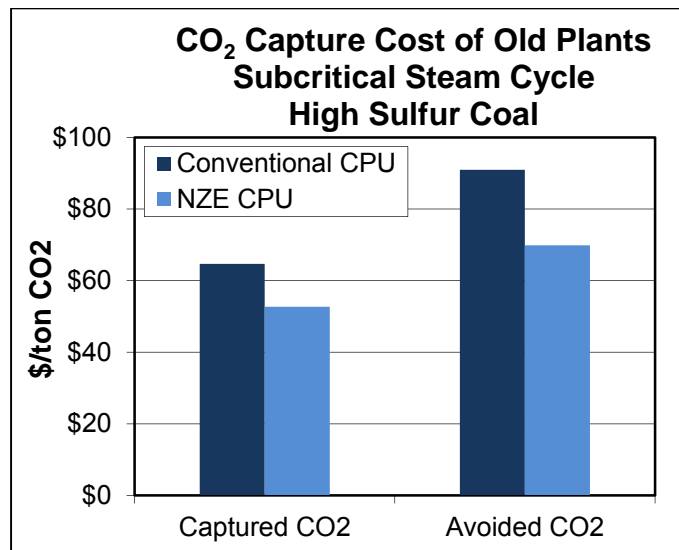


Figure 5.13 Cost of CO₂ Capture for Old Plants using High Sulfur Coal

Table 5.50 Economic Estimates for Old Plants with High Air Ingress – High Sulfur Coal

Case No.	20a	23a	27a
Air or Oxy Firing	Air	Oxy	Oxy
Fuel	High S	High S	High S
CPU Type	na	Conv	Praxair
Partial Condensation or Distillation CPU	na	PC	PC
CPU SO _x /NO _x Removal	na	None	None
Steam Cycle	Sub	Sub	Sub
Air Intrusion	2%	10%	10%
SCR	No	Yes	No
FGD	Yes	Yes	Yes
Stream Treated by FGD	None	PA + Partial SA + CPU Feed	PA + Partial SA
Total Capital, \$MM	344	1125	1183
Capex, \$/kW (net)	630	2040	2150
Total Operating & Fixed Costs, \$MM/yr	165.3	227.7	232.1
Cost of Electricity			
Capital, \$/MWh	13.9	47.9	50.5
Operating & Fixed Costs, \$/MWh	40.3	55.6	56.7
Pipeline & Injection Wells, \$/MWh		7.9	9.4
Total Cost of Electricity (COE), \$/MWh	54.2	111.5	116.6
Increase in COE Compared to Base Case, \$/MWh		57.3	62.4
CO₂ Capture Cost			
Basis of Comparison		Case 20a	Case 20a
CO ₂ Emission Before Capture, t/MWh	0.925	1.181	1.216
CO ₂ Emission After Capture, t/MWh		0.296	0.032
Capture Cost, \$/ton		64.67	52.72
Avoided Cost, \$/ton		90.97	69.89

Greenfield Plants using the Supercritical Steam Cycle

Comparisons are shown for a new plant using the supercritical steam cycle in Figures 5.14 and 5.15, which contain results for Cases 4 (air fired), 12 (conventional CPU), and 17 (NZE CPU). Inclusion of CCS increases COE by \$63.4/MWh using a conventional CPU and by \$60.0/MWh using a NZE CPU. The lower COE of the system using the NZE CPU compared to the system using the conventional CPU is due to the elimination of the SCR and the smaller FGD used in the NZE CPU. The cost of captured CO₂ is about \$7.2/ton less expensive using the NZE CPU compared to the cost using a conventional CPU. The cost of avoided CO₂ is about \$10.4/ton less expensive. As explained earlier, the main reasons for lower capture costs in the NZE CPU are lower capex for SO_x/NO_x removal and higher CO₂ capture rate. Details of the cost estimates are in Table 5.51.

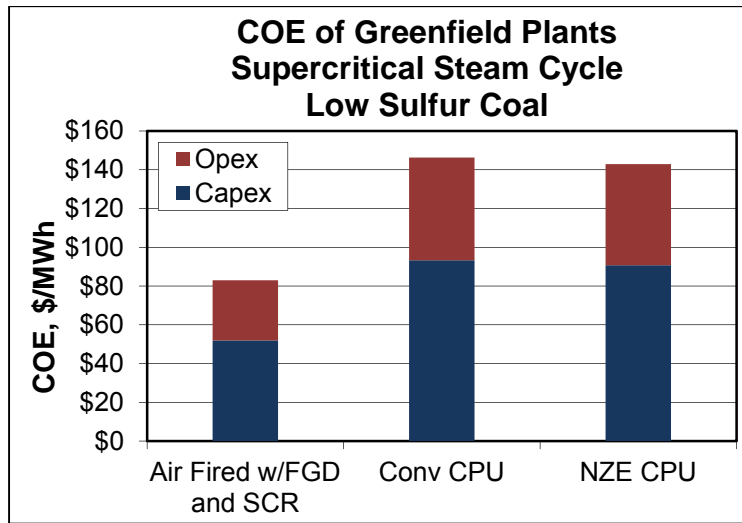


Figure 5.14 COE for Greenfield Supercritical Plants with and without CCS

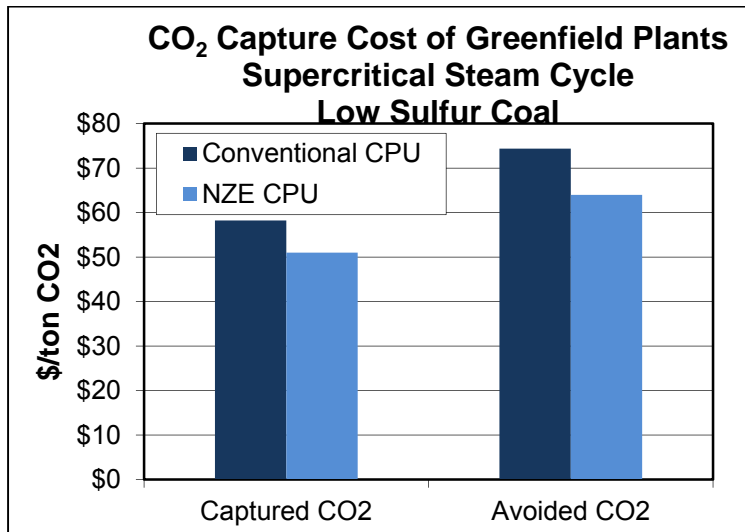


Figure 5.15 Cost of CO₂ Capture for Greenfield Supercritical Plants

Table 5.51 Economic Estimates for Greenfield Plants Using the Supercritical Steam Cycle

Case No.	4	12	17
Air or Oxy Firing	Air	Oxy	Oxy
Fuel	Low S	Low S	Low S
CPU Type	na	Conv	Praxair
Partial Condensation or Distillation CPU	na	PC	PC
CPU SO _x /NO _x Removal	na	None	None
Steam Cycle	SC	SC	SC
Air Intrusion	2%	2%	2%
SCR	Yes	Yes	No
FGD	Yes	Yes	Yes
Stream Treated by FGD	Entire FG	PA + CPU Feed	PA

Case No.	4	12	17
Total Capital, \$MM	1300	2184	2125
Capex, \$/kW (net)	2360	3970	3860
Total Operating & Fixed Costs, \$MM/yr	126.9	180.6	175.5
Cost of Electricity			
Capital, \$/MWh	52.0	93.3	90.7
Operating & Fixed Costs, \$/MWh	31.0	44.1	42.9
Pipeline & Injection Wells, \$/MWh	0.0	8.9	9.3
Total Cost of Electricity (COE), \$/MWh	83.0	146.3	142.9
Increase in COE Compared to Base Case, \$/MWh		63.4	60.0
CO₂ Capture Cost			
Basis of Comparison		Case 4	Case 4
CO ₂ Emission Before Capture, t/MWh	0.946	1.182	1.184
CO ₂ Emission After Capture, t/MWh		0.094	0.009
Capture Cost, \$/ton		58.23	51.01
Avoided Cost, \$/ton		74.36	64.00

Greenfield Plants using the Ultrasupercritical Steam Cycle

Results for new plants using the ultrasupercritical steam cycle are shown in Figures 5.16 and 5.17, which contain results for Cases 5 (air fired), 13 (conventional CPU) and 18 (NZE CPU). Addition of CCS using a conventional CPU increases COE by \$59.3/MWh, while the NZE CPU increases COE by \$51.7. As with the supercritical systems, the COE associated with the NZE CPU is lower due to the elimination of the SCR and the use of a smaller FGD. Cost of captured CO₂ is about \$7.6/ton less and cost of avoided CO₂ is about \$10.5/ton less using the NZE CPU compared to a conventional CPU. Details of the cost estimates are in Table 5.52.

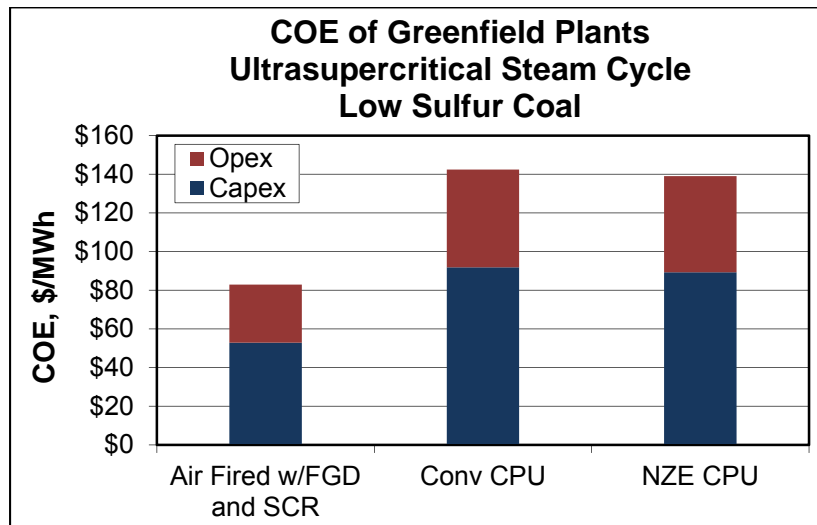


Figure 5.16 COE for Greenfield Ultrasupercritical Plants

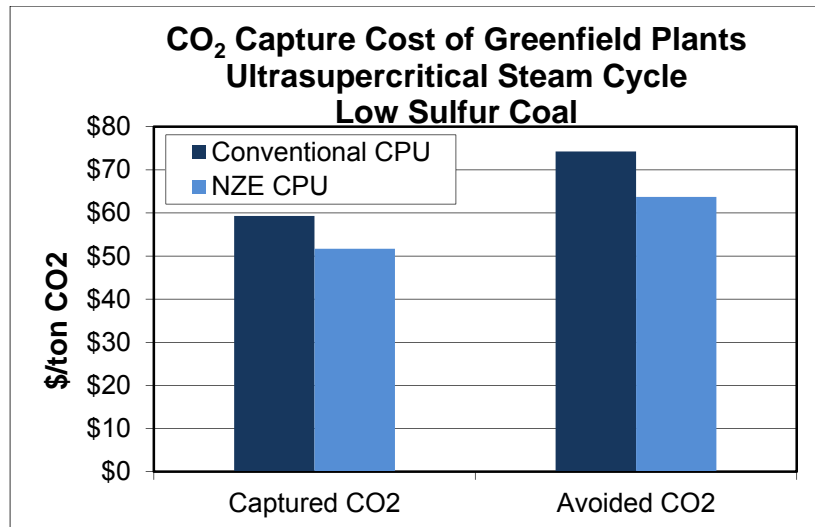


Figure 5.17 Cost of CO₂ Capture of Greenfield Ultrasupercritical Plants

Table 5.52 Economic Estimates for Greenfield Plants Using the Ultrasupercritical Steam Cycle

Case No.	5	13	18
Air or Oxy Firing	Air	Oxy	Oxy
Fuel	Low S	Low S	Low S
CPU Type	na	Conv	Praxair
Partial Condensation or Distillation CPU	na	PC	PC
CPU SO _x /NO _x Removal	na	None	None
Steam Cycle	USC	USC	USC
Air Intrusion	2%	2%	2%
SCR	Yes	Yes	No
FGD	Yes	Yes	Yes
Stream Treated by FGD	Entire FG	PA + CPU Feed	PA
Total Capital, \$MM	1320	2149	2087
Capex, \$/kW (net)	2400	3910	3800
Total Operating & Fixed Costs, \$MM/yr	123.2	172.2	166.9
Cost of Electricity			
Capital, \$/MWh	52.9	91.9	89.3
Operating & Fixed Costs, \$/MWh	30.1	42.0	40.8
Pipeline & Injection Wells, \$/MWh	0.0	8.5	8.9
Total Cost of Electricity (COE), \$/MWh	82.9	142.5	139.0
Increase in COE Compared to Base Case, \$/MWh		59.5	56.1
CO₂ Capture Cost			
Basis of Comparison		Case 5	Case 5
CO ₂ Emission Before Capture, t/MWh	0.888	1.090	1.093
CO ₂ Emission After Capture, t/MWh		0.086	0.008
Capture Cost, \$/ton		59.29	51.68
Avoided Cost, \$/ton		74.25	63.71

Impact of Steam Cycle Efficiency

The impact of steam cycle efficiency is summarized in Table 5.53. The results are extracted from Tables 5.46, 5.51 and 5.52. As steam cycle efficiency increases, the increase in COEs for the CCS cases decrease while CO₂ capture costs increase for both the conventional and NZE CPUs. The CO₂ avoided cost goes up for supercritical steam cycle compared to the subcritical cycle, however, they decrease somewhat for ultrasupercritical cycle compared to the supercritical cycle.

Table 5.53 Impact of Steam Cycle Efficiency on COE and CO₂ Capture Costs

Steam Cycle	SubC	SC	USC
Air fired cases			
Case No.	3	4	5
Total Cost of Electricity (COE), \$/MWh	82.3	83.0	82.9
Oxy fired cases with conventional CPU			
Case No.	10	12	13
Total Cost of Electricity (COE), \$/MWh	147.9	146.3	142.5
Increase in COE Compared to Base Case, \$/MWh	65.6	63.4	59.5
Basis of Comparison for CO ₂ capture costs	Case 3	Case 4	Case 5
Capture Cost, \$/ton	56.61	58.23	59.29
Avoided Cost, \$/ton	71.88	74.36	74.25
Oxy fired cases with NZE CPU			
Case No.	14	17	18
Total Cost of Electricity (COE), \$/MWh	146.0	142.9	139.0
Increase in COE Compared to Base Case, \$/MWh	63.6	60.0	56.1
Basis of Comparison for CO ₂ capture costs	Case 3	Case 4	Case 5
Capture Cost, \$/ton	50.23	51.01	51.68
Avoided Cost, \$/ton	63.34	64.00	63.71

Comparison of Partial Condensation vs. Distillation in the CPU Cold Box

The results from Cases 14 and 19 are compared in Figures 5.18 and 5.19 to show the impact of using a distillation process in the CPU to produce ~99.9% CO₂ purity instead of a partial condensation process, which produces >95% CO₂ purity. Case 3 is used as the basis for calculating captured and avoided CO₂ costs. The distillation process increases COE by about \$2.3/MWh compared to the partial condensation process. Cost of captured CO₂ increases by about \$1.7/ton and cost of avoided CO₂ increases by about \$2.5/ton, using the distillation process. Details of the cost estimates are in Table 5.54.

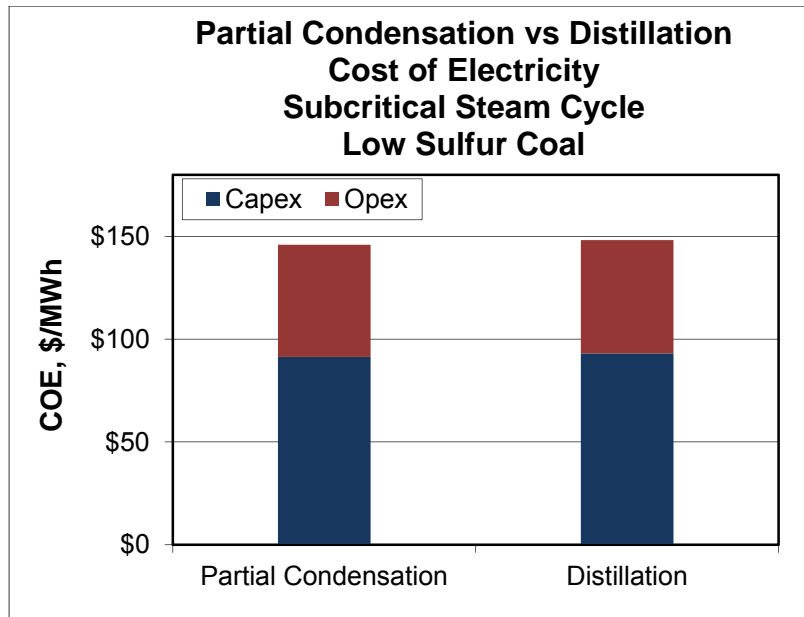


Figure 5.18 COE for Partial Condensation CPU vs. Distillation CPU

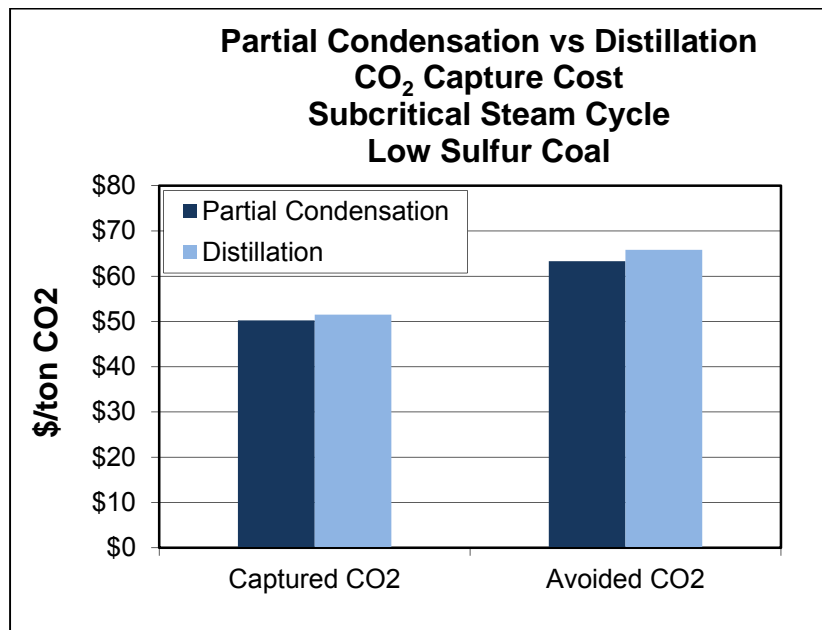


Figure 5.19 CO₂ Capture Costs for Partial Condensation CPU vs. Distillation CPU

Table 5.54 Economic Estimates for Comparison of Partial Condensation CPU to Distillation CPU

Case No.	3	14	19
Air or Oxy Firing	Air	Oxy	Oxy
Fuel	Low S	Low S	Low S
CPU Type	na	Praxair	Praxair
Partial Condensation or Distillation CPU	na	PC	Distil.
CPU SOx/NOx Removal	na	None	None
Steam Cycle	Sub	Sub	Sub
Air Intrusion	2%	2%	2%
SCR	Yes	No	No
FGD	Yes	Yes	Yes
Stream Treated by FGD	Entire FG	PA	PA
Total Capital, \$MM	1259	2133	2176
Capex, \$/kW (net)	2290	3890	3960
Total Operating & Fixed Costs, \$MM/yr	130.6	182.6	185.7
Cost of Electricity			
Capital, \$/MWh	50.4	91.4	93.1
Operating & Fixed Costs, \$/MWh	31.9	44.8	45.3
Pipeline & Injection Wells, \$/MWh		9.8	9.8
Total Cost of Electricity (COE), \$/MWh	82.3	146.0	148.2
Increase in COE Compared to Base Case, \$/MWh		63.6	65.9
CO₂ Capture Cost			
Basis of Comparison		Case 3	Case 3
CO ₂ Emission Before Capture, t/MWh	1.014	1.276	1.292
CO ₂ Emission After Capture, t/MWh		0.009	0.013
Capture Cost, \$/ton		50.23	51.51
Avoided Cost, \$/ton		63.34	65.82

Potential for Cost Reduction if FGD is Completely Eliminated

To prevent corrosion of the coal pulverizers, an FGD is used to treat the primary recirculated flue gas when burning low sulfur coal with oxygen. When burning high sulfur coal, corrosion of the boiler also becomes a concern, necessitating a portion of the secondary recirculated flue gas be sent to an FGD as well as the primary recirculated flue gas. Cases 6, 9 and 10 (conventional CPU) and Cases 14 and 16 (NZE CPU) are compared to estimate the potential for cost savings (for low sulfur coal) if a modified pulverizer is developed which can tolerate high concentrations of SO_x and would enable the FGD to be eliminated. Results are summarized in Table 5.55.

Table 5.55 Impact of Partial or Complete FGD Elimination

Case No	6	9	10	14	16
CPU Type	Conv	Conv	Conv	NZE	NZE
Streams Treated by FGD	None	CPU Feed	PA + CPU Feed	PA	None
SO _x Removed by FGD, tpd	0	129.2	130.3	62.6	0
% of SO _x Removed by FGD	0%	98.0%	98.9%	47.0%	0%
SO _x in Purified CO ₂ , ppmv	4426	99	65	2	4
COE, \$/MWh	141.3	146.2	147.9	146	143.1
Capture Cost, \$/ton	51.20	54.93	56.61	50.23	48.40
Avoided Cost, \$/ton	64.26	70.02	71.88	63.34	60.48

Case 10 is used as the basis of comparison for evaluating the cost savings for conventional CPU's. In Case 10, the PA stream is sent to an FGD in order to protect the pulverizer and the CPU feed is sent to the FGD to meet the target SO_x concentration in the purified CO₂. SO_x concentrations of the purified CO₂ are shown in Table 5.55. In Case 6, it is assumed a SO_x-tolerant pulverizer is available and the FGD is eliminated. Since there is no SO_x removal process in the conventional CPU, most of the SO_x exits the CPU in the purified CO₂ at a concentration of 4426 ppmv. Case 6 would be applicable only if there are no restrictions on the concentration of SO_x in the purified CO₂. In Case 9, it is assumed a SO_x-tolerant pulverizer is available, but it is still desired to meet the SO_x concentration target in the purified CO₂. In Case 9, only the CPU feed is sent to an FGD. The SO_x concentration of the purified CO₂ in Case 9 is 99 ppmv.

Case 14 is the base case for comparing NZE CPU's. In Case 14, the PA stream is sent to an FGD to protect the pulverizer. The CPU feed does not need to be sent to an FGD because the NZE CPU includes a SO_x removal process. In Case 16, no FGD is used as it is assumed a SO_x-tolerant pulverizer is available. SO_x concentrations in the purified CO₂ are 2 ppmv for Case 14 and 4 ppmv for Case 16.

The impacts of partial or complete elimination of FGD on COE and CO₂ capture costs are shown in Figure 5.20 and Figure 5.21, respectively. The potential reduction in COE, if the FGD is completely eliminated, is estimated to be \$6.6/MWh for conventional CPU's and \$2.9/MWh for NZE CPU's. For Case 9, the FGD is reduced in size and the reduction in COE is \$1.7/MWh. For conventional CPU, partial elimination of FGD (Case 9) reduces CO₂ capture cost by \$1.7/ton and the avoided CO₂ cost by \$2.8/ton. When FGD is completely eliminated for conventional CPU, the CO₂ avoided cost approaches that of the base NZE CPU case. For NZE CPU, elimination of FGD reduces the CO₂ avoided cost by \$3/ton. Comparison of conventional CPU and NZE CPU shows that even with no FGD, the CO₂ capture and avoided costs are lower for the NZE CPU while it produces much higher purity CO₂. Details of the cost estimates are in Table 5.56.

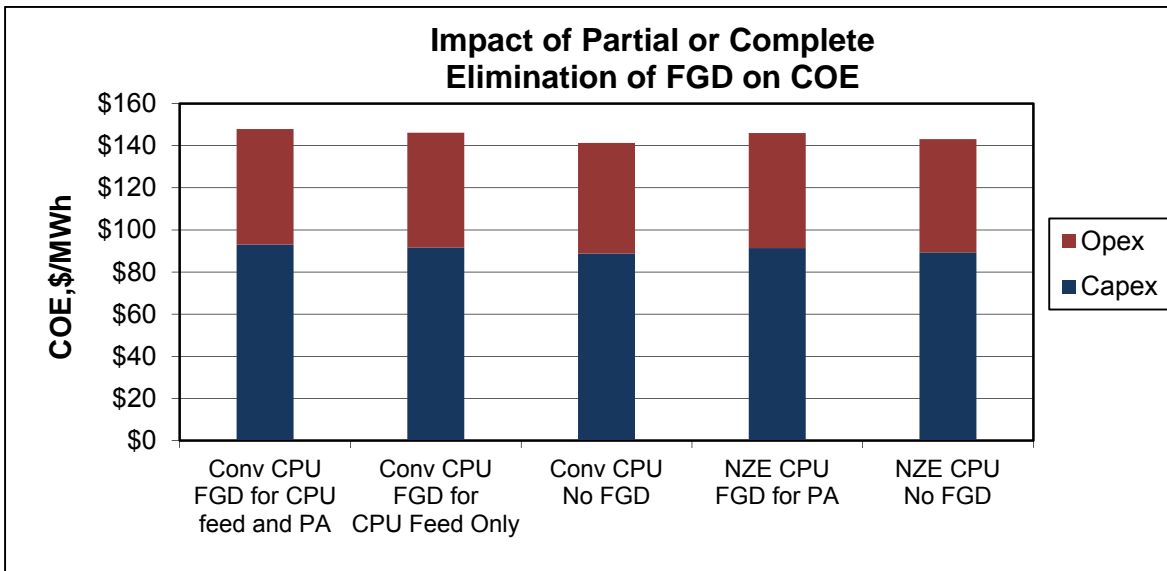


Figure 5.20 Impact on COE when FGD is Partially or Completely Eliminated

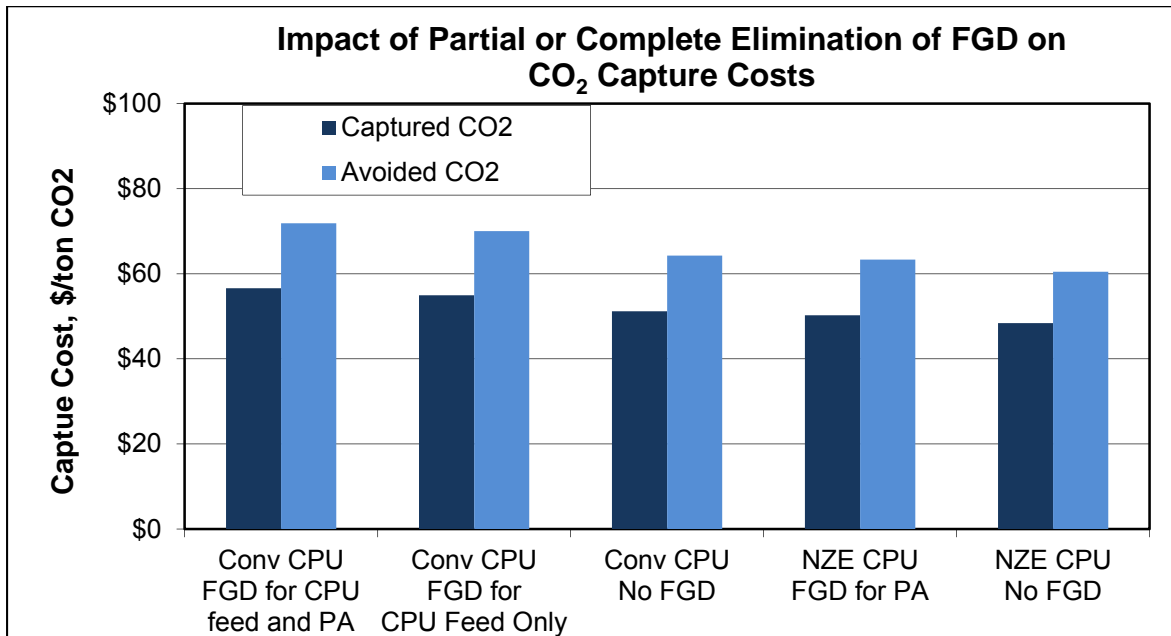


Figure 5.21 CO₂ Capture Costs when FGD is Partially or Completely Eliminated

Table 5.56 Economic Estimates for Evaluation of Savings if FGD is Eliminated

Case No.	6	9	10	14	16
Air or Oxy Firing	Oxy	Oxy	Oxy	Oxy	Oxy
Fuel	Low S	Low S	Low S	Low S	Low S
CPU Type	Conv	Conv	Conv	NZE	NZE
Partial Condensation or Distillation CPU	PC	PC	PC	PC	PC
CPU SO _x /NO _x Removal	None	None	None	Act C	Act C
Steam Cycle	Sub	Sub	Sub	Sub	Sub
Air Intrusion	2%	2%	2%	2%	2%
SCR	Yes	Yes	Yes	No	No
FGD	No	Yes	Yes	Yes	No
Stream Treated by FGD	None	CPU Feed	PA + CPU Feed	PA	None
Total Capital, \$MM	2076	2143	2180	2133	2089
Capex, \$/kW (net)	3780	3900	3960	3890	3800
Total Operating & Fixed Costs, \$MM/yr	176.8	185.1	186.6	182.6	180.4
Cost of Electricity					
Capital, \$/MWh	88.8	91.7	93.1	91.4	89.3
Operating & Fixed Costs, \$/MWh	43.2	45.2	45.6	44.8	44.1
Pipeline & Injection Wells, \$/MWh	9.2	9.3	9.3	9.8	9.7
Total Cost of Electricity (COE), \$/MWh	141.3	146.2	147.9	146.0	143.1
Increase in COE Compared to Base Case, \$/MWh	58.9	63.8	65.6	63.6	60.8
CO₂ Capture Cost					
Basis of Comparison	Case 3	Case 3	Case 3	Case 3	Case 3
CO ₂ Emission Before Capture, t/MWh	1.248	1.265	1.260	1.276	1.265
CO ₂ Emission After Capture, t/MWh	0.097	0.103	0.102	0.009	0.009
Capture Cost, \$/ton	51.20	54.93	56.61	50.23	48.40
Avoided Cost, \$/ton	64.26	70.02	71.88	63.34	60.48

Comparison of a New Plant without CCS to an Old Plant with CCS

Reductions in CO₂ emissions can be achieved by replacing old inefficient plants with new high efficiency plants or by adding CO₂ capture and sequestration processes to existing plants. Figure 5.22 shows the COE for a new plant using the ultrasupercritical steam cycle (Case 5), an existing subcritical boiler retrofitted with CCS with 2% air intrusion (Case 14a), and a similar retrofitted subcritical boiler with 10% air intrusion (Case 15a). Details of the cost estimates are in Table 5.57.

The COE of the retrofitted plant with 2% air intrusion is about \$9.5MWh more than the COE of the new ultrasupercritical plant. The COE of the retrofitted plant with 10% air intrusion is \$14.8/MWh more than the COE of the new ultrasupercritical plant.

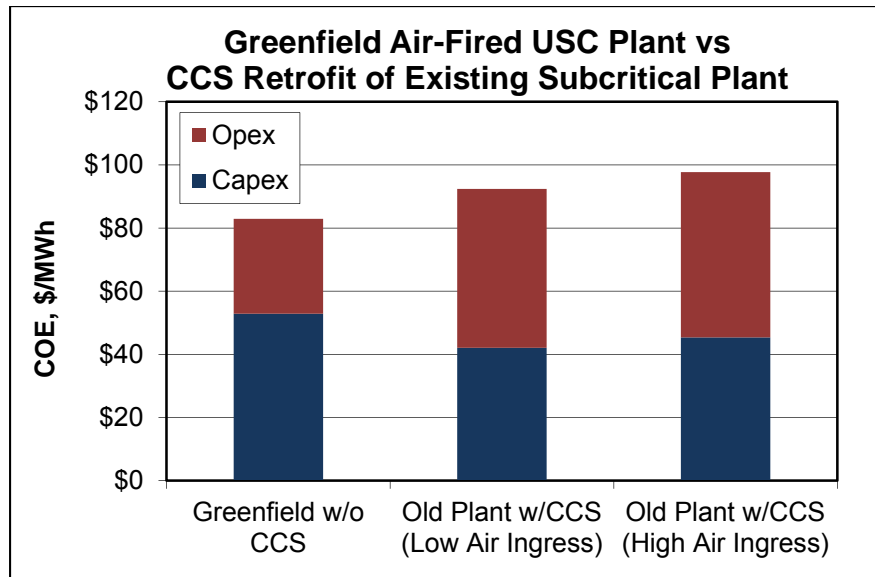


Figure 5.22 COE for New Plant without CCS vs. Old Plants with CCS

Table 5.57 Economic Estimates for Comparing New Plant without CCS to Old Plants with CCS

Case No.	5	14a	15a
Air or Oxy Firing	Air	Oxy	Oxy
Fuel	Low S	Low S	Low S
CPU Type	na	NZE	NZE
Partial Condensation or Distillation CPU	na	PC	PC
CPU SOx/NOx Removal	na	None	None
Steam Cycle	USC	Sub	Sub
Air Intrusion	2%	2%	10%
SCR	Yes	No	No
FGD	Yes	Yes	Yes
Stream Treated by FGD	Entire FG	PA	PA
Total Capital, \$MM	1320	984	1059
Capex, \$/kW (net)	2400	1790	1930
Total Operating & Fixed Costs, \$MM/yr	123.2	165.3	173.6
Cost of Electricity			
Capital, \$/MWh	52.9	42.1	45.4
Operating & Fixed Costs, \$/MWh	30.1	40.5	42.4
Pipeline & Injection Wells, \$/MWh	0.0	9.8	9.9
Total Cost of Electricity (COE), \$/MWh	82.9	92.4	97.7
Increase in COE Compared to Base Case, \$/MWh		9.5	14.8
CO₂ Capture Cost			
Basis of Comparison	Case 5	Case 5	Case 5
CO ₂ Emission Before Capture, t/MWh	0.888	1.276	1.331
CO ₂ Emission After Capture, t/MWh	0.888	0.009	0.031
Capture Cost, \$/ton		7.47	11.36
Avoided Cost, \$/ton		10.77	17.23

Subtask 5.5 – Integration and Operability

General comments received from AES regarding the Near Zero Emissions process are:

- Synthesized flue gas in the laboratory does not contain several contaminants found in power plant flue gases, including HCl, HF, PM and Hg. It is recommended to test the processes on a flue gas slipstream, at a suitable point in the development program.
- The SO_x/NO_x removal processes produce acidic byproduct, either as a waste or as saleable product. An acidic waste effluent would presumably require neutralization before disposal.
- There would be safety concerns around handling the acidic byproducts.
- A full-scale system would require compression of very large amounts of flue gas, with high capital and operating costs.
- Flue gases tend to be erosive and corrosive, raising concerns about compressor reliability.
- In air fired plants, operational upsets can result in flammable mixtures existing downstream of the combustion section of the furnace and causing “puffs” or explosions. Protections in air-fired plants include the burner management system, CO monitor in the flue gas, and multiple O₂ monitors at the inlet to the economizer. In an oxy-combustion plant, these flammable mixtures could potentially enter the CPU.

AES provided the following information regarding operations of pulverized coal power plants:

Operability

Plant Organization and Day-to-Day Operations

Most pulverized coal plants are organized with Operations, Maintenance, Material Handling, Water Treatment, Stores, Safety, Technical Support, and Clerical Support. Maintenance is typically comprised of Mechanical, Electrical and I&C departments, along with a planning function. Operations are continuous. Operators enter maintenance job orders which are prioritized by the planner and scheduled accordingly. Technical Support reviews key operating data and heat rate and assists on major maintenance. Material Handling is responsible for unloading and reclaiming coal, ash handling and lime/limestone unloading.

Water Treatment is responsible for operations and maintenance of the water purification system. Technical Support reviews key operating data and trends, provides major maintenance, Capex planning and preventive/predictive maintenance. Safety is responsible for required training and reporting. Stores purchases and inventories spare parts and equipment. Clerical Support is responsible for payroll and benefits administration, fuels accounting, ash and limestone administration, accounts payable, and treasury functions.

Typical Operational Issues

Factors affecting daily operations are age of the plant, design, fuel quality, equipment condition, maintenance practices and history, water chemistry, major equipment redundancy, number of units, amount of auxiliary equipment and staffing. Good preventive and predictive maintenance practices are particularly important. Typical operational issues include coal flow pluggage in chute, hoppers, feeders and mill inlets. Boiler tube leaks in high velocity sections of the boiler can be problematic, often due to dissimilar weld failures.

Safety

Main safety concerns are related to material handling, new equipment, abnormal conditions, furnace slagging. Proper isolation and tagging of high energy equipment while on line is particularly important.

Startup and Shutdown Operations

Startups are characterized as either cold, warm or hot depending on the temperatures of the turbine shell, throttle valve, or governor valve. Cold starts can take 16-20 hours. Warm and hot starts can be accomplished in 8-12 hours. Planned shutdown frequency varies according to plant and state inspection requirements. Some are on two year or 18 month or 12 month cycles for the boiler, while turbine majors are in the 7-10 year frequency range.

Start up begins with ensuring proper water levels within the drum and boiler. Once this is accomplished, warm up guns and igniters (oil or gas) are inserted to begin building up pressure and temperature. Boiler pressure is raised per the manufacturer's schedule, usually 100 psi per hour. Firing rates are increased as necessary to achieve required turbine temperatures, and required superheat. Usually at least 100 F of superheat is required. The turbine is then "rolled off" of turning gear (3-5 rpm), and speed is increased at a rate of 100 rpm per minute (cold), 200 rpm per minute (warm or hot) until soak speed is attained. Soak speed varies per unit, but is usually in the 2300-2400 rpm range.

The turbine is maintained at this speed for some amount of time. Typically 3-4 hours are needed for the inner shells to achieve proper temperature. This is because the rotor heats up and expands much faster than the stationary shells. If temperatures are not within requirements, the rotor will rub against seals resulting in higher clearances, affecting turbine efficiency and potentially resulting in mechanical damage or failure. An important consideration for operators during start up is to be aware when the rotor approaches and runs thru a critical speed. The number of critical speeds a rotor has varies by unit, but typically there are 3- 4 critical speeds in the ramp up to 3600 rpm. Operators need to avoid prolonged operation at a critical speed as vibration can increase dramatically at the various bearings.

During the soak period, the field is put on the generator. Once proper temperatures are achieved, the turbine is then brought up to a little over 3600 and synchronized to the transmission system. It is typically at this point coal is introduced to the furnace at minimum feed rates. The generator is then brought to some minimum load (<10%) and held for some period to allow temperatures to stabilize. Once this period expires, load is gradually applied in concert with increases in boiler pressure. Water chemistry is closely monitored for silica levels to avoid solid particle erosion of the turbine blades. Load is gradually increased as operators place high pressure heaters in service. Once silica is at an acceptable level, pressure is increased to its normal maximum setting and load is increased to its maximum setting, or as dispatch requires.

Outages and Seasonal Load Variations

Depending on system load, planned outages are usually in spring or fall. Planned outages typically start on a Friday night to allow weekend cooling and isolation and tagging. Actual maintenance work starts the following Monday. Planned outage frequency is dictated by a number of variables: 1) authorized inspector requirements for the pressure parts, or 2) wear amount of critical components, typically mills, or high gas velocity areas in the convective sections or sometimes 3) downstream gas ducts.

Load is generally reduced per normal schedules – this varies by unit, but ramp rates of anywhere from 1-2 mw/min up to 10-15mw/min are typical. As far as seasonal variations these vary by region but in New York, peak load occurs in the summer and winter. Load tends to reduce in the spring and fall. This can

also be affected by transmission outages which can affect pricing in different areas of the State, and could drive a plant up or down, depending on actual transmission flow conditions.

Planned outages are necessary in order to overhaul key pieces of equipment subject to high wear, i.e., mills, exhausters, burners, coal pipes, ash handling equipment. Also, in a coal plant with old design casings, dust tends to settle in motor windings, necessitating shutdowns on a yearly frequency. Depending on the number of boiler pressure excursions, safety valves develop leaks and need repairs/re-setting on a yearly basis.

Unplanned or forced outages can occur for any number of reasons: boiler tube leaks, transient condition in the transmission system tripping generator breakers, loss of vacuum due to issues with circulating water pumps, faulty instrument output causing a trip, or a hot spot in a critical breaker or transformer bushing.

Avoiding outages requires competent operating practices, good maintenance practices, and paying attention to various operating parameters. Availability for a well-run coal plant should be greater than 90%.

Typical issues besides those described above are often fuel related problems. For example fine, wet coal causes issues in hoppers and chutes, feeder and mill inlets. Pluggage within a feeder or mill immediately causes load to be reduced, thus necessitating the control system to function according to design and quick action by the operator.

Ambient Conditions

Ambient conditions can cause problems during the winter, especially in extreme conditions. Coal unloading and re-claim become problematic, as train cars tend to freeze solid requiring heating and soaking with attendant flow issues. Mobile equipment tends to experience problems also.

During the summer months, if a plant is located on a river, inlet water temperatures can affect turbine vacuum, and reduce load.

Coal Composition

Coal composition significantly affects boiler performance and operation. While designers can attempt to use a range of coal, practical considerations and economics usually result in a narrow bandwidth of fuels. Hardness, measured on the Hargrove scale, directly affects pulverizer performance similar to the effect of moisture content. Eastern bituminous fuels are lower in moisture than western coals (4 - 6% for eastern versus 25 - 30% for western). The higher moisture levels require more retention time in the mill, or higher temperature and flow of primary air to properly dry the coals for furnace input. Coal air temperatures leaving the mill should be at least 150 F to avoid firing issues and possible layout in the coal pipes. The desired range of coal air is 150 – 180 F.

Ash content has a major impact on back end erosion – erosion rates vary to the fourth power as ash content increases. It also affects precipitator performance and ash handling equipment. Heat content of the coal directly affects boiler performance, as the boiler is designed for a specific amount of energy. If lower than designed heat content fuels are used, then greater amounts of material must be fed into the furnace. This affects heat transfer rates, erosion rates, slagging, and gas flows which all impact other major support equipment.

Sulfur content directly affects precipitator performance. Precipitators are generally designed for sulfur contents of 2 - 4% sulfur. Coals containing less than 1% sulfur tend to be highly resistive and generate “back corona” within the precipitator. This phenomenon results in coating or clamping of the ash on the wires and plates. This reduces collection efficiency, and raises opacity levels. If not acted on quickly, the clamping can become so intense that collection efficiency reduces to unacceptable levels. This necessitates removal of the boiler from service

Process Parameters

Process Control

Coal plants today typically employ what is known as coordinated control: this process looks at generator output and boiler or throttle pressure simultaneously. As a megawatt signal comes from the dispatch system model, a megawatt controller takes the signal and produces a control signal that uses actual generator output to close the loop. The megawatt control signal is sent in parallel to the turbine and boiler control system. The signal to the turbine is demand for steam flow. The boiler signal is a feed forward signal to the firing system and a pressure controller for throttle pressure. Main systems in support of the coordinated control system are 1) combustion control which controls feeder speeds, and FD fans, 2) pulverizer control which controls mill outlet temps and feeder speeds, 3) furnace draft control which controls the ID Fans, 4) secondary air control which controls windbox pressure, 5) feed water flow and 6) superheat and reheat temperature control.

Most plants have distributed control systems with uninterruptible power supplies and back up drops. In addition, there are data acquisition and historian modules available along with performance monitoring.

Most plants are highly automated with main and auxiliary systems completely automated. This is desirable because systems are highly complex. Manual operation would likely result in numerous operating errors. The number of operating personnel depend on plant complexity, number of boilers and turbines, amount of auxiliary equipment, environmental equipment, age, and plant condition. Typically, on a shift basis one control operator is necessary per unit along with 1 chief or shift supervisor, 1 auxiliary equipment operator, and 1 person in FGD if the plant is so equipped. For larger plants with extensive waste water treatment and sludge (from FGD) handling equipment an additional 1-2 people are required per shift.

Air Ingress

Air ingress comes from six main areas: 1) furnace setting depending on age and design of the boiler, 2) furnace and roof penetrations 3) duct work and duct work expansion joints, 4) air heater leakage, 5) observation and maintenance doors, and 6) ash hopper casing. High levels of air in-leakage negatively impact boiler performance in several ways. Excess air as a practical matter is measured at economizer outlet due to temperature limitations of the probes. Air leakage tends to fool the probes into thinking excess air in the furnace is higher than actual; thus the furnace becomes starved of combustion air resulting in higher levels of unburned carbon and CO. As air leakage increases, mass gas flow increases thus overloading ID Fans potentially resulting in slagging.

Excess Air

A rule of thumb in coal boilers is that 20% excess air, or 3.2% oxygen measured at economizer exit is optimum for combustion efficiency and lower CO levels.

Air Preheaters

Rotary heat recovery systems are typically Ljungstrom air pre-heaters. These air heaters have a vertical shaft rotating continuously from 1 - 3 rpm, depending on design. The rotor has metal “baskets” attached in two layers, hot and cold. The air heater is located within a set of ductwork with flue gas entering from the top at about 550 F - 600 F on one side, and air entering at ambient from the bottom at the other side. Exit gas temperatures are typically in the 280 - 300 F range depending on efficiency, age and cleanliness. Air leaves the air heaters in the 500 F range. Leakage is controlled by rotor post, radial and axial seals. These are wear items requiring checking/replacement/repairs on a yearly basis. The baskets are constructed of steel sheets, which are corrugated or notched to smooth the flow. Pressure drop across the elements are monitored for soot blowing and cleaning requirements. Leakage can be in the 10% range or greater depending on age and maintenance practices.

There are two types of stationary air heaters: tubular and heat pipes. Tubular air heaters are constructed with steel tubes arranged vertically between two tube sheets. Typically, the tubes are rolled into the sheets at each end. Gas enters into the tubes with air passing around the tubes externally. Tubular heaters are much simpler than regenerative heaters. But major issues with them are cold end corrosion and mechanical failures of the joints. The cold end corrosion varies with sulfur content of the coal. The main problem is the ambient air temperatures almost assures some level of corrosion because at least a portion of each tube will have a wall temperature below the acid dew point, thus necessitating some level of regular tube replacement.

Heat pipes are relatively new to coal fired boilers (last 20 years) and theoretically offer many advantages over the Ljungstrom and tubular type heaters. They are highly efficient and have no moving parts. A heat pipe consists of dozens of finned steel tubes; each filled with toluene or naphthalene, and is installed at a slight angle (5 degrees). Tubes are closely spaced (1” or less), and are arranged in a staggered pattern from top to bottom. While leakage can be very low, maintenance can be a major issue. The tube spacing and arrangement patterns can cause ash build up and leaks. Some boilers with heat pipes require two outages per year for cleaning. Cold end corrosion also is an issue depending on exit gas temperatures and sulfur content. Ten to fifteen year life cycles are not uncommon for heat pipes.

Dispatch Orders – Market Issues

Dispatch order in NY State is as follows: A number of units across the state are mandated as “must run”. These are typically nuclear units, hydro units and plants designated as necessary for local transmission security. Following these units, dispatch order is dictated by strike price of each specific unit, in terms of \$/MWh. Historically coal plants have the lowest strike price due to the low cost of coal. This is beginning to change as natural gas prices decline and additional environmental equipment adds to strike price i.e., ammonia for SCR, and limestone or hydrated lime for FGD.

Environmental Drivers

Environmental regulations govern allowable flue gas opacity, NO_x and SO₂ emissions and mercury emissions. Opacity is limited to 20% maximum continuously or 29% on a 6 minute average. NO_x emissions are limited to 0.1 lb/MMBTU. SO₂ emissions are limited to 0.17 lb/MMBTU. Hg emissions limitations are under development. A requirement equivalent to at least 90% removal is anticipated by the industry.

Available control technologies include:

Opacity:	Precipitators and bag-houses
NO _x :	SCR, SNCR and over fire air or a combination of any of the two
SO ₂ :	Dry or wet scrubbing

Hg: Carbon injection/ in combination with a dry scrubber and bag house, removal rates of 95% can be achieved.

Summary

Some of the challenges that have been identified in this technoeconomic evaluation include:

- Potential to develop high temperatures in the furnace which could result in slagging, overheating of refractory or furnace tubes.
- Potential for flue gas recycle to result in corrosion due to high SO_x concentration.
- Developing operating procedures for switching from air-firing to oxy-firing to air-firing.
- Potential for high air intrusion rates to negatively impact CPU effectiveness.
- Potential for high concentrations of oxygen to reach the activated carbon beds in the CPU and possibly ignite the carbon.
- The need to develop control schemes to supply the proper amount of oxygen from ASU and to maintain CPU effectiveness as the power output from the power plant ramps up and down.
- Reluctance on the part of power plant companies to deal with the risks of handling the acidic byproduct or waste from a NZE CPU.

It is expected that none of these challenges will be insurmountable.

Subtask 5.6 – Plan for Pilot Demonstration

Oxy-Coal Furnace

The University of Utah has completed a $\pm 30\%$ cost estimate of the oxy-coal furnace. A preliminary schematic of the furnace is shown in Figure 5.23. The furnace includes two pulverized coal burners rated at 4 MMBtu/h each. To provide continuous operation, the furnace includes ash removal capability.

The furnace design includes the following major items:

- Primary/secondary blowers
- Primary, secondary, tertiary, and staging air/oxygen/FGR flow trains
- Natural gas train (used for startup and to maintain temperature when coal feed is interrupted)
- Coal feed system
- Exhaust handling system
- Temperature and pressure measurements
- Digital control hardware
- Supporting structure
- Steel furnace shell
- Refractory and insulating materials
- Burners
- Convective zone heat exchangers
- Pulsed-jet baghouse
- SO₂ scrubber
- Coal preparation (truck dump equipment, crusher, pulverizer, storage and conveying equipment)
- Small steam boiler (for soot blowing)
- All plumbing and electrical supplies required for construction.

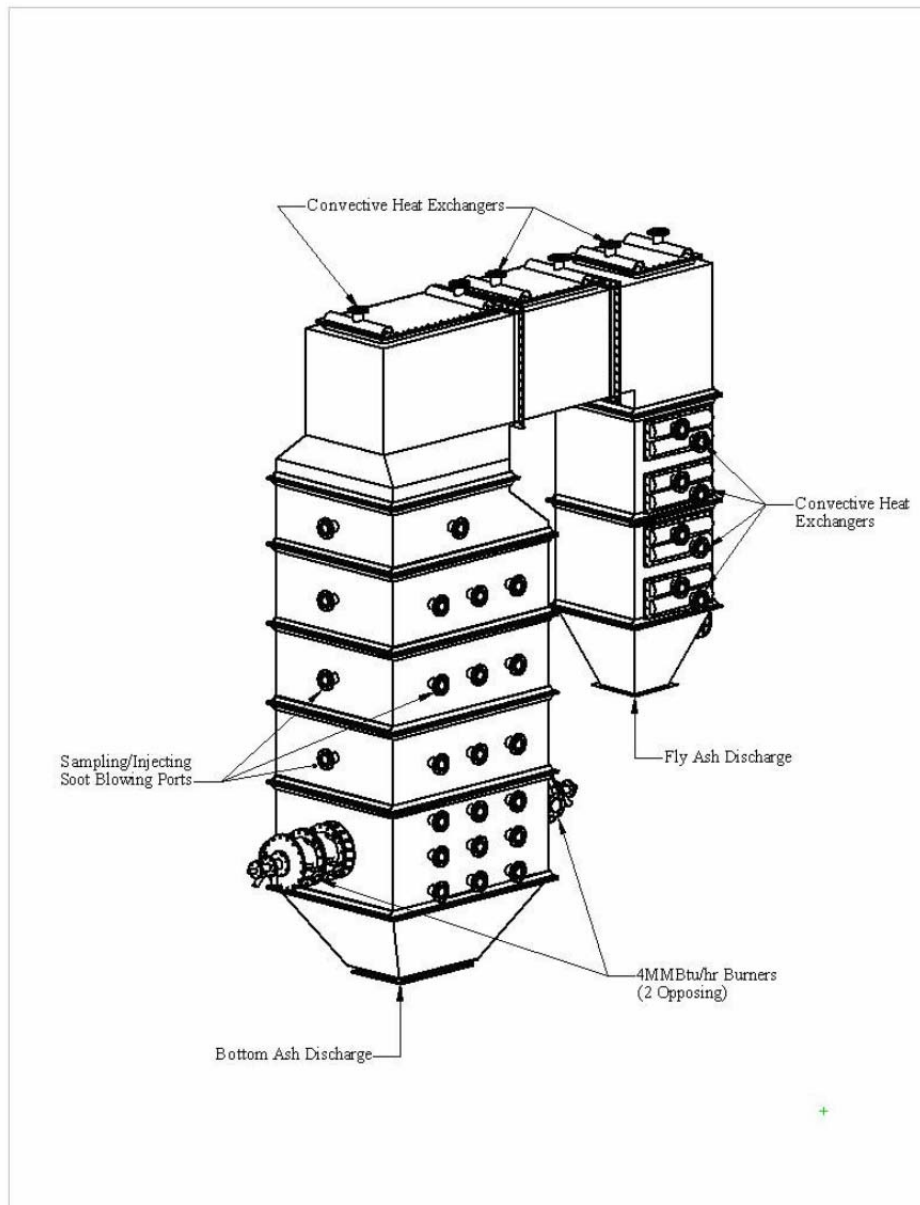


Figure 5.23 Preliminary Schematic of Oxy-Coal Furnace

Subscale Near Zero Emissions CPU

A process schematic for a full-scale CPU using Near Zero Emissions technology is shown in Figure 5.1. A process flow diagram for the subscale CPU is shown in Figure 5.24. Differences between the sub-scale and a full-scale CPU include:

- Elimination of the product compressor.
- Elimination of the power recovery turbine.
- Elimination of waste heat recovery in the flue gas cooler.
- Use of a single Hg guard bed instead of 2 beds in lead/lag configuration.

Process Description

1. Direct Contact Cooler

The direct contact cooler is used to cool the flue gas, reduce the amount of water in the flue gas, and remove HCl and HF.

The direct contact cooler consists of a packed tower with at least 2 sections of packing. Flue gas is sent to the bottom. Water from the bottom of the column is pumped, cooled in an indirect heat exchanger, and sent to the top of the lower section of packing. Fresh water is sent to the top section of the column to ensure complete removal of HF and HCl. Excess water is split from the recirculation loop at an appropriate location and sent out of battery limits.

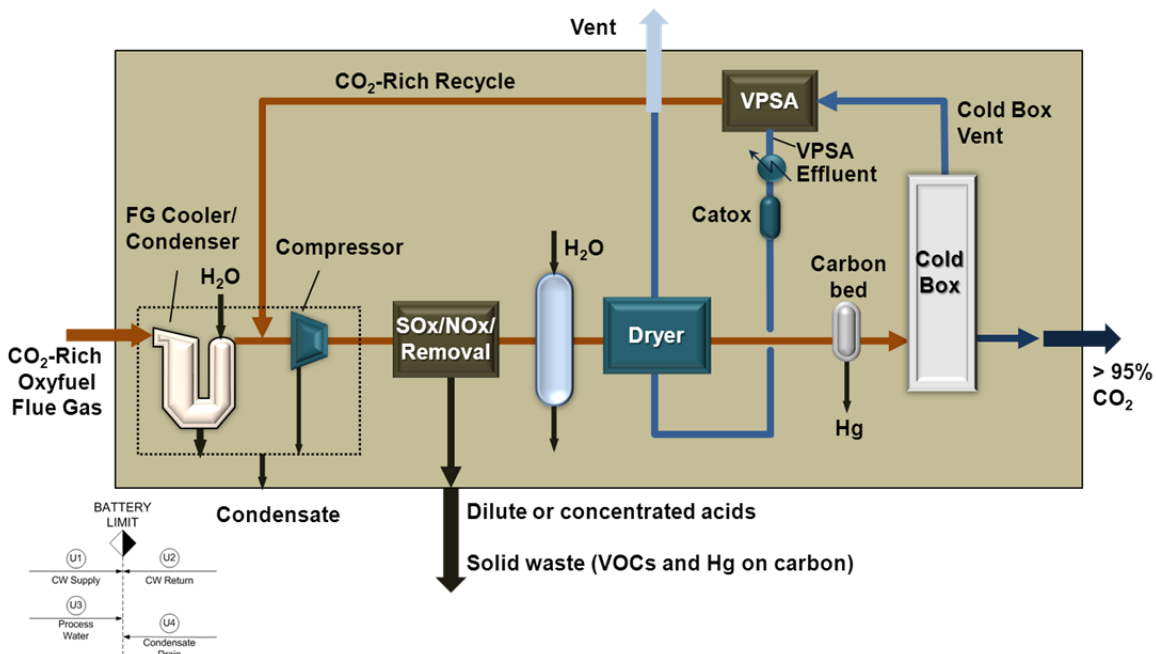


Figure 5.24 Process Schematic of 20 tpd Demonstration CPU

2. Multistage Compression System (Raw Gas Compressor)

The compressor consists of a 5-stage non-lubricated reciprocating compressor with water-cooled heat exchangers and phase separators after each stage of compression, including the final stage. It is anticipated that significant amounts of SOx and NOx contained in the flue gas will form H₂SO₄ and HNO₃ in the compressor condensate.

3. SOx/NOx Removal System

The SOx/NOx removal system is based on the activated carbon process. It reduces SOx concentration by 99.9% and NOx concentration by 95%. The activated carbon process causes SOx and NOx to react with oxygen and water to form H₂SO₄ and HNO₃ and exit the process as an aqueous acid.

4. Water Wash Column

The purpose of the water wash column is to reduce SOx/NOx concentration in the gas stream in the event a breakthrough occurs in the SOx/NOx removal process.

5. *Dryer Beds*

The dryer reduces the moisture content of the gas to < 1 ppmv. Two adsorption beds are used. One bed is used to dry the gas, while the other is thermally regenerated. The hot gas from the Catox is used to heat and regenerate the bed. An indirect heat exchanger is used to reduce the regeneration gas temperature during the cooling step of the regeneration cycle. Regeneration gas leaving the dryer is vented to atmosphere.

6. *Mercury Guard Bed*

To protect downstream equipment, mercury is removed from the gas using a fixed bed of activated carbon.

7. *Dual Purity Cold Box*

The gas stream from the mercury guard bed is sent to a cold box which separates the raw gas into

- (a) A purified CO₂ stream, which is vented to atmosphere, and
- (b) A waste stream which contains most of the nitrogen, oxygen, argon and carbon monoxide that was contained in the flue gas, as well as some CO₂.

CPU cold boxes can contain either a partial condensation process (single stage phase separator) that can make ~95% CO₂ or a distillation process that can make 99.9% CO₂. For the sub-scale CPU, both types of processes are provided in a single cold box, thus allowing the performance of both processes to be evaluated and optimized. The concept is illustrated in Figure 5.25.

8. *CO₂ VPSA*

The waste stream from the dual purity cold box contains significant amounts of CO₂. Rather than venting this stream directly to atmosphere, the waste stream is sent to a CO₂ VPSA where much of the CO₂ is recovered. Recovered CO₂ is blended with raw gas leaving the direct contact cooler and sent to the multistage compression system. The CO₂ VPSA also produces a CO₂-depleted waste stream which is sent to the Catox system.

9. *Catox System*

The Catox system is used to reduce emissions of CO. The waste stream from the CO₂ VPSA is sent to the Catox system, where it is (electrically) heated and sent to a catalytic reactor. The catalytic reactor promotes the reaction of carbon monoxide with oxygen to form CO₂. Hot gas from the catalytic oxidation process is used to regenerate the dryer beds.

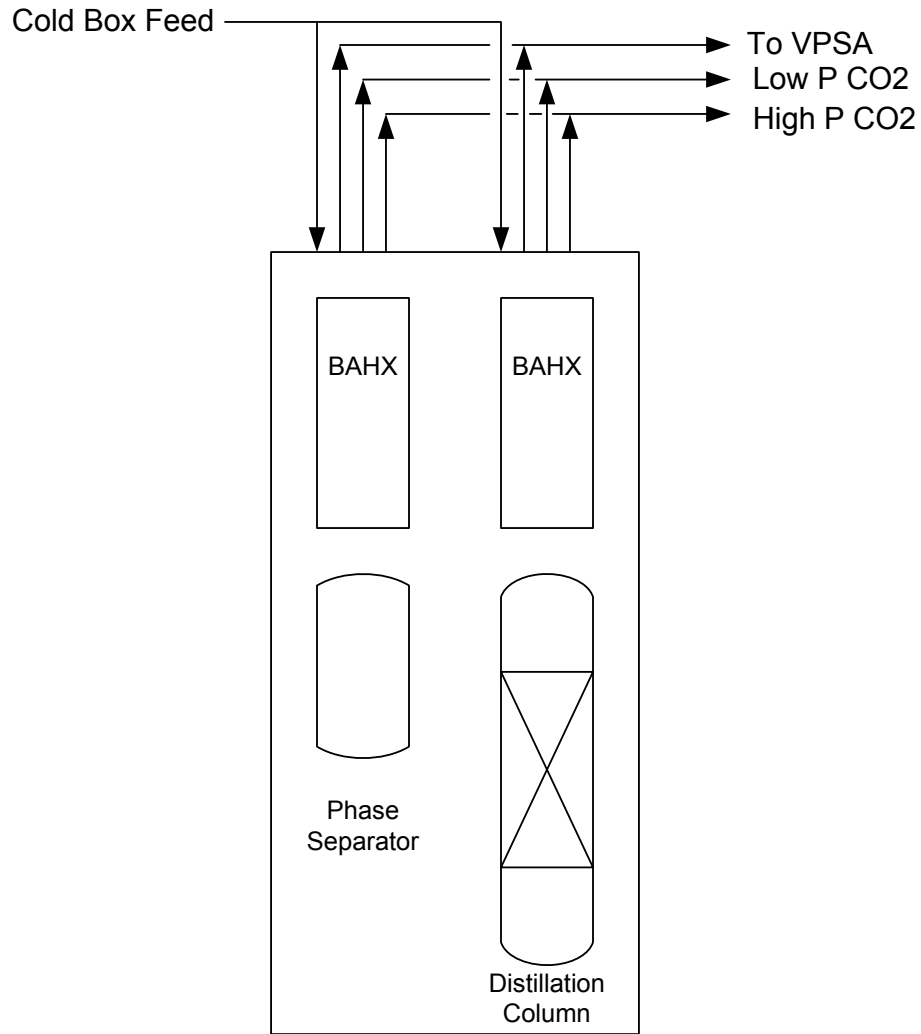


Figure 5.25 Dual Purity Cold Box for Pilot Demonstration CPU

The coal composition in Table 5.58 was used for predicting oxyfuel flue gas composition.

Table 5.58 Coal Composition for Pilot Demonstration CPU

Component	wt. %
Moisture	10.81%
Ash	10.75%
Hydrogen	4.14%
Carbon	62.51%
Nitrogen	1.11%
Sulfur	0.36%
Oxygen	10.32%
Chlorine	0.00%
Total	100.00%

Stream summaries for the two different cold box processes are shown in Tables 5.59 and 5.60. Major assumptions for calculating flue gas rate and composition from the boiler to the CPU include:

- FGD is not in operation
- Excess oxygen in furnace flue gas = 2.5%.
- Flue gas recycle ratio = 0.694
- Air ingress rate = 7.3%

Table 5.59 Stream Summary – Partial Condensation CPU

Stream ID	A	B	C	D	U1	U2	U3	U4
Stream Name	CO ₂ -Rich Oxyfuel Flue Gas	Dilute Acid	Vent to Atm (Dry Basis)	Gaseous Product CO ₂	CW Supply	CW Return	Process Water	Condens. Drain
Temperature, deg F	250	67	Varies	18	60	80	60	103
Pressure, psia	14.7	14.7	14.7	14.7	50	40	50	20.49
Molar Flow, lb mol/h	58.38	1.56	12.77	38.24	1,854	1,854	14.88	13.82
Mass Flow, lb/hr	2191	33	371	1683	33,390	33,390	268	370
Composition, Mol Fr								
CO ₂	0.658473	0	0.015413	0.999967	0	0	0	0.000373
N ₂	0.176613	0	0.807357	0.000002	0	0	0	0.000003
O ₂	0.037417	0	0.167834	0.000010	0	0	0	0.000002
Ar	0.002053	0	0.009385	0	0	0	0	0
SO ₂	0.001309	0	0	0.000001	0	0	0	0.000773
SO ₃	0.000024	0	0	0	0	0	0	0.000069
NO	0.000274	0	0.000012	0	0	0	0	0.000156
NO ₂	0.000034	0	0	0.000020	0	0	0	0.000098
CO	0.000036	0	0	0	0	0	0	0
HCl	0.000028	0	0	0	0	0	0	0.000080
HF	0.000051	0	0	0	0	0	0	0.000145
H ₂ O	0.123688	0.953491	0	0	1.00	1.00	1.00	0.998302
H ₂ SO ₄	0	0.038886	0	0	0	0	0	0
HNO ₃	0	0.007623	0	0	0	0	0	0

Table 5.60 Stream Summary – Distillation CPU

Stream ID	A	B	C	D	U1	U2	U3	U4
Stream Name	CO ₂ -Rich Oxyfuel Flue Gas	Dilute Acid	Vent to Atm (Dry Basis)	Gaseous Product CO ₂	CW Supply	CW Return	Process Water	Condens. Drain
Temperature, deg F	250	67	Varies	20	60	80	60	103
Pressure, psia	14.7	14.7	14.7	14.7	50	40	50	14.7
Molar Flow, lb mol/h	58.38	1.56	10.93	40.16	1,743	1,743	14.88	20.41
Mass Flow, lb/hr	2191	33	316	1739	31,410	31,410	268	369
Composition, Mol Fr								
CO ₂	0.658473	0	0.010042	0.954152	0	0	0	0.000361
N ₂	0.176613	0	0.818443	0.033995	0	0	0	0.000003
O ₂	0.037417	0	0.161904	0.009343	0	0	0	0.000002
Ar	0.002053	0	0.009431	0.000418	0	0	0	0
SO ₂	0.001309	0	0	0.000001	0	0	0	0.000776
SO ₃	0.000024	0	0	0	0	0	0	0.000069
NO	0.000274	0	0.000011	0.000001	0	0	0	0.000157
NO ₂	0.000034	0	0	0.000019	0	0	0	0.000098
CO	0.000036	0	0.000168	0.000007	0	0	0	0
HCl	0.000028	0	0	0	0	0	0	0.000080
HF	0.000051	0	0	0	0	0	0	0.000146
H ₂ O	0.123688	0.953492	0	0.002065	1.00	1.00	1.00	0.998309
H ₂ SO ₄	0	0.038889	0	0	0	0	0	0
HNO ₃	0	0.007619	0	0	0	0	0	0

Cost Estimate of Pilot Facility:

The boiler cost estimate in Table 5.61 is based on a boiler capacity of 8 MMBtu/h and CPU capacity of 20 tpd.

Table 5.61 Capex of Pilot CPU Demonstration Facility

Boiler and Infrastructure, \$MM	\$4.5
CPU, \$MM	\$10.2
Total, \$MM	\$14.7

The operating scenario, defined in Table 5.62, results in a total of 258 days/yr of pilot testing. The length of the test program is 3 years.

Table 5.62 Operating Scenario for Pilot CPU Demonstration Facility

Heating Days/Campaign	5
Oxy-Coal Operating Days/Campaign	43
Cooling Days/Campaign	5
Maintenance Days/Campaign	7
No of Campaigns/yr	6

Operating cost breakdown is shown in Table 5.63.

Table 5.63 Opex of Pilot CPU Demonstration Facility

Year	2014	2015	2016	Total
Labor, \$MM/yr	\$2.2	\$2.2	\$2.2	\$6.6
Consumables, \$MM/yr	\$2.1	\$2.1	\$2.1	\$6.3
M&R, \$MM/yr	\$1.1	\$1.1	\$1.1	\$3.3
Total Opex, \$MM/yr	\$5.4	\$5.4	\$5.4	\$16.2

The overall spending by year is shown in Table 5.64.

Table 5.64 Cost Summary by Year for Pilot CPU Demonstration Facility

Year	2012	2013	2014	2015	2016	Total
Capex, \$MM	\$5.0	\$9.7	\$0.0	\$0.0	\$0.0	\$14.7
Opex, \$MM	\$0.0	\$0.0	\$5.4	\$5.4	\$5.4	\$16.2
Total, \$MM	\$5.0	\$9.7	\$5.4	\$5.4	\$5.4	\$30.9

Conclusions

Subtask 5.1 - Process and Systems Engineering

The NZE CPU is capable of achieving near zero emissions of SO_x, NO_x, CO, Hg, HCl, HF and VOC's. The NZE CPU is able to achieve significantly higher capture of CO₂ than a conventional CPU. The advantage becomes more pronounced at high air infiltration rates. The purified CO₂ from the NZE CPU contains significantly less SO_x and NO_x than the purified CO₂ from a conventional CPU. CO₂ purity >99.9% vol. is achievable by using a distillation column in the cold box.

Subtask 5.2 - Oxyfuel Power Plant Performance

Key findings from the Foster Wheeler report are:

- The oxyfuel retrofit at the existing power plant is technically feasible.
- The investment cost of the retrofit in the boiler island is between \$95 - \$99 MM.

Subtask 5.4 – Economic Feasibility

Cost analysis reveals the several trends:

- Advantage of NZE CPU is highest for old plants with high air ingress and without FGD and SCR. The benefit of NZE CPU over conventional CPU is not apparent when only COEs are compared

as CO₂ capture rates are much higher for the NZE CPU. The advantage of NZE CPU is more clearly seen when CO₂ avoided costs are compared.

- For new plants, increases in COE compared to air-fired base cases for the conventional CPU and the NZE CPU are \$66 and \$64/MWh, respectively. Cost of avoided CO₂ and cost of captured CO₂ are generally about 11-14% lower using the NZE CPU compared to using a conventional CPU. Lower capture costs for NZE CPU are due to lower capital investment in FGD/SCR and higher CO₂ capture rates.
- Relative contribution from activated carbon process and VPSA in lowering CO₂ avoided costs are ~67% and ~33%, respectively.
- With no credits for sale of sulfuric acid byproduct, the Task 2 sulfuric acid process for SO_x/NO_x removal does not provide any cost advantage compared to the Task 3 activated carbon process.
- For older plants with high air intrusion, increase in COE compared to air-fired base cases is higher for NZE technology at \$63.0/MWh compared to \$61.1/MWh using conventional CPU. For older plants, the cost of avoided CO₂ and capture CO₂ are about 18-24% lower using the NZE CPU. Larger benefit of the NZE CPU for high air intrusion case is due to larger difference in the CO₂ capture rate when compared to the conventional CPU.
- The avoided CO₂ and captured CO₂ cost advantage of the NZE CPU increases with air intrusion.
- Cost of electricity is generally slightly lower using the NZE CPU compared to using the conventional CPU, except at high air intrusion rates.
- The use of distillation to make high purity CO₂ increases COE by about \$2.3/MWh. Captured CO₂ cost increases by \$1.3/ton and avoided CO₂ cost increases by \$2.5/ton.
- If the FGD is eliminated from the boiler island, the potential cost savings is about \$2.9/MWh, when using an NZE CPU. The potential reduction in captured CO₂ cost is \$1.8/ton and the potential reduction in avoided CO₂ cost is \$2.9/ton.
- The COE for retrofitting CCS to an existing subcritical plant is only 11% - 18% more than COE for a new ultrasupercritical plant without CCS.

Subtask 5.5 – Integration and Operability

Integrating a full-scale ASU and CPU with a pulverized coal power plant will present several challenges, most of which will need to be identified and resolved during the engineering phase of a project. From power producer's perspective, areas of concern are management of temperatures and corrosion within the boiler, transition from air-firing to oxy-firing mode, ability to follow load, disposal of acidic waste streams and keeping oxygen levels within safe limits.

Subtask 5.6 – Plan for Pilot Demonstration

A cost estimate has been completed for the sub-scale oxy-coal furnace, building improvements and CPU. Capex is \$14.7 million \pm 30%. Lead time is 18 months. Opex is about \$5.4 million/yr. The total cost over the life of the program is about \$31 million.

Project Conclusions

Experimental program was successfully completed to determine technical feasibility of two SO_x/NO_x removal processes and VPSA process for increasing CO₂ recovery. Commercial viability assessment was completed to determine economic feasibility and to define path to commercialization.

The activated carbon process exceeded performance targets for SO_x and NO_x removal efficiencies and it was found to be suitable for power plants burning both low and high sulfur coals. This process was able to achieve simultaneous SO_x and NO_x removal in a single step. The removal efficiencies were >99.9% for SO_x and >98% for NO_x.

The sulfuric acid process for high sulfur coal plants met performance expectations with regards to SO_x/NO_x removal from flue gas, however, it did not meet performance targets for sulfuric acid product specifications. Key stumbling block for this process was inability to remove the absorbed NO_x from the acid. It was decided not to pursue this technology further after the required tasks were completed.

The VPSA process met or exceeded the performance targets set at in the project. In pilot scale tests, the VPSA process could recover > 95% of CO₂ at >80% purity (by vol.) from simulated cold box feed streams. The VPSA process and system were optimized by performing technoeconomic analysis. The six-bed VPSA process with adsorbent Q and one stage of vacuum pump were found to be optimum. The optimum CO₂ purity from VPSA was found to be ≥80% (by vol.) in order to minimize processing costs in CPU. Based on these results, process simulations were performed for the NZE CPU. The overall CO₂ recovery was projected to be >99% for plants with low air ingress (2%) and >97% for plants with high air ingress (10%).

The commercial viability assessment for retrofitting existing and new power plants with oxyfuel technology was carried out. Foster Wheeler performed power plant performance assessment and concluded that the retrofit is technically feasible. Their study pointed out that the recirculated flue gas stream used as 'primary air' must be treated in FGD for SO_x removal and the SO_x level in the boiler must be below 4000 ppm.

Praxair performed economic feasibility study using the DOE's guidelines for 550 MW net power plants. The efficiency penalty for 99.3% CO₂ capture was estimated to be ~8.0 percentage points. The study compared COE and CO₂ capture costs using conventional and NZE CPU technologies in order to determine the value of technology developed in this project. The cost of electricity (COE) for existing plant without CCS (CO₂ capture and storage) increased from \$35/MWh to \$96/MWh for CCS with conventional CPU and to \$98/MWh for CCS with NZE CPU. The CO₂ avoided costs for NZE CPU and conventional CPU were \$65/ton and \$86/ton, respectively. Large reduction in CO₂ mitigation cost for NZE CPU compared to conventional CPU were due to higher capture rate and savings in capital investment for FGD and SCR. For greenfield plant, the COE increased from \$82/MWh to \$148/MWh for conventional CPU and \$146/MWh for NZE CPU. The CO₂ avoided costs were ~12% lower for NZE CPU at \$63/ton compared to \$72/ton for conventional CPU. Relative contribution from activated carbon process and VPSA in lowering CO₂ avoided costs were ~67% and ~33%, respectively.

For scale-up towards commercialization, about one year of further development is recommended for the activated carbon process with the emphasis on adsorption-regeneration cycle optimization. Next step for scaling up this technology is a demonstration of entire NZE CPU at a 20 tpd (tons per day) scale. Cost estimation for this demonstration was estimated with U. of Utah as a potential host site. The total capital cost for a demonstration unit was estimated to be ~\$15 MM and the operating costs for a three year operation were estimated to be ~\$16 MM.

In summary, one technology option for NZE CPU based on the activated carbon process and coldbox-VPSA hybrid process was successfully developed. Although proposed for only low sulfur coal plants, activated carbon process was demonstrated to work for SO_x levels expected from high sulfur coal plants as well. The NZE CPU technology was projected to achieve near zero stack emissions, produce high purity CO₂ relatively free of trace impurities and achieve ~99% CO₂ capture rate while lowering the CO₂ capture costs.

References

- [1] Degenstein, N. J., Shah, M. M. and Kumar, R., “Multi-stage process for purifying carbon dioxide and producing acid”, US Patent 7,927,573, April 19, 2011.
- [2] Degenstein, N. J. and Shah, M. M., “Purifying carbon dioxide and producing acid”, US Patent 7,927,572, April 19, 2011.
- [3] Degenstein, N. J., Shah, M. M. and Neu, B. T., “Purifying carbon dioxide using activated carbon”, US Patent Application 20100083697 A1, April 8, 2010.
- [4] D.K. Louie. *Handbook of Sulphuric Acid Manufacture*, 1st ed.; DKL Engineering Inc.; Ontario, Canada, 2005.
- [5] A.M. Fairlie. *Sulfuric Acid Manufacture*, International Textbook Press, Scranton PA, 1936.
- [6] Sulfuric Acid and Sulfur Trioxide. *Ullmanns Encyclopedia of Industrial Chemistry*, 5th ed.; Wiley-VCH: Weinheim, Germany: 2005.
- [7] W.G. Davenport, M.J. King. *Sulfuric Acid Manufacture*, 1st ed.; Elsevier; New York, 2005.
- [8] Hultbom, K.G., “Industrially Proven Methods for Mercury Removal from Gases”, EPD Congress 2003, The Minerals, Metals & Materials Society (TMS), 2003
- [9] Sulphuric Acid Market Outlook, 2008-2012, British Sulphur, Presented at Sulphur 2008, Rome Italy, 2008.
- [10] Sulphuric Acid Market Outlook, British Sulphur, Presented at Sulphur 2009, Vancouver, Canada, 2009.
- [11] Chilton, T. H., *Strong Water; Nitric Acid: Sources, Methods of Manufacture, and Uses*, M.I.T. Press, 1968.
- [12] Mochida I., Korai, Y., Shirahama, M., Kawano S., Hada T., Seo Y., Yoshikawa M., Yasutake, “Removal of SO_x and NO_x over activated carbon fibers”, *Carbon vol. 38*, p 227-239, 2000.
- [13] Santos S., “Impact of Mercury on Oxy-Coal Combustion Technology for Power Generation with CO₂ Capture”, IEA Greenhouse Gas R&D Programme, Stoke Orchard, Cheltenham, UK, 2010.
- [14] Tan Y., Mortazavi R., Dureau B., Douglas M.A. “An investigation of mercury distribution and speciation during coal combustion”, *Fuel vol. 83* p 2229-2236, 2004.
- [15] Chu, P. and Schmidt C., “Hazardous Air Pollutant Emissions from Coal Fired Power Plants”, (Pittsburgh: Pittsburgh Coal Conference, 1994), p 551-556, 1994.
- [16] Meij, R., “Trace element behavior in coal-fired power plants”, *Fuel Process. Technol. Vol. 39*, p 199–217, 1994.

[17] Prestbo, E. M. and Bloom, N. S., “Mercury speciation adsorption MESA method for combustion flue gas: methodology, artifacts, intercomparison, and atmospheric implications”, *Water, Air, Soil Pollut.* 80, p 145–158, 1995.

[18] Kumar, R. “Process and Apparatus to Recover High Purity Carbon Dioxide”, US Patent 7,550,030 B2, June 23, 2009.

[19] Kumar, R. “Process and Apparatus to Recover Medium Purity Carbon Dioxide”, US Patent 7,618,478 B2, November 17, 2009.

[20] Kumar, R. “Process and Apparatus for Carbon Dioxide Recovery”, US Patent 7,740,688 B2, June 22, 2010.

[21] Seltzer, A. and Fan, Z. “Near-Zero Emissions Oxy-Combustion Flue Gas Purification – Power Plant Performance” Topical Report, DOE Award No. DE-NT0005341, submitted to OSTI, March 2011.

Appendix A – Literature Review for Task 4 VPSA Process

As a first step in the project a literature search was conducted. The following literature is organized under two categories: Adsorbents and Processes. In addition, existing patents for CO₂ capture by adsorption are also reviewed:

Adsorbent Literature

In this section, various published literature about different adsorbents and their sorption characteristics for CO₂ as a pure gas or their selective capability for CO₂ as a component in a mixture of other gases like N₂, CH₄, CO, O₂, are summarized.

Based upon pure and binary equilibrium data for CO₂ and N₂, Li and Tezel⁽⁴⁵⁾ claimed that Silicalite is a promising adsorbent for the separation of CO₂ and N₂. Li and Tezel⁽⁴⁴⁾ also claimed that β- zeolite is a good candidate for flue gas separation. This was based upon pure component equilibrium isotherms using pulse chromatography.

Lu et al.⁽⁴⁶⁾ modified three adsorbents - carbon nanotubes, activated carbon and zeolites with 3-aminopropyl-triethoxysilane. The modified carbon nanotubes showed the highest equilibrium capacity for CO₂.

Rivera-Ramos et al.⁽⁶³⁾ measured pure component equilibrium isotherms for CO₂, CH₄, H₂, N₂, O₂, and CO on ion-exchanged Silicoaluminophosphates (SAPOs). The overall adsorption performance of the ion-exchanged materials was as follows: Sr²⁺ > Na⁺ > Ag⁺ > Ca²⁺ > Mg²⁺ > Ti³⁺ > Ce³⁺. A simulator was used to assess the performance of a VPSA (Vacuum Pressure Swing Adsorption) process for CO₂ removal from CH₄ mixtures, and results showed that Sr²⁺-SAPO-34 was the best option.

Soares et al.⁽⁷²⁾ provide basic data for Hydrotalcite to remove CO₂ from post-combustion flue gas. Soares et al.⁽⁷³⁾ also suggest the use of CMS (Carbon Molecular Sieve) to separate CO₂ from an O₂/N₂ mixture.

Dreisbach et al.⁽⁸⁾ present complete pure, binary and ternary equilibrium data and co-relations for CO₂, CH₄ and N₂ on Activated Norit R1 carbon.

Siriwardane et al.⁽⁷⁰⁾ reported equilibrium and some breakthrough data for CO₂, N₂, O₂ and H₂ on Zeolite 13X, activated Carbon and natural zeolite ZS500A. Zeolite 13X is recommended for CO₂ separation. Siriwardane et al.⁽⁶⁹⁾ also reported that the zeolite with the highest sodium content gave the best separation of CO₂ from the gas mixtures.

Lee et al.⁽⁴⁰⁾ provided equilibrium and column dynamic (adsorption and desorption) data for chemisorption of carbon dioxide from inert nitrogen at 150, 350 and 450 °C on a sample of sodium oxide promoted alumina. Heats of CO₂ chemisorption are also reported. Regeneration by N₂ purge was at 350 °C. Stable CO₂ sorption capacity was achieved after a few cycles. A thermal swing chemisorption (TSC) process for the production of CO₂ from a flue gas using Na₂O promoted alumina was summarized by Lee and Sircar⁽³⁹⁾.

Lee et al.⁽⁴¹⁾ presented equilibrium and kinetic data for CO₂ on physisorbents like NaX zeolite, Maxsorb Carbon, BPL Activated Carbon, Alumina and Silica Gel. Chemisorbents like CaO, Li₂ZrO₃, K₂CO₃ promoted hydrotalcite and Na₂O promoted alumina were also studied. Physisorbents are usually limited to be used at operating temperatures below 100°C to have practical equilibrium sorption capacities. The feed gas also requires pre-drying because H₂O selectively adsorb over CO₂, reducing sorption capacity for

CO₂. On the other hand, chemisorbents provide acceptable sorption capacities for CO₂ at elevated temperatures (150-500°C) even in the presence of water.

Ram Reddy et al. ⁽⁵⁵⁾ found that SO_x is irreversibly adsorbed on layered double hydroxide (LDH) adsorbent. Hence, LDH derivatives for CO₂ capture require a de-SO_x unit operation upstream.

Hutson and Attwood ⁽²³⁾ tested various hydrotalcite-like compounds (HTlc) and showed that the synthetic analogue of the naturally occurring hydrotalcite mineral, [Mg_{0.73}Al_{0.27}(OH)₂](CO₃)_{0.13}·xH₂O], had the best overall adsorption capacity and kinetics for CO₂ at 603 K. At the end of 10 equilibrium adsorption and desorption cycles, the HTlc had maintained approximately sixty-five percent of its initial capacity.

Himeno et al. ⁽¹⁸⁾ synthesized Clathrasil Deca-dodecasil 3R (DD3R) zeolite. Based upon pure component equilibrium they concluded that all-silica DD3R is an effective adsorbent or zeolite membrane material that can separate carbon dioxide and methane gaseous mixtures. Henry's law selectivity is ~ 10.

Harlick, and Tezel ⁽¹⁵⁾ screened on thirteen Zeolite based adsorbents: 5A, 13X, NaY, NaY-10, H-Y-5, H-Y-30, H-Y-80, HiSiv 1000, H-ZSM-5-30, H-ZSM-5-50, H-ZSM-5-80, H-ZSM-5-280 and HiSiv 3000. Based upon working capacity calculations NaY and 13X were recommended for CO₂ recovery.

Xu et al. ⁽⁷⁹⁾ reported that MCM-41 modified with PEI (polyethylenimine) has high CO₂ capacity from CO₂/N₂/O₂ mixture. Adsorbent is not stable above 100 C. Isotherm is extremely non-linear. This work was done at Penn. State. Additional work was also going on at Penn. State (Maroto-Vater, M. M., Lu, Z., Tang Z. and Zhang, Y.) on PEI modified carbons. These also have very high CO₂ capacity.

Millward and Yaghi ⁽⁵¹⁾ presented pure component isotherms for Metal-Organic Framework (MOF) adsorbents and an activated carbon for comparison. CO₂ equilibrium capacities at 35 bar and at room temperature are in the order MOF -177 > IRMOF-1 > IRMOF-6 > IRMOF-3 > IRMOF-11 > CU₃(BTC)₂ > MOF-74 > MOF-505 > Activated Carbon Norit RB2 > MOF-2. Also, MOF-177 was found to have higher capacity than 13X or MAXSORB. A container filled with MOF-177 can store 9 times more CO₂ than an empty container or two times more CO₂ than a container filled with 13X or MAXSORB at 35 bar and room temperature.

Siriwardane et al. ⁽⁶⁸⁾ reported 13X and UOP WEG-592 results for a PSA/TSA process. Process cycle was not outlined. A novel sorbent utilizing liquid impregnation technique was developed. It is water insensitive and can be thermally regenerated at 80 °C. Other novel adsorbents were also developed at NETL to adsorb at 315 °C and thermally regenerate at 700 °C. Details were not given.

Hutson et al. ⁽²⁴⁾ proposed to use Hydrotalcite like compound (HTlc) to carryout CO₂ PSA at ~ 200 to 300 °C. Process cycle was not outlined.

Hiyoshi et al. ⁽¹⁹⁾ found that adsorption capacities of aminosilane modified SBA-15 under wet condition were comparable to that under dry condition (~1.28 mole/kg in presence of water at 333K). Adsorbents were completely regenerated by heating up to 423 K in Helium flow.

Bonhomme et al. ⁽²⁾ found high Silica ZSM-5 membranes grown on porous α-Alumina to permeate CO₂ out of Synthesis Gas mixture (CO₂, H₂, CH₄, N₂, CO and O₂). It is selective for CO₂ over H₂. However, after ~ 60 hrs of operation, CO₂ permeability dropped to ~ 1/3rd. Heating the membrane brought the value to about ½ of the original.

Harlick and Tezel ⁽¹⁶⁾ investigated working capacities for PSA, TSA and PTSA processes on NaY Zeolite for the removal of CO₂ from flue gas. Pure CO₂ equilibrium data is fitted by a temperature-dependent form of the Toth isotherm.

Walton et al. ⁽⁷⁶⁾ studied the effect of ion exchanging X and Y Zeolites on CO₂ capacity. They used Li, Na, K, Rb and Cs ions. Equilibrium isotherms were measured at one temperature and the Toth equation was used to model the data. LiY (with > 75% exchange was found to be the best material for CO₂ removal.

Franchi et al. ⁽¹¹⁾ developed a high capacity, water-tolerant adsorbent for CO₂. It consisted of diethanolamine (DEA) loaded pore-expanded MCM-41 silica.

Xu et al. ⁽⁸⁰⁾ developed a “molecular basket” adsorbent (MCM-41-PEI) for CO₂ capture from flue gas of a natural gas-fired boiler. It is claimed to have high adsorption capacity and high CO₂ selectivity.

Hiyoshi et al. ⁽²⁰⁾ developed an Amine modified Silica gel (SBA-15). It is claimed to have higher capacity for CO₂ compared to NaY. It is also a water-tolerant adsorbent.

Kimura et al. ⁽²⁷⁾ developed a new adsorbent based upon Lithium Silicate to capture CO₂ at high-temperature. It may be used in a fluidized bed.

Macario et al. ⁽⁴⁷⁾ synthesized mesoporous material in pure silica form (MCM-41 and MCM-48) containing Al, Fe, Cu and Zn. These materials have high CO₂ adsorption capacity, high selectivity and high working capacity.

Knowles et al. ⁽²⁸⁾ prepared several new materials and analyzed for CO₂ adsorption.

Shigemoto and Yanagihara ⁽⁶⁵⁾ outlined the use of Potassium carbonate supported on activated carbon for efficient recovery of CO₂ from moist flue gas.

Ebner et al. ⁽⁹⁾ synthesized and explored the working capacity of K-Promoted Hydrotalcite-like Compound (HTLc) at high temperature. It exhibited maximum working capacity of ~ 0.55 mol/ kg at 450 °C between 65 to 980 torr. However, the kinetics was found to be very slow.

Key commercial adsorbents identified from the literature review are listed below:

Activated Carbon(s),
NaX Zeolite,
Activated Alumina(s),
Silica Gel(s),
NaY Zeolite,
Carbon Molecular Sieve,
NaA Zeolite,
CaA Zeolite,
Silicalite,
HiSiv(s),
HY Zeolite, and
ZSM(s)

Process Literature

In this section, a summary of the various published literature about different adsorption processes and operating conditions for CO₂ capture from gas mixtures is presented.

Theoretical study by Radosz et al. ⁽⁵⁴⁾ on flue gas (CO₂ / N₂) separation to capture CO₂ on two activated carbons, Charcoal and virgin bituminous coal was reported. CO₂ capture cost from VPSA was ~ \$37/ton and from TSA ~ \$20/ton for one of the activated carbons. The target purity and target recovery was 90% respectively.

Ho et al. ⁽²¹⁾ claimed that for CO₂ recovery from post combustion flue gas (CO₂ / N₂) using 13X zeolite, Vacuum Swing Adsorption process (i.e VSA, 22 psia to 0.7 psia) is better than a Pressure Swing Adsorption process (i.e. PSA; 87 psia to 14.7 psia). The size of the adsorber vessels is very large. They suggested that a better adsorbent is needed. CO₂ purity of 58% at 85% recovery was reported.

Merel et al. ⁽⁵⁰⁾ investigated a Thermal Swing Adsorption (TSA) process with indirect heating by internal coils for CO₂ post-combustion capture. The process shows that Zeolite 5A has better performance than Zeolite 13X to recover CO₂ from a 90% N₂ and 10% CO₂ flue gas mixture. CO₂ recovery of $\geq 94\%$ was claimed.

Chaffe et al. ⁽³⁾ presented an experimental – simulation study. Two VSA cycles; 6 steps without purge and 9 steps with purge were considered on 13X adsorbent for a CO₂ - N₂ flue gas mixture. The 6-step process had CO₂ purity from 60%-80% at CO₂ recovery from 82%-83%. The 9-step process had CO₂ purity from 60%-70% at CO₂ recovery from 90%-95%. In all the cases, recovery decreased as purity increased. Inorganic-organic (amines) hybrid adsorbents were also suggested but not tested in the process.

Zhang et al. ^(81, 82) also presented an experimental – simulation study for CO₂ recovery from CO₂ - N₂ flue gas mixtures using 13X adsorbent. Many VSA cycles were considered and the effect of process parameters on power was evaluated. The maximum purity (~ 70%) and highest recovery (~ 70%) was for the case with evacuation pressure ~ 0.9 psia and feed pressure ~ 17 psia @ feed CO₂ ~ 12%.

Xio et al. ⁽⁷⁸⁾ used a validated simulator to study CO₂ recovery on 13X Zeolite from a 12% CO₂ plus dry air gas mixture. Both recovery and purity quickly drop as the evacuation pressure rises from ~ 0.6 psia to ~ 1.5 psia. The power consumption goes up as the evacuation pressure goes lower. For a 9-step cycle with two pressure equalizations and evacuation pressure ~ 0.6 psia, CO₂ purity > 70% at CO₂ recovery > 90% was reported. For a 12-step cycle with two pressure equalizations, purge and evacuation pressure ~ 0.6 psia, CO₂ purity > 70% at CO₂ recovery > 95% was reported.

Li et al. ⁽⁴³⁾ experimentally examined the effect of humidity on CO₂ capture on 13X zeolite using a VSA cycle. Feed had 12% CO₂ and 95% RH at 30 °C. Water causes “cold spot“ formation. This results in a CO₂ recovery drop from 79% to 60% and productivity drop by 22%.

Zhang et al. ⁽⁸⁴⁾ provide data for an RPSA (Rapid Pressure Swing Adsorption) process with Silica Gel as the adsorbent. Feed gas is 81% N₂ and 19% CO₂ at ~ 145 psia. A single-bed process yields ~ 90% CO₂ product purity at 70% recovery. A two-bed process yields ~ 94% CO₂ product purity at 72% recovery.

Ko et al. ⁽²⁹⁾ describe a gPROMS based mathematical model investigating PSA using 13X for CO₂ recovery through dynamic simulation and optimization. Feed is a mixture of N₂ and CO₂ at ~ 2.5 atm. Optimization study shows that the optimal feed pressure should not be high.

Konduru et al. ⁽³⁰⁾ presented experimental data for a (TSA Thermal Swing Adsorption) process using 13 X Zeolite. Feed has 1.5% CO₂. 135 °C thermal regeneration is used. Adsorbent capacity at 90% saturation decreased from ~ 8 to 6 wt% in five cycles.

Lee and Sircar⁽³⁹⁾ reported simulation results for a fast novel Thermal Swing Chemisorption process (TSC). The process uses Na₂O promoted alumina as a reversible CO₂ selective chemisorbent. Wet feed gas is 15% CO₂ + N₂ at ~ 1.1 atm and T > 150 °C. CO₂ product purity ~ 100% at > 93% recovery is claimed. Steam is used for indirect heating / regeneration: high pressure steam (13.5 atm at 500 °C) requirement is 0.44 tons per ton of CO₂ and low pressure steam (1.3 atm at 200-500 °C) requirement is 3.1 tons per ton of CO₂.

Reynolds et al.⁽⁵⁸⁾ theoretically studied nine PSA cycle configurations for concentrating CO₂ from stack and flue gas at high temperature (575 K) using a K-promoted HTlc. They concluded that the best cycle based on overall performance was a 5-bed 5-step stripping PSA cycle with some light reflux step (LR) and heavy reflux (HR) from countercurrent depressurization (CnD). The process produced 98.7% CO₂ purity, 98.7% CO₂ recovery and 5.8 LSTP/hr/kg feed throughput.

Chou and Chen⁽⁵⁾ presented simulation and experimental results for several two and three bed VPSA cycles to recover CO₂ from flue gas (20% CO₂ and 80% N₂) mixture. 13X adsorbent was used. The process steps were: feed re-pressurization, co-current depressurization to collect N₂ product, countercurrent depressurization to sub-ambient pressure to collect CO₂ product and product pressurization. In the two-bed process CO₂ product concentration was ~ 30 - 40% at 90% recovery. In the three-bed process CO₂ product concentration was ~ 60% at ~ 60% to 80% recovery.

Hoffman and Pennline⁽²²⁾ NETL presentation deals with thermally regenerating 13X beds saturated with flue gas. Beds are very shallow.

Chen's⁽⁴⁾ doctoral thesis presented dual-bed VSA processes for CO₂ removal from flue gas and concentrate CO₂ in the desorbed stream. Highest CO₂ concentration was ~ 90% and CO₂ recovery is between 90-95%.

Gomes and Yee⁽¹³⁾ reported results from a four-bed PSA to separate N₂/CO₂ from exhaust gas. Feed mixture is N₂ (~30%), CO₂ (~10%) and an inert (Helium). Experimental and simulation studies were done with 13X Zeolite. N₂ purity increased from 30 to 90%.

Park et al.⁽⁵³⁾ recommended a two-stage VPSA process to get 99% CO₂ from flue gas containing 10-15% CO₂. First stage of the process was numerically analyzed. Specific blower power is inversely proportional to CO₂ recovery. Specific vacuum power is independent of the recovery but inversely proportional to CO₂ purity and directly proportional to compression ratio.

Na et al.⁽⁵²⁾ presented results on a PSA experimental study. CO₂ at purity ~ 99% at a recovery ~ 55% was claimed. Feed gas is 83% N₂, 13% CO₂ and 4% O₂. Adsorbent was Activated Carbon.

Takamura et al.⁽⁷⁵⁾ presented simulation and experimental results for a bed filled with NaA and NaX adsorbents. Boiler exhaust gas has 13% CO₂, 79% N₂ and 8% O₂. Process cycle steps for the PSA process are: feed re-pressurization, feed, purge by the recovered gas, pressure equalization, desorption, regeneration purge, pressure equalization and idle. A four bed PSA system results in CO₂ recovery from ~ 80% to 90%. Corresponding product purity is ~ 50 to 60%. NaX to NaA ratio of 2:1 in the vessels showed the best performance.

Suzuki et al.⁽⁷⁴⁾ showed experimentally and numerically that production capacity of piston-driven Ultra-Rapid PSA was about one order of magnitude higher than those of conventional PSA. Still, the performance of the Ultra-Rapid PSA was low.

Chue et al.⁽⁶⁾ concluded that Zeolite 13X is a better adsorbent than Activated Carbon for flue gas separation using their PSA process.

Kikkinides et al.⁽²⁶⁾ show that based upon simulation studies Activated Carbon is better than CMS (Carbon Molecular Sieve) for producing CO₂ from flue gas (~ 17% CO₂). Almost 100% CO₂ purity at ~ 68% recovery was claimed.

Xiao et al.⁽⁷⁷⁾ presented simulation results for a 3-bed VSA process for CO₂/N₂ separation from flue gas using 13X zeolite. NaY zeolite was also mentioned for CO₂ VSA. Six-step cycle was feed to waste, feed to provide RP gas, provide PE, evacuation, receive PE, RP. Nine-step cycle was feed to waste, Feed to provide RP gas, Provide PE, Product Purge, Evacuation, Receive PE, RP. Feed pressure ~ 1.3 bara, evacuation pressure ~ 0.05-0.06 bara. CO₂ purity ~ 90% and recovery ~ 80% was claimed. Zhang et al.⁽⁸³⁾ experimentally simulated the above mentioned cycles using NaX Zeolite. 6-step process had CO₂ purity from 80%-83% at CO₂ recovery from 70%-80%. 9-step process had CO₂ purity from 90%-95% at CO₂ recovery from 60%-70%.

Reynolds et al.⁽⁵⁹⁾ presented simulation results for a VSA process for CO₂/N₂ separation from flue gas using K-promoted HTlc adsorbent at high temperature. The VSA process has four steps: N₂ RP, feed to produce N₂ product, countercurrent blow down to sub-ambient pressure to produce CO₂ product, counter current N₂ purge under sub-ambient pressure to get extra CO₂ product. Process cycle and adsorbent are very encouraging.

Reynolds et al.⁽⁶⁰⁾ compared simulation results for many PSA cycles at high temperature using K-Promoted Hydrotalcite-like Compound (HTlc). They obtained best performances from a 4-bed 4-step stripping PSA cycle with CO₂ product purity ~ 83% and recovery ~ 17% and a 5-bed 5-step stripping PSA cycle with CO₂ product purity ~ 76% and recovery ~ 49%. Flue gas feed contained 15% CO₂, 75% N₂ and 10% moisture. Feed temperature was 575 °K.

Malhotra et al.⁽⁴⁸⁾ tested the selectivity of copper terephthalate complex adsorbent for CO₂ over N₂ and the selectivity was 8. They also simulated a PSA process to capture CO₂ from a 400 MW gas-fired power plant that would meet the specifications of 90% capture and 96% CO₂ purity. Because pressurizing the total plant exhaust (1586.1 MMSCFD) would place a very high parasitic load (about 260 MW), they opted for a design in which the beds are charged at the pressure of the exhaust, and the CO₂ product is recovered by pulling vacuum. The highest purity obtained in the experiments was 67.9% CO₂ with 34.1% recovery. The production rate was 0.0113 SL/min. Additional simulations of the PSA process revealed that CO₂-rich product with 97% purity is achievable by a 2-bed/5-step PSA process using the copper terephthalate adsorbent; however, it would require a long rinse (with part of the CO₂-rich stream) and purging at low absolute pressure to obtain a high-purity CO₂-rich product. The power requirement by using either the copper terephthalate or Hisiv 3000 adsorbent is twice the power production of the power plant.

Patents' Literature

There are many U.S. patents for CO₂ recovery from various sources. Some claim very high CO₂ purity (99.99+ %) at high (99.9+ %) recovery. The process configuration we are exploring is different than in the patent literature. Details on these patents are listed below:

Gauthier et al.⁽¹²⁾ propose to use H₂ PSA tail gas to recover CO₂ by compression and condensation/separation. Many integrations including membrane are outlined.

Gueret et al. ⁽¹⁴⁾ propose an integrated process for adsorption and cryogenic separation for the production of CO₂ and installation to perform the process.

Shen and Radoz ⁽⁶⁴⁾ outline polymerizable ionic liquid monomers and their corresponding polymers and found these to exhibit high CO₂ sorption.

Reddy ⁽⁵⁶⁾ outlines an integrated process to produce CO₂ and H₂ from SMR/ Shift Syngas. The process has a first separation unit which produces raw CO₂, a second separation unit which produces high purity H₂ and a CO₂ liquefaction unit. The first unit may be absorption, adsorption or membrane or any other separation technology based. The second unit may be adsorption or any other separation technology based. The liquefaction unit may have auto refrigeration.

Kane et al. ⁽²⁵⁾ outline a process to produce CO₂ from a low-pressure gas mixture at constant purity. It employs simultaneous purge and evacuation steps. The counter current purge is carried out by the less strongly adsorbed species.

Kumar ⁽³⁸⁾ outlines a process with five steps: adsorption, depressurization, low pressure purge, evacuation, pressure equalization by part of the depressurized and low pressure purge effluent gas and repressurization. The novel feature is that first part (higher pressure) of the depressurized gas is recycled whereas the second part (lower pressure) and part of the low pressure purge effluent gas is used for pressure equalization.

Kumar ⁽³⁷⁾ outlines a process with four steps: adsorption, depressurization, evacuation, pressure equalization by part of the depressurized gas and repressurization. The novel feature is that first part (higher pressure) of the depressurized gas is recycled whereas the second part (lower pressure) is used for pressure equalization.

Krishnamurthy and Andrecovich ⁽³¹⁾ outlined an integrated process to produce CO₂ and N₂ from combustion off-gas. The process steps are: (a) particulate removal from the exhaust gas, (b) gas compression, (c) trace removal, (d) produce a CO₂ rich and a N₂ rich stream. This process could be absorption or adsorption or any other separation technology based, (e) liquefy CO₂ and distill off volatile contaminants, (f) purify the N₂ rich fraction to remove contaminants, and (g) cryogenically distill N₂ rich stream to produce N₂.

Leitgeb and Leis ⁽⁴²⁾ outline a PSA process to produce the more strongly adsorbed species (CO₂) from a gas mixture at high purity. This process employs a co-current purge step by the high purity strongly adsorbed species. This purge stream and product are obtained during the evacuation step. Effluent from the purge step is recycled for re-pressurization. Primary process improvement is claimed in the pressure build-up steps.

Kumar ⁽³⁴⁾ outlines a process to produce two products at high purity and high recovery from a multi component gas mixture. This process employs a single train of beds. The bed is purged by the more strongly adsorbed species obtained during the evacuation step. This purge is at low pressure and is carried out after the bed has been depressurized. Effluent during the purge step and depressurization steps is recompressed and recycled as feed.

Krishnamurthy et al. ⁽³³⁾ outlined an integrated SMR/Shift-H₂ PSA – CO₂ PSA and CO₂ liquefaction unit. The tail gas from H₂ PSA is compressed and processed in the CO₂ PSA unit. Evacuated CO₂ product from the PSA unit is compressed and further processed in a liquefaction unit to produce food grade CO₂. Part of the compressed CO₂ product from PSA is retrieved after a few stages of compression and used for high

pressure rinse in CO₂ PSA. The rinse effluent and waste from the liquefaction unit is recycled as feed to the CO₂ PSA unit. H₂ rich waste from CO₂ PSA is fed to the SMR.

Krishnamurthy and MacLean⁽³²⁾ outlined an integrated hybrid (distillation and PSA) process for producing pure liquid CO₂ from low concentration CO₂ feed streams (~35% to 98%). Recovery and purity are enhanced by integration.

Kumar⁽³⁵⁾ outlines a process to produce two products at high purity and high recovery from a binary gas mixture. This process employs a single train of beds. The bed is purged by the more strongly adsorbed species obtained during the evacuation step. This purge is at low pressure and is carried out after the bed has been depressurized. Effluent during the purge step and depressurization steps is recompressed and recycled as feed.

Kumar⁽³⁶⁾ outlines a process to produce two products at high purity. This process employs two trains of beds, which are integrated during the feed and re-pressurization steps. The train producing the more strongly adsorbed species (CO₂) is purged by the more strongly adsorbed species obtained during the evacuation step. This purge is at low pressure and is carried out after the bed has been depressurized. Effluent during the purge step is recompressed and recycled as feed.

DiMartino⁽⁷⁾ outlines a process to produce carbon dioxide from a gas mixture. At the end of the feed step the discharge end of the feed column is connected with the inlet end of the evacuated bed to provide an internal purge. This results in higher purity of the evacuated (CO₂) gas product.

Hay⁽¹⁷⁾ outlines a process to produce $\geq 95\%$ carbon dioxide from a feed stream containing 10-30% CO₂ at ambient pressure. The process steps are feed, co-current evacuation, countercurrent evacuation to produce product and re-pressurization step. Co-current evacuated gas is used for PE / re-pressurization and mixed with feed.

Sircar et al.⁽⁶⁷⁾ outlines a process to produce Methane and Carbon dioxide from landfill gas. It is an integrated thermal (TSA) and pressure swing adsorption (PSA) process. The waste produced from the PSA regenerates the TSA. There are no pressure equalization steps in the PSA process. In the first embodiment, a high-pressure rinse and recycle step is used. In the second embodiment, the depressurized gas is re-compressed and recycled by mixing with the feed gas.

Benkmann⁽¹⁾ outlines a process to produce two products at high purity and high recovery. This process employs two trains of beds, which are integrated during the feed and co-current depressurization steps. The train producing the more strongly adsorbed species (CO₂) is purged by the co-current depressurized gas after it has been recompressed. Part of the co-current depressurized gas may be recycled for re-pressurization. Evacuation and blowdown steps produce part of the more strongly adsorbed species and part of the purge gas.

Sircar⁽⁶⁶⁾ outlines a process to produce very high purity CO₂ (99.99⁺%) and very high purity H₂ (99.99⁺%) at high CO₂ (99.9⁺%) recovery from Syngas. This process has two trains of adsorption beds, which are in-communication with each other during the feed and re-pressurization steps. Beds in the CO₂ train employ a rinse step by high purity CO₂ at high pressure. Depressurization and evacuation of the same bed follow this step. Depressurized gas is re-compressed and used for high-pressure rinse. The effluent from the high pressure, high purity rinse step is recycled to the feed.

Richard et al.⁽⁶²⁾ outline an integrated adsorption and cryogenic process for separation for the production of CO₂ and installation to perform the process.

Reddy et al. ⁽⁵⁷⁾ outline an integrated Adsorption and Absorption process for the production of CO₂ and H₂.

Sirwardane ⁽⁷¹⁾ discloses synthesis of a new adsorbent material. It is an amine-enriched sorbent. The sorbents may be used in a TSA process to capture CO₂ from flue gas.

Richard et al. ⁽⁶¹⁾ outline an integrated adsorption and cryogenic process for separation for the production of CO₂. Different process configurations are described.

References

1. Benkmann, C. "Adsorption Process for the Separation of Gaseous Mixtures", US Patent # 4,299,596 Issued to Linde November 120, 1981.
2. Bonhomme, F., Welk M. E. and Nenoff, T. M. "CO₂ selectivity and lifetimes of high silica ZSM-5 membranes", *Microporous and Mesoporous Materials*, 66, 181, 2003.
3. Chaffe, A. L.; Knowles, G. P.; Liang, Z. ; Zhang, J. ; Xiao, P. and Webley, P. A. "CO₂ capture by adsorption: Materials and process development" *International Journal of Greenhouse Control*, 1, 11 , 2007.
4. Chen, C. Y. "Study of Carbon Dioxide Recovery and Utilization by Pressure Swing Related Process"; Doctoral dissertation submitted in 2003 defended in July 2004. Chinese language.
5. Chou, C-T and Chen, C-Y; "Carbon dioxide recovery by vacuum swing adsorption", *Separation and Purification Technology*, 39, 51, 2004.
6. Chue, K. T. , Kim, J. N. , Yoo, Y. J. , Cho, S. H. and Yang R. T. "Comparison of Activated Carbon and Zeolite 13X for CO₂ Recovery from Flue Gas by Pressure Swing Adsorption"; *Ind. Eng. Chem. Res.*, 34, 591, 1995.
7. DiMartino, S. P. "Vacuum Swing Adsorption Process with Vacuum Aided Internal Rinse", US Patent # 4,857,083 Issued to Air Products and Chemicals August 15, 1989.
8. Dreisbach, F., Staudt, R. and Keller, J.U. "High Pressure Adsorption Data of Methane, Nitrogen, Carbon Dioxide and their Binary and Ternary Mixtures on Activated Carbon", *Adsorption*, 5, 215, 1999.
9. Ebner, A. D., Reynolds, S. P. ad Ritter, J. A. "Understanding the Adsorption and Desorption of CO₂ on K-Promoted Hydrotalcite-like Compound (HTlc) through Nonequilibrium Dynamic Isotherms", *I & EC Res.*, 45, 6387, 2006.
10. Energy Information Administration. Annual Energy Outlook 2009 with projections to 2030. Report No. DOE/EIA-0383, 2008.
11. Franchi, R.S., Harlick, P. J. E. and Sayari, A. "Applications of Pore-Expanded Mesoporous Silica. Development of High-Capacity, Water-Tolerant Adsorbent for CO₂", *I&EC Research*, 44, 8007, 2005.
12. Gauthier P-R, Polster, B. and Marty, P. "Method and Installation for Combined Production of Hydrogen and Carbon Dioxide" Air Liquide Application # WO 2006/054008 A1, Filed October 27, 2005.
13. Gomes, V. G and Yee, K.W.K.; "Pressure Swing Adsorption for Carbon dioxide Sequestration from Exhaust Gases"; *Separation and Purification Technology*, 28, 161, 2002.
14. Gueret, V., Lockwood, F. and Dubettier, G. R. "Process for Upgrading the Pressurization Gas of a VPSA CO₂ Unit" Air Liquide Application #288,9971, Filed August 29, 2005.
15. Harlick, P.J.E. and Tezel, F. H.; "An Experimental adsorbent screening study for CO₂ removal from N₂", *Microporous and Mesoporous Materials*, 76, 71, 2004.
16. Harlick, P.J.E. and Tezel, F.H. "Equilibrium Analysis of Cyclic Adsorption Process: CO₂ Working Capacity with NaY"; *Separation Science and Technology*, 40, 2569, 2005.

17. Hay, L. "Process for Treating a Gaseous Mixture by Adsorption", US Patent # 4,840,647 Issued to Air Liquide June 20, 1989.
18. Himeno, S., Tomita, T., Suzuki, K and Yoshida, S. "Characterization and selectivity for methane and carbon dioxide adsorption on the all-silica DD3R zeolite" *Microporous and Mesoporous Materials*, 98 (1-3, 5), 62, 2007.
19. Hiyoshi, N., Yogo, K. and Yashima, T. "Reversible Adsorption of Carbon Dioxide on Amine-Modified SBA-15 from Flue Gas Containing Water Vapor", *Studies in Surface Science and Catalysis* 153, 417, 2004.
20. Hiyoshi, N., Yogo, K. and Yashima, T. "Adsorption of Carbon Dioxide on Aminosilane-modified Mesopore Silica", *J. of the Japan Petroleum Institute*, 48(1), 29, 2005.
21. Ho, M. T.; Allinson, G. W. and Wiley, D. E. "Reducing the Cost of CO₂ Capture from Flue Gases Using Pressure Swing Adsorption" *Ind. Eng. Chem. Res.*, 47, 4883, 2008.
22. Hoffman, J. and Pennline, H. "Capture of Carbon Dioxide using Zeolite Molecular Sieve"; Presentation at the 3rd Annual Conference on Carbon Capture & Sequestration, May 3-6, 2004; Alexandria, Virginia.
23. Hutson, N. D. and Attwood, B. C. "High temperature adsorption of CO₂ on various hydrotalcite-like compounds" *Adsorption*, 14 (6) 781, 2008.
24. Hutson, N., Attwood, B., Reynolds, S., Gadre, S., Ebner, A. and Ritter, J. "Separation and Capture of CO₂ using a High Temperature Pressure Swing Adsorption (PSA) system"; 3rd Annual Conference on Carbon Capture and Sequestration, Alexandria, Virginia, May 3-6, 2004.
25. Kane, M. S., Leavitt, F. W., Ackley, M. W. and Notaro, F. "Pressure Swing Adsorption Process and Apparatus", US Patent # 6,245,127 B1, Issued to Praxair Technology June 12, 2001.
26. Kikkinides, E. S., Yang, R. and Cho, S. H. and Yang R. T. "Concentration and Recovery of CO₂ from Flue Gas by PSA"; *Ind. Eng. Chem. Res.*, 324, 2714, 1993.
27. Kimura, S., Adachi, M., Noda, R. and Horio, M. "Particle Design and Evaluation of dry CO₂ recovery sorbent with liquid holding capability", *Chemical Engineering Science*, 60, 4061, 2005.
28. Knowles, G. P., Delaney, S. W. and Chaffee, A.L. "Diethylenetriamine [propyl (silyl) - Functionalized (DT) Mesoporous Silicas as CO₂ Adsorbents"; *Ind. Eng. Chem. Res.*, 45, 2626, 2006.
29. Ko, D., Siriwardane, R. and Biegler, T. "Optimization of Pressure-Swing Adsorption Process Using Zeolite 13X for CO₂ Sequestration", *I&EC Research*, 42, 339, 2003.
30. Konduru, N., Lindner, P. and Assaf-Anid, M. N. "Curbing the greenhouse effect by carbon dioxide adsorption with Zeolite 13X", *AIChE Journal*, 53 (12), 3137, 2007.
31. Krishnamurthy, R. and Andrecovich, M. A. "Carbon Dioxide Production from Combustion Exhaust Gases with Nitrogen and Argon by-product Recovery", US Patent # 5,185, 139, Issued to The BOC Group February 9, 1993.
32. Krishnamurthy, R. and MacLean, D. L. "Method and Apparatus of Producing Carbon Dioxide in High Yields from Low Concentration Carbon Dioxide Feeds", US Patent # 4,952, 223, Issued to The BOC Group August 28, 1990.
33. Krishnamurthy, R., Malik, V. A. and Stockley, A. G. "Hydrogen and Carbon Dioxide Co Production Apparatus", US Patent # 5,000, 925, Issued to The BOC Group May 19, 1991.
34. Kumar, R. "Adsorption Process for Producing Two Gas Streams from a Gas Mixture", US Patent # 5,026, 406, Issued to Air Products and Chemicals June 25, 1991.
35. Kumar, R. "Adsorption Process for Producing Two Gas Streams from a Gas Mixture", US Patent # 4,915, 711 Issued to Air Products and Chemicals April 10, 1990.
36. Kumar, R. "Adsorption Process for Recovering Two High Purity Gas Products from a Multi Component Gas Mixture", US Patent # 4,913, 709 Issued to Air Products and Chemicals

- April 3, 1990.
37. Kumar, R. "Depressurization Effluent Repressurized Adsorption Process", US Patent # 5,284, 322, Issued to Air Products and Chemicals September 28, 1993.
 38. Kumar, R. "Purge Effluent Repressurized Adsorption Process", US Patent # 5,354, 346, Issued to Air Products and Chemicals October 11, 1994.
 39. Lee, K. B. and Sircar, S. "Removal and Recovery of Compressed CO₂ from Flue Gas by a Novel Thermal Swing Chemisorption Process" *AIChE Journal*, 54 (9), 2293, 2008.
 40. Lee, K. B., Beaver, M. G. and Caram, H. S. "Chemisorption of Carbon Dioxide on Sodium Oxide Promoted Alumina" *AIChE Journal*, 53 (11), 2824, 2007.
 41. Lee, K. B., Beaver, M. G., Caram, H. S. and Sircar, S. "Reversible Chemisorbents for Carbon Dioxide and their Potential Applications" *Industrial & Engineering Chemistry Research*, 47(21), 8048, 2008.
 42. Leitgeb, P. and Leis, J. "Pressure Swing Adsorption Process" US Patent # 5,051, 115, Issued to Linde September 24, 1991.
 43. Li, G.; Xiao, P.; Webley, P.; Zhang, J.; Singh, R.; Marshall, M. "Capture of CO₂ from high humidity flue gas by vacuum swing adsorption with zeolite 13X", *Adsorption*, 14, 415, 2008.
 44. Li, P. and Tezel, H. "Adsorption Separation of N₂, O₂, CO₂ and CH₄ gases by β- zeolite" *Microporous and Mesoporous Materials* 98, 94, 2007.
 45. Li, P. and Tezel, H. "Pure and Binary Adsorption Equilibria of Carbon Dioxide and Nitrogen on Silicalite" *J. Chem. Eng. Data*, 53, 2479, 2008.
 46. Lu, C.; Bai, H.; Wu, Bi; Su, F. and Hwang, J. F. "Comparative Study of CO₂ Capture by Carbon Nanotubes, Activated Carbons, and Zeolites" *Energy & Fuels*, 22, 3050, 2008.
 47. Macario, A., Katovic, A., Giordano, G., Iucolano, F. and Caputo "Synthesis of mesoporous materials for carbon dioxide sequestration", *Microporous and Mesoporous Materials*, 81, 139, 2005.
 48. Malhotra, R., Hirschon, A.S., Venturelli, A., Seki, K., Knaebel, K.S., Shin, H., Reinhold, H. Chapter 9 – Self-Assembled Nanoporous Materials for CO₂ Capture: Part 2: Experimental Studies. *Carbon Dioxide Capture for Storage in Deep Geologic Formations. Results from the CO₂ Capture Project 2005*, pp 177-188.
 49. Marland, G., Boden, T.A., and Andres, R.J. Global, Regional, and National CO₂ Emissions. In *Trends: A Compendium of Data on Global Change*. Carbon Dioxide Information Analysis Center, Oak Ridge National Laboratory, U.S. Department of Energy, Oak Ridge, Tenn., U.S.A. 2008.
 50. Merel, J.; Clause, M. and Meunier, F. "Experimental Investigation on CO₂ Post-Combustion Capture by Indirect Thermal Swing Adsorption Using 13 X and 5A Zeolites" *Ind. Eng. Chem. Res.*, 47, 209, 2008.
 51. Millward, A. R. and Yaghi, O. M. "Metal-Organic Frameworks with Exceptionally High Capacity for Storage of Carbon Dioxide at Room Temperature", *J. Am. Chem. Soc.*, 127, 17998, 2005.
 52. Na, B-K., Lee H., Koo K-K. and Song, H-K.; "Effect of Rinse and Recycle Methods on PSA Process to Recover CO₂ from Power Plant Flue Gas using Activated Carbon"; *I&EC Research*, 41, 5498, 2002.
 53. Park, J-H., Beum H-T., Kim J-N. and Cho, S-H.; "Numerical Analysis on the Power Consumption of the PSA Process for Recovering CO₂ from Flue Gas"; *I&EC Research*, 41, 4122, 2002.
 54. Radosz, M.; Hu, X.; Kaspars, K. and Shen, Y. "Flue-Gas Carbon Capture on Carbonaceous Sorbents: Toward a Low-Cost Multifunctional Carbon Filter for "Green" Energy

- Producers” *Ind. Eng. Chem. Res.*, 47, 3748, 2008.
55. Ram Reddy, M. K. , Xu, Z. P. Lu, G. Q. and Costa, D. d. “Effect of SO_x Adsorption on Layered Double Hydroxides for CO₂ Capture”” *Industrial & Engineering Chemistry Research*, 47(19), 7357, 2008.
 56. Reddy, S. “Hydrogen and Carbon Dioxide Co-Production” Flour Corporation Application. # US 2002/0073845 A1, Filed Dec. 19, 2000.
 57. Reddy, S. and Ravikumar, R. “Recovery of CO₂ and H₂ from PSA Offgas in an H₂ Plant”, US Patent # 6,551,380 B1 Issued to Flour Corporation April 22, 2003.
 58. Reynolds, S. P., Mehrotra, A., Ebner, A. D. and Ritter, J. A. “Heavy reflux PSA cycles for CO₂ recovery from flue gas: Part I. Performance evaluation”, *Adsorption*, 14 (2-3), 399, 2008.
 59. Reynolds, S.P., Ebner, A. D. and Ritter, J. A. “New Pressure Swing Adsorption Cycles for Carbon Dioxide Sequestration”, *Adsorption*, 11, 531, 2005.
 60. Reynolds, S.P., Ebner, A. D. and Ritter, J. A. “Stripping PSA Cycles for CO₂ Recovery from Flue Gas at High Temperature Using a Hydrotalcite-Like Adsorbent” *I & EC Res.*, 45, 4278, 2006.
 61. Richard, D. G., Frederic L. and Vincent G. “Integrated Method and Installation for Cryogenic Adsorption and Separation for Producing CO₂”, WO 2006/106253 A2 Air Liquide Patent Application October 10, 2006.
 62. Richard, D. G., Vincent G. and Frederic L. “Integrated Process for Adsorption and Cryogenic Separation for the Production of CO₂ and installation to Perform the Process”, FR 287,2889 A1 Air Liquide Patent Application August 8, 2005.
 63. Rivera-Ramos, M. E.; Ruiz-Mercado, G. J. and Hernandez-Maldonado, A. J. “Separation of CO₂ from Light Gas Mixtures using Ion-Exchanged Silicoaluminophosphate Nanoporous Sorbents” *Ind. Eng. Chem. Res.*, 47, 5602, 2008.
 64. Shen, Y. and Radosz, M. “Novel Ionic Liquids and Poly(ionic liquid)s as new materials gas separation and other applications” University of Wyoming Application # WO 2006/026064 A2, Filed August 5, 2004.
 65. Shigemoto, N. and Yanagihara, T. ”Material Balance and Energy Consumption for CO₂ Recovery from Moist Flue Gas Employing K₂CO₃-on-Activated Carbon and Its Evaluation for Practical Adaption”, *Energy & Fuels*, 20, 721, 2006.
 66. Sircar, S. “Separation of Multicomponent Gas Mixtures”, US Patent # 4,171,206 Issued to Air Products and Chemicals October 16, 1979.
 67. Sircar, S., Kumar, R., Koch, W.R., and VanSloun, J. “Recovery of Methane from Lanfill Gas”. US Patent # 4,770,676 Issued to Air Products and Chemicals September 13, 1988.
 68. Siriwardane, R., Shen M., Fisher, E. and Losch, J. “CO₂ Capture Utilizing Solid Sorbents” publication from National Energy Technology Laboratory (NETL).
 69. Siriwardane, R.V., Shen, M. and Fisher, E. “Adsorption of CO₂, N₂, and O₂ on Natural Zeolites”, *Energy Fuels*, 17(3), 571, 2003.
 70. Siriwardane, R.V., Shen, M., Fisher, E. and Poston, J.; Shamsi, A. “Adsorption and Desorption of CO₂ on Solid Adsorbents” DOE Publication.
 71. Sirwaradane, S. “Solid Sorbents for Removal of Carbon Dioxide Gas Streams at Low Temperatures” US Patent # 6,908,497 B1 Issued to The United States of America as represented by the Department of Energy June 21, 2005.
 72. Soares, J.L., Casarin, G.L., Jose, H.J. and Moreira, R.F.P.M. “Experimental and Theoretical Analysis for the CO₂ Adsorption on Hydrotalcite”, *Adsorption*, 11, 237, 2005.
 73. Soares, J.L., Jose, H.J. and Moreira, R.F.P.M. “Preparation of a carbon molecular sieve and application to separation of N₂, O₂, and CO₂ in a fixed bed”, *Brazilian Journal of Chemical Engineering*, 20, 1, 2003.

74. Suzuki, T., Sakoda, A., Suzuki, M. and Izumi, J. "Recovery of Carbon Dioxide from Stack Gas by Piston-Driven Ultra-Rapid PSA"; *Journal of Chemical Engineering of Japan*, 30(6), 1026, 1997.
75. Takamura, Y. T., Narita, S., Akoi, J., Horonaka, S. and Uchida, S; "Evaluation of dual-bed pressure swing adsorption for CO₂ recovery from boiler exhaust gas"; *Separation and Purification Technology*, 24, 519, 2001.
76. Walton, K. S., Abney, M. B. and LeVan, M. D. "Roles of Steric and Acid-Base Factors in CO₂ Adsorption in Alkali-Metal Cation Exchanged Y and X Zeolites", Annual AIChE Meeting, Oct. 31- Nov. 4, 2005, Cincinnati, OH.
77. Xiao, P., Webley, P. A. and Zhang, T. "Recovery of Carbon Dioxide from Flue Gas Streams by Vacuum Swing Adsorption"; Annual AIChE Meeting, Oct. 31- Nov. 4, 2005, Cincinnati, OH.
78. Xiao, P., Zhang, J., Webley, P., Li, G. and Singh, R.; Todd, R. "Capture of CO₂ from flue gas streams with zeolite 13X by vacuum-pressure swing adsorption" *Adsorption*, 14, 575, 2008.
79. Xu, X., Song C., Anderson, J.M., Miller B.G. and Scaroni, A. W. "Adsorption Separation of CO₂ from Simulated flue gas Mixture by novel 'molecular basket' adsorbents", *Int. J. Environmental Technology and Management* 4, (1/2), 2004.
80. Xu, X., Song, C., Miller, B.G. and Scaroni, A. "Influence of Moisture on CO₂ Separation from Gas Mixture by a Nanoporous Adsorbent Based on Polyethylenimine-Modified Molecular Sieve MCM-41", *I&EC Research*, 44, 8113, 2005.
81. Zhang, J. and Webley, P. "Cycle Development and Design for CO₂ Capture from Flue Gas by Vacuum Swing Adsorption" *Environ. Sci. Technology*, 42, 563, 2008.
82. Zhang, J., Webley and Xiao P. "Effect of Process parameters on power requirements of vacuum swing adsorption technology for CO₂ capture from flue gas" *Energy Conversion and Management*, 49, 346, 2008.
83. Zhang, T., Xiao, P., and Webley, P. A. "Experimental Pilot-Scale Study of Carbon Dioxide Recovery from Flue Gas Streams by Vacuum Swing Adsorption"; Annual AIChE Meeting, Oct. 31- Nov. 4, 2005, Cincinnati, OH.
84. Zhang, Z., Guan, J. and Ye, Z. "R&D Note: Separation of a Nitrogen-Carbon Dioxide Mixture by Rapid Pressure Swing Adsorption", *Adsorption*, 4, 173, 1998.